MARIANA PINHEIRO FERNANDES

ATIVIDADE DE LECTINAS DE SEMENTES DE *Cratylia mollis* SOBRE A FUNÇÃO MITOCONDRIAL E VIABILIDADE DE *Trypanosoma cruzi*

Campinas-SP

2010

MARIANA PINHEIRO FERNANDES

ATIVIDADE DE LECTINAS DE SEMENTES DE *Cratylia mollis* SOBRE A FUNÇÃO MITOCONDRIAL E VIABILIDADE DE *Trypanosoma cruzi*

Tese apresentada ao curso de Pós-Graduação em Fisiopatologia Médica, da Universidade Estadual de Campinas, área de concentração em Biologia Estrutural, Celular e do Desenvolvimento, para obtenção do título de Doutor em Fisiopatologia Médica.

ORIENTADOR: PROF. DR. ANIBAL EUGENIO VERCESI
COLABORADORA: PROFA. DRA. FERNANDA RAMOS GADELHA

Campinas-SP

2010

FICHA CATALOGRÁFICA ELABORADA PELA

BIBLIOTECA DA FACULDADE DE CIÊNCIAS MÉDICAS DA UNICAMP

Bibliotecário: Sandra Lúcia Pereira – CRB-8ª / 6044

F391a

Fernandes, Mariana Pinheiro
Atividades de lectinas de sementes de *Cratylia mollis* sobre a função mitocondrial e viabilidade de *Trypanosoma cruzi* / Mariana Pinheiro Fernandes. Campinas, SP : [s.n.], 2010.

Orientadores : Aníbal Eugenio Vercesi; Fernanda Ramos Gadelha
Tese (Doutorado) Universidade Estadual de Campinas. Faculdade de Ciências Médicas.

1. *Trypanosoma cruzi*. 2. Mitocôndria. 3. Cálcio. 4. Espécies reativas de oxigênio. 5. Morte celular. 6. Lectina. I. Vercesi, Aníbal Eugenio. II. Gadelha, Fernanda Ramos. III. Universidade Estadual de Campinas. Faculdade de Ciências Médicas. IV. Título.

Título em inglês : Activity of *Cratylia mollis* seed lectins on mitochondrial function and *Trypanosoma cruzi* viability

Keywords:

- *Trypanosoma cruzi*
- Mitochondria
- Calcium
- Reactive oxygen species
- Cell death
- Lectin

Titulação: Doutor em Fisiopatologia Médica

Área de concentração: Biologia Estrutural,Celular e do Desenvolvimento

Banca examinadora:
Profº. Drº. Aníbal Eugênio Vercesi
Profº. Drº. José Roberto Meyer Fernandes
Profª. Drª. Nadja Cristhina de Souza Pinto Lardner
Profª. Drª. Maria Luiza Vilela Oliva
Profº. Drº. Fábio Maranhão Costa

Data da defesa: 24-02-2010

Banca examinadora da tese de Doutorado

Mariana Pinheiro Fernandes

Orientador(a) : Prof(a). Dr(a). Aníbal Eugenio Vercesi

Membros:

1. Prof(a). Dr(a). Aníbal Eugenio Vercesi
2. Prof(a). Dr(a). José Roberto Meyer Fernandes
3. Prof(a). Dr(a). Nadja Cristhina de Souza Pinto Lardner
4. Prof(a). Dr(a). Maria Luiza Vilela Oliva
5. Prof(a). Dr(a). Fabio Maranhão Costa

Curso de pós-graduação em Fisiopatologia Médica da Faculdade de Ciências Médicas da Universidade Estadual de Campinas.

Data: 24/02/2010

O presente trabalho foi realizado no Laboratório de Bioenergética, Núcleo de Medicina e Cirurgia Experimental (NMCE), Departamento de Patologia Clínica, Faculdade de Ciências Médicas, Universidade Estadual de Campinas (UNICAMP), sob orientação do Prof. Dr. Aníbal Eugênio Vercesi, na vigência de auxílios concedidos pela Coordenação de Aperfeiçoamento de Pessoal de Nível Superior (CAPES), Fundação de Amparo à Pesquisa do Estado de São Paulo (FAPESP), Conselho Nacional para o Desenvolvimento Científico e Tecnológico (CNPq) e Fundação de Amparo ao Ensino, Pesquisa e Extensão da Universidade Estadual de Campinas (FAEPEX-UNICAMP).

Àqueles que sempre foram para mim

modelo, força e orgulho:

MEUS PAIS.

“Se, a princípio, a idéia não é absurda,
então não há esperança para ela”.

"Algo só é impossível até que alguém duvide
e acabe provando o contrário."

Albert Einstein.

AGRADECIMENTOS

Ao Prof. Dr. Aníbal E. Vercesi, pela oportunidade de fazer parte desse grupo e desenvolver este trabalho, pelos ensinamentos científicos e, principalmente pela amizade estabelecida durante este período.

À Profa. Dra. Fernanda Ramos Gadelha, por sua colaboração científica, incentivo, amizade e confiança.

Às Profas. Dras. Luana Cassandra B. B. Coelho, Maria Julia Manso Alves e Maria Tereza dos Santos Correia, pela amizade e colaboração.

Ao Prof. Dr. Roger Castilho e a amiga Márcia Fagian por sempre estarem à disposição e pela ajuda diária no laboratório.

Ao Luiz Henrique G. Ribeiro, pela atenção dedicada à minha pessoa, amizade, ajuda constante com as culturas de *Trypanosoma cruzi* e por sempre acreditar em mim.

A todos que fazem o Laboratório de Bioenergética do Departamento de Patologia Clínica da UNICAMP, pela colaboração, companheirismo e pelos laços de amizade que se formaram durante este período de convivência; em especial, Bárbara, Bruno, Carina, Carlos, Carol, Daniela, Edilene, Fabiane, Franco, Karina, Leandro, Luciane, Paolo, Rafael, Roberto, Rodrigo Catharino, Rute e Tiago.

Aos amigos Felipe Ravagnani e Marcos Chiaratti pela dedicada amizade, apoio e incentivos contantes.

Às minhas amigas Juliana Ronchi e Natalia Inada pela amizade, paciência, companhia fiel em todos os momentos, e por não medirem esforços para me ajudar nas horas difíceis.

À amiga Ana Catarina com a qual compartilhei momentos difíceis, como também muitos momentos alegres que jamais serão esquecidos. Depois de muito trabalho, conseguimos mais essa conquista.

À minha família por compreenderem a minha ausência durante esses quatro anos; em especial aos meus pais, Mauro e Ana, por toda dedicação, amor e ensinamentos ao longo da minha vida. Vocês são o meu porto seguro.

Ao meu amor Fernando Teixeira, que sempre esteve ao meu lado em todos os momentos fazendo dos meus objetivos os seus e por sempre me apoiar, com suas palavras de carinho, incentivo e força. A você declaro todo meu amor e admiração.

A todos aqueles que direta ou indiretamente contribuíram para esta conquista.

Agradeço de um modo especial a DEUS, pela oportunidade de viver este momento e por sua constante presença na minha vida.

SUMÁRIO

LISTA DE ABREVIATURAS

AA – antimicina A

AIF – "apoptosis inducing factor" (fator de indução de apoptose)

ANT - "adenine nucleotide transporter" (translocador de nucleotídeos de adenina)

Apaf-1 – "apoptosis activating factor 1" (fator 1 de ativação de apoptose)

AT(D)P – adenosina tri (di) – fosfato

BAPTA/AM – 1,2 – bis (2-aminophenoxy)-ethane-*N,N,N',N'*- tetracetic acid

BSA – albumina soro bovina

$[Ca^{2+}]$ – concentração de cálcio

CCCP – carbonyl cyanide p-(Trifluoromethoxy) hydrazone

ConA – concanavalina A

Cramoll 1,4 – Lectina de sementes de *Cratylia mollis*, isoformas 1 e 4

CsA – ciclosporina A

CTE – cadeia de transporte de elétrons

CyD - ciclofilina-D

Cyt-c – citocromo c

EGTA – etileno glico – bis(β-aminoetil éter)-N,N,N´,N´-ácido tetraacético

EROs – espécies reativas de oxigênio

$FADH_2$ – flavina adenina dinucleotídeo reduzido

H_2DCF-DA - diacetato de diclorodihidrofluoresceína

H_2O_2 – peróxido de hidrogênio

HEPES – (N-[2-Hydroxyethyl]piperazine-N´-[2-ethanesulfonic acid])

MFR – mitocôndria de fígado de rato

MnSOD – Mn–superóxido dismutase

MTc – Fração mitocondrial de *T.cruzi*

NADH – nicotinamida adenina dinuclotídeo (estado reduzido)

NADPH – nicotinamida adenina dinuclotídeo fosfato (estado reduzido)

NAD^+ – nicotinamida adenina dinuclotídeo (estado oxidado)

$NADP^+$ – nicotinamida adenina dinuclotídeo fosfato (estado oxidado)

PARP-1 - Poli(ADP-ribose)polimerase-1

P_i – fosfato inorgânico

PTPM – poro de transição de permeabilidade mitocondrial

$O_2^{\bullet -}$ - ânion superóxido

OH^- - radical hidroxil

Rot – rotenona

Succ –succinato

SERCA - "sarco/endoplasmic reticulum Ca^{2+} -ATPase"

TcCPX - triparedoxina peroxidase citosólica

TcMPx - triparedoxina peroxidase mitocondrial

TPM – transição de permeabilidade mitocondrial

UCP – proteína desacopladora

UQ – ubiquinona (forma oxidada da coenzima Q)

$UQH^{\bullet}$ - radical ânion semiquinona

UQH_2 – ubiquinona (forma reduzida da coenzima Q)

VDAC – "voltage-dependent anion channel" (canal aniônico voltagem-dependente)

$\Delta\mu H^+$ - gradiente eletroquímico de prótons

$\Delta\Psi_m$ – potencial elétrico de membrana mitocondrial

$\Delta\Psi$ - potencial elétrico de membrana

ΔpH – gradiente químico de prótons

LISTA DE FIGURAS

INTRODUÇÃO **PÁG.**

RESULTADOS

RESUMO

Lectinas são proteínas ou glicoproteínas que reconhecem glicoconjugados de superfície celular. Neste trabalho, nós investigamos se a lectina de sementes de *Cratylia mollis* (Cramoll 1,4) tem efeitos tóxicos em *Trypanosoma cruzi*. Cramoll 1,4 reconheceu glicoconjugados presentes na superfície celular dos parasitas, levando a aglutinação de epimastigotas e tripomastigotas, de uma maneira dose dependente (1-50 µg/ml). Além disso, Cramoll 1,4 diminuiu a proliferação de epimastigotas; 93% de inibição foi obtida com 50 µg/ml. A incubação de células (1.25×10^8 /ml) na presença de Cramoll 1,4 (50 µg/ml) e Ca^{2+} (10 µM) por 1 h induziu permeabilização de membrana plasmática seguida por influxo de Ca^{2+} e acúmulo de Ca^{2+} mitocondrial, resultado que se assemelha ao efeito clássico da digitonina. Cramoll 1,4 estimulou (cinco vezes) a produção de espécies reativas de oxigênio (EROs) mitocondrial, diminuiu de maneira significativa o potencial elétrico de membrana mitocondrial ($\Delta\Psi_m$) e prejudicou a fosforilação de ADP. A geração de EROs induzida por Cramoll 1,4 foi diminuída de forma significativa por EGTA. A permeabilização de membrana plasmática por digitonina (20 µM) em meio contendo Ca^{2+} também estimulou a geração de EROs mitocondrial, mas numa proporção menor que Cramoll 1,4. A velocidade de respiração desacoplada em epimastigotas não foi afetada pelo tratamento com Cramoll 1,4 + Ca^{2+}, mas a respiração de repouso induzida por oligomicina foi 65% maior nas células tratadas do que nos controles. Experimentos usando frações mitocondriais de *T. cruzi* (MTc) mostraram que, em contraste com a digitonina, a lectina diminuiu de forma significativa o $\Delta\Psi_m$ por um mecanismo sensível a EGTA. Em concordância com os resultados da permeabilização de membrana plasmática e prejuízo da fosforilação oxidativa pela lectina, experimentos de microscopia de fluorescência usando iodeto de propídeo revelaram que Cramoll 1,4 induziu morte de epimastigotas por necrose. Experimentos feitos com mitocôndrias isoladas de fígado de rato (MFR) mostraram que Cramoll 1,4 induziu transição de permeabilidade mitocondrial, dependente de Ca^{2+}, com aumento na produção de EROs. Em contraste ao que foi observado em MFR, o efeito de Cramoll 1,4 em MTc é insensível a ciclosporina A, um inibidor clássico do poro de transição de permeabilidade mitocondrial. Nós mostramos que a toxicidade de Cramoll 1,4 em epimastigotas parece resultar de uma ação conjunta nas membranas plasmática e mitocondrial do parasita, sobrecarga de Ca^{2+} mitocondrial e produção de EROs.

ABSTRACT

Lectins are proteins or glycoproteins that recognize cell surface glycoconjugates. In this work, we investigated whether *Cratylia mollis* seed lectin (Cramoll 1,4) has toxic effects on *Trypanosoma cruzi*. Cramoll 1,4 recognized glycoconjugates present on the cell surfaces of parasites, leading to agglutination of both epimastigotes and trypomastigotes in a dose-dependent manner (1-50 μg/ml). In additional, Cramoll 1,4 decreased epimastigote proliferation; 93% inhibition was attained at 50 μg/ml. Incubation of cells (1.25 x 10^8 /ml) in the presence of 50 μg/ml Cramoll 1,4 and 10 μM Ca^{2+} for 1 h induced plasma membrane permeabilization followed by Ca^{2+} influx and mitochondrial Ca^{2+} accumulation, a result that resembles the classical effect of digitonin. Cramoll 1,4 stimulated (five-fold) mitochondrial reactive oxygen species (ROS) production, significantly decreased the electrical mitochondrial membrane potential ($\Delta\Psi_m$) and impaired ADP phosphorylation. ROS generation induced by Cramoll 1,4 was significantly diminished by EGTA. Plasma membrane permeabilization by 20 μM digitonin in a Ca^{2+}-containing medium also stimulated mitochondrial ROS generation but at a lower rate than Cramoll 1,4. The rate of uncoupled respiration in epimastigotes was not affected by Cramoll 1,4 plus Ca^{2+} treatment, but oligomycin-induced resting respiration was 65% higher in treated cells than in controls. Experiments using *T. cruzi* mitochondrial fractions (MTc) showed that, in contrast to digitonin, the lectin significantly decreased $\Delta\Psi_m$ by a mechanism sensitive to EGTA. In agreement with the results showing plasma membrane permeabilization and impairment of oxidative phosphorylation by the lectin, fluorescence microscopy experiments using propidium iodide revealed that Cramoll 1,4 induced epimastigote death by necrosis. Experiments performed with rat liver mitochondria (RLM) showed that Cramoll 1,4 induced Ca^{2+}-dependent mitochondrial permeability transition increasing the ROS production. In contrast to RLM, the Cramoll 1,4 effect in MTc is insensitive to cyclosporin A, a classic inhibitor of mitochondrial permeability transition pore. We showed that Cramoll 1,4 toxicity to *T. cruzi* epimastigotes seems to result from a concerted action on the parasite's plasma and mitochondrial membranes, mitochondrial Ca^{2+} overload and ROS production.

1 – INTRODUÇÃO

CONSIDERAÇÕES GERAIS SOBRE LECTINAS

Histórico, características estruturais, distribuição na natureza e funções

O termo "lectina" (do latim *lectus*, significa selecionado, escolhido) foi proposto por Boyd e Shapleigh em 1954 para designar um grupo de proteínas que apresentava a característica comum de seletividade na interação com carboidratos. O termo aglutinina é usado como sinônimo para lectina, em referência à habilidade de aglutinar eritrócitos ou outras células (Peumans e Van Damme, 1995). Em 1980, Goldstein e colaboradores definiram as lectinas como proteínas ou glicoproteínas de origem não imune, possuidoras de pelo menos dois sítios moleculares de ligação através dos quais interagem com carboidratos levando à aglutinação de células ou precipitação de polissacarídeos sem alterar suas respectivas estruturas.

Atualmente, a definição mais aceita é a baseada em suas estruturas, que define lectinas como proteínas de origem não imune contendo pelo menos um sítio não-catalítico de ligação reversível a mono ou oligossacarídeos específicos (Peumans e Van Damme, 1995, 1998a; Peumans et al., 2001). O(s) sítio(s) de ligação a carboidratos tende(m) a se dispor na superfície da molécula protéica, e a seletividade da ligação é obtida através de pontes de hidrogênio, interações de van der Walls e hidrofóbicas (Surolia et al., 1996; Elgavish e Shaanan, 1997).

Quanto ao número de sítios de ligação a carboidratos, a maioria das lectinas são di ou polivalentes. Algumas lectinas não apresentam um monossacarídeo inibidor e são inibidas apenas por oligossacarídeos (Lis e Sharon, 1981). Segundo Sharon e Lis (1990), algumas lectinas apresentam interações mais fortes com oligossacarídeos em comparação com monossacarídeos, enquanto outras são quase exclusivas para oligossacarídeos. De acordo com essas propriedades de ligação a carboidratos, as lectinas podem ser classificadas como específicas quando apresentam interação com um monossacarídeo ou não específicas quando interagem com diferentes oligossacarídeos.

Em virtude da capacidade de reconhecimento a carboidratos, as lectinas são usadas como ferramentas para a investigação funcional e estrutural de carboidratos complexos, especialmente para a análise de mudanças que ocorrem nas proteínas da superfície celular

durante os processos fisiológicos e patológicos, da diferenciação celular ao câncer (Sharon e Lis, 2001).

As lectinas possuem ampla distribuição na natureza podendo ser encontradas em microorganismos (Bhowal et al., 2005; Tsivileva et al., 2008), animais (Podolsky et al., 2006; Sprong et al., 2009) e plantas (Vega et al., 2006; Oliveira et al., 2008). O reino vegetal tem demonstrado ser uma ótima fonte de lectinas, servindo como fonte para a purificação dessas macromoléculas. Diferentes funções têm sido creditadas às lectinas de plantas, incluindo transporte de carboidratos, empacotamento e/ou mobilização de proteínas estocadas (Nomura et al., 1998, Ratanapo et al., 2001), defesa contra o ataque de insetos e outros predadores (Sengupta et al., 1997); muitas lectinas são potentes imunomoduladores (Oudrhiri et al., 1985), influenciando a proliferação de linfócitos humanos (Ghosh et al., 1999).

As lectinas de plantas são agrupadas de acordo com a ligação aos carboidratos e os grupos de especificidade, compreendem: fucose, manose, ácido siálico, N-acetilglicosamina, N-acetilgalactosamina-galactose e grupo glicanos complexos (Peumans e Van Damme, 1998b). A definição da especificidade da lectina e confirmação da presença da mesma em uma amostra podem ser feitas por ensaios de inibição da atividade hemaglutinante (AH) com diferentes monossacarídeos, oligossacarídeos ou glicoproteínas, ou por ensaios de precipitação de moléculas glicídicas (Sharon e Lis, 1990).

Uma outra classificação para lectinas de plantas baseia-se no número de domínios de ligação a carboidratos e outros de natureza não catalítica, dividindo-as em quatro principais tipos: merolectinas, hololectinas, quimerolectinas (Peumans e Van Damme, 1998a) e superlectinas (Peumans et al., 2001). Merolectinas são proteínas formadas exclusivamente por um domínio de ligação a carboidrato e, por conta de sua natureza monovalente, são incapazes de precipitar glicoconjugados ou aglutinar células. Como exemplo deste grupo tem-se a proteína que se liga à quitina obtida do látex da seringueira (*Hevea brasiliensis*). Hololectinas são proteínas formadas exclusivamente de domínios de ligação a carboidratos, que contêm dois ou mais destes domínios idênticos ou muito semelhantes. Este grupo compreende as lectinas que possuem múltiplos sítios de ligação, com capacidade de aglutinar células ou precipitar glicoconjugados. A maioria das lectinas de plantas pertence ao grupo das hololectinas. Quimerolectinas compreendem as proteínas que possuem um domínio de ligação a carboidrato e um domínio não relacionado que atua de forma independente. Como exemplos de

quimerolectinas temos as proteínas que inativam ribossomos tipo 2. As superlectinas são proteínas com dois sítios de ligação a carboidratos, estruturalmente diferentes, reconhecendo carboidratos distintos (Peumans et al., 2001).

As lectinas de sementes podem diferir estruturalmente. Por exemplo, a lectina de *Vatairea macrocarpa* é uma mistura de moléculas constituídas por uma única ou duas cadeias polipeptídicas, que mantêm 55% de sua atividade após aquecimento a 100°C durante 5 min (Cavada et al., 1998). Similarmente, a lectina isolada de sementes de *Sphenostyles stenocarpa* (Machuka et al., 1999) também apresenta uma estrutura oligomérica, um tetrâmero de massa molecular 122.000 Da, porém sua atividade foi totalmente abolida após tratamento térmico (80°C). Em folhas de *Bauhinia monandra* foi detectada quantidade em miligramas de uma lectina galactose-específica, purificada por cromatografia de afinidade, que apresentou atividade anti-inseticida (Coelho e Silva, 2000, Macedo et al., 2007).

Duas lectinas de folhas de amoreira (*Morus alba*) MLL 1 e MLL 2 apresentam alta especificidade de ligação ao ácido siálico; inibição do crescimento de uma bactéria fitopatogênica chamada *Pseudomonas syringae pv mori* foi observada com MLL 1. O ácido siálico encontrado freqüentemente em carboidratos de glicoconjugados tem um papel importante em muitos mecanismos de reconhecimento biológico. Lectinas com especificidade para diferentes formas de ácido siálico têm sido usadas como ferramenta diagnóstica na identificação de bactérias patogênicas e tumores malignos (Ratanapo et al., 1998; 2001). Algumas lectinas incluindo aquelas de *Helix pomatia*, *Agaricus bisporus* e lectina de *Arisaema helleborifolium*, conhecida como AHL, estão sendo investigadas para seu possível uso em terapia contra o câncer (Kaur et al., 2006).

Em protozoários observou-se que uma lectina de látex de *Synadenium carinatum* (ScLL) mostrou efeito protetor em camundongos BALC/c infectados com *Leishmania amazonensis* (Afonso-Cardoso et al ., 2007).

A ligação de lectinas a oligossacarídeos na membrana celular é uma importante etapa na morte celular mediada pela lectina (Coelho et al., 2007; Macedo et al., 2007). Células que perderam esses carboidratos tornaram-se resistentes aos efeitos citotóxicos dessas proteínas (Gastman et al., 2004). Em *Trypanosoma cruzi*, as lectinas também foram utilizadas para avaliar mudanças na composição e distribuição de açúcares na superfície celular durante o

processo de transformação de epimastigotas a tripomastigotas metacíclicos, que é a forma infectante em humanos (Bourguignon et al., 1998).

Purificação e caracterização de lectinas

As lectinas têm sido purificadas principalmente a partir de sementes de leguminosas maduras, representando até 10% do conteúdo de proteína total (Konozy et al., 2003). Além disso, também podem ser obtidas de diferentes tecidos vegetais tais como raízes (Wu et al., 2000), cascas de árvores (Sá et al., 2009), folhas (Konozy et al., 2002), flores (Ito, 1986), frutos (Cheung et al., 2009), bulbos (Mo et al., 1994) e rizomas (Ng et al., 2001).

A purificação é baseada em características como tamanho molecular, solubilidade, carga e afinidade específica de ligação a carboidratos (Correia e Coelho, 1995). As técnicas utilizadas para eliminar moléculas que não sejam de interesse (contaminantes) são diversas.

As condições de extração envolvem vários parâmetros como, a seleção da solução extratora, temperatura e tempo. A maioria das lectinas são solúveis em água e em solução salina (Oshikawa et al., 2000; Moure et al., 2001). A preparação obtida, dita extrato bruto, é então avaliada quanto à concentração protéica e utilizada como material inicial para o isolamento da proteína.

A partir do extrato bruto, as proteínas podem ser fracionadas por métodos tais como a precipitação seletiva de proteínas com sais (Paiva e Coelho, 1992) ou elevadas temperaturas (Bezerra et al., 2001). O sulfato de amônio é o sal mais comumente utilizado (Coelho e Silva, 2000) devido à sua elevada solubilidade.

O fracionamento salino é um processo que se baseia no princípio de que a solubilidade da maioria das proteínas é diminuída em altas concentrações de sais. Esse efeito é chamado *salting-out* e o sulfato de amônio é muito utilizado para este fim. Em geral as lectinas podem ser parcialmente purificadas por este processo, uma vez que o sal retira a camada de solvatação existente ao redor das proteínas fazendo com que as mesmas precipitem. A precipitação com sulfato de amônio pode estabilizar a atividade hemaglutinante da proteína, mesmo após longos períodos de armazenamento (Kennedy et al., 1995; Coelho e Silva, 2000).

A técnica de diálise é utilizada para separar as lectinas, de moléculas pequenas, através da utilização de uma membrana (celulose) semipermeável (Kabir et al., 1998). As moléculas

com dimensões maiores são retidas dentro do saco de diálise e as menores e os íons atravessam os poros da membrana e permanecem na solução.

Vários métodos cromatográficos são realizados para purificar lectinas. As técnicas cromatográficas utilizadas incluem cromatografia de filtração em gel (Rego et al., 2002), de troca iônica (Ng e Yu, 2001) e cromatografia de afinidade (Coelho e Silva, 2000). Contudo, devido à propriedade de ligação a carboidrato, cromatografia de afinidade em colunas contendo suportes polissacarídeos (Cavada et al., 1998; Machuka et al; 1999; Coelho e Silva, 2000) ou glicoproteínas (Nomura et al., 1998; Kawagishi et al., 2001) tem sido a técnica mais comumente utilizada.

Na cromatografia de filtração em gel ou exclusão molecular as moléculas são separadas através do tamanho. A cromatografia de troca iônica separa as proteínas em função de sua carga; as proteínas com carga negativa (aniônicas) ligam-se em coluna de DEAE-Celulose, contendo cargas positivas; as proteínas com cargas positivas (catiônicas) podem ser separadas em colunas de CM-Cellulose, de carga negativa. Outro método eficiente é a cromatografia de afinidade, técnica que se baseia na ligação da lectina a grupamentos químicos específicos existentes no suporte insolúvel, como é o exemplo da ligação de lectinas que reconhecem glicose à Sephadex, matriz formada por dextrana, biopolímero produzido pela ação bacteriana sobre a sacarose, um dissacarídeo, formado por unidades de glicose (Brazil e Entlicher, 1999). A proteína desejada é obtida com alto grau de pureza, alterando-se as condições de pH (Datta et al., 2001), força iônica (Chung et al., 2001) ou pela eluição com solução contendo um competidor (Lima et al., 1997).

Na caracterização estrutural de lectinas utilizam-se métodos eletroforéticos baseados no princípio que uma molécula com carga elétrica líquida mover-se-á em um campo elétrico. A velocidade de migração de uma proteína depende da intensidade do campo, da carga líquida da proteína e do coeficiente de atrito. As separações eletroforéticas são quase sempre feitas em gel, onde os de poliacrilamida são os escolhidos por serem quimicamente inertes e porque o tamanho dos seus poros pode ser controlado (Stryer, 2004). A inclusão do detergente sulfato sódico de dodecila (SDS) no sistema possibilita a desnaturação da molécula protéica e, como conseqüência, a definição da massa molecular de subunidades (Coelho e Silva, 2000). Outra caracterização que pode ser feita é a definição da seqüência aminoacídica ou estrutura primária

da lectina e a subseqüente determinação da homologia com outras proteínas através de espectrometria de massa (Rego et al., 2002).

Isolectinas e Isoformas

Sharon e Lis (1990) definiram isolectinas como um grupo de proteínas intimamente relacionadas, resultantes da expressão de diferentes genes. A denominação pode ser dada em relação a diferentes atividades biológicas, como a atividade hemaglutinante e mitogênica (Aragon et al., 1993). Também pode estar relacionada ao padrão de migração em gel de poliacrilamida em condições não desnaturantes (Wongkham et al., 1995); quanto à diferente especificidade para carboidratos, pequenas alterações na estrutura da molécula protéica podem levar a modificações na orientação do açúcar ligado a ela alterando, portanto, a especificidade da lectina (Guzmán-Partida et al., 2004), diferença de carga (Kawagishi et al., 1997) ou quando são constatadas modificações pós-tradução (Mandal et al., 1994). Três isolectinas da aglutinina de germe de trigo (WGA-1, WGA-2 e WGA-3) interagiram em diferentes graus com células leucêmicas e manifestaram citoaglutinação e atividade citotóxica diferentes (Ohba et al., 2003).

O termo isoforma é utilizado para designar múltiplas formas de lectinas presentes na mesma espécie ou variedade de origem genética não definida (Paiva e Coelho, 1992). Algumas espécies de plantas contêm duas ou mais proteínas com atividade hemaglutinante, por exemplo, *Vicia villosa* e *Sambucus nigra* (Kaku et al., 1990). Várias técnicas podem ser utilizadas para a separação de isoformas como, focalização isoelétrica, cromatofocalização, ou cromatografia de interação hidrofóbica são mais comumente utilizadas para suas separações. Contudo, a elucidação das diferenças estruturais das isoformas por métodos de química de proteínas pode ser trabalhosa. Um método baseado em partículas não porosas e monolítico poliestireno-divinilbenzeno (PS-DVB) de fase estacionária e espectrometria de massa foi utilizado para separar isolectinas de três espécies de plantas, *Lens culinaris*, *Triticum vulgaris* e C*anavalia ensiformis* (Hochleitner et al., 2003).

Lectinas e mitocôndria

O efeito citotóxico de muitas lectinas resulta em processos de morte celular, por apoptose, necrose e/ou autofagia, que podem ou não ter participação da mitocôndria. Gastman et al. (2004) demostraram que a lectina de gérmen de trigo, WGA, promove apoptose em células Jurkat através de uma via mitocondrial com ativação de caspase-9. Outra lectina de planta, conhecida como VCA (*Viscum album* L. *coloratum* aglutinina) induziu apoptose por ativação de caspases-3 em células de leucemia mielocítica humana (HL-60) (Lyu et al., 2001). Além disso, uma outra lectina de *Viscum album*, a ML-1, ativa caspase-8 independentemente de receptor de morte e promove apoptose por liberação de citocromo c (Bantel et al., 1999).

O uso de Concanavalina A (ConA) como potencial agente anti-hepatoma tem sido intensamente estudado. Após a ligação de ConA a domínios de manose presentes em glicoconjugados de membrana celular, ocorre a internalização da lectina por endocitose mediada por clatrina. A lectina acumula-se preferencialmente na mitocôndria e subseqüentemente altera a permeabilidade de membrana mitocondrial (Lei e Chang, 2007). Já em melanoma (células A375) foi observado que a ConA exerce atividade anti-proliferativa e induz morte celular de uma maneira dependente de caspases com participação da via apoptótica mitocondrial (Liu et al., 2009).

Cratylia mollis

Cratylia mollis Mart. é o nome dado a uma planta nativa, perene da Região Semi-Árida do sertão do Estado de Pernambuco pertencente à família das *Fabaceae*, popularmente conhecida como feijão camaratuba ou camaratú (Figura 1). É utilizada como forrageira na alimentação de caprinos e bovinos, principalmente nos períodos de estiagem prolongada, quando esta apresenta uma maior importância por permanecer verde. Esta planta é de porte arbustivo e produz grandes quantidades de sementes (Santos et al, 2004).

Figura 1: *Cratylia mollis* Mart

As sementes de *C. Mollis* foram avaliadas quanto à presença de lectinas (Cramoll) obtendo-se três isolectinas a partir de diferentes frações (F) de precipitados salinos (F0-40%, F40-60% e F60-80%). Cramoll 1, a isolectina mais abundante nas sementes desta planta, foi purificada através de F40-60%; desta fração obteve-se também por cromatografia de afinidade uma preparação purificada (Cramoll 1,4) (Figura 2), mistura de Cramoll 1 e sua isoforma, Cramoll 4, as quais podem ser separadas por cromatografia de troca iônica (Correia e Coelho, 1995). Cramoll 2 e Cramoll 3 foram isoladas por Paiva e Coelho (1992). A classificação das isolectinas foi feita de acordo com a migração eletroforética em gel para proteínas básicas nativas; Cramoll 1 apresenta a maior migração (proteína mais básica), seguida de Cramoll 2; Cramoll 3 é a menos básica das três. Cramoll 1,4, Cramoll 1 e Cramoll 2 pertencem à classe das lectinas que se ligam à glicose/manose, Cramoll 3 é galactose específica, além de ser uma glicoproteína.

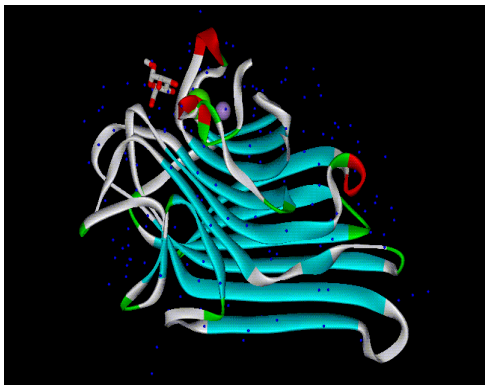

Figura 2: Estrutura terciária da lectina Cramoll 1,4 (De Souza et al., 2003).

As lectinas Cramoll 1,4 e Cramoll 1 vêm sendo estudadas quanto a suas aplicações em ensaios biológicos onde observou-se uma forte ligação destas lectinas a tecidos transformados, particularmente aqueles originados de tecidos mamários (Beltrão et al., 1998). Cramoll 1,4 imobilizada em Sepharose 4B foi capaz de isolar a enzima lecitina colesterol aciltransferase, como também glicoproteínas do plasma humano (Lima et al., 1997). Cramoll 1 já foi cristalizada por técnica convencional e através da sua cristalização no espaço, experiência idealizada pelo Prof. Dr. Glaucius Oliva, em colaboração com a Agência Espacial Norte Americana (NASA); a seqüência de aminoácidos e estrutura terciária dessa lectina foi definida (De Souza et al., 2003). Os estudos das estruturas tridimensionais das diferentes formas moleculares de *C. mollis* permitirão uma caracterização mais fina da relação estrutura-função destas moléculas, especialmente no que diz respeito às diferentes isoformas, ampliando tanto o conhecimento na área básica como direcionando a utilização biotecnológica de cada família de proteínas. Com esses resultados, pretende-se, em uma fase mais avançada, clonar e expressar as lectinas que mostrem uma atividade biológica mais relevante, através do uso de biologia molecular, além da utilização de ressonância magnética nuclear (RMN) para resolver a estrutura ou domínios das referidas proteínas.

MITOCÔNDRIAS

Breve Histórico

As mitocôndrias são organelas responsáveis pela conversão de energia de óxido-redução para a forma de energia química necessária para os eventos celulares. Além dessa função, nos últimos 40 anos, as mitocôndrias têm emergido como organela central em processos de sinalização, injúria e morte celular, após a descoberta de novas proteínas e moduladores metabólitos nessas organelas (Inada et al., 2008). As mitocôndrias variam de tamanho, formato, quantidade e localização, dependendo do tipo e função celular (Nelson e Cox, 2000).

Entre os primeiros pesquisadores que descobriram as mitocôndrias como organelas citoplasmáticas, merece destaque o cientista Köllinker, que descreveu a existência de grânulos organizados no sarcoplasma de músculo esquelético e os estudou por vários anos,

a partir de 1850. Esses grânulos, que por volta de 1890 foram chamados por Retzius de "sarcossomos", eram na verdade as mitocôndrias de tecido muscular (Lehninger, 1964).

A "nova era" das pesquisas com mitocôndrias iniciou-se com o trabalho de Bensley em 1930, que tentou isolar mitocôndrias de células de tecido hepático por centrifugação diferencial. Apesar de todo o esforço, Bensley não conseguiu isolar mitocôndrias intactas, porém o pioneirismo de seu trabalho foi destacado por reunir as pesquisas citológicas com as primeiras pesquisas bioquímicas de respiração mitocondrial. Em 1948, Hogeboom, Schneider e Palade alcançaram êxito em isolar mitocôndrias intactas de fígado de rato, por centrifugação diferencial (Lehninger, 1964). Em 1949, os bioquímicos norte-americanos Eugene Kennedy e Albert Lehninger isolaram mitocôndrias hepáticas e demonstraram que essa organela é o sítio celular responsável pela síntese de ATP, associada à oxidação de coenzimas (NADH + H^+ e $FADH_2$). Essa observação deu origem à fase moderna da investigação sobre os mecanismos de conversão de energia em sistemas que consomem oxigênio (Nelson e Cox, 2000). Durante cerca de 20 anos houve uma busca infrutífera por um suposto intermediário químico que seria responsável pelo acoplamento entre os processos de respiração e síntese de ATP. Em 1961, o bioquímico inglês Peter Mitchell, baseado na constatação de que a redução do oxigênio (O_2) a água (H_2O) pela cadeia respiratória gera um gradiente de prótons (H^+) entre o meio interno (matriz) da mitocôndria e o espaço entre suas membranas interna e externa, propôs a teoria quimiosmótica da fosforilação oxidativa (Mitchell, 1961).

Cadeia transportadora de elétrons e Fosforilação oxidativa

A energia necessária para o processo de fosforilação oxidativa provém do potencial eletroquímico de prótons gerado pela cadeia de transporte de elétrons que reduz o O_2 à H_2O. Esta energia é utilizada pela ATP sintetase para fosforilar o ADP à ATP. Assim, a cadeia respiratória converte a energia redox gerada pelo catabolismo em potencial de membrana mitocondrial, que é a força motriz para a fosforilação oxidativa (Mitchell, 1961).

Normalmente, os elétrons provenientes das coenzimas NADH + H^+ e $FADH_2$, reduzidas durante a oxidação de carboidratos, aminoácidos e ácidos graxos, são transferidos ao átomo de ferro da NADH desidrogenase (complexo I, Figura 3). O complexo I transfere

seus elétrons à forma oxidada da coenzima Q (UQ), gerando a forma reduzida desta coenzima (UQH_2). Elétrons originados a partir do succinato passam para a UQ através do complexo II, resultando também na redução da coenzima Q. Em alguns tecidos a coenzima Q pode também ser reduzida pela glicerol-3-fosfato desidrogenase (na presença de glicerol-3-fosfato citosólico) ou pela ubiquinona oxirredutase (como resultado da β-oxidação de ácidos graxos). A UQH_2 é então desprotonada, resultando na formação da espécie aniônica semiquinona ($UQH^{\bullet}$), a forma que doa elétrons ao citocromo c. Existem dois conjuntos separados de $UQH^{\bullet}$, um na face citoplasmática e outro na face matricial da membrana mitocondrial interna, e as duas formas de $UQH^{\bullet}$ são oxidadas juntas, regenerando UQ e doando elétrons para o citocromo c. O citocromo c transfere elétrons para a citocromo oxidase (complexo IV, Figura 3). Este complexo é responsável pela transferência de elétrons para o oxigênio, resultando na geração de água, em um processo envolvendo quatro passos consecutivos de transferência de um elétron (Nicholls e Ferguson, 2002).

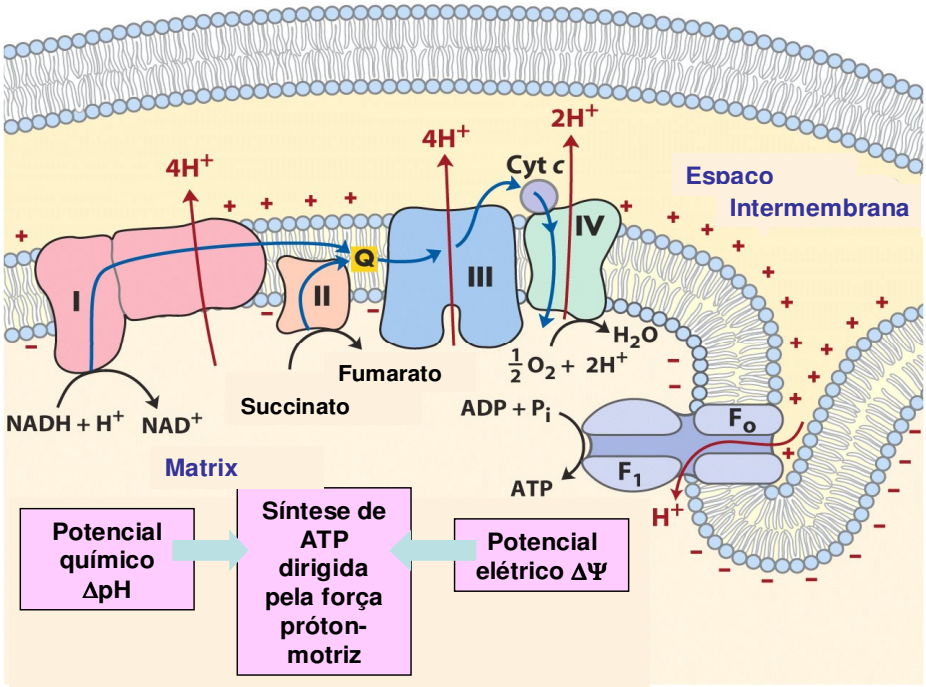

Figura 3: Cadeia respiratória mitocondrial e teoria quimiosmótica (adaptado de Nelson e Cox, 2000). Os números romanos indicam os quatro complexos respiratórios. Os elétrons do NADH + H^+ e de outros substratos oxidáveis passam através de uma cadeia de transportadores arranjados assimetricamente na membrana. O fluxo de elétrons é acompanhado pela transferência de prótons através da membrana mitocondrial, produzindo tanto um gradiente químico (ΔpH) quanto elétrico (ΔΨ). A membrana mitocondrial interna é impermeável aos prótons, os quais podem reentrar na matriz através de canais específicos

de prótons (F_o). A força próton-motora que impulsiona esses prótons de volta para a matriz fornece a energia para a síntese do ATP, catalisada pelo complexo F_1 associado com F_o.

Segundo Mitchell (1961), a passagem de elétrons através da seqüência de intermediários redox da cadeia respiratória permite um fluxo de H^+ da matriz mitocondrial ao espaço intermembrana, contra um gradiente de concentração. A formação deste potencial eletroquímico transmembrânico seria o elemento inicial do acoplamento entre a oxidação de substratos e a utilização desta energia. O componente elétrico ($\Delta\Psi$) deste potencial atinge valores de aproximadamente 180 mV no estado de repouso, enquanto o componente químico (ΔpH) oscila na faixa de 0 a 1 unidade de pH. O fluxo de H^+ através da F_oF_1-ATP sintase, de volta ao interior da mitocôndria, desta vez a favor do gradiente, estaria diretamente acoplado à fosforilação do ADP. A ATP sintase, responsável por esta reação, é constituída de duas subunidades distintas denominadas F_1, solúvel e localizada na matriz mitocondrial, e Fo, hidrofóbica e mergulhada na membrana mitocondrial interna, onde estão também localizados os complexos da cadeia respiratória (Mitchell, 1961).

A geração de um gradiente eletroquímico transmembrânico de prótons ($\Delta\mu H^+$) é um elemento central no aproveitamento de energia em sistemas biológicos. Evolutivamente este mecanismo é fundamental, já que é aproveitado tanto na fosforilação oxidativa em mitocôndrias quanto na fotossíntese, em cloroplastos. Além disso, este gradiente pode ser usado diretamente para processos endergônicos sem a participação de ATP. São exemplos deste mecanismo de acoplamento direto as trocas eletroforéticas de ATP^{4-} por ADP^{3-}, a redução de $NAD(P)^+$ pela transidrogenase específica e a captação eletroforética de Ca^{2+} que transporta duas cargas positivas para o interior da mitocôndria (Nicholls e Ferguson, 2002).

Alguns mecanismos, denominados mecanismos de desacoplamento, são capazes de desviar o gradiente de H^+ da síntese de ATP. Ânions de ácidos graxos (AG) possuem essa habilidade quando protonados, pois atravessam facilmente as membranas mitocondriais, carregando um próton para a matriz por mecanismo de "flip-flop" (Walter e Gutknecht, 1984; Andreyev et al., 1989). Devido à alcalinidade da matriz em relação ao espaço intermembranas, o ácido graxo livre (AGL) é desprotonado no interior da mitocôndria e, em sua forma aniônica, pode ser transportado de volta ao espaço intermembranas por dois processos eletroforéticos: 1) pelo translocador de nucleotídeos de adenina (ANT), na

ausência de seus substratos específicos – ADP e ATP (Skulachev, 1991) e 2) por proteínas desacopladoras (UCPs) (Garlid et al., 1996). Esse transporte de ânions de AGLs para o espaço intermembranas é seguido pelo seu rápido retorno na forma protonada, constituindo um ciclo fútil, que resulta na transferência de um H^+ para a matriz mitocondrial.

A proteína desacopladora (UCP) foi descoberta em estudos com mitocôndrias de tecido adiposo marrom, sendo a responsável pelo desacoplamento da fosforilação oxidativa para a geração de calor (Nicholls, 1976). Posteriormente, essas proteínas foram também identificadas em plantas (PUMP) (Vercesi et al., 1995). Em mamíferos, foram identificadas outras isoformas de UCP em outros tecidos, designadas de UCP2 a UCP4. Sugere-se que essas proteínas podem atuar no controle de peso e na redução da geração de espécies reativas de oxigênio (EROs). No entanto, a função dessas novas isoformas ainda é incerta (para revisão Krauss et al., 2005).

Homeostase de cálcio, EROs e Sistemas antioxidantes

O cálcio (Ca^{2+}) desempenha um importante papel como segundo mensageiro no controle de muitos processos biológicos, assim como, crescimento e diferenciação, motilidade e contração, endocitose, exocitose e secreção, e regulação do metabolismo intermediário (Campbell et al., 1983; Putney e Bird, 1993; Moreno et al., 1994).

A captação e liberação do Ca^{2+} através da membrana plasmática e organelas intracelulares ocorre pela ação conjunta de distintos sistemas de transporte responsáveis pelo controle da concentração de Ca^{2+} intracelular (Moreno et al., 2003). Para funcionar apropriadamente, a célula deve manter essa concentração a níveis baixos. Em células de mamíferos, a concentração de Ca^{2+} livre no citosol, em condições de repouso, é mantida na ordem de 0,1 μM, muito abaixo da concentração do Ca^{2+} extracelular, de 1 mM (Carafoli, 1987; Reed, 1990; Nicotera et al., 1992). A estrutura de ácidos nucléicos e algumas proteínas podem ser danificadas por altas concentrações de Ca^{2+}, entretanto níveis intermediários podem interferir no controle de quinases específicas e ativar proteases sensíveis a Ca^{2+} ou fosfolipases levando à morte celular. Falhas nos sistemas envolvidos na "proteção" citosólica contra altos níveis de Ca^{2+} é freqüentemente associada a danos irreversíveis (Gunter e Pfeiffer, 1990). O aumento de Ca^{2+} intramitocondrial pode levar à inibição da fosforilação oxidativa, uma vez que o complexo Ca-ADP formado compete

com Mg-ADP na ligação no sítio ativo da F_oF_1-ATP sintase (Vercesi et al., 1990). Assim, o aumento da concentração de Ca^{2+} intramitocondrial com a redução do nível de ATP pode conduzir à morte celular.

Alterações na permeabilidade da membrana mitocondrial interna induzidas por Ca^{2+} podem ocorrer em conseqüência da ação de EROs geradas na mitocôndria (Vercesi et al., 1993; Vercesi e Hoffmann, 1993). Essas organelas são particularmente propensas à lesão oxidativa por EROs geradas continuamente pela cadeia respiratória mitocondrial (Boveris e Chance, 1973; Turrens, 1997; Kowaltowski et al., 1999) ou produzidas através do metabolismo de compostos endógenos, como o ácido 5-aminolevulínico, um precursor do heme, ou xenobióticos (Hermes-Lima, 1995). Muitos estudos associam a disfunção mitocondrial causada por EROs à morte celular tanto por necrose quanto por apoptose (Zamzami et al., 1997; Zhang et al., 1997; Zecchin et al., 2007).

Normalmente, o oxigênio é reduzido à água pela citocromo c oxidase, em quatro passos consecutivos de um elétron, pois o oxigênio molecular apresenta uma configuração triplete (Depierre e Ernster, 1977). Esta enzima é altamente especializada neste processo, sendo capaz de se ligar fortemente ao oxigênio parcialmente reduzido, impedindo sua liberação antes da obtenção de sua redução total (para revisão, veja Turrens, 1997). Deste modo, a produção de ânions superóxido ($O_2^{\bullet-}$) através da redução monoeletrônica do O_2 pela citocromo c oxidase é praticamente inexistente. No entanto, até 2% do oxigênio consumido pela mitocôndria é convertido a $O_2^{\bullet-}$ em passos intermediários da cadeia respiratória mitocondrial (Boveris e Chance, 1973; Turrens, 1997), principalmente nos complexos I (Turrens e Boveris, 1980) e III (Cadenas et al., 1977). A produção de $O_2^{\bullet-}$ no complexo I é promovida pelos substratos dependentes de NAD tais como malato, glutamato, e piruvato e estimulada por rotenona, um inibidor da transferência de elétrons do complexo I à coenzima Q (Turrens e Boveris, 1980; Turrens, 1997; Kowaltowski et al., 2009).

O vazamento de elétrons da cadeia respiratória na coenzima Q ocorre provavelmente durante a doação de elétrons do ânion semiquinona, que é um radical livre, para o oxigênio. O vazamento de elétrons neste ponto é estimulado por succinato, cianeto e antimicina A (Boveris et al., 1976; Cadenas et al., 1977; Kowaltowski et al., 1998; Turrens, 1997; Turrens et al., 1985). A antimicina A tem notadamente um grande papel

estimulatório, por bloquear a formação de $UQH^{\bullet}$ na face matricial da membrana mitocondrial interna, promovendo um acúmulo de ânions semiquinona formados anteriormente na face citosólica da membrana mitocondrial interna. Mixotiazol, um inibidor da formação da $UQH^{\bullet}$ na face citosólica da membrana interna mitocondrial, previne a geração de $O_2^{\bullet-}$ neste ponto (Cadenas e Boveris, 1980; Kowaltowski et al., 1998; Turrens, 1997; Turrens et al., 1985).

Como a geração mitocondrial de $O_2^{\bullet-}$ é um processo contínuo e fisiológico, a mitocôndria possui eficientes sistemas antioxidantes, como enzimas tiólicas, superóxido dismutase dependente de manganês (MnSOD), glutationa, NADPH, vitaminas E e C (Sutton e Winterbourn, 1989; Watabe et al., 1997; Netto et al., 2002).

Além dos sistemas antioxidantes, a mitocôndria possui mecanismos que promovem um leve desacoplamento da fosforilação oxidativa e podem diminuir a geração de EROs (Skulachev, 1991). Entre eles estão as UCPs (Klingenberg et al., 2001), o translocador de nucleotídeos de adenina (ANT) (Samartsev et al., 1997) e os canais de K^+ sensíveis a ATP (mitoK_{ATP}) (Ferranti et al., 2003). Eles promovem uma pequena diminuição do potencial eletroquímico de H^+ suficiente para aumentar o consumo de O_2 e mudar o estado redox dos transportadores de elétrons da cadeia respiratória. Essa alteração é suficiente para diminuir a redução monoeletrônica de oxigênio em estágios intermediários da cadeia de transporte de elétrons, principalmente nos complexos I e III (Skulachev, 1991).

Quando ocorre um desequilíbrio com predominância de EROs em relação aos sistemas antioxidantes gera-se um estado de estresse oxidativo, que pode causar danos mitocondriais. Tanto os lipídeos, como as proteínas de membrana e o DNA mitocondrial são alvos de ação de EROs (Mehrotra et al., 1991; Vercesi 1993a; Vercesi e Hoffmann, 1993; Castilho et al., 1994; Mertens et al., 1995; Kowaltowski et al., 2009).

Transição de Permeabilidade Mitocondrial (TPM)

A transição de permeabilidade mitocondrial (TPM) é caracterizada por uma permeabilização progressiva da membrana mitocondrial interna, que gradativamente se torna permeável a prótons, íons, suporte osmótico e até mesmo pequenas proteínas. O Ca^{2+}

parece ser o principal agente estimulador da geração mitocondrial de EROs (Kowaltowski et al., 2001). Este fenômeno foi primeiramente caracterizado por Hunter e Haworth, no final dos anos 70, e foi sugerido ser o resultado da abertura de um poro de tamanho discreto, que permite a passagem de moléculas com aproximadamente 1,5 kDa, na membrana mitocondrial interna (Haworth e Hunter, 1979). A estrutura básica do poro de transição de permeabilidade mitocondrial (PTPM) é sugerida contendo o canal ânion voltagem dependente (VDAC), o translocador de nucleotídeos de adenina (ANT) e a ciclofilina-D (CyD), um membro de uma família de isomerases de alta homologia *cis-trans* peptil-prolil (Haworth e Hunter, 1979; Zoratti e Szabò, 1995; Brustovetsky e Klingenberg, 1996; Green e Reed, 1998; Woodfield et al., 1998; Crompton, 1999; Scheffler, 2001). Acredita-se que essas proteínas interagem com sítios específicos entre as membranas mitocondriais externa e interna e formam a estrutura básica do PTPM, interagindo possivelmente com outros constituintes, incluindo o receptor benzodiazepínico, bem como com a creatina e adenilato quinases (Fagian et al., 1990; Zoratti e Szabò, 1995; Crompton et al., 1998; Green e Reed, 1998; Crompton, 2000; Breckenridge e Xue, 2004). Estudos recentes com nocautes gênicos contestaram a validade desse modelo mostrando que em mitocôndrias deficientes em ANT, VDAC e mesmo CyD ocorre transição de permeabilidade mitocondrial, tendo no entanto algumas propriedades alteradas (Kokoszka et al., 2004; Krauskopf et al., 2006; Juhaszova et al., 2008). Por exemplo, em mitocôndrias deficientes de ANT, o ligante do ANT, atractilosídeo, não promove a abertura do PTPM (Lemasters et al., 2009). Estudos recentes do nosso grupo demonstraram a abertura do PTPM em mitoplastos, que são mitocôndrias sem a membrana externa, mostrando que mesmo na ausência de VDAC (que localiza-se na membrana mitocondrial externa) ocorre a abertura do PTPM na presença de Ca^{2+} e de outros indutores (Ronchi et al – dados não publicados).

A CyD contribui para a abertura do PTPM provavelmente devido uma mudança conformacional das proteínas da membrana interna. Recentes estudos com animais deficientes de CyD mostraram que essa estrutura é importante para a TPM e que esses camundongos são resistentes à morte celular causada por injúria isquêmica e a indução de TPM nesses animais requer elevadas concentrações de Ca^{2+} (Nakagawa et al., 2005; Baines et al., 2005; Lemasters et al., 2009). A ciclosporina A (CsA) é um dos mais efetivos

membros da família dos endecapeptídeos cíclicos, que atuam como imunossupressores e foi descoberta como um potente inibidor do PTPM (Fournier et al., 1987; Crompton et al., 1988; Broekemeier et al., 1989). Estudos têm demonstrado que o efeito inibitório da CsA na abertura do PTPM é mediado pela CyD (Halestrap et al., 1998).

A TPM induzida por Ca^{2+} pode ser estimulada por um grande número de compostos conhecidos como indutores (Zoratti e Szabò, 1995), que incluem o fosfato inorgânico (P_i) (Rossi e Lehningher, 1964), oxidantes de nucleotídeos de piridina (Lehninger et al., 1978; Castilho et al., 1995; Kowaltowski et al., 1996a, 1996b; Vercesi et al., 1997), protonóforos (Bernardi, 1992) e reagentes ditiólicos (Lenartowicz et al., 1991; Bernardes et al., 1994). A maioria destes indutores são compostos capazes de aumentar o estresse oxidativo mitocondrial promovido pelo Ca^{2+} (Castilho et al., 1995; Kowaltowski et al., 1996a, 1996b; Vercesi et al., 1997).

A primeira evidência de que a TPM era causada por EROs geradas pela mitocôndria foi apresentada quando Lehninger e co-autores demonstraram que o estado oxidado de nucleotídeos de piridina estimulava o efluxo de Ca^{2+} mitocondrial (Lehninger et al., 1978), resultados estes confirmados por trabalhos posteriores (Vercesi 1984a, 1984b; Vercesi e Pereira-da-Silva, 1984). Este efluxo foi posteriormente atribuído a uma permeabilização mitocondrial não específica (Nicholls e Brand, 1980). Os oxidantes de nucleotídeos de piridina promovem o acúmulo de H_2O_2 em mitocôndrias porque o sistema glutationa peroxidase/glutationa redutase mitocondrial é reduzido por nucleotídeos de piridina (Meister e Anderson, 1983; Chance et al., 1979). Experimentos comprovando que a catalase, o quelante de Fe^{2+} o-fenantrolina e a anóxia inibem a TPM induzida por Ca^{2+} e próoxidantes (Valle et al., 1993; Castilho et al., 1995) confirmaram que a TPM é dependente de EROs geradas pela mitocôndria.

A Figura 4 representa o modelo proposto para explicar a formação do poro induzido pelo Ca^{2+} e EROs. O Ca^{2+} intramitocondrial liga-se a cardiolipina na face interna da membrana mitocondrial interna causando alteração ultraestrutural da cadeia respiratória que facilita a produção de $O_2^{\bullet-}$ e conseqüentemente de H_2O_2 (Grijalba et al., 1999). Este lipídeo possui cabeça polar eletronegativa e está presente em altas concentrações (14-23%) na membrana mitocondrial interna, em uma grande variedade de tecidos. Simultaneamente, o Ca^{2+} mobiliza Fe^{2+} na matriz mitocondrial que estimula a reação de Fenton e a produção de

radical hidroxil que ataca tióis de proteínas, lipídeos e DNA mitocondrial (Merryfield e Lardy, 1982; Castilho et al., 1995; Vercesi et al., 1997). A diminuição de NAD(P)H e GSH causada por pró-oxidantes prejudica a eliminação de H_2O_2 pelas enzimas glutationa peroxidase (GP) e glutationa redutase (GR). Na presença de altas concentrações de fosfato inorgânico (P_i), a enolização de aldeídos (Indig et al., 1988) formados por lipoperoxidação de ácidos graxos poliinsaturados (PUFA) leva a produção final de espécies tripletes que estimulam o processo de lipoperoxidação dos PUFA da membrana (Kowaltowski et al., 1996a, 1996b).

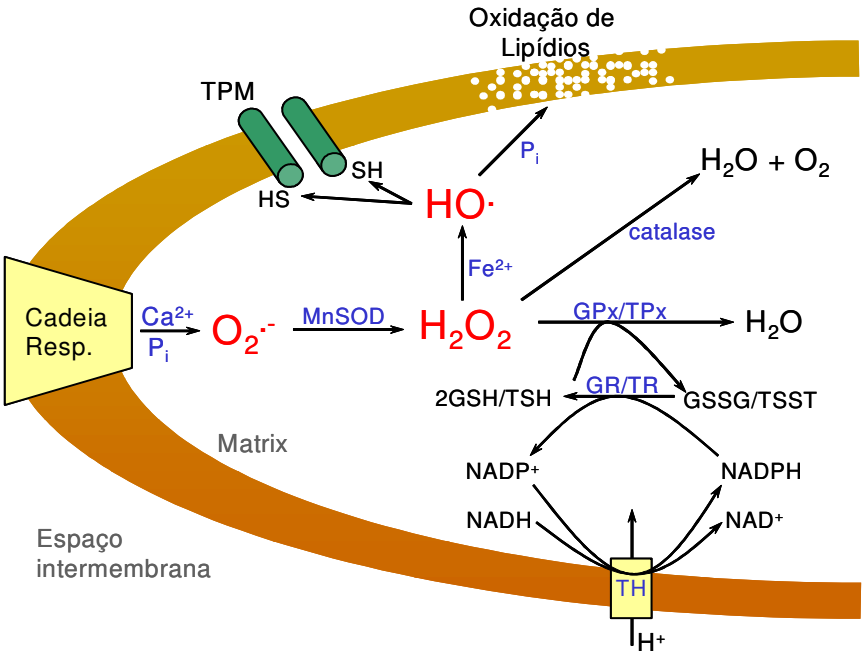

Figura 4: Modelo proposto para explicar a formação do poro de transição de permeabilidade induzido por Ca^{2+} e EROs na membrana mitocondrial interna (Kowaltowski et al., 2001)**.** A cadeia respiratória, inserida na membrana mitocondrial interna, constantemente gera pequenas quantidades de radicais $O_2^{\bullet-}$. Estes radicais são normalmente removidos pela Mn-superóxido dismutase (MnSOD), que promove a geração de H_2O_2. O H_2O_2 é então reduzido à H_2O pela glutationa peroxidase (GP), tioredoxina peroxidase (TP) ou catalase (em mitocôndria de coração). GSH, oxidado pela GP, e TSH, oxidado pela TP, são recuperados pelo sistema enzimático glutationa e tioredoxina redutases (GR e TR), que usam NADPH como doador de elétrons. NADH, que está presente em quantidades reguladas pela respiração, reduz então $NADP^+$ usando a NAD(P) transidrogenase (TH). Quando a geração de $O_2^{\bullet-}$ aumenta na presença de Ca^{2+} e P_i, e/ou os mecanismos de remoção de H_2O_2 estão inativados, H_2O_2 acumula-se e na presença de Fe^{2+}, gera o radical $OH^{\bullet}$ altamente reativo. $OH^{\bullet}$ oxida grupos tiólicos (-SH) do complexo do poro de TPM, levando à formação e abertura do poro. Alternativamente, $OH^{\bullet}$ pode promover permeabilização da membrana através da peroxidação lipídica, um processo fortemente estimulado por P_i.

O conteúdo protéico das membranas mitocondriais pode chegar a 75% na membrana mitocondrial interna (Lehninger, 1964; Nicholls e Ferguson, 2002). Devido ao alto conteúdo protéico da membrana mitocondrial interna, é esperado que estas proteínas sejam um dos principais alvos das EROs geradas pela mitocôndria e induzidos por Ca^{2+} (Fagian et al., 1990; Valle et al., 1993; Castilho et al., 1995; Kowaltowski et al., 1996a, 1996b). As EROs, principalmente o radical hidroxil, são capazes de oxidar resíduos de cisteína e metionina protéicos, levando à formação de ligações cruzadas S-S e sulfóxido de metionina, respectivamente. A disfunção mitocondrial devido à oxidação de proteínas da membrana mitocondrial parece estar associada principalmente, à oxidação de resíduos de cisteína (Fagian et al., 1990; Castilho et al., 1996).

Mitocôndrias e o Processo de Morte Celular

A morte celular, segundo Kroemer et al. (2009), pode ser classificada de acordo com vários aspectos: aparência morfológica (que pode ser apoptótica, necrótica, autofágica ou associada com mitose), critérios enzimáticos (com e/ou sem envolvimento de nucleases ou de distintas classes de proteases, como caspases, calpainas, catepsinas e transglutaminases), aspectos funcionais (programada ou acidental, fisiológica ou patológica) ou características imunológicas (imunogênica ou não imunogênica).

Para que uma célula seja considerada morta um dos seguintes critérios morfológicos ou moleculares devem ser encontrados: perda da integridade de membrana plasmática, pela incorporação de corantes vitais *in vitro* (como o iodeto de propídeo); ou quando a célula, incluindo seu núcleo, sofre completa fragmentação em corpos discretos (conhecidos como "corpos apoptóticos"); e/ou quando verifica-se *in vivo* o englobamento da célula morta (ou fragmentos celulares) por uma célula adjacente (Kroemer et al., 2009). Esses eventos de morte celular podem ou não ter participação da mitocôndria.

A TPM é um mecanismo comum de disfunção da mitocôndria que ocorre na morte celular, e está relacionado à liberação de fatores pró-apoptóticos mitocondriais, devido ao inchamento da organela, com ruptura da membrana mitocondrial externa (Green e Reed, 1998; Green e Kroemer, 2005). A morte celular apoptótica ocorre de forma regulada e

apresenta várias características como arredondamento celular, retração de pseudópodes, redução de volume celular (piquinose), condensação de cromatina, fragmentação nuclear, discreta ou nenhuma modificação ultra-estrutural de organelas citoplasmáticas, protrusões de membrana plasmática, porém com manutenção de sua integridade até os estágios finais do processo e englobamento por fagócitos mononucleares (*in vivo*) (Kroemer et al., 2009).

Há vários mecanismos descritos pelos quais as proteínas mitocondriais regulatórias de apoptose podem ser liberadas para o citosol. Esses mecanismos são divididos em dois grupos: (i) aqueles que envolvem permeabilização da membrana interna com inchamento mitocondrial, perda do potencial de membrana e habilidade de sintetizar ATP, como ocorre após a TPM e (ii) aqueles que envolvem apenas a permeabilização da membrana externa e permitem a manutenção da função mitocondrial (Green e Reed, 1998; Crompton, 1999; Spierings *et al*., 2005). O primeiro mecanismo é típico de condições em que ocorre "apoptose acidental". O segundo mecanismo pode ser observado tanto na "apoptose acidental" quanto na morte celular programada (Crompton, 1999). Neste caso, ocorre uma permeabilização da membrana externa provocada por membros pró-apoptóticos da família Bcl-2 como Bax, Bak e Bok. Essas proteínas, habitualmente citosólicas, formam poros na membrana externa de modo estimulado por membros da família Bcl-2 que contém apenas o domínio BH3 (Bid e Bad) e inibido por Bcl-2, Bcl-xl e Bcl-w (Adams e Cory, 2001; Zimmermann et al. 2001; Green e Kroemer, 2005).

A apoptose é coordenada por um conjunto de proteases cisteína/aspartato-específicas conhecidas como caspases (Thornberry e Lazebnik, 1998, Zimmermann et al., 2001; Strasser et al., 2000; Green, 2000). Essas proteases são sintetizadas como precursores inativos e, mediante estímulos apoptóticos, sofrem ativação proteolítica. Várias proteínas podem regular a ativação de caspases, um número grande dessas proteínas tem localização ou interação mitocondrial (Ravagnan et al., 2002). O citocromo *c*, normalmente localizado no espaço intermembranas mitocondrial, pode ser liberado para o citosol, onde se liga a Apaf-1 ("apoptosis activating factor 1") e caspase 9, formando o apoptosomo, complexo de alto peso molecular responsável pela clivagem de várias pró-caspases (Zimmermann et al., 2001, Ravagnan et al., 2002). As mitocôndrias também contém a proteína Smac/DIABLO, que inativa proteínas citosólicas responsáveis pela inibição de caspases (Du et al., 2000,

Verhagen et al., 2000, Ravagnan et al., 2002). Também merece destaque, o AIF ("apoptosis inducing factor"), uma proteína capaz de induzir condensação da cromatina nuclear de modo independente da ativação de caspases, e a endonuclease G, capaz de promover diretamente a fragmentação de DNA nuclear, estão normalmente localizados no espaço intermembranas mitocondrial e migram para o citosol mediante estímulos pró-apoptóticos (Lorenzo et al., 1999, Van Loo et al., 2001, Ravagnan et al., 2002).

Uma outra forma de morte celular, a necrose, durante muito tempo foi avaliada como um processo de morte acidental e descontrolado, mas vários trabalhos têm mostrado evidências que a execução de morte celular necrótica pode ser finamente regulada por um conjunto de vias de transdução de sinais e mecanismos catabólicos. Por exemplo, domínios de receptores de morte (TNFR1, Fas/CD95 e TRAIL-R) e receptores "Toll-like" (TLR3 e TLR4) têm demonstrado que provocam necrose, particularmente na presença de inibidores de caspases (Festjens et al., 2006). Embora ainda não seja um consenso, alguns autores têm sugerido o termo "necroptose" para indicar uma necrose regulada, que depende principalmente da atividade serina/treonina quinase de RIP1, a fim de diferenciá-la de uma necrose acidental (Kroemer et al., 2009).

Diversos mediadores, organelas e processos celulares têm sido implicados na morte celular necrótica, mas ainda não é claro como esses eventos interagem uns com os outros (Kroemer et al., 2009). No entanto, é conhecido que esse fenômeno inclui alterações mitocondriais (desacoplamento, produção de espécies reativas de oxigênio, estresse nitroxidativo por óxido nítrico ou compostos similares e permeabilização de membrana mitocondrial, freqüentemente controlada pela ciclofilina D), alterações lisossomais (produção de espécies reativas de oxigênio por reação de Fenton e permeabilização de membrana lisossomal), mudanças nucleares (hiperativação de PARP-1 e concomitante hidrólise de NAD^+), degradação lipídica (ativação de fosfolipases, lipoxigenases e esfingomielinases), aumento na concentração de Ca^{2+} citosólico que resulta em sobrecarga mitocondrial e ativação de proteases não caspases (calpainas e catepsinas). Ainda hoje, apesar do conhecimento de todas essas alterações, a caracterização de uma morte celular por necrose é avaliada principalmente por permeabilização de membrana plasmática precoce e ausência de marcadores apoptóticos ou autofágicos (Kroemer et al., 2009).

ASPECTOS GERAIS DA TRIPANOSSOMÍASE AMERICANA

O parasita *Trypanosoma cruzi*

O *T. cruzi*, descoberto pelo cientista brasileiro Carlos Chagas em 1909 e causador da conhecida doença de Chagas ou tripanossomíase americana, é um protozoário flagelado pertencente ao gênero *Trypanosoma*; família *Trypanosomatidae*; ordem *Kinetoplastida*; superclasse *Mastigophora*; sub-filo *Sarcomastigophora* e filo *Protozoa*. Apresenta três formas evolutivas: tripomastigota, epimastigota e amastigota, morfologicamente distintas pela posição do cinetoplasto em relação ao núcleo e a inserção do flagelo. O cinetoplasto é uma estrutura bastante especializada onde se concentra todo DNA mitocondrial do parasita. As formas tripomastigotas têm seu cinetoplasto na parte posterior do parasita em relação ao flagelo; nas epimastigotas, o mesmo se encontra na região entre o núcleo e a base do flagelo e nas formas amastigotas, o cinetoplasto encontra-se próximo ao núcleo e na região do flagelo que é muito reduzido ou ausente nesta forma (Brener, 1992).

O *T. cruzi* é transmitido por mais de 130 espécies de insetos da ordem *Hemíptera*, família *Reduviidae*, subfamília *Triatominae* (Barret et al., 2003). Cinco espécies têm especial importância epidemiológica: *Triatoma infestans*, *T. brasiliensis*, *T. dimidiata*, *Rhodinius prolixus* e *Panstrongylus megistus*. Não apenas o hospedeiro humano, mas um grande espectro de mamíferos pode ser infectado e atuar como reservatório do parasita (WHO, 2002).

A organização mundial de saúde estima que 100 milhões de pessoas correm o risco de serem infectadas, principalmente pela picada de insetos triatomíneos (Branche et al., 2006). A infecção humana prevalece em 21 países da América Latina, desde o México até Argentina e Chile (WHO, 2002; OPS, 2006). A maior parte dos casos de infecção humana, ou de outros vertebrados, é causada pela via vetorial, importante via de disseminação do parasita, conseqüência do contato da pele ou mucosas com as fezes ou urina de insetos hematófagos contaminados pelo *T. cruzi* (Schumuñis, 2000). Com relação a esse tipo de transmissão, em 2006, o Brasil recebeu o certificado de eliminação da transmissão pelo *Triatoma infestans*, considerado o principal vetor.

A transmissão congênita e a transfusão sangüínea são causas preocupantes de infecção, sendo a congênita a mais importante, por conta dos efeitos colaterais causados

nas mães e bebês pelos medicamentos disponíveis (Gürtler et al., 2003). Existem outras formas de transmissão do *T. cruzi*, como a transmissão oral por ingestão de alimentos contaminados, transplantes de órgãos infectados e acidentes laboratoriais (WHO, 2002).

O ciclo de vida do *T. cruzi* alterna entre mamíferos e insetos vetores com diferentes formas evolutivas em cada hospedeiro. No intestino de insetos triatomíneos (região mediana) encontram-se as formas replicativas denominadas epimastigotas, que se diferenciam para formas não replicativas denominadas tripomastigotas metacíclicos que são encontrados na parte posterior do intestino do inseto e são eliminados através das fezes quando o inseto vetor pica o hospedeiro mamífero. Uma vez no hospedeiro vertebrado, os tripomastigotas metacíclicos invadem vários tipos de células e transformam-se em amastigotas, que se reproduzem por fissão binária. Os amastigotas se diferenciam em tripomastigotas e, após ruptura celular, vão para corrente sangüínea e invadem novas células. Quando os tripomastigotas sangüíneos são ingeridos por um inseto triatomíneo, transformam-se em epimastigotas fechando assim o ciclo biológico do parasita (Figura 5).

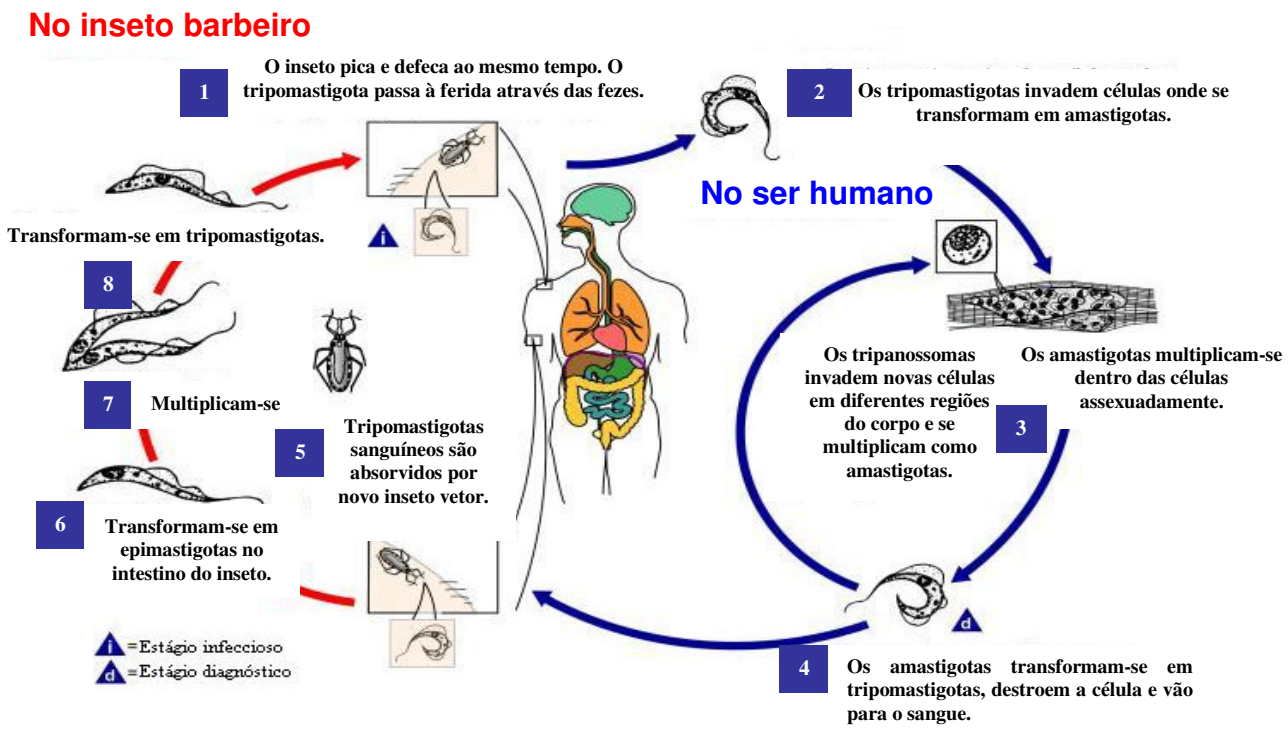

Figura 5: Ciclo Biológico do *Trypanosoma cruzi*. Fonte: Adaptado do Centro para Controle de Doenças e Prevenção(CDC): http://www.dpd.cdc.gov/dpdx.

A doença de Chagas

A doença de Chagas é um sério problema de saúde que afeta aproximadamente 15 milhões de pessoas nas Américas Central e do Sul sendo registradas de 50.000 a 200.000 novas infecções a cada ano (Tarleton et al., 2007). Nos últimos anos, diversos casos têm sido registrados no Brasil, com destaque para a região amazônica, antes considerada de baixa endemicidade (Dias et al., 2002). Essa região atualmente registra aproximadamente 600 casos da forma aguda da doença de Chagas caracterizando essa doença como emergente nessa região (Valente et al., 2009). Fatores econômicos e/ou políticos têm aumentado a migração de pessoas de países endêmicos para outros países, onde estão sendo detectados casos de infecção humana através de transfusões de sangue, transplante de órgãos infectados e infecção congênita (Schmunis et al., 2007a), transformando a doença de Chagas de um problema rural da América Latina para um problema global (Schmunis et al., 2007).

Em relação às fases clínicas, a doença de Chagas pode ser dividida em aguda e crônica, sendo a crônica subdividida em indeterminada, cardíaca, digestiva e nervosa.

A fase aguda da doença, cujas características aparecem de 7 a 10 dias após a infecção, faz com que o paciente apresente sintomas atípicos e de difícil diagnóstico; os sinais da infecção são caracterizados por inchaço na região da picada semelhante a um furúnculo ao qual se dá o nome de "chagoma de inoculação" (Brener, 1992). Durante a fase aguda da doença, o *T. cruzi* conduz a um estado de imuno-comprometimento envolvendo as células do timo e uma intensa ativação policlonal de linfócitos (Reina-San Martin et al., 2000).

Na fase crônica indeterminada da doença de Chagas, ocorre baixo nível de parasitemia e alto teor de anticorpos. Após a fase aguda, a maioria dos pacientes evolui durante uma ou duas décadas nesta forma indeterminada, na qual, embora exista a infecção ativa, praticamente não há lesões clinicamente demonstráveis e os órgãos e sistemas se encontram preservados (Cimerman e Cimerman, 1999). Nesta fase, as pessoas infectadas que moram em áreas endêmicas são importantes reservatórios do parasita (WHO, 2002).

Em média, 20 anos após a infecção, cerca de 40 % dos pacientes desenvolvem sinais patológicos característicos da doença de Chagas, como cardiomiopatia, danos do

sistema nervoso periférico e disfunção do sistema digestivo que conduz ao megaesôfago e/ou megacólon (WHO, 2002).

A forma crônica cardíaca é a mais importante por sua elevada morbimortalidade nas áreas endêmicas. Inflamação crônica, miocitólise e fibrose ocorrem progressivamente nos três folhetos do órgão, cujo volume pode ser normal, pequeno ou aumentado. As principais lesões ocorrem no miocárdio, com importante destruição de miocélulas e do sistema excitocondutor, o que origina as síndromes básicas, respectivamente, de insuficiência cardíaca e arritimias. Na fase crônica digestiva, todo o tubo digestivo é acometido e as lesões predominam no esôfago e cólon terminal. Macroscopicamente, o segmento pode apresentar-se absolutamente normal (estágios iniciais, ocorrendo somente disfunção motora) ou progressivamente dilatado (megaesôfago, megacólon, megaestômago). No cólon, complicação freqüente e grave nos casos mais avançados é uma torção de alça, mais comum na sigmóide (Cimerman e Cimerman, 1999).

A forma nervosa crônica atinge o sistema nervos autônomo, provocando disfunções motoras e secretórias periféricas, geralmente discretas e pouco perceptíveis. As lesões no sistema nervoso central podem ocorrer nos casos de reativação da doença em pacientes imunodeficientes (Pittella, 1993; Acquatella, 1998).

A terapia utilizada no tratamento da doença de Chagas é baseada no benznidazol e nifurtimox, drogas capazes de eliminar a parasitemia e reduzir títulos sorológicos na fase aguda da infecção, mas não são efetivas na fase crônica da mesma. Além disso, essas drogas podem causar sérios problemas de saúde decorrentes da sua alta toxicidade (Leite et al., 2006).

O nifurtimox não está mais sendo comercializado no Brasil devido à resistência apresentada pelas cepas brasileiras (Coura e Castro, 2002). O aparecimento de resistência torna imprescindível a descoberta de novos agentes terapêuticos de origem natural (Newman et al., 2000), semi-sintéticos ou sintéticos, além da utilização da biologia molecular para caracterizar a suscetibilidade das cepas infectantes às substâncias em questão (Murta et al., 1998).

O uso de novos compostos de origem natural tem sido usado com sucesso no tratamento de algumas doenças parasitárias. Alguns extratos, como também compostos

puros obtidos de plantas tem sido reportado por apresentar significantes atividades anti-protozoárias sem grandes efeitos adversos (Güida et al., 2007).

Por ser um parasita que apresenta diversas formas evolutivas durante seu ciclo biológico e uma alta capacidade de se adaptar ao meio que vive faz-se necessário estudos científicos no sentido de compreender melhor a maquinaria celular do parasita a fim de possibilitar o desenvolvimento de drogas mais específicas, sem grandes efeitos citotóxicos ao paciente.

Metabolismo energético de Tripanossomatídeos

As formas epimastigotas de *T. cruzi* podem consumir ativamente carboidratos e aminoácidos do meio. A oxidação da glicose, pelas diferentes formas desse parasita, resulta na produção de CO_2 e outras moléculas, principalmente succinato e L-alanina (Cazzulo, 1994). O *T. cruzi* não apresenta reservas intracelulares de glicose, como glicogênio ou amido. Por conseguinte, a glicose é importada constantemente do meio externo (a partir do sangue de mamíferos, por exemplo) através de transportadores de hexoses (Miletti et al., 2006). Foi observado que epimastigotas degradam preferencialmente glicose, mas possuem capacidade de metabolizar aminoácidos, principlamente a L-prolina, quando a glicose do meio é esgotada (Cazzulo, 1994).

Ao contrário da maior parte dos eucariotos onde a via glicolítica ocorre no citoplasma, nos tripanossomatídeos esta via ocorre dentro de uma organela denominada glicossomo, exceto a síntese de fosfoenolpiruvato que ocorre no citosol (Cazzulo, 1994; Bringaud et al., 2006). O oxaloacetato, o produto final da oxidação da glicose, é reduzido a malato pela malato desidrogenase glicossomal. Na matriz mitocondrial, o malato pode ser reduzido a fumarato, que por ação da NADH-fumarato redutase pode ser reduzido a succinato (principal doador de elétrons) que é oxidado pela cadeia respiratória.

O *T. cruzi* também apresenta uma via alternativa de oxidação de glicose, a via das pentoses fosfato, que leva à produção de ribose-5-fosfato e NADPH. Esta coenzima atua como doadora de hidrogênio em sínteses redutoras (como síntese de ácidos graxos e colesterol) e em reações de proteção contra agentes oxidantes (Maugeri e Cazzulo, 2004).

Em tripanossomatídeos, as enzimas dessa via encontram-se tanto no glicossomo quanto no citosol (Heise et al., 1999; Duffieux et al., 2000).

Tem sido descrito que nos três estágios de desenvolvimento de *T. cruzi* (epimastigota, amastigota e triomastigota) o parasita apresenta ciclo de Krebs e cadeia respiratória (Docampo et al., 1978; Cazzulo, 1994).

Um fato que merece bastante importância nesses parasitas é a existência de uma mitocôndria única, multilobulada, que ocupa aproximadamente 12 % do volume celular (Paulin et al., 1975). Na matriz mitocondrial encontra-se o cinetoplasto (DNA mitocondrial) que é responsável pela síntese dos citocromos a, a_3 e b (Docampo et al., 1978) podendo assim, regular o metabolismo aeróbico destes parasitas (Affranchino et al., 1986).

Semelhantemente como ocorre em mamíferos, o *T. cruzi* apresenta uma completa maquinaria enzimática voltada para o metabolismo oxidativo. Isto inclui uma cadeia de transporte de elétrons funcional, que contém citocromos, além de outros componentes, capaz de gerar um gradiente de prótons que é utilizado pela F_1F_o-ATP sintase para a produção de ATP. É desconhecido o mecanismo exato pelo qual os tripanossomatídeos regulam a fosforilação oxidativa. No entanto, os níveis de substratos disponíveis, oxigênio, ADP e equivalentes reduzidos podem ter um papel importante, assim como o grau de acoplamento entre a respiração e a fosforilação oxidativa (Bringaud et al., 2006).

O complexo I (NADH: ubiquinona oxidoredutase) da cadeia respiratória desse parasita apresenta características particulares que o diferencia do complexo I de humanos. Vários autores questionam a funcionabilidade desse complexo na transferência de elétrons por conta de algumas observações específicas: a oxidação de NADH é insensível a rotenona (inibidor clássico do complexo I em humanos); nenhum substrato dependente de NADH é capaz de promover a fosforilação de ADP em formas procíclicas de *T. brucei* permeabilizadas com digitonina; e a redução do citocromo c por NADH ou por substratos dependentes de NADH é insensível a antimicina A, indicando que os elétrons do NADH não alcançam o citocromo c via complexo III (Turrens, 1989). Recentemente, Carranza et al., 2009 demonstraram que cepas de *T. cruzi* com deleções em genes específicos do complexo I não apresentaram diferenças no potencial elétrico de membrana mitocondrial e no consumo de oxigênio quando comparado com cepas normais. Além disso, esse estudo

mostrou que uma considerável fração de NADH mitocondrial é oxidada pela fumarato redutase NADH dependente. Acredita-se que apesar de não ter uma clara função no transporte de elétrons ao longo da cadeia, o complexo I atuaria na formação de super-complexos possibilitando uma transferência de elétrons mais eficiente (Lazarou et al., 2007).

Conforme descrito, o metabolismo energético de tripanossomatídeos apresenta características particulares, além de um sistema enzimático bastante especializado que permite o parasita se adaptar às diferentes condições do meio. Isso ressalta a importância de estudos bioquímicos com ênfase na bioenergética mitocondrial a fim de se conhecer melhor a maquinaria celular desse parasita.

Homeostase de Ca^{2+} em Tripanossomatídeos

O *T. cruzi* tem um complexo ciclo de vida envolvendo diferentes estágios morfológicos que se adaptam a uma variedade de condições impostas pelo vetor e hospedeiro mamífero. Enquanto a forma sanguínea tripomastigota e o estágio epimastigota de *T. cruzi* encontrado no inseto vetor proliferam em meio onde a concentração de cálcio é muito alta (da ordem de 1 mM), os amastigotas vivem em um meio intracelular onde a concentração de cálcio livre é muito baixa (da ordem de 0,1 μM). Essas mudanças dramáticas na concentração de cálcio livre no meio durante o ciclo de vida deste parasita sugere que a homeostase de Ca^{2+} deve diferir entre amastigotas e os outros estágios do parasita, assim como, entre amastigotas e células hospedeiras (Vercesi et al., 1994).

Em tripanosomatídeos, a participação de Ca^{2+} durante o processo de invasão celular tem sido demonstrada, embora a exigência para a elevação do cálcio citosólico na célula hospedeira tenha variado entre os parasitas. Em *T. cruzi*, um aumento na concentração de Ca^{2+} intracelular é requerido para invasão celular, em adição à mobilização de Ca^{2+} na célula hospedeira (Moreno et al., 1994; Burleigh e Andrews, 1998). Uma baixa internalização dos parasitas ocorreu quando células hospedeiras foram tratadas, antes e durante suas interações com tripomastigotas, com um quelante de cálcio (EDTA) ou verapamil, um bloqueador do canal de cálcio (Osuna et al, 1990) ou quando tripomastigotas foram tratados com quin-2AM (quin 2 acetoximetil ester), um quelante de cálcio (Moreno

et al., 1994). No sentido inverso, quando tripomastigotas foram pré-tratados com ionomicina, um ionóforo de cálcio, alta taxa de infectividade foi observada (Yakubu et al, 1994).

A elevação do Ca^{2+} intracelular também foi observada em promastigotas de *L. mexicana amazonensis* após a invasão de macrófagos, mas diferentemente de *T. cruzi*, um aumento transitório no Ca^{2+} intracelular foi detectado nessas células e rapidamente retornaram aos níveis basais. Após tratamento de macrófagos com BAPTA-AM, outro quelante de cálcio, não houve mudança na taxa de infecção (Lu et al, 1997).

Os sistemas de transporte de cálcio em *T. cruzi* precisa ser bastante eficiente para manter a grande diferença existente entre os meios externo e interno. No soro e fluidos extracelulares a concentração de Ca^{2+} livre ionizado (na faixa de mM) é 10.000 vezes maior que os níveis citosólicos (variando de 100 a 300 nM) (Gunter e Pfeiffer, 1990). Em tripanosomatídeos, a operação conjunta de distintos mecanismos transportadores de Ca^{2+} na membrana plasmática, mitocôndria e retículo endoplasmático regulam a concentração citosólica de Ca^{2+} na faixa de 70-150 nM (Vercesi et al, 1991) dependendo do parasita.

Em *T. cruzi*, a captação de cálcio mitocondrial através de um uniporter de Ca^{2+}, depende da presença do potencial elétrico de membrana mitocondrial, gerado pela respiração ou hidrólise de ATP, que fornece a força motriz para o acúmulo de Ca^{2+} (Vercesi et al., 1991), de uma maneira similar a mitocôndrias de mamíferos. Como nestas células, o transporte de cálcio em *T. cruzi* é estimulado por fosfato e inibido por vermelho de rutênio (Docampo e Vercesi, 1989a), um inibidor do uniporter de Ca^{2+} (Kowaltoswski, 2000). Uma alta capacidade de retenção de Ca^{2+} por mitocôndrias de *T. cruzi* foi observado na presença de fosfato (Docampo and Vercesi, 1989a), que compensa as mudanças no gradiente de pH mitocondrial através da membrana mitocondrial (Kowaltoswski, 2000). No entanto, o efluxo de Ca^{2+} da mitocôndria parece ocorrer por troca eletroneutra de Ca^{2+} da matriz por Na^{+} ou prótons externos (Moreno e Docampo, 2003).

Em muitas células eucarióticas, a membrana plasmática possui um canal para influxo de Ca^{2+} (Vercesi et al., 1991). Uma vez no citosol, o Ca^{2+} pode interagir com proteínas ligantes de cálcio ou podem ser captados por diferentes organelas (Figura 6). Liberação de Ca^{2+} para o meio extracelular ocorre principalmente por Ca^{2+}-ATPases da membrana plasmática (Moreno e Docampo, 2003).

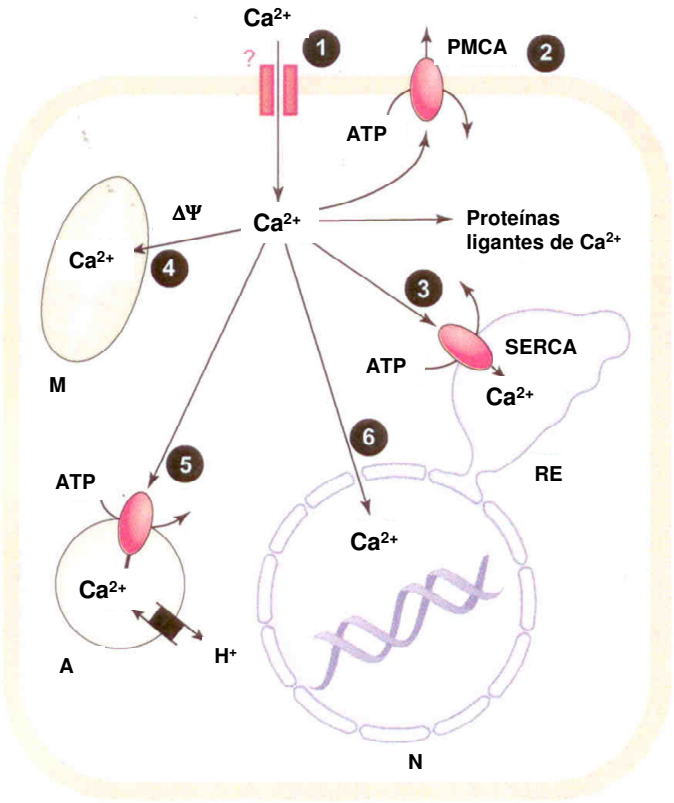

Figura 6: Representação esquemática da distribuição de Ca^{2+} em protozoários parasitas (Adaptado de Moreno e Docampo, 2003). A entrada de Ca^{2+} ocorre provavelmente através de canais de Ca^{2+}(1). Uma vez dentro da célula, o Ca^{2+} pode ser translocado novamente para o meio extracelular, primariamente pela ação de Ca^{2+}-ATPase de membrana plasmática (2). Além disso, o Ca^{2+} pode interagir com proteínas ligantes de Ca^{2+} ou ser seqüestrado pelo reticulo endoplasmático (3), mitocôndria (4), acidocalcisoma (5) ou núcleo (6). O retículo endoplasmático contém a Ca^{2+}-ATPase de retículo sarco-endoplasmático. A mitocôndria capta Ca^{2+} através do seu potencial elétrico de membrana ($\Delta\Psi$). Os acidocalcisomas contém uma Ca^{2+}-ATPase de membrana plasmática. O Ca^{2+} parece difundir livremente para dentro do núcleo. RE, retículo endoplasmático; M, mitocôndria; N, núcleo; A, acidocalcisoma; SERCA, Ca^{2+}-ATPase do retículo sarcoplasmático; PMCA, Ca^{2+}-ATPase de mebrana plasmática.

Como em mamíferos, quando ocorre uma perda na capacidade desses sistemas reguladores de transporte de Ca^{2+} ou quando ocorre uma permeabilização de membrana plasmática do parasita, há um grande influxo de Ca^{2+} na célula com conseqüente acúmulo pela mitocôndria podendo levar a uma situação de estresse oxidativo e sinalização para morte celular (Irigoin et al., 2009).

Produção de EROs e Sistemas Antioxidantes em Tripanossomatídeos

Como descrito anteriormente, o *T. cruzi* utiliza o oxigênio molecular como aceptor final de elétrons gerando moléculas de água na mitocôndria. Acoplado a este processo ocorre a síntese de ATP. O oxigênio molecular também pode ser parcialmente reduzido, aceitando um, dois ou três elétrons gerando, respectivamente, o ânion superóxido ($O_2^{\cdot-}$), peróxido de hidrogênio (H_2O_2) e radicais hidroxila ($OH^{\cdot-}$).

Durante seu ciclo de vida, o *T. cruzi* é exposto a diferentes EROs geradas pelo metabolismo aeróbico do parasita, na resposta imune do hospedeiro e/ou, ocasionalmente, produzidas por medicamentos utilizados no tratamento da doença de Chagas (Turrens, 2004).

A eficácia de uma infecção em um ambiente oxidante depende, em grande parte, da habilidade do parasita em detoxificar as espécies reativas. Apesar de os tripanossomatídeos não possuírem catalase, ou glutationa peroxidades dependentes de selênio (Fairlamb et al., 1992; Flohe et al., 1999), eles apresentam um sistema de detoxificação particular (Figura 7), representado por enzimas dependentes da tripanotiona (N^1,N^8-bis-glutatinilespermidina). A tripanotiona é mantida na forma reduzida pela tripanotiona redutase (Fairlamb et al., 1992), que por sua vez, serve como fonte de redução da triparedoxina, que é uma proteína doadora de elétrons para a redução de peróxidos pela triparedoxina peroxidase (Alphey et al., 1999; 2000). A tripanotiona tem um importante papel no metabolismo dos tripanossomatídeos, similar ao da glutationa em outros organismos.

Em *T. cruzi* foram caracterizadas a triparedoxina peroxidase citosólica (CPX) e a triparedoxina peroxidase mitocondrial (MPX). Estas enzimas catalisam a redução de H_2O_2 usando triparedoxina como substrato reduzível, em combinação com a tripanotiona, tripanotiona redutase e NADPH (Wilkinson et al., 2002). Essa proteína parece proteger o parasita das oscilações na produção de EROs geradas durante o seu metabolismo, uma vez que, em condições de estresse, observou-se um aumento no níveis citosólicos de CPX (Finzi et al.,2004).

Com relação à superóxido dismutase (SOD), o *T. cruzi* apresenta SOD dependente de ferro (Fe-SOD), tanto no citosol quanto na mitocôndria, que dismuta o ânion superóxido à H_2O_2 (Marin et al., 2008).

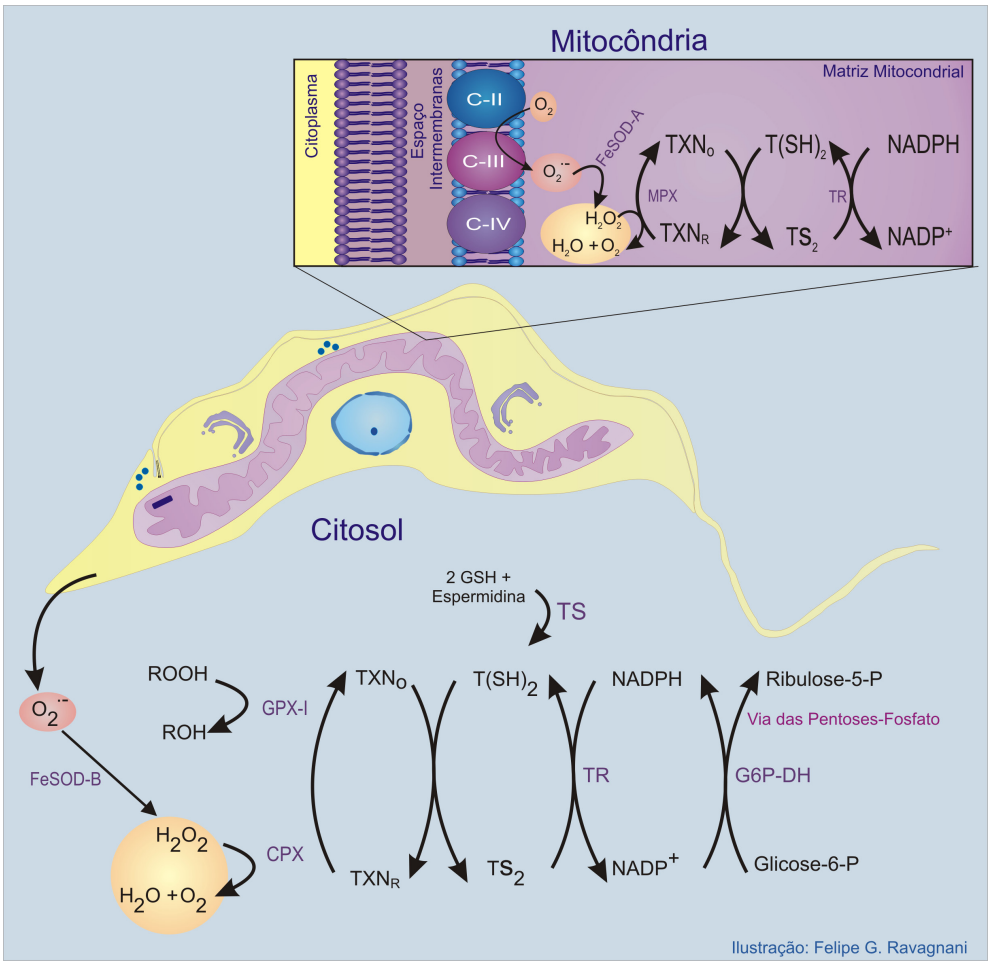

Figura 7: Sistemas antioxidantes em *Trypanosoma cruzi* (Adaptado de Piacenza et al., 2009). Nesse esquema, representamos os sitemas antioxidantes presentes no citosol e na mitocôndria de *T. cruzi*. O doador final de elétrons para todos os sistemas enzimáticos é o NADPH, derivado da via das pentoses-fosfato. Mitocôndria: a cadeia transportadora de elétrons (Complexo II: succinato desidrogenase, C-II; Complexo III: ubiquinol citocromo c redutase, C-III e complexo IV: citocromo oxidase, C-IV) é um dos principais sítios para a geração de ânion superóxido ($O_2^{\bullet-}$), principalmente em C-III. A isoforma mitocondrial da superóxido dismutase dependente ferro (FeSOD-A) catalisa a dismutação do $O_2^{\bullet-}$ a H_2O_2. A triparedoxina peroxidase mitocondrial (MPX) cataliticamente decompõe H_2O_2 usando triparedoxina reduzida (TXN_R) como substrato redutor. Citosol: As enzimas antioxidantes incluem: triparedoxina peroxidase citosólica (CPX), FeSOD-B e glutationa peroxidase I (GPX-I). A tripanotiona reduzida ($T(SH)_2$) é sintetizada a partir de duas moléculas de glutationa (GSH) e uma de espermidina, em uma reação catalisada pela enzima tripanotiona sintetase (TS). Tripanotiona redutase (TR); triparedoxina oxidada (TXN_O); tripanotiona oxidada (TS_2); glicose-6-fosfato desidrogenase (G6P-DH).

2 - OBJETIVOS

OBJETIVO GERAL

Este trabalho teve como objetivo o estudo da atividade de lectinas de *Cratylia mollis* (Cramoll 1,4) sobre a função mitocondrial e viabilidade de *Trypanosoma cruzi*.

OBJETIVOS ESPECÍFICOS

PARTE I

Mediante o reconhecimento de glicoconjugados de superfície em *T. cruzi* pela Cramoll 1,4, foi avaliado o efeito da lectina na:

- Viabilidade e inibição da proliferação do parasita;
- Homeostase intracelular do Ca^{2+};
- Função mitocondrial de células inteiras: Potencial elétrico de membrana mitocondrial e consumo de oxigênio;
- Produção de EROs;
- Determinação do tipo de morte celular.

PARTE II

Analisar o mecanismo de ação da Cramoll 1,4 em mitocôndrias isoladas de *Trypanosoma cruzi* e de fígado de rato em relação a (ao):

- Abertura do poro de transição de permeabilidade mitocondrial (TPM);
- Potencial elétrico de membrana mitocondrial
- Produção de peróxido de hidrogênio

ARTIGO ACEITO PARA PUBLICAÇÃO NO
JOURNAL OF BIOENERGETICS AND BIOMEMBRANES

(APÊNDICE 1)

3 - RESULTADOS

PARTE I

Mechanism of *Trypanosoma cruzi* death induced by *Cratylia mollis* seed lectin

Fernandes, M. P.[1]; Inada, N. M.[1#]; Chiaratti, M. R.[1,2]; Araújo, F. F. B.[3]; Meirelles, F. V.[2]; Correia, M. T. S.[3]; Coelho, L. C. B. B.[3]; Alves, M. J. M.[4]; Gadelha, F. R.[5] and Vercesi, A. E.[1*]

[1]Departamento de Patologia Clínica, Faculdade de Ciências Médicas, Universidade Estadual de Campinas, Campinas, Brazil; [2]Departamento de Ciências Básicas, Faculdade de Zootecnia e Engenharia de Alimentos, Universidade de São Paulo, Pirassununga, Brazil; [3]Departamento de Bioquímica, Centro de Ciências Biológicas, Universidade Federal de Pernambuco, Recife, Brazil; [4]Instituto de Química, Universidade de São Paulo, São Paulo, Brazil and [5]Departamento de Bioquímica, Instituto de Biologia, Universidade Estadual de Campinas, Campinas, Brazil.

***Corresponding author:** Aníbal E. Vercesi, Universidade Estadual de Campinas, Departamento de Patologia Clínica, Faculdade de Ciências Médicas, CEP: 13083-887, Campinas, SP, Brazil, Tel: +55-19-35217370, Fax: +55-19-35217330, e-mail: anibal@unicamp.br

 # Current address: Laboratório de Biofotônica, Instituto de Física, Universidade de São Paulo, São Carlos, Brazil.

Abstract

Incubation of *T. cruzi* epimastigotes with the lectin Cramoll 1,4 in Ca^{2+} containing medium led to agglutination and inhibition of cell proliferation. The lectin (50 μg/ml) induced plasma membrane permeabilization followed by Ca^{2+} influx and mitochondrial Ca^{2+} accumulation, a result that resembles the classical effect of digitonin. Cramoll 1,4 stimulated (five-fold) mitochondrial reactive oxygen species (ROS) production, significantly decreased the electrical mitochondrial membrane potential ($\Delta\Psi_m$) and impaired ADP phosphorylation. The rate of uncoupled respiration in epimastigotes was not affected by Cramoll 1,4 plus Ca^{2+} treatment, but oligomycin-induced resting respiration was 65% higher in treated cells than in controls. Experiments using *T. cruzi* mitochondrial fractions showed that, in contrast to digitonin, the lectin significantly decreased $\Delta\Psi_m$ by a mechanism sensitive to EGTA. In agreement with the results showing plasma membrane permeabilization and impairment of oxidative phosphorylation by the lectin, fluorescence microscopy experiments using propidium iodide revealed that Cramoll 1,4 induced epimastigotes death by necrosis.

Keywords: *Trypanosoma cruzi*, mitochondria, calcium, ROS, cell death, Cramoll 1,4 lectin

Abbreviations: AA, antimycin A; ADP, adenosine 5'-diphosphate; CCCP, carbonyl cyanide p-trifluoromethoxyphenylhydrazone; Cramoll 1,4, *Cratylia mollis* seed lectin (Isoform 1,4); EGTA, Ethylene glycol-bis(2-aminoethylether)-*N,N,N′,N′*-tetraacetic acid; H_2DCF-DA, dichlorodihydrofluorescein diacetate; MTT, 3-[4,5-dimethylthiazol-2-yl]-2,5-diphenyltetrazolium bromide; PI, propidium iodide; ROS, reactive oxygen species; $\Delta\Psi_m$, electrical mitochondrial membrane potential.

Introduction

Chagas' disease is caused by the protozoan *Trypanosoma cruzi*, and it is still an important health problem in Latin America affecting several million people in rural regions (http://www.who.int/tdr/diseases/chagas/swg_chagas.pdf). Current chemotherapeutics for Chagas' disease are based on the use of non-specific drugs, such as benznidazole, which appears to exert its trypanocidal effect through reactive oxygen species (ROS) generation and/or through the decrease in glutathione and trypanothione levels (Maya et al. 2007; Wilkinson et al. 2008). Unfortunately, treatment is associated with a high frequency of serious side effects in the host (Buá et al. 2004; Carraro et al. 2007; Pedrosa et al. 2001; Urbina and Docampo 2003).

The *T. cruzi* lifecycle was identified a hundred years ago (Chagas 1909), but until now, many aspects of its cell biology have remained a mystery. Therefore, a better understanding of the *T. cruzi* cell machinery could lead to the identification of targets for the development of more specific trypanocidal agents. The search for new compounds from natural sources is a widely used approach employed in the treatment of some parasitic diseases. Extracts and pure compounds obtained from plants have been reported to possess significant anti-protozoan activities without side effects (Güida et al. 2007). Artemisin and its derivatives are a potent new class of anti-malarials originating from *Artemisia annua*, L. (Asteraceae) (Kayser et al. 2003). Quinine is one of the best known alkaloids with anti-plasmodial activity, and licochalcone A from *Glycyrrhiza inflata* is a strong inhibitor of mitochondrial functions in *Leishmania* species (Kayser et al. 2003).

Compounds isolated from several plants from the Brazilian semi-arid region have revealed trypanocidal activity against *T. cruzi* epimastigotes (Vieira et al. 2008). In this regard, the seed lectin Cramoll 1,4 (Isoform 1,4) isolated from *Cratylia mollis*, a native forage from the semi-arid region in Northeast Brazil, is a protein that recognizes and binds to specific carbohydrates on the cell surface inducing mitogenic activity (Maciel et al. 2004). It also exhibits anti-tumour activity when encapsulated into liposomes (Andrade et al. 2004). Concanavalin A (ConA), a lectin with high homology to Cramoll 1,4, exerts a potent anti-hepatoma effect. After binding to the mannose moiety on hepatoma cell membrane glycoproteins, ConA is internalized and accumulates in the mitochondria causing cell death (Lei and Chang. 2007). Some other lectins, including those from *Helix*

pomatia, *Agaricus bisporus* and the *Arisaema helleborifolium* lectin (AHL), are being investigated for their possible use in cancer therapy (Kaur et al. 2006).

With regard to parasites, a lectin from *Synadenium carinatum* latex (ScLL) showed a protective effect against *Leishmania amazonensis* infection in BALB/c mice (Afonso-Cardoso et al. 2007). Binding of some lectins to specific oligosaccharides on the cell membrane seems to mediate cell death (Coelho et al. 2007; Macedo et al. 2007). Cells that do not possess these carbohydrates are resistant to the cytotoxic effect of these proteins (Gastman et al. 2004). Lectins can also be used to evaluate changes in the sugar composition and distribution on cell surfaces during the process of *T. cruzi* transformation from epimastigotes to the mammalian-infective metacyclic trypomastigotes (Bourguignon et al. 1998).

T. cruzi has only one mitochondrion, and the study on the mechanisms by which different compounds interfere with its bioenergetics could be useful for the search and development of new chemotherapies. Considering the property of ConA, a homologue of Cramoll 1,4, to cross the cell membrane and localize to mitochondria, we evaluated the effects of Cramoll 1,4 on *T. cruzi* epimastigote mitochondrial functions and cell viability.

Material and Methods

Chemicals

Arsenazo III, MTT, Safranine O, Succinate, Digitonin, EGTA, CCCP, ADP, Antimycin A and Oligomycin were purchased from Sigma (St. Louis, USA). H_2DCF-DA was purchased from Molecular Probes Inc. (Eugene, Oregon, USA). CAT was purchased from Calbiochem of EMD Chemicals Inc. (Affiliate of Merck KGaA, Darmstadt, Germany). All other reagents were of the highest purity grade available.

Cell cultures

T. cruzi epimastigotes (Tulahuen 2 strain) were grown in LIT medium, containing 20 mg l^{-1} hemin and 10% fetal bovine serum, as described (Castellani et al. 1967). After 5

days, cells were harvested by centrifugation (1,000 *g* at 4°C) and washed once in phosphate buffered saline (PBS), pH 7.2. The number of cells ml^{-1} was determined using a Neubauer chamber. *T. cruzi* trypomastigotes (Y strain) were grown and maintained as described (Andrews and Colli 1982). HaCaT keratinocyte, a spontaneously transformed human epithelial cell line, were grown in RPMI-1640 medium supplemented with 2 mM L-glutamine and 10% fetal bovine serum in a humidified atmosphere with 5% CO_2 (v/v) at 37°C. For the experiments, keratinocytes grown to ~80 % confluence were used.

Preparation of T. cruzi mitochondrial fraction

Epimastigotes (log phase) were harvested by centrifugation (1,000 *g*, 10 min at 4°C), washed in 0.12 M sodium phosphate, pH 8.0 buffer, containing 86.3 mM NaCl and 56 mM glucose. After centrifugation, the pellet was mixed with 3 ml of acid-washed glass beads (150-212 μm – SIGMA), 100 μl of protease inhibitor cocktail (Sigma) and 80 μl of 0.1 M phenylmethanesulphonyl fluoride (PMSF). Cells were disrupted by abrasion in a chilled mortar until 90% disruption was achieved (as determined under an optical microscope), resuspended in 4 ml of 50 mM HEPES-NaOH, pH 7.2 buffer, containing 0.27 M sucrose, 1 mM EDTA, and 1 mM $MgCl_2$, and centrifuged at 1,000 *g* for 5 min at 4°C in order to remove the glass beads, unbroken cells and large debris. The supernatant was submitted to another centrifugation (1,000 *g* for 10 min at 4°C) for total removal of the glass beads. The supernatant was then centrifuged at 16,000 *g* for 10 min at 4°C to obtain the mitochondrial fraction, which was washed in 2 ml of 10 mM potassium phosphate, pH 7.5 buffer, containing 0.25 M sucrose and 1 mM EDTA. After another centrifugation at 16,000 *g* for 10 min at 4°C, the pellet was resuspended in 200 μl of reaction medium (10 mM HEPES, pH 7.2, 125 mM sucrose, 65 mM KCl, 1 mM $MgCl_2$ and 2 mM K_2PO_4), and the total protein concentration was determined by the Biuret method (Gornall et al. 1949).

Lectin preparation

Seeds of *C. mollis* Mart. (camaratu bean) were collected in the State of Pernambuco (Brazil), and the lectin (Cramoll 1,4) was purified according to (Correia and Coelho 1995).

The seed extract (10% w/v in 0.15 M NaCl) was ammonium sulphate-fractionated (40–60%) and then purified by affinity chromatography on a Sephadex G-75 column. Cramoll 1,4 elution was performed with 0.3 M glucose in 0.15 M NaCl, and protein concentration was determined according to (Lowry et al. 1951).

Microscopy

Epimastigotes or trypomastigotes (1.25 x 10^8 cells/ml) were incubated in PBS, pH 7.2, + 1 mM $MgCl_2$ with 2.5 or 50 µg/ml Cramoll 1,4 for 1 h. Phase contrast microscopic images were captured on a Leica DM IRB inverted microscope (Leica Microsystems, Wetzlar, Germany) coupled to an acquisition image system (CoolSnap-Pro/Colour). In order to evaluate cell death caused by necrosis, epimastigotes (1 x 10^7 cells/ml) were incubated in PBS, pH 7.2, + 1 mM $MgCl_2$ with 50 µg/ml Cramoll 1,4 for 2 h at 28°C. Next, cells were stained with 10 µg/ml propidium iodide (590 excitation/535 emission) for 10 min, and images were captured using an epifluorescence microscope (Axioplan, Carl Zeiss, NY, USA).

DNA agarose gel electrophoresis

DNA fragmentation was evaluated based on the method described by (Piacenza et al. 2001). Briefly, epimastigotes (1.25 x 10^8 cells/ml) were incubated in PBS, pH 7.2, + 1 mM $MgCl_2$ with 50 µg/ml Cramoll 1,4 for 1, 2, 4, 8, 18 or 24 h. Parasites were then collected by centrifugation at 13,000 *g* for 5 min. Cell pellets were resuspended in 0.5 ml of TE buffer (10 mM Tris-HCl + 1 mM EDTA, pH 8.0) containing 5% Triton X-100 and kept on ice for 15 min. Next, samples were centrifuged at 13,000 *g* for 15 min at 4°C to separate intact chromatin (pellet) from DNA fragments (supernatant). After the addition of 5 µl of 1 M $MgCl_2$ + 100 µl of 5 M NaCl + 1 ml of isopropyl alcohol, the supernatant was incubated overnight at -20°C to precipitate DNA fragments. Intact chromatin and DNA fragment pellets were resuspended in 50 µl of TE buffer and treated with 100 µg/ml RNase at 37°C for 1 h. Then, samples were treated with 500 µg/ml proteinase K at 55°C for 1 h and separated by electrophoresis on a 2% agarose gel at 80 V for 3 h. DNA was stained with

ethidium bromide (10 µg/ml for 15 min) and visualized in a Fuji Fla 3000G Laser Scanner (Fuji Film Co., Japan).

Determination of Cramoll 1,4 effect on cell viability and proliferation rates

T. cruzi epimastigotes (1.25 x 10^8 cells/ml) were incubated in PBS, pH 7.2, + 1 mM $MgCl_2$ with different lectin concentrations (1, 2.5, 5, 10, 20 or 50 µg/ml) for 1 h at 28°C, and cell viability was verified by the MTT method (Muelas-Serrano et al. 2000). This method assesses viability by cellular conversion of the soluble tetrazolium salt MTT (3-[4,5-dimethylthiazol-2-yl]-2,5-diphenyltetrazolium bromide) into the insoluble formazan by mitochondrial enzymes. After cell treatment with the lectin as described above, cells were centrifuged (1,000 *g* for 5 min at 4°C), and the pellet resuspended and incubated for 1.5 h in PBS containing MTT (2.5 mg/ml). Formazan extraction was performed using 10% SDS dissolved in 0.01 N HCl. Formazan formation was quantified in a spectrophotometer at 540 nm. In order to establish the effect of Cramoll 1,4 on cell proliferation rates after incubation with different lectin concentrations, as described above, cells were centrifuged (1,000 *g* for 5 min) and grown in LIT medium for five days. The number of cells was determined in a Neubauer chamber.

Treatment of the keratinocytes (1 x 10^6 cells/ml) with the lectin was performed after trypsinization (0.05% trypsin + 0.025% EDTA solution). Keratinocyte viability was analyzed by annexin V FITC and propidium iodide staining in a FACSCalibur flow cytometer (BD Biosciences, San Jose, CA, USA) equipped with an argon laser and CellQuest software (version 4.1). Briefly, 10^6 cells were incubated with different lectin concentrations (1, 2.5, 5, 10, 20 or 50 µg/ml) for 1h at 28°C, washed in PBS and resuspended in binding buffer (10 mM HEPES, pH 7.4, 150 mM NaCl, 5 mM KCl, 1 mM $MgCl_2$, and 1.8 mM $CaCl_2$) containing annexin V-FITC (1:500). After 20 min incubation in the dark at room temperature, cells were also stained with propidium iodide (PI, 1:50). Apoptosis was quantified by FACS analysis as the number of annexin V-FITC-positive and PI-negative cells divided by the total cell number, while necrosis was quantified as the number of PI-positive cells divided by the total cell number.

Measurement of Ca^{2+} movements

Variations in free Ca^{2+} concentrations in whole cells were followed by measuring the changes in the absorbance spectrum of arsenazo III (Scarpa 1979), using an SLM Aminco DW 2000 spectrophotometer at the wavelength pair 675-685 nm (Docampo et al. 1983). Calibration was performed by recording changes in absorbance after addition of known amounts of $CaCl_2$.

Estimation of mitochondrial membrane potential ($\Delta\Psi_m$)

$\Delta\Psi_m$ was estimated by following safranine O fluorescence (Vercesi et al. 1991a), recorded on a F-4500 Hitachi spectrofluorimeter operating at excitation and emission wavelengths of 495 and 586 nm, respectively, and a slit width of 2.5 nm. Relative changes in membrane potential were expressed as fluorescence arbitrary units (A.U.)

Cellular oxygen consumption

Oxygen consumption was measured in a high resolution respirometry OROBOROS Oxygraph-2k (Oroborus Instruments, Innsbruck, Austria) in PBS, pH 7.2, + 1mM $MgCl_2$ at 28^{o}C. DatLab 4 software was used for data acquisition (Gnaiger 2001).

Reactive oxygen species production

After treatment for 1 h under the conditions described in the Figure 7 legend, cells were incubated for 40 min in the dark with 5µM dichlorodihydrofluorescein diacetate (H_2DCF-DA) under constant stirring. Fluorescence was determined on an F-4010 Hitachi spectrofluorimeter at 488 and 525 nm for excitation and emission wavelengths, respectively, and a slit width of 5 nm.

Data analysis

All results are expressed as the mean ± the standard error of the mean (SEM) for at least four independent experiments. Statistical significance was determined by one way ANOVA followed by Tukey's test, with a significance level of $p<0.05$. The cell viability and proliferation experiments were analyzed by polynomial regression (SigmaStat®, version 2.0, 1992-1995, Jandel Corporation).

Results

Recognition of glycoconjugates on the T. cruzi cell surface by Cramoll 1,4

Using phase-contrast microscopy (Fig. 1), we observed that *T. cruzi* epimastigotes (*a-c*) or trypomastigotes (*a'-c'*) incubated for 1 h in the presence of lectin (either 2.5 or 50 µg/ml) underwent agglutination, likely due to the recognition of glycoconjugates present on parasite cell surface. In contrast, incubation of keratinocytes with Cramoll 1,4 did not generate the stable cell agglutination observed for *T. cruzi* (data not shown).

In order to evaluate whether the lectin-glycoconjugate interaction decreased parasite survival, we used the epimastigotes form in the following experiments.

Cramoll 1,4 inhibited T. cruzi epimastigote survival and proliferation but had no effect on keratinocyte viability

Fig. 2A shows that treatment of epimastigotes with Cramoll 1,4 for 1 h caused a dose-dependent impairment of cell viability, reaching a maximum decrease of 60% upon treatment with 20 µg/ml. In order to ascertain whether the remaining cells were still capable of proliferating, parasites (treated with Cramoll 1,4 for determination of cell viability) were washed twice to remove unbound lectin, resuspended in culture medium, and after five days, the number of live parasites was determined. As can be seen in Fig. 2B, a significant decrease in the proliferation rate was observed with Cramoll 1,4 at concentrations higher than 20 µg/ml, reaching almost 100% inhibition at 50 µg/ml. These results indicate that the

parasites able to reduce MTT to formazan after lectin treatment were not capable of proliferating in culture. This lectin had no significant effect on keratinocyte viability under the same incubation conditions (Fig. 3). In that case, cell viability was analyzed by flow cytometry because the agglutination promoted by the lectin in these cells was not stable as in *T. cruzi* and could be reversed with gentle stirring.

Cramoll 1,4 promoted T. cruzi epimastigote plasma membrane permeabilization followed by medium Ca^{2+} internalization and accumulation by the mitochondrion

Digitonin has been used over the years to permeabilize the plasma membrane of trypanosomatids, allowing for the estimation of the mitochondrial membrane potential and the study of oxidative phosphorylation and Ca^{2+} transport by mitochondria *in situ* (Vercesi et al. 1991 a, b; Vercesi et al. 1993). Indeed, when cells were incubated in the presence of digitonin (Fig. 4, *line a*) permeabilization of the plasma membrane was followed by mitochondrial Ca^{2+} uptake, as evidenced through the release of accumulated Ca^{2+} caused by the respiratory inhibitor antimycin A. Interestingly, incubation of *T. cruzi* epimastigotes in the same reaction medium containing Cramoll 1,4, instead of digitonin, was also followed by a slightly slower decrease in medium Ca^{2+} that was reversed by antimycin A. This indicates that, similar to digitonin, Cramoll 1,4 has the ability to permeabilize *T. cruzi* epimastigote plasma membranes to Ca^{2+} (Fig. 4, *line b*). In both cases, addition of the ionophore A23187 after antimycin A resulted in an additional release of Ca^{2+} from other intracellular stores (Moreno et al. 1992 a, b). No Ca^{2+} uptake was observed when *T. cruzi* was incubated in the presence of heat-denatured lectin or in the absence of digitonin (Fig. 4, *lines c* and *d*).

Cramol 1,4 treatment decreased mitochondrial membrane potential ($\Delta\Psi_m$) and impaired oxidative phosphorylation

As illustrated in Fig. 5A, digitonin was used to permeabilize epimastigote plasma membrane allowing for the determination of $\Delta\Psi_m$ and ADP phosphorylation, as indicated by the fluorescence increase caused by ADP (100 μM) and reversed by

carboxyatractylosyde (CAT, 5 μM), an inhibitor of the ADP/ATP carrier. At the end of the experiment, a total elimination of $\Delta\Psi_m$ was caused by the classical uncoupler, carbonyl cyanide m-chlorophenylhydrazone (CCCP, 1 μM) (*line a*). The *line b* of Figure 5 A shows that even after a preincubation period of 1 h with digitonin, epimastigotes could still phosphorylate added ADP. In contrast, when the parasites were submitted to lectin treatment for the same period (1 h), a very low increase in fluorescence was observed after ADP addition, indicating a significant impairment of oxidative phosphorylation (*line c*). On the other hand, when heat-inactivated Cramoll 1,4 was preincubated for 1 h with the epimastigotes, no safranine O uptake was observed, again indicating that denatured lectin had no ability to permeabilize the plasma membrane of the epimastigotes (*line d*). It should be noted that all experiments were performed in the presence of 10 μM Ca^{2+}.

In the experiments of Fig. 5B, the parasites were incubated during a longer period of time (2 h), either in the presence of lectin (*line a*) or digitonin (*line b*), in reaction medium containing 10 μM Ca^{2+}. In both cases, $\Delta\Psi_m$ was significantly lower than in the experiments of Fig. 5A, and no ADP phosphorylation could be observed (*lines a* and *b*). The presence of EGTA significantly protected $\Delta\Psi_m$ and ADP phosphorylation in the presence of either digitonin (*line c*) or lectin (*line d*), indicating that Ca^{2+} had a major effect on mitochondrial dysfunction under both situations.

Cramoll 1,4 did not modify the uncoupled epimastigote respiration rate but released state 4 respiration

In the experiments of Fig. 6, we investigated the effect of Cramoll 1,4 (50 μg/ml for 1 h) on oligomycin-induced state 4 or CCCP-uncoupled epimastigote respiration. The lectin caused a 65% increase in state 4 respiration in the presence of Ca^{2+} and a 52% increase in free Ca^{2+} in the medium (EGTA present). In contrast, Cramoll 1,4 did not alter the CCCP-uncoupled respiration rate either in the presence or absence of Ca^{2+}.

After 2 h incubation in the presence of Cramoll 1,4, respiration rates were similar in the presence of oligomycin and CCCP, indicating that respiration was completely uncoupled (data not shown). Accordingly, the results depicted in Fig. 5B (*line a*) showed

that under these same experimental conditions, no changes in $\Delta\Psi_m$ was caused by ADP addition.

Stimulation of ROS generation by epimastigotes treated with Cramoll 1,4 or digitonin: effect of Ca^{2+}

T. cruzi epimastigotes were treated with either lectin or digitonin for 1 h and subsequently loaded with H_2DCF-DA. Cramoll 1,4, but not denaturated Cramoll, increased ROS generation 5.4-fold, while digitonin increased it 4.2-fold (Fig. 7). ROS formation induced either by the lectin or digitonin was partially inhibited by EGTA. In agreement with the $\Delta\Psi_m$ experiments, Cramoll 1,4 had a higher effect on ROS production than digitonin (5.4- vs. 4.2-fold).

Cramoll 1,4, but not digitonin, decreased $\Delta\Psi_m$ in epimastigote mitochondrial fractions

All of the previous results suggested that, in addition to permeabilizing the epimastigote plasma membrane, Cramoll 1,4 also exerted a direct effect on mitochondria. This is possible because ConA, a plant lectin with high homology to Cramoll 1,4, is internalized via endocytosis and accumulates in mitochondria after it binds to the mannose moiety of the cell membrane glycoproteins (Lei and Chang 2007). Therefore, we investigated the direct effect of Cramoll 1,4 on isolated epimastigote mitochondria (Fig. 8). Similar to the experiments performed with permeabilized epimastigotes, isolated mitochondria incubated in the presence of Cramoll 1,4 and EGTA (Ca^{2+}-free medium) generated a $\Delta\Psi_m$ similar to that exhibited by the control mitochondria, and both phosphorylated added ADP (Fig. 8A). In contrast, Figure 8B shows that in the presence of 10 μM Ca^{2+}, Cramoll 1,4 significantly decreased $\Delta\Psi_m$, relative to the control experiment, confirming that it interacts directly with the organelle. This result is in agreement with the experiments showing that ConA penetrates in hepatoma cells and increases the permeability of the inner mitochondrial membrane (Lei and Chang 2007).

Cramoll 1,4-induces epimastigote death by necrosis

After epimastigote treatment with 50 µg/ml Cramoll 1,4 (2 h), the parasites were stained with propidium iodide (PI), and images were captured by fluorescence microscopy. The intense fluorescence signal obtained is compatible with cell death by necrosis (Fig. 9). This is in agreement with the results of the plasma membrane permeabilization (Fig. 4) and the impairment of epimastigote oxidative phosphorylation (Fig. 5A) after Cramoll 1,4 treatment. DNA fragmentation, which is characteristic of death by apoptosis, could not be detected by electrophoresis, even when the epimastigotes were treated with Cramoll 1,4 for up to 24 h (data not shown).

Discussion

Since the first description of the reactivity of epimastigotes and trypomastigotes with ConA (Alves and Colli 1974), lectins have been used as cell surface markers in order to evaluate changes in *T. cruzi* membrane glycoconjugate composition in different stages of the parasitic cell cycle (Bourguignon et al. 1998). Herein, we report that the interaction between Cramoll 1,4 and *T. cruzi* surface glycoconjugates results in plasma membrane permeabilization followed by medium Ca^{2+} influx and cell death. The action of Cramoll 1,4 on *T. cruzi* allowed for a better understanding of both the mechanisms of lectin toxicity and the molecular events that govern cell death in this parasite.

A large body of evidence demonstrates that mitochondrial calcium homeostasis plays an important role in the modulation of numerous physiological cellular processes, including cell death (Giacomello et al. 2007). The *T. cruzi* mitochondrion is very active in calcium accumulation and has a high storage capacity (Docampo and Vercesi 1989; Moreno et al. 1992 a, b), but under certain experimental conditions, *T. cruzi* mitochondrial calcium overload may lead to mitochondrial dysfunction. Indeed, it was observed that *T. cruzi* epimastigotes exposed to Ca^{2+} in the presence of fresh human serum underwent cell death mediated by permeabilization of the plasma membrane by membrane attack complex (MAC) deposition on the cell surface. This permeabilization was followed by cell Ca^{2+} influx and mitochondrial Ca^{2+} overload, a condition that stimulated ROS generation by the

mitochondria (Irigoin et al. 2009). In this regard, Grijalba et al. (1999) demonstrated that mitochondrial Ca^{2+} overload alters the lipid organization of the inner mitochondrial membrane by interacting with the anionic head of cardiolipin, an abundant component of the inner mitochondrial membrane. These alterations in membrane organization may affect the respiratory chain function, including coenzyme Q mobility, favouring monoelectronic oxygen reduction (superoxide radical generation) at intermediate steps of the respiratory chain and leading to mitochondrial oxidative damage followed by cell death.

It has also been shown that *T. cruzi* epimastigote lysis by fresh human serum is dependent upon the alternative pathway of complement activation (Nogueira et al. 1975). In contrast, in trypomastigotes, the classical activation pathway of the human complement system is inhibited *in vitro* by parasitic calreticulin, a phosphoprotein phosphatase (Ferreira et al. 2004; Moreno et al. 2007) that renders this evolutionary form resistant to human serum.

In the current study, we showed that Cramoll 1,4, a protein of non-immune origin, is able to recognize glycoconjugates on the *T. cruzi* cell surface, leading to epimastigote agglutination (Fig. 1A), thus decreasing cell viability and proliferation (Fig. 2). Cramoll 1,4 was also able to recognize *T. cruzi* trypomastigote surface membrane glycoconjugates causing agglutination (Fig. 1B) and membrane permeabilization (data not shown). In contrast, this lectin was unable to agglutinate and kill keratinocytes, a human cell line. This indicates that the lectin-glycoconjugate interaction in this model was not strong enough to cause pore formation (Fig. 3).

As in the case of fresh human serum, Cramoll 1,4 induced plasma membrane permeabilization and mitochondrial calcium overload (Fig. 4). These processes were followed by increased production of ROS (Fig. 7), a $\Delta\Psi_m$ decrease and impairment in oxidative phosphorylation (Fig. 5) that culminated with cell death by necrosis (Fig. 9). As proposed by Grijalba et al. 1999, the attack of ROS to the inner mitochondrial membrane caused oxidative damage to lipids and proteins that led to increased membrane permeability with a consequent release of the resting respiration, as observed in Fig. 6.

In order to verify whether the lectin effect against *T. cruzi* epimastigotes was strictly the consequence of cell membrane permeabilization, we used digitonin as a positive control. The comparison indicated that although calcium uptake promoted by digitonin was

slightly higher when compared to that induced by the lectin (Fig. 4), the Cramoll 1,4 effects on mitochondria were stronger than that caused by digitonin, as illustrated by higher production of ROS (Fig. 7) and larger decreases of both $\Delta\Psi_m$ and oxidative phosphorylation (Fig. 5A). This prompted us to investigate a direct effect of the lectin on isolated epimastigote mitochondria. Indeed, the results indicated that Cramoll 1,4, but not digitonin, caused a significant decrease in $\Delta\Psi_m$ from isolated epimastigote mitochondria incubated in medium containing Ca^{2+} (Fig. 8B). In contrast, in Ca^{2+}-free medium, Cramoll 1,4 did not affect the ability of mitochondria to phosphorylate added ADP (Fig. 8A). The direct effect of Cramoll 1,4 on mitochondria may explain the different mechanism of epimastigote death caused by this lectin (necrosis) when compared to that caused by fresh human serum. The latter also permeabilizes the plasma membrane and causes Ca^{2+}-dependent *T. cruzi* epimastigote death by apoptosis (Irigoin et al. 2009).

To our knowledge, this is the first report investigating the mechanism of a seed lectin on *T. cruzi* mitochondrial function and cell death. We showed that Cramoll 1,4 toxicity to *T. cruzi* epimastigotes seems to result from a concerted action on the parasite's plasma and mitochondrial membranes, mitochondrial Ca^{2+} overload and ROS production. The nature of lectin interactions with the mitochondrial membranes is currently under investigation.

Acknowledgments

We would like to thank Luis Henrique Gonzaga Ribeiro and Roberto Zangrandi for excellent technical assistance, and Juliana Giusti for help with the DNA fragmentation experiments. This work was supported by Conselho Nacional de Desenvolvimento Científico e Tecnológico (CNPq), Fundação de Amparo à Pesquisa do Estado de São Paulo (FAPESP) and Coordenação de Aperfeiçoamento de Pessoal de Nível Superior (CAPES).

References

Afonso-Cardoso, S. R., Rodrigues, F. H., Gomes, M. A., Silva, A. G., Rocha, A., Guimarães, A.H., Candelouro, I., Favoreto Jr, S., Ferreira, M. S., and de Souza, M. A. (2007) Korean J Parasitol 45:255-266

Alves, M. J., and Colli, W. (1974) J Protozool 21:575-578

Andrade, C. A., Correia, M. T., Coelho, L. C., Nascimento, S. C., and Santos-Magalhães, N. S. (2004) Int J Pharm 278:435-445

Andrews, N. W., and Colli, W. (1982) J Protozool 29:264-269

Bourguignon, S. C., de Souza, W., and Souto-Padron, T. (1998) Histochem Cell Biol 110:527-534

Búa, J., Ruiz, A. M., Potenza, M., and Fichera, L. E. (2004) Bioorg Med Chem Lett 14:4633-4637

Carraro, R., Búa, J., Ruiz, A., and Paulino, M. (2007) J Mol Graph Model 26:48-61

Castellani, O., Ribeiro, L. V., and Fernandes, J. F. (1967) J Protozool 14:447-451

Chagas, C. (1909) Bulletin de la Société de Pathologie Exotique 2:304-307

Coelho, M. B., Marangoni, S., and Macedo, M. L. (2007) Comp Biochem Physiol C Toxicol Pharmacol 146:406-414

Correia, M. T., and Coelho, L. C. (1995) Appl Biochem Biotechnol 55:261-273

Docampo, R., Moreno, S. N., and Mason, R. P. (1983) J Biol Chem 258:14920-14925

Docampo, R., and Vercesi, A. E. (1989) J Biol Chem 264:108-111

Ferreira, V., Valck, C., Sánchez, G., Gingras, A., Tzima, S., Molina, M. C., Sim, R., Schwaeble, W., and Ferreira, A. (2004) J Immunol 172:3042-3050

Gastman, B., Wang, K., Han, J., Zhu, Z. Y., Huang, X., Wang, G. Q., Rabinowich, H., and Gorelik, E. (2004) Biochem Biophys Res Commun 316:263-271

Giacomello, M., Drago, I., Pizzo, P., and Pozzan, T. (2007) Cell Death Differ 14:1267-1274

Gnaiger, E. (2001) Respir Physiol 128:277-297

Gornall, A. G., Bardawill, C. J., and David, M. M. (1949) J Biol Chem 177:751-766

Grijalba, M. T., Vercesi, A. E., and Schreier, S. (1999) Biochemistry 38:13279-13287

Güida, M. C., Esteva, M. I., Camino, A., Flawia, M. M., Torres, H. N., and Paveto, C. (2007) Exp Parasitol 117:188-194

Irigoin, F., Inada, N. M., Fernandes, M. P., Piacenza, L., Gadelha, F. R., Vercesi, A. E., and Radi, R. (2009) Biochem J 418:595-604

Kaur, M., Singh, K., Rup, P. J., Saxena, A. K., Khan, R. H., Ashraf, M. T., Kamboj, S. S., and Singh, J. (2006) Arch Biochem Biophys 445:156-165

Kayser, O., Masihi, K. N., and Kiderlen, A. F. (2003) Expert Rev Anti Infect Ther 1:319-335

Lei, H. Y., and Chang, C. P. (2007) Autophagy 3:402-404

Lowry, O. H., Rosebrough, N. J., Farr, A. L., and Randall, R. J. (1951) J Biol Chem 193:265-275

Macedo, M. L., das Graças Machado Freire, M., da Silva, M. B., and Coelho, L. C. (2007) Comp Biochem Physiol A Mol Integr Physiol 146:486-498

Maciel, E. V., Araujo-Filho, V. S., Nakazawa, M., Gomes, Y. M., Coelho, L. C., and Correia, M. T. (2004) Biologicals 32:57-60

Maya, J. D., Cassels, B. K., Iturriaga-Vasquez, P., Ferreira, J., Faundez, M., Galanti, N., Ferreira, A., and Morello, A. (2007) Comp Biochem Physiol A Mol Integr Physiol 146:601-620

Moreno, S. N., Docampo, R., and Vercesi, A. E. (1992a) J Biol Chem 267:6020-6026

Moreno, S. N., Vercesi, A. E., Pignataro, O. P., and Docampo, R. (1992b) Mol Biochem Parasitol 52:251-261

Moreno, V. R., Aguero, F., Tekiel, V., and Sánchez, D. O. (2007) Acta Trop 101:80-89

Muelas-Serrano, S., Nogal-Ruiz, J. J., and Gómez-Barrio, A. (2000) Parasitol Res 86:999-1002

Nogueira, N., Bianco, C., and Cohn, Z. (1975) J Exp Med 142:224-229

Pedrosa, R. C., De Bem, A. F., Locatelli, C., Geremias, R., and Wilhelm Filho, D. (2001) Redox Rep 6:265-270

Piacenza, L., Peluffo, G., and Radi, R. (2001) Proc Natl Acad Sci U S A 98:7301-7306

Scarpa, A. (1979) Methods Enzymol 56:301-338

Urbina, J. A., and Docampo, R. (2003) Trends Parasitol 19:495-501

Vercesi, A. E., Bernardes, C. F., Hoffmann, M. E., Gadelha, F. R., and Docampo, R. (1991a) J Biol Chem 266:14431-14434

Vercesi, A. E., Hoffmann, M. E., Bernardes, C. F., and Docampo, R. (1991b) Cell Calcium 12:361-369

Vercesi, A. E., Hoffmann, M. E., Bernardes, C. F., and Docampo, R. (1993) Braz J Med Biol Res 26:355-363

Vieira, N. C., Espindola, L. S., Santana, J. M., Veras, M. L., Pessoa, O. D., Pinheiro, S. M., de Araujo, R. M., Lima, M. A., and Silveira, E. R. (2008) Bioorg Med Chem 16:1676-1682

Wilkinson, S. R., Taylor, M. C., Horn, D., Kelly, J. M., and Cheeseman, I. (2008) Proc Natl Acad Sci USA 105:5022-5027

Figure Legends

Fig. 1 Phase-contrast microscopy of untreated and Cramol 1,4-treated *T. cruzi* epimastigotes and trypomastigotes. Epimastigotes (*a-c*) or trypomastigotes (*a*'-*c*') were incubated in the absence (*a, a*'), or in the presence of 2.5 µg/ml Cramoll 1,4 (*b,b*') or 50 µg/ml Cramoll 1,4 (*c,c*') for 1 h. (*a, a*',*b, b*', and *c*'x 500); (*c* x 125). Bars represent 100 µM. The results shown are representative of four independent experiments.

Fig. 2 Effect of Cramoll 1,4 on *T. cruzi* viability and proliferation rates. Epimastigotes (1.25 x 10^8 cells/ml) were incubated in PBS (pH 7.2), 1 mM $MgCl_2$ and 10 µM Ca^{2+} in the presence of different lectin concentrations for 1 h at 28°C. (A) Cell viability was determined by the MTT assay and expressed as the percentage of viable cells related to control (r^2 =0.90). (B) After treatment as in A, cells were washed in PBS, resuspended in culture medium, and after five days in culture, the number of cells was determined in a Neubauer chamber (r^2 =0.97). Data are the average ± SEM of four independent experiments.

Fig. 3 HaCaT keratinocyte viability after Cramoll 1,4 treatment. **A**fter trypsinization, keratinocytes (1 x 10^6 cells/ml) were incubated in RPMI-1640 medium with 1% fetal bovine serum in the presence of different Cramoll 1,4 concentrations for 1 h. Data are the average ± SEM of four independent experiments. $p>0.05$.

Fig. 4 Effect of Cramoll 1,4 or digitonin on Ca^{2+} uptake by *T. cruzi* epimastigotes. Parasites (1.25 x 10^8 cells/ml) were added to a reaction medium containing PBS (pH 7.2), 1 mM $MgCl_2$, 10 µM calcium, 5 mM succinate and 40 µM arsenazo III in a total volume of 2 ml. Antimycin A (AA, 5 µM) and the ionophore A23187 (10 µM) were added at time points indicated by the arrows. Lines represent incubation with: 20 µM digitonin (*line a*), 50 µg/ml Cramoll 1,4 (*line b*), reaction medium (*line c*), or denatured lectin (*line d*). The results shown are representative of four independent experiments. A.U., arbitrary units.

Fig. 5 *T. cruzi* epimastigote mitochondrial membrane potential ($\Delta\Psi_m$) after exposure to Cramoll 1,4. Epimastigotes (1.25 x 10^8 cells/ml) were added to a reaction medium containing PBS (pH 7.2), 1 mM $MgCl_2$, 5 µM safranine O and 5 mM succinate in a total volume of 2 ml. $\Delta\Psi_m$ was determined after 1 h (A) or 2 h (B) of treatment. (A) *Line a* represents the control with direct addition (no preincubation period) of digitonin (50 µM), *lines b-c* represent experiments performed after 1 h incubation with either 20 µM digitonin or 50 µg/ml Cramoll 1,4, respectively, and *line d* represents an experiment in the presence of denatured lectin. All of the experiments were performed in the presence of 10 µM Ca^{2+}. (B) *Line a* indicates cells incubated in the presence of 50 µg/ml Cramoll 1,4 + 10 µM Ca^{2+}, *line b* incubation with 20 µM digitonin + 10 µM Ca^{2+}, and *lines c-d* with 20 µM digitonin + 500 µM EGTA (Ca^{2+} free medium) or 50 µg/ml Cramoll 1,4 + 500 µM EGTA (Ca^{2+} free medium), respectively, for 2 h. Additions are indicated by the arrows: 100 µM ADP, 5 µM CAT and 1 µM CCCP. The results shown are representative of four independent experiments. A.U., arbitrary units.

Fig. 6 O_2 consumption rates in epimastigotes exposed to Cramoll 1,4. Epimastigotes (1.25 x 10^8 cells/ml) were incubated with Cramoll 1,4 (50 µg/ml) in PBS (pH 7.2) + 1 mM $MgCl_2$ in the presence of 10 µM Ca^{2+} or 500 µM EGTA (Ca^{2+} free medium) for 1 h at 25°C, in a total volume of 2 ml. Cells were then diluted to 1 x 10^7 cells/ml, and oxygen consumption was determined in the presence of oligomycin (2 µg/ml) or CCCP (0.5 µM). Data are the average ± SEM of four independent experiments performed in duplicate. *$p < 0.05$ between the oligomycin control + Ca^{2+} vs. oligomycin + Cramoll 1,4 + Ca^{2+}. **$p<0.05$ between the oligomycin control + EGTA vs. oligomycin + Cramoll 1,4 + Ca^{2+}.

Fig. 7 ROS generation induced by Cramoll 1,4. Epimastigotes (1.25 x 10^8 cells/ml) were treated with 50 µg/ml Cramoll 1,4 or 20 µM digitonin for 1 h in the presence of 10 µM Ca^{2+} or 500 µM EGTA (Ca^{2+} free medium). After H_2DCF-DA loading, cells were added to the reaction medium containing PBS (pH 7.2), 1 mM $MgCl_2$ and 5 mM succinate in a total volume of 2 ml. Fluorescence was determined as described in the Materials and Methods section. Data are the average ± SEM of four independent experiments. Statistical analysis: $p < 0.05$ among distinct groups.

Fig. 8 Effect of Cramoll 1,4 on $\Delta\Psi_m$ of isolated epimastigote mitochondria. $\Delta\Psi_m$ was determined in the presence of 100 µM EGTA (A) or 10 µM Ca^{+2} (B). Cramoll 1,4 (50 µg/ml) or digitonin (20 µM) was added to the reaction medium. This reaction medium consisted of 125 mM sucrose, 65 mM KCl, 10 mM HEPES, 1 mM $MgCl_2$, 2 mM K_2PO_4, 0.05% BSA, 5 µM safranine and 5 mM succinate in a total volume of 500 µl. *T. cruzi* mitochondrial fractions (MTc, 0.5 mg/ml), 200 µM ADP, 1 µg/ml oligomycin and 1 µM CCCP were added where indicated by the arrows. The results shown are representative of four independent experiments.

Fig. 9 Cramoll 1,4-induced epimastigote cell death occurs by necrosis. Epimastigotes (1 x 10^7 cells/ml) were incubated in the absence (*a, a*'), or in the presence of 50 µg/ml Cramoll 1,4 (*b, b*') for 2 h. The parasites were stained with 10 µg/ml propidium iodide. Bars represent 50 µM. The results shown are representative of two independent experiments performed in duplicate.

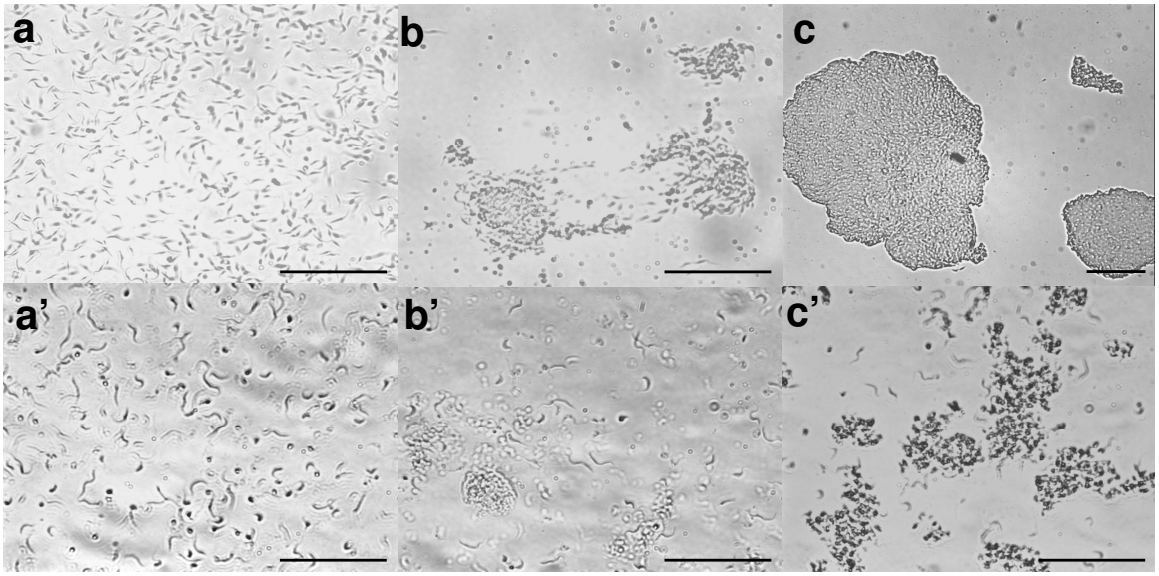

Fig. 1 – Fernandes et al.

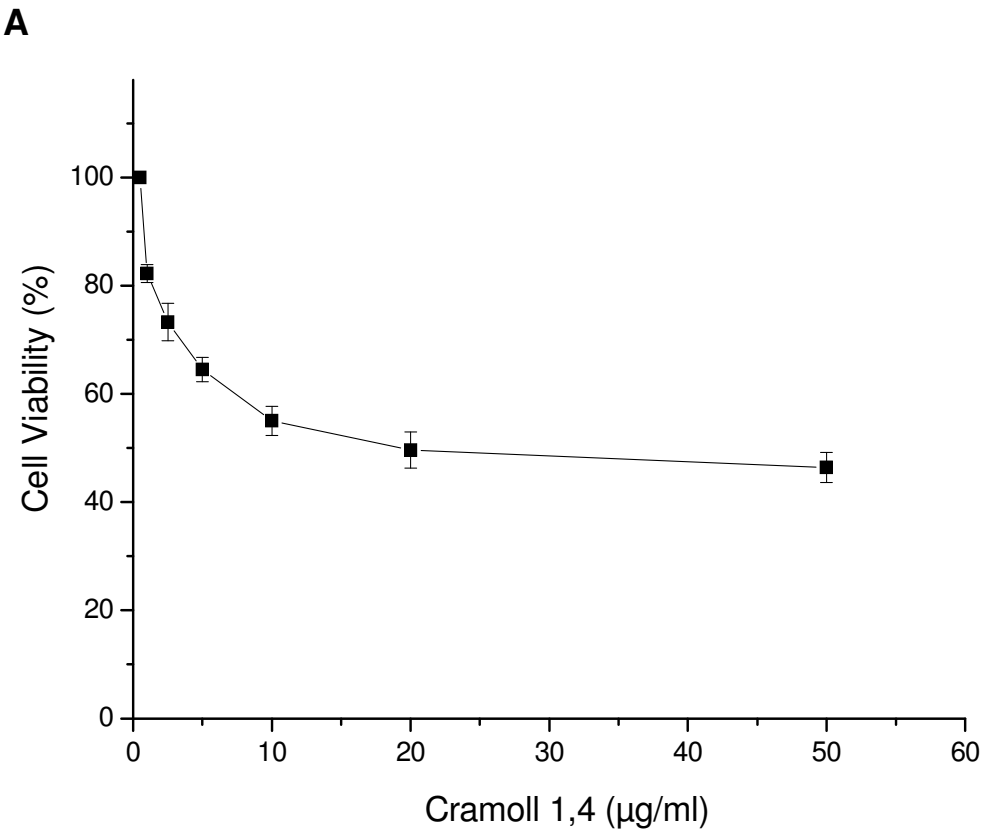

Fig. 2A – Fernandes et al.

B

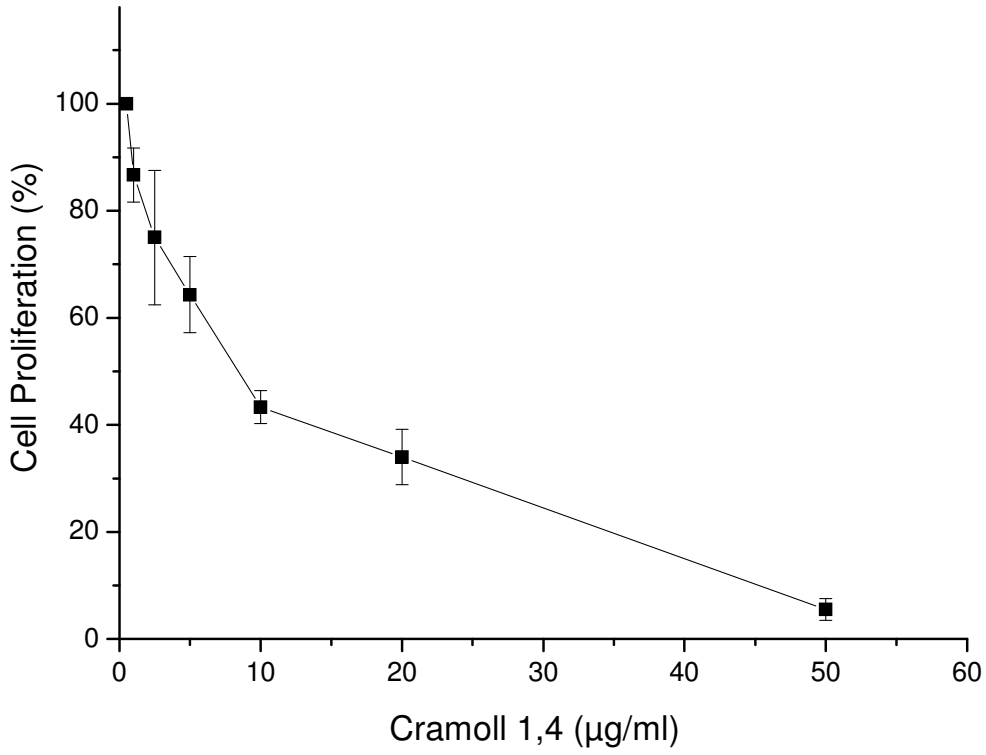

Fig. 2B – Fernandes et al.

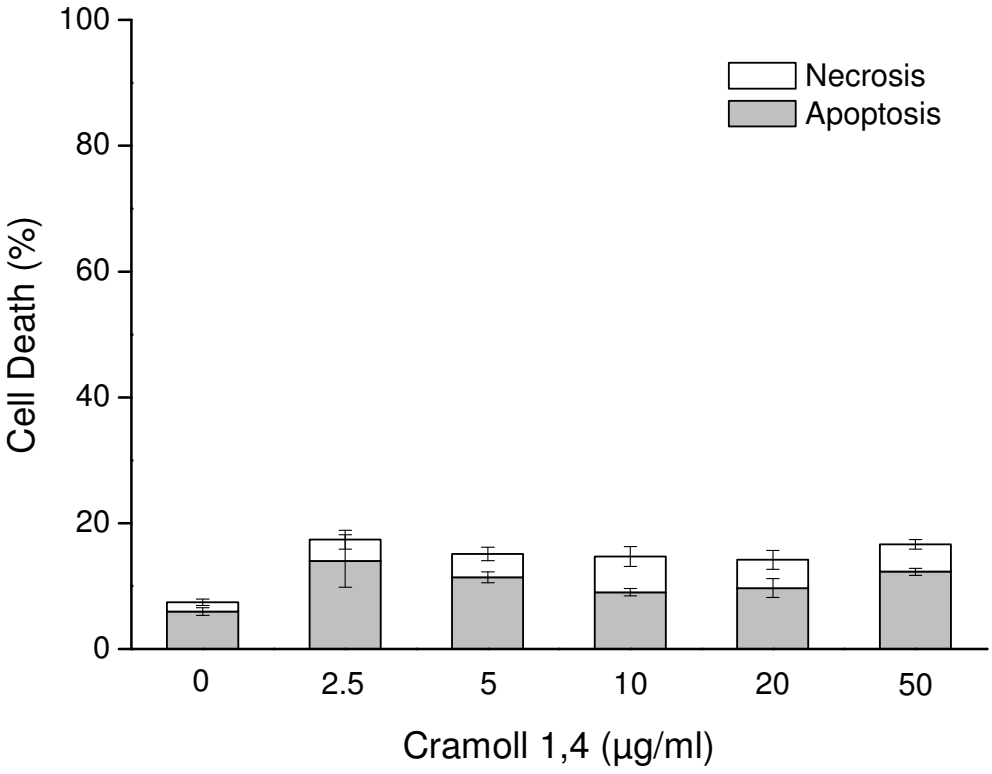

Fig. 3 – Fernandes et al.

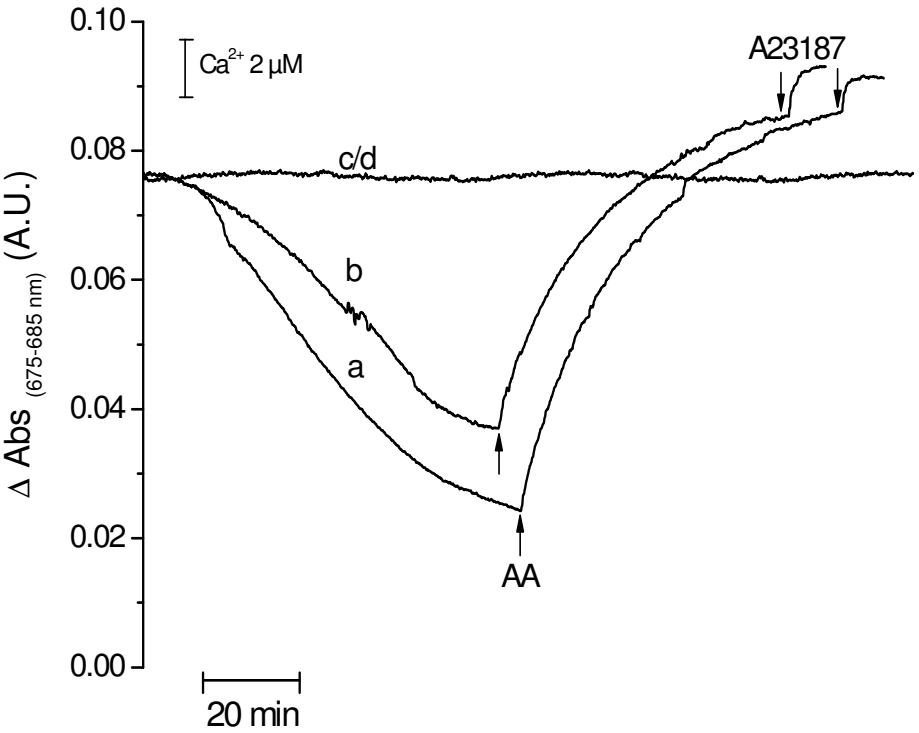

Fig. 4 – Fernandes et al.

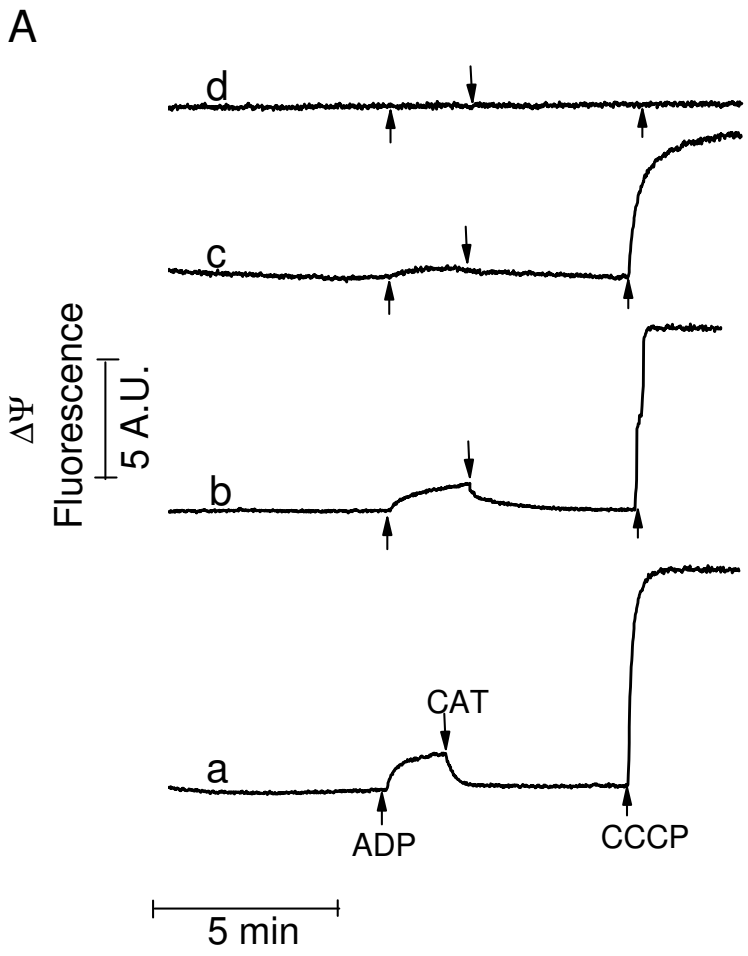

Fig. 5A – Fernandes et al.

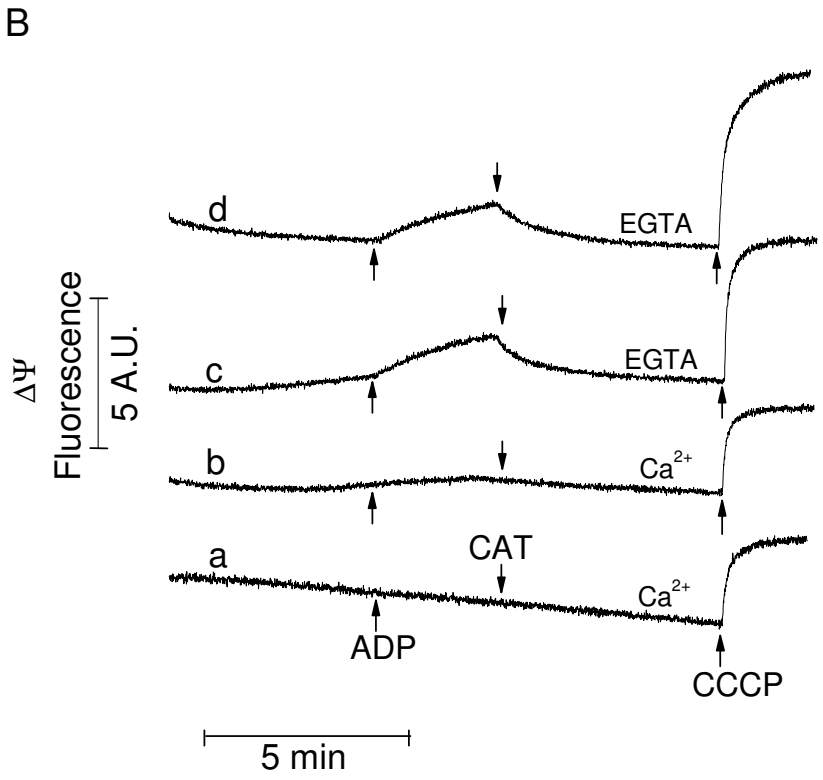

Fig. 5B – Fernandes et al.

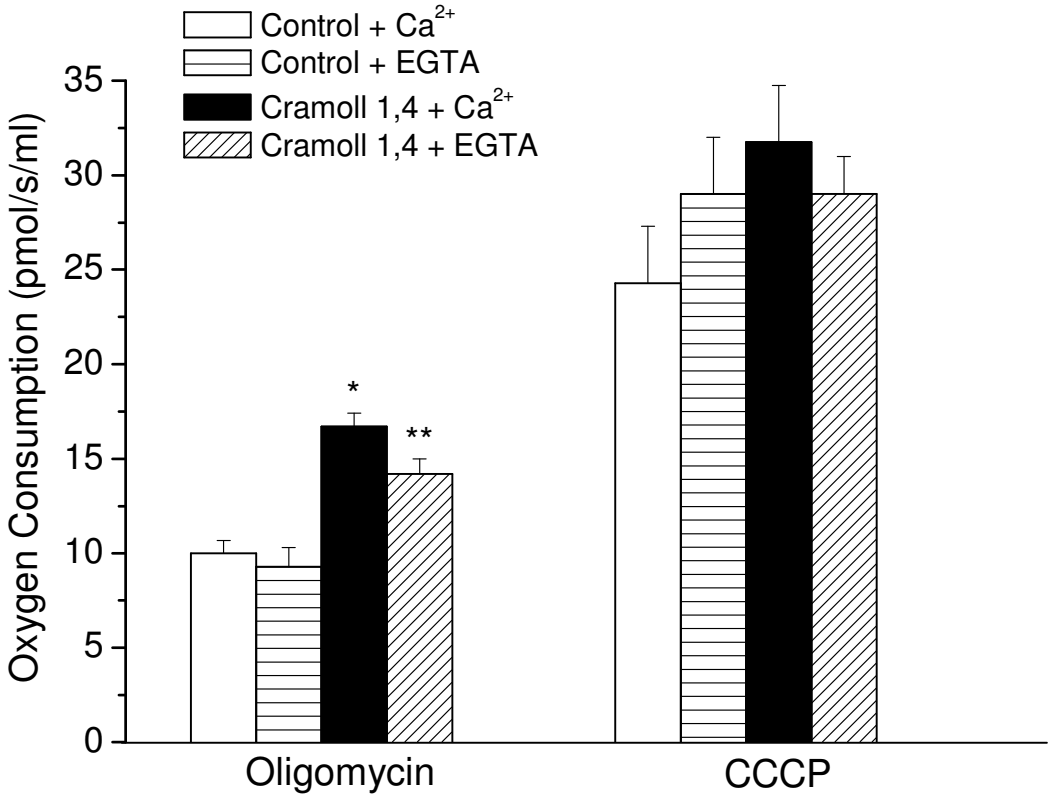

Fig. 6 – Fernandes et al.

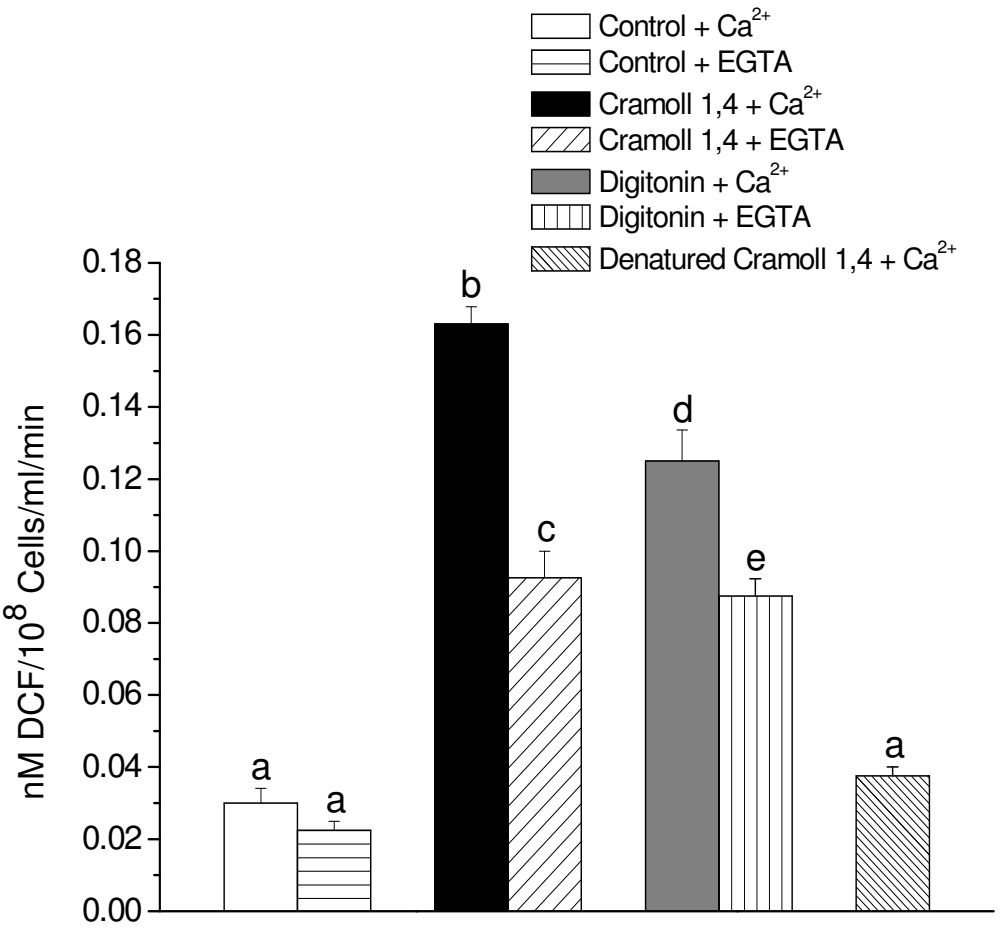

Fig. 7 – Fernandes et al.

A

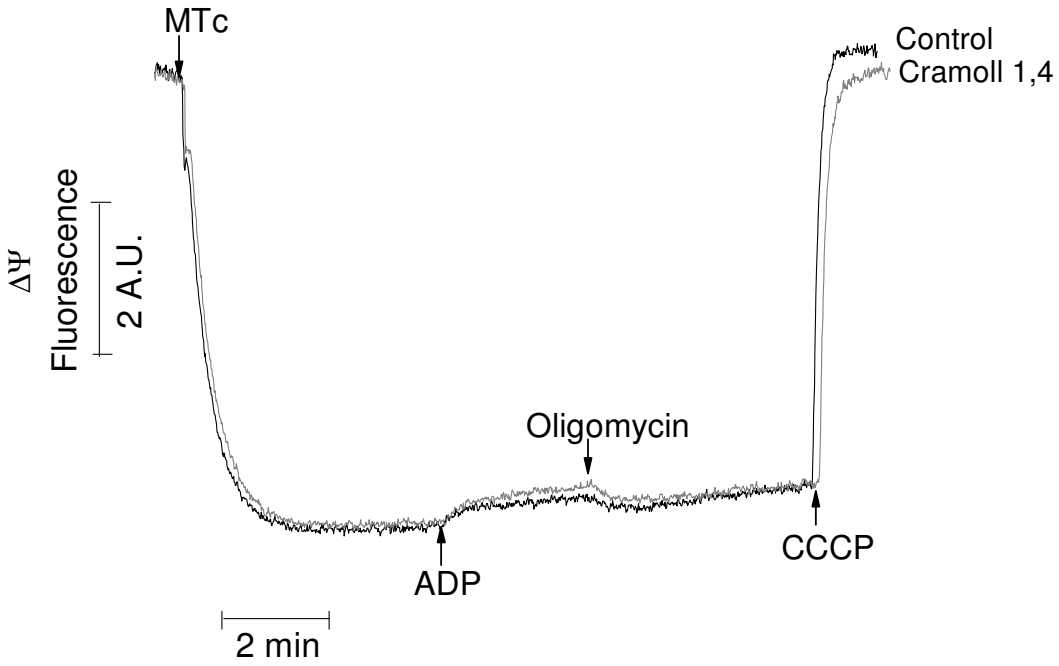

Fig. 8A – Fernandes et al.

B

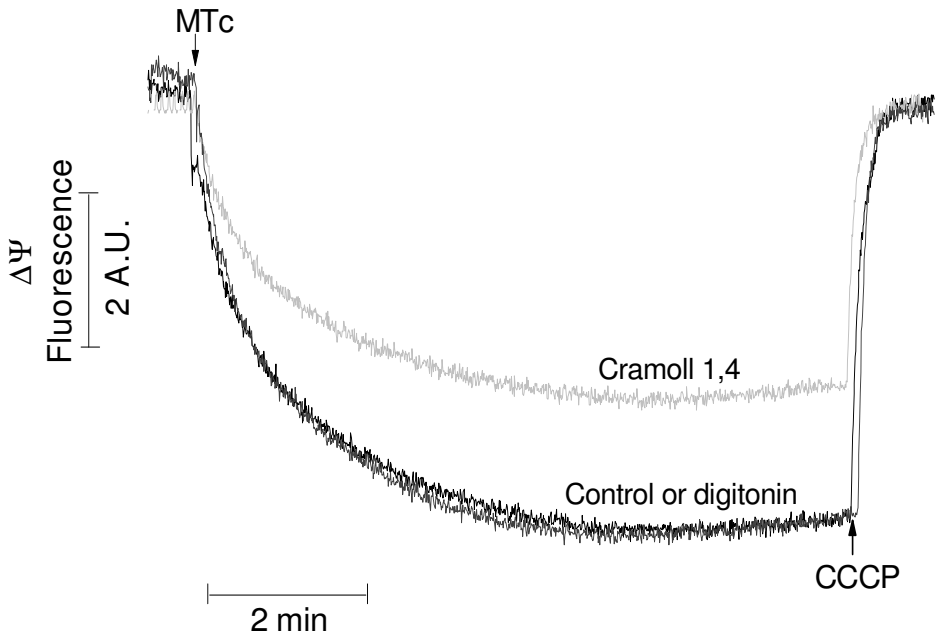

Fig. 8B – Fernandes et al.

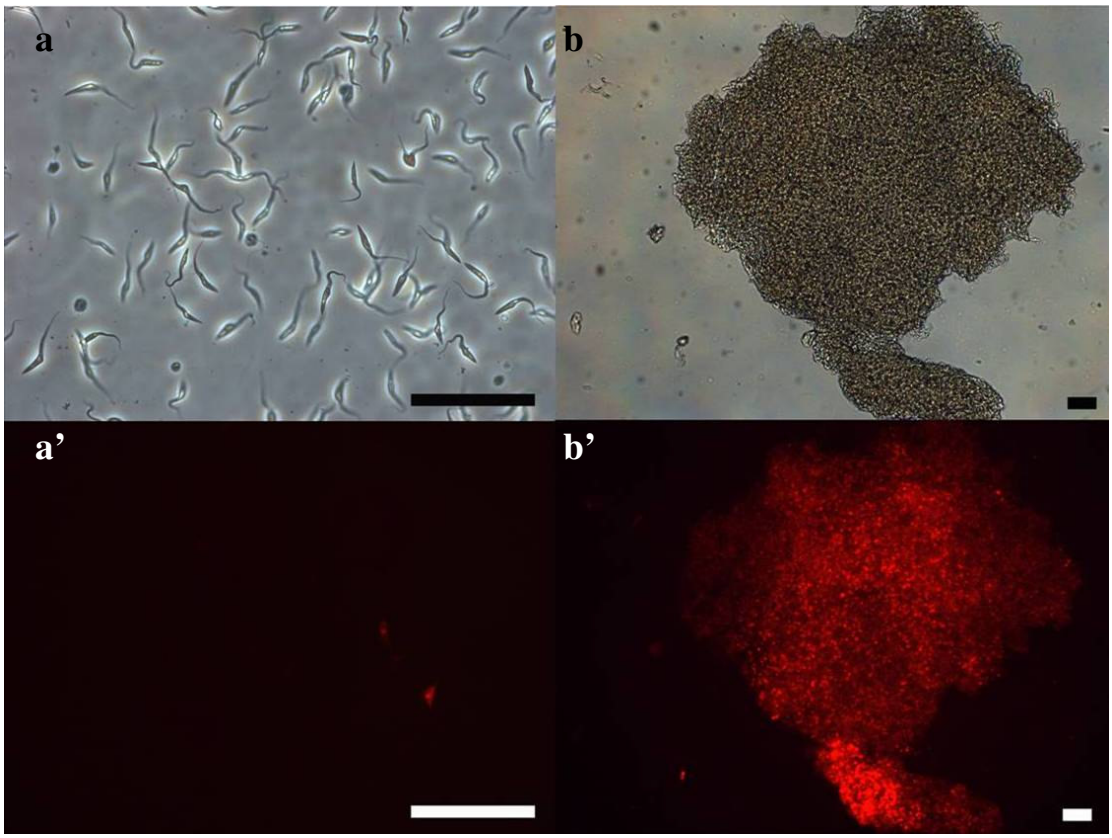

Fig. 9 – Fernandes et al.

MECANISMOS DE AÇÃO DA LECTINA, CRAMOLL 1,4, EM MITOCÔNDRIAS ISOLADAS DE *Trypanosoma cruzi* E DE FÍGADO DE RATO

3 – RESULTADOS

PARTE II

MATERIAIS E MÉTODOS

Animais

Para os experimentos com mitocôndrias isoladas, utilizamos fígados de ratos da linhagem Wistar, fêmeas adultas e adquiridas do Centro Multidisciplinar para Investigação Biológica (CEMIB) da UNICAMP.

Cultura de epimastigotas

Epimastigotas de *T. cruzi*, cepa Tulahuen 2, foram cultivados no Laboratório de Bioenergética e Defesas Antioxidantes em *Trypanosoma cruzi* no Departamento de Bioquímica do Instituto de Biologia da UNICAMP.

Epimastigotas foram crescidos à 28^{o}C em meio LIT contendo hemina (20mg/l^{-1}) e soro fetal bovino (10%) como descrito por Castelani et al. (1967). No início da fase estacionária, os parasitas foram coletados por centrifugação (5 min, 2.500 rpm, a 4^{o}C) lavados e ressuspensos em PBS (137 mM NaCl, 2,7 mM KCl, 8,1 mM Na_2HPO_4 e 1,5 mM KH_2PO_4, pH 7,2) e $MgCl_2$ (1 mM). A contagem das células foi feita em câmara de Neubauer.

Isolamento de mitocôndrias de fígado de rato

As mitocôndrias foram isoladas de fígado de ratos adultos utilizando-se a técnica de centrifugação diferencial, segundo Schneider e Hogeboom (1951). O fígado, retirado após a morte do animal, foi lavado em solução de sacarose 250 mM contendo tampão 10 mM de HEPES (pH 7,2) e 0,5 mM de EGTA, picado com tesoura e homogeneizado em homogeneizador Potter-Elvehjem. O material foi centrifugado a 2500 rpm por 10 minutos. O sobrenadante resultante foi centrifugado durante 10 minutos a 8000 rpm sendo a fase lipídica superior retirada com pipeta Pasteur. O sobrenadante foi descartado e o precipitado ressuspenso em 250 mM de sacarose, 5 mM de HEPES (pH 7,2) e 0,3 mM de EGTA, e novamente centrifugado como na condição anterior. A fração mitocondrial foi ressuspensa na mesma solução, porém isenta de EGTA, numa concentração de aproximadamente 80 mg de proteína por mililitro de suspensão mitocondrial.

Preparação da fração mitocondrial de *T. cruzi*

Epimastigotas (fase log) foram coletados por centrifugação (1.000 *g*, 10 min a 4°C), lavados em tampão contendo 0,12 M de fosfato de sódio (pH 8,0), 86,3 mM de NaCl e 56 mM de glicose e após centrifugação, o precipitado foi misturado a 3 ml de pérolas de vidro (150-212 microns – Sigma), previamente lavadas em PBS, 100 µl de um coquetel de inibidor de protease (Sigma) e 80 µl de uma solução 0,1 M de fluoreto de fenilmetanosulfonil (PMSF). As células foram rompidas por abrasão em um cadinho de porcelana até a obtenção de aproximadamente 90 % de rompimento, determinado por microscopia óptica. A seguir, 4 ml de tampão contendo 50 mM de HEPES-NaOH (pH 7,2), 0,27 M de sacarose, 1mM de EDTA e 1mM de $MgCl_2$ foram adicionados e a suspensão foi centrifugada a 1.000 *g*, por 5 mim a 4°C para remoção das pérolas de vidro, células que não romperam e debris celulares. O sobrenadante foi submetido a outra centrifugação (1.000 *g*, por 10 mim a 4°C) para total remoção das pérolas de vidro. O sobrenadante foi então centrifugado a 16.000 *g*, por 10 min a 4°C para obtenção da fração mitocondrial, a qual foi lavada em 2 ml de tampão contendo 10 mM de fosfato de potássio (pH 7,5), 0,25 M de sacarose e 1 mM de EDTA. Após uma nova centrifugação a 16.000 *g*, por 10 min a 4°C, o precipitado foi ressuspenso em 200 µl de meio de reação (125 mM de sacarose, 65 mM de KCl, 10 mM de HEPES, 1 mM de $MgCl_2$ e 2 mM de K_2HPO_4) obtendo-se assim a fração mitocondrial de *T. cruzi*.

Dosagem de proteína

A concentração de proteína das suspensões mitocondriais foi determinada pelo método de biureto (Gornall et al., 1949), modificado pela adição de colato 1% (Kaplan e Pedersen, 1983). O princípio do método baseia-se na determinação da concentração de ligações peptídicas através da medida da absorbância do complexo cobre-nitrogênio. Este complexo absorve em comprimento de onda de 540 nm. A absorbância é considerada diretamente proporcional à concentração de proteína na solução analisada, onde uma solução de BSA a 1% foi utilizada como padrão.

Condições experimentais

Os experimentos com mitocôndrias isoladas foram realizados a 28 °C em meio de reação padrão contendo 125 mM de sacarose, 10 mM de HEPES (pH 7,2), 65 mM de cloreto de potássio, 2 mM de fosfato de potássio e 1 mM de cloreto de magnésio. Como substrato respiratório foi utilizado 5 mM de succinato nos experimentos com mitocôndrias de *T. cruzi* e uma mistura de substratos para o complexo I (2mM de malato, 1mM de piruvato, 1mM de α-cetoglutarato e 1mM de glutamato) nos experimentos com mitocôndrias de fígado de rato. Os experimentos foram feitos na presença ou ausência de 0,5 mM de EGTA. Outros reagentes adicionados estão indicados nas figuras.

Medida de inchamento mitocondrial

As suspensões mitocondriais são turvas e espalham a luz incidente. A luz espalhada é uma função da diferença entre o índice de refração da matriz e do meio, e, qualquer processo que diminua esta diferença irá diminuir a luz espalhada e aumentar a transmitância (Nicholls e Åkerman, 1982). Assim, um aumento no volume da matriz mitocondrial, associado com a entrada de solutos permeáveis, resulta numa aproximação entre o índice de refração da matriz e do meio de reação com a conseqüente diminuição da luz espalhada. Esta propriedade das mitocôndrias fornece um método qualitativo simples para se estudar o fluxo de solutos através da membrana mitocondrial interna. As mitocôndrias são ideais à aplicação desta técnica porque sua matriz pode sofrer grandes variações de volume, já que a membrana interna sofre apenas desdobramento de suas pregas. O acompanhamento espectrofotométrico da redução da absorbância a 520 nm (Macedo et al, 1988) foi feito em um espectrofotômetro U-3000 utilizando mitocôndrias isoladas de fígado de rato (0,5 mg de proteína/ml).

Estimativa do potencial elétrico de membrana mitocondrial ($\Delta\Psi_m$)

A estimativa do potencial elétrico de membrana mitocondrial foi avaliada através do indicador safranina O (5 μM), que apresenta um deslocamento no espectro visível associado a sua ligação à membrana de mitocôndrias energizadas. Esta adsorção foi seguida de alteração de espectro de absorbância da safranina na faixa de 500 a 600 nm.

Nestas condições as diferenças de absorbância nos comprimentos 511-533 são diretamente proporcionais à amplitude do potencial até valores de aproximadamente 170 mV (Åkerman & Wikström, 1976; Vercesi et al, 1991). As mudanças na fluorescência da safranina foram monitoradas em um espectrofluorimetro Hitachi (F4500), nos comprimentos de onda de excitação e emissão de 495 e 586 nm, respectivamente, com largura de fenda de 2,5 nm.

Medida da geração mitocondrial de peróxido de hidrogênio

A produção de peróxido de hidrogênio (H_2O_2) pelas mitocôndrias isoladas foi determinada fluorimetricamente através da conversão de Amplex Red® 10 μM (Molecular Probes, Invitrogen, Carlsbad, CA), na presença de peroxidase 1 U/ml, a um composto altamente fluorescente, resofurina (Zhou et al., 1997). A fluorescência foi monitorada ao longo do tempo em um espectrofluorímetro Hitachi F-4500 usando comprimentos de onda de excitação e emissão de 563 e 587 nm, respectivamente, com largura da fenda de 5 nm. Sob estas condições, um aumento linear na fluorescência indica um aumento da taxa de liberação do H_2O_2 pelas mitocôndrias. Uma curva de calibração foi feita através da adição de concentrações conhecidas de peróxido de hidrogênio.

Análises Estatísticas

Os dados são apresentados como média ± epm. Todas as figuras apresentadas nos resultados são representativas de pelo menos 4 experimentos realizados com preparações biológicas independentes. As análises estatísticas foram feitas utilizando ANOVA para comparações múltiplas, seguida pelo pós teste de Tukey com nível de significância $p<0,05$.

RESULTADOS

Indução de transição de permeabilidade mitocondrial por Cramoll 1,4 em mitocôndrias de fígado de rato

A obtenção de um bom protocolo de isolamento da fração mitocondrial de *T. cruzi*, mitocôndria acoplada e com capacidade de fosforilar ADP, levou-nos a estudar mais

detalhadamente a ação de Cramoll 1,4 na mitocôndria do parasita. Para isso avaliamos, em paralelo, a ação dessa lectina em mitocôndrias isoladas de fígado de rato (MFR), uma vez que nesse modelo o mecanismo de transição de permeabilidade mitocondrial é amplamente estudado.

A incubação de MFR na presença de Cramoll 1,4 (50 μg/ml) em meio de reação padrão contendo Ca^{2+} resultou em um significativo inchamento da organela visualizado pela queda na absorbância, em virtude de uma menor turbidez da suspensão mitocondrial (Fig. 10, *linha cinza claro*) quando comparado com o controle (Fig. 10, *linha preta*).

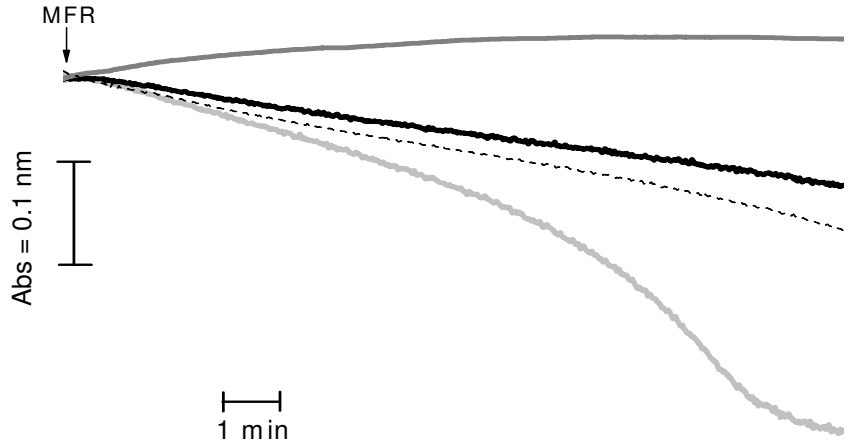

Fig. 10: Inibição do inchamento mitocondrial induzido por Cramoll 1,4 em mitocôndrias de fígado de rato por inibidores do poro de transição de permeabilidade. Mitocôndrias de fígado de rato (MFR, 0,5 mg/ml) foram incubadas em meio de reação padrão contendo 30 μM de Ca^{2+} (*linha preta*) ou 50 μg/ml de Cramoll 1,4 + 30 μM de Ca^{2+} (*linha cinza claro*) na presença de inibidores do poro de transição de permeabilidade mitocondrial: catalase (2 μM, *linha pontilhada*), EGTA (0,5mM, *linha cinza escuro*) ou ciclosporina A (CsA, 1μM, *linha cinza escuro*). Os gráficos mostrados são representativos de quatro experimentos independentes.

A abertura do poro de transição de permeabilidade mitocondrial (PTPM) é induzida por Ca^{2+}, substâncias químicas e estresse oxidativo e pode ser inibida na presença de ciclosporina A (CsA), agentes redutores de grupamentos tióis, antioxidantes e pH menor que 7,0 (Kowaltowski et al., 2009; Lemasters et al., 2009). A fim de avaliarmos se o efeito da lectina na organela foi decorrente da abertura do PTPM incubamos Cramoll 1,4 na

presença de catalase (Fig. 10, *linha pontilhada*), EGTA ou CsA (Fig. 10, *linha cinza escuro*) e verificamos uma proteção total do inchamento. Esses resultados mostram que a lectina causa permeabilização da membrana mitocondrial, dependente de Ca^{2+}, com conseqüente abertura do PTPM.

Ciclosporina não previne contra a perda do potencial elétrico de membrana mitocondrial ($\Delta\Psi_m$) induzido pela lectina em mitocôndrias de *T. cruzi*

A fim de compreendermos melhor a ação de Cramoll 1,4 na mitocôndria realizamos experimentos de $\Delta\Psi_m$ com mitocôndrias de fígado de rato, uma vez que através dos experimentos de inchamento verificamos que a lectina também tem uma ação direta nessas mitocôndrias. A abertura do PTPM permite a entrada de moléculas (1,5 kDa) e água resultando no inchamento da organela. Este processo causa eliminação do $\Delta\Psi_m$ e conseqüentemente da fosforilação oxidativa (Inada et al., 2008).

Cramoll 1,4 dissipou completamente o $\Delta\Psi_m$ em mitocôndrias de fígado de rato (Fig. 11A, *linha cinza claro*) em comparação com o controle (Fig. 11A, *linha preta*). Em concordância com os experimentos de inchamento, na presença de catalase (Fig. 11A, *linha pontilhada*), EGTA ou CsA (Fig. 11B, *linha cinza escuro*) houve proteção contra a perda do $\Delta\Psi_m$ e da fosforilação oxidativa.

Na primeira parte do trabalho vimos que em *T. cruzi,* tanto em células inteiras quanto em mitocôndrias isoladas na presença de Ca^{2+}, Cramoll 1,4 causou uma redução no $\Delta\Psi_m$ (Fig. 5B e 8B). Uma vez que verificamos a abertura do poro de transição de permeabilidade em MFR, o próximo passo foi avaliar se o mesmo estava ocorrendo nas frações mitocondriais de *T. cruzi*. No entanto, diferentemente do que foi observado em MFR, em mitocôndrias de *T. cruzi* não verificamos uma proteção contra a perda do $\Delta\Psi_m$ na presença de CsA (Fig. 11B, *linha cinza escuro*). Interessantemente, a catalase conferiu proteção (Fig. 11B, *linha pontilhada*).

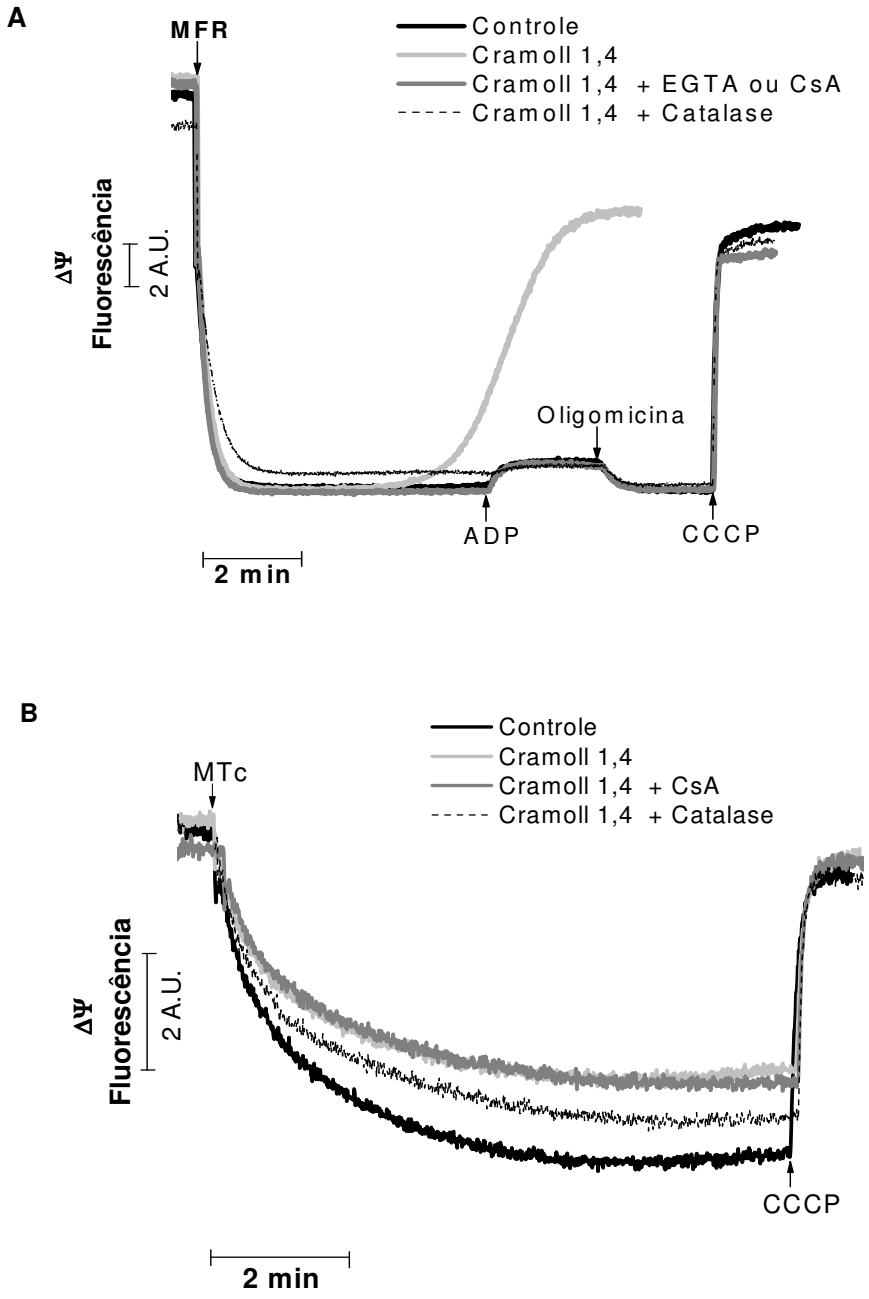

Fig. 11: Efeito de Cramoll 1,4 no potencial elétrico (ΔΨ) de mitocôndrias isoladas na presença de inibidores do poro de transição de permeabilidade. Mitocôndrias isoladas (0,5 mg/ml) de fígado de rato (MFR, Figura A) ou frações mitocondriais de *T. cruzi* (MTc, Figura B) foram incubadas em meio de reação padrão contendo Cramoll 1,4 (50 µg/ml) + Ca^{2+} (10 µM) na presença de inibidores do poro de transição de permeabilidade mitocondrial: ciclosporina A (CsA, 1µM), EGTA (0,5 mM) ou catalase (2 µM). ADP (200 µM), oligomicina (1 µg/ml) e CCCP (1 µM) foram adicionados onde indicado pelas setas. Nos exprimentos com MTc foi adicionado BSA (0,05 %) ao meio de reação. Os gráficos mostrados são representativos de quatro experimentos independentes.

Cramoll 1,4 aumenta a produção de H_2O_2 mitocondrial

Os experimentos feitos com células inteiras revelaram que o tratamento com Cramoll 1,4 causava uma condição de estresse oxidativo no parasita (Fig. 7).

Como pode ser observado na Fig. 12, avaliando essa situação em mitocôndrias isoladas com uma sonda específica para H_2O_2, demonstramos a participação da mitocôndria na produção de EROs induzida pela lectina. Observamos um significativo aumento na produção de H_2O_2, sensível a EGTA, tanto em mitocôndrias de fígado de rato quanto em mitocôndrias de *T. cruzi* (Fig. 12A e B), no entanto como observado nos experimentos de $\Delta\Psi_m$ (Fig. 11B, linha *cinza escuro*) esse efeito foi insensível a CsA, no parasita (Fig. 12B).

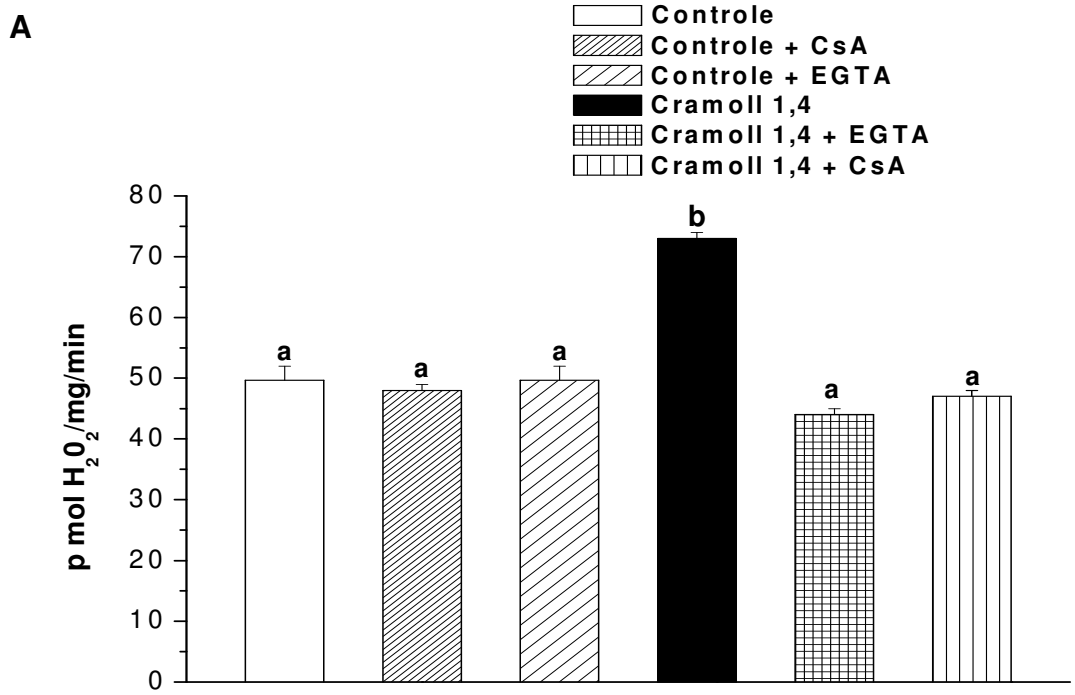

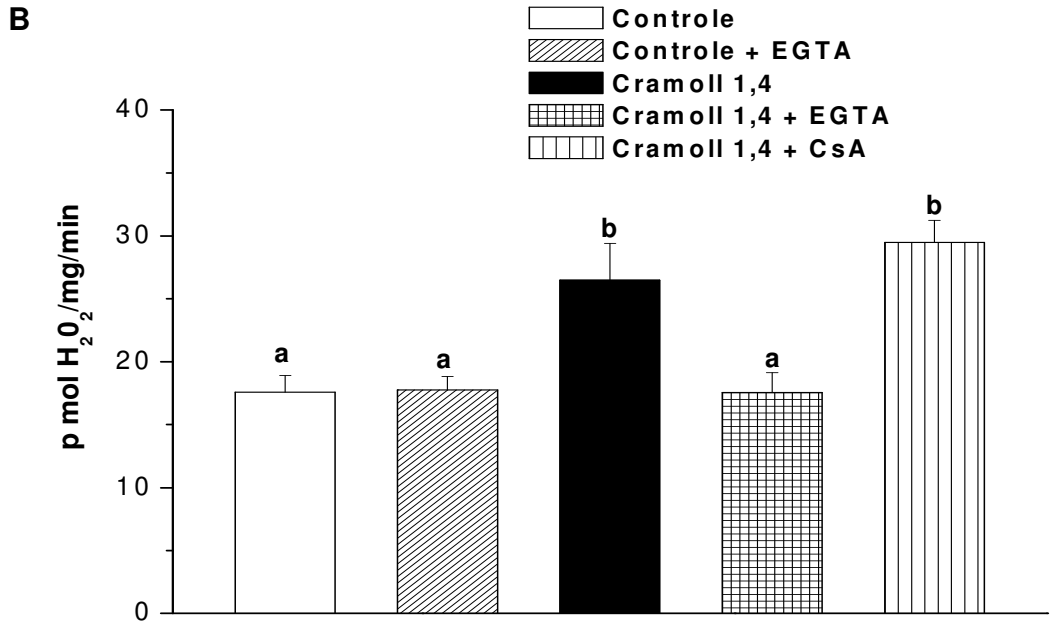

Fig. 12: Efeito de Cramoll 1,4 na produção de H_2O_2 em mitocôndrias isoladas na presença de inibidores do poro de transição de permeabilidade. Mitocôndrias isoladas (0,5 mg/ml) de fígado de rato (MFR, Figura A) ou frações mitocondriais de *T. cruzi* (MTc, Figura B) foram incubadas em meio de reação padrão contendo Cramoll 1,4 (50 µg/ml) + Ca^{2+} (10 µM) na presença de inibidores do poro de transição de permeabilidade mitocondrial: ciclosporina A (CsA, 1µM) ou EGTA (500 µM). Os gráficos mostrados são representativos de quatro experimentos independentes. $p<0,05$ entre grupos distintos, representados por letras diferentes.

4 – DISCUSSÃO

O uso de lectinas em *T. cruzi* durante muito tempo esteve limitado ao reconhecimento de glicoconjugados de superfície celular, para avaliar mudanças na composição de membrana entre as diferentes formas evolutivas ou diferentes fases do ciclo celular do parasita (Alves e Colli, 1974; Bourguignon et al., 1998).

No presente trabalho, demonstramos que a lectina Cramoll 1,4 liga-se a glicoconjugados presentes na superfície celular de epimastigotas e tripomastigotas levando à aglutinação do parasita de forma dose dependente (Fig. 1). Como conseqüência dessa ligação, ocorre permeabilização da membrana plasmática promovendo um influxo de Ca^{2+} do meio externo e posterior acúmulo pela mitocôndria, levando a uma situação de estresse oxidativo e morte do parasita.

Em contraste, a lectina não causou morte em queratinócitos, outro modelo celular (Fig. 3). Isso pode ser explicado pelo fato de uma lectina ligar-se a glicoconjugados de superfície celular e não necessariamente levar à permeabilização da membrana plasmática e sinalização para morte celular. A Cramoll 1,4, dentre outras lectinas, apresenta atividade mitogênica a partir da ligação a domínios específicos na membrana (Maciel et al., 2004; Zheng et al., 2007). O tipo de receptor ao qual a lectina se liga é que determina o tipo de sinal que será desencadeado na célula (Benoist et al., 2009). Diferente do que ocorre em *T. cruzi*, em queratinócitos a Cramoll 1,4, provavelmente, não se liga a um domínio que resulte em permeabilização de membrana plasmática e conseqüente morte celular.

Em *T. cruzi* foi visto que a interação Cramoll 1,4-glicoconjugado reduz a viabilidade (Fig. 2A) e inibe a proliferação celular (Fig. 2B), causando a morte do parasita (Fig. 9). Os eventos celulares que precedem essa morte foram, então, investigados com a forma epimastigota de *T. cruzi*.

Em decorrência da permeabilização de membrana plasmática, observamos um influxo de Ca^{2+} e posterior acúmulo pela mitocôndria (Fig. 4). Vários estudos demonstram que a homeostase mitocondrial de Ca^{2+} desempenha um papel importante na modulação de vários processos celulares fisiológicos e que alterações nessa homeostase podem sinalizar o início do processo de morte celular (Giacomelo et al., 2007; Kowaltowski et al., 2001). Um importante processo relacionado ao Ca^{2+}, tanto na apoptose, necrose ou necroptose, é a transição de permeabilidade mitocondrial (TPM). A sobrecarga mitocondrial de Ca^{2+} é suficiente para induzir TPM (Kowaltowski et al., 2001). Apesar de a mitocôndria de *T.*

cruzi apresentar alta capacidade de estocar esse Ca^{2+} (Docampo e Vercesi, 1989), quando comparado a mitocôndrias de eucariotos, sob certas condições experimentais, sobrecarga de Ca^{2+} na mitocôndria pode levar à disfunção mitocondrial e morte do parasita (Irigoin et al., 2009). Entretanto, até o momento não foi observado o processo de TPM em *T. cruzi*.

Como tínhamos visto que o Ca^{2+} internalizado pelo *T. cruzi* estava sendo acumulado na mitocôndria (Fig. 4), avaliamos também o $\Delta\Psi_m$ e o consumo de oxigênio após incubação dos parasitas com a lectina. Após 2h de incubação com Cramoll 1,4, na presença de Ca^{2+}, verificamos diminuição significativa do $\Delta\Psi_m$ do parasita, com prezuízo da fosforilação oxidativa (Fig. 5B). Os experimentos de respiração mostraram que a lectina age como um desacoplador uma vez que, na presença de oligomicina, verificamos um aumento de 65% na velocidade de consumo de oxigênio (Fig. 6).

Em trabalho prévio (Irigoin et al., 2009), mostramos que epimastigotas de *T. cruzi* expostos a soro humano fresco na presença de Ca^{2+} sofrem morte celular mediada pela permeabilização de membrana plasmática através da deposição do complexo de ataque à membrana (MAC) na superfície celular do parasita. Essa permeabilização antecedeu um influxo de Ca^{2+} na célula e sobrecarga de Ca^{2+} mitocondrial, condição que estimulou a produção de EROs pela mitocôndria. Grijalba et al. (1999) mostraram que a sobrecarga de Ca^{2+} mitocondrial altera a organização de lipídeos da membrana mitocondrial interna devido à interação com a cabeça aniônica da cardiolipina, um fosfolipídeo abundante na membrana mitocondrial interna. Essas alterações na organização da membrana podem afetar a cadeia respiratória, incluindo mobilidade da coenzima Q, favorecendo a redução monoeletrônica do O_2 (geração $O_2^{\bullet-}$) como etapa intermediária da cadeia respiratória, que resulta em dano oxidativo mitocondrial seguido de morte celular. Semelhante ao que foi verificado com o soro humano fresco, a permeabilização da membrana plasmática de epimastigotas pela lectina também estimulou significativamente a produção de EROs pelo parasita (Fig. 7).

Os protozoários da ordem Kinetoplastida, como o *T. cruzi*, apresentam uma única mitocôndria, ocupando até 12 % do volume celular do parasita (Paulin et al., 1975). A complexidade ultraestrutural e algumas características dos processos bioenergéticos que ocorrem nessa organela, até o presente momento, são pouco conhecidas. Esse fato deve-se, principalmente, à dificuldade de se obter uma mitocôndria intacta após o rompimento da

membrana plasmática do parasita, devido às dimensões da organela e à presença de microtúbulos aderidos ao lado interno da membrana plasmática. Por conta disso, o estudo da bioenergética mitocondrial de parasitas flagelados tem sido feito com células inteiras permeabilizadas com digitonina, um glicosídeo esteróide com propriedades detergentes capazes de permeabilizar a membrana plasmática (Vercesi et al., 1991).

Nesse sentido, para verificar se o efeito da lectina em epimastigotas era estritamente conseqüência da permeabilização da membrana plasmática, utilizamos a digitonina como controle positivo. Apesar de a captação de Ca^{2+} promovida pela digitonina ter sido ligeiramente maior quando comparada àquela induzida pela lectina (Fig. 4), os efeitos da Cramoll 1,4 na mitocôndria foram mais intensos do que aqueles causado pela digitonina, como ilustrado pela maior produção de EROs (Fig. 7) e pela diminuição significativa no $\Delta\Psi_m$ e na fosforilação oxidativa (Fig. 5A). No entanto, a incubação do parasita com digitonina por longos períodos de tempo causa disfunção mitocondrial (Fig. 5B). Conhecendo essa limitação em relação ao estudo *in situ* da mitocôndria do parasita, nós estabelecemos um protocolo de isolamento que proveu uma fração mitocondrial acoplada e com capacidade de fosforilar ADP. Isso nos incentivou a investigar mais direta e detalhadamente a ação da Cramoll 1,4 em mitocôndrias isoladas de *T. cruzi*.

Os resultados indicaram que a Cramoll 1,4, mas não a digitonina, causou uma diminuição significativa no $\Delta\Psi_m$ em mitocôndrias isoladas de epimastigotas incubadas em meio de reação padrão contendo Ca^{2+} (Fig. 8B). Quando em meio livre de Ca^{2+}, a Cramoll 1,4 não afetou a capacidade da mitocôndria de fosforilar o ADP adicionado (Fig. 8A). O efeito direto da lectina na mitocôndria pode explicar a diferença no mecanismo de morte de epimastigotas causado por esta lectina (necrose) (Fig. 9) quando comparado àquele induzido pelo soro humano fresco, que também permeabiliza a membrana plasmática e causa morte de epimastigotas de *T. cruzi* por apoptose (Irigoin et al., 2009).

A determinação do tipo de morte celular não é um processo fácil. Muitos autores têm questionado as metodologias utilizadas para definir esses tipos de morte e as interpretações dos resultados, uma vez que as vias de apoptose e necrose programada (necroptose) se interligam em alguns pontos (para revisão, ver Galluzi e Kroemer, 2008). É preciso que vários indicadores demonstrem a ocorrência predominante de um tipo de morte celular em relação a outro. Nossos resultados, segundo o estabelecido por Kroemer et al.

(2009), são mais condizentes com morte predominantemente por necrose, uma vez que constatamos: 1. permeabilização precoce de membrana plasmática, através da incorporação de iodeto de propídeo (Fig. 9); 2. sobrecarga mitocondrial de Ca^{2+} (Fig. 4); 3. disfunções mitocondriais, com prezuízo da fosforilação oxidativa e privação de ATP (Fig. 5), desacoplamento (Fig. 6), aumento na produção de EROs (Fig. 7) e 4. ausência de fragmentação de DNA (essa fragmentação é característica de morte apoptótica).

A fim de compreendermos melhor a ação da lectina realizamos também experimentos com mitocôndrias isoladas de fígado de rato (MFR), uma vez que nesse modelo a bioenergética mitocondrial é bastante estudada e conhecida (Coelho e Vercesi, 1980; Vercesi, 1987; Kowaltowski et al., 2001). Observamos que a Cramoll 1,4 promove inchamento em MFR decorrente da abertura do poro de transição de permeabilidade mitocondrial (PTPM), uma vez que, na presença de inibidores desse poro, como CsA, catalase ou EGTA, houve uma proteção total do inchamento da organela promovido pela lectina (Fig. 10). Para confirmar esse resultado, analisamos o $\Delta\Psi_m$ e a produção de H_2O_2, uma vez que a abertura do poro causa dissipação do $\Delta\Psi_m$ e conseqüente prejuízo à fosforilação oxidativa (Inada et al., 2008), podendo haver aumento na produção de EROs pela mitocôndria. Verificou-se que a Cramoll 1,4 causa um colapso no $\Delta\Psi_m$ em MFR, podendo ser prevenido por CsA, catalase ou EGTA (Fig. 11A). A produção de H_2O_2 induzida por Cramoll 1,4 também foi reduzida por CsA ou EGTA (Fig. 12A), indicando que aumento na produção de EROs induzido pela lectina ocorre em decorrência da abertura do PTPM. Embora os mecanismos que ligam a captação mitocondrial de Ca^{2+} à produção de EROs ainda não estejam claramente definidos, trabalhos da literatura tem demonstrado que o processo de TPM ocorre com a participação de Ca^{2+} e aumento de EROs (Kowaltowski et al., 2009). Em mitocôndrias isoladas de cérebros de roedores e de fígado humano, por exemplo, foi demonstrado que a geração de EROs induzida por Ca^{2+} é mediada pela transição de permeabilidade (Hansson et al., 2008).

Nas frações mitocondriais de *T. cruzi* também foi observada permeabilização da membrana mitocondrial do parasita pela lectina, com significativa perda do $\Delta\Psi_m$ (Fig. 8B). No entanto, diferente do que foi observado em MFR, não houve proteção na presença de CsA, apenas com EGTA ou catalase (Fig. 11B). Essa falta de proteção pela CsA pode ocorrer pela ausência de ciclofilina D na mitocôndria do parasita. Artigos da literatura tem

mostrado a existência de genes da família das ciclofilinas em *T. cruzi* (Búa et al., 2001; Carraro et al., 2006; Potenza et al., 2006) e muitas dessas isoformas de ciclofilinas, dentre elas a TcCyP 19, TcCyP 22, TcCyP 28 e TcCyP 40 apresentam afinidade de ligação à CsA. No entanto, esses trabalhos foram feitos com extratos de *T. cruzi* e nenhum deles investigou a localização dessas proteínas no parasita. É conhecido que as ciclofilinas de eucariotos estão localizadas em diferentes estruturas celulares como citoplasma (Hanschumacher et al., 1984), mitocôndria (Schneider et al., 1994), retículo endoplasmático (Bergsma et al., 1991), spliceossomo (Tiegelkamp et al., 1998), núcleo e membrana nuclear (Anderson et al., 1993; Yokoyama et al., 1995).

Com base em nosso protocolo de isolamento de frações mitocondriais de *T. cruzi,* estudos podem ser feitos para investigar a existência de ciclofilinas em mitocôndria do parasita. Independente da presença ou não de ciclofilina mitocondrial em *T. cruzi*, nossos resultados mostraram que a Cramoll 1,4 induz transição de permeabilidade mitocondrial dependente de cálcio, tanto em MFR quanto em frações mitocondriais de *T. cruzi*. Esse processo leva ao acúmulo de cálcio na mitocôndria, aumento na geração de EROs e morte do parasita por necrose.

5 – CONCLUSÕES

Neste trabalho mostramos que, após a ligação da Cramoll 1,4 a glicoconjugados presentes na superfície celular de epimastigotas e tripomastigotas de *T. cruzi*, houve aglutinação do parasita de forma dose dependente. Essa ligação lectina-glicoconjugado reduziu a viabilidade celular e inibiu a capacidade de proliferação de epimastigotas em decorrência da permeabilização da membrana plasmática, levando à internalização de Ca^{2+} do meio externo e acúmulo pela mitocôndria, com conseqüente disfunção mitocondrial, aumento da produção de EROs e conseqüente morte do parasita.

Nossos estudos sobre a ação da Cramoll 1,4 em mitocôndrias isoladas mostraram que a lectina causa TPM, dependente de Ca^{2+}, tanto em mitocôndrias de fígado de rato quanto em frações mitocondriais de *T. cruzi*, promovendo aumento na produção de H_2O_2. Entretanto, ao contrário do que foi observado em mitocôndrias de fígado de rato, o efeito de Cramoll 1,4 em frações mitocondriais de *T. cruzi* é insensível a CsA, um inibidor clássico do poro de transição de permeabilidade mitocondrial em células eucarióticas.

6 – REFERÊNCIAS BIBLIOGRÁFICAS

Acquatela H. Heart pathology of extracardiac origin (V). Recent advances in chagasic cardiomyopathy. Rev Esp Cardiol. 1998;51:152-7.

Adams JM, Cory S. Life-or-death decisions by the Bcl-2 protein family. Trends Biochem Sci. 2001;26(1):61-6.

Affranchino JL, Schwarcz de Tarlovsky MN, Stoppani AO. Terminal oxidases in the trypanosomatid *Trypanosoma cruzi*. Comp Biochem Physiol B. 1986;85(2):381-8.

Afonso-Cardoso SR, Rodrigues FH, Gomes MA, Silva AG, Rocha A, Guimaraes AH, et al. Protective effect of lectin from *Synadenium carinatum* on *Leishmania amazonensis* infection in BALB/c mice. Korean J Parasitol. 2007;45(4):255-66.

Åkerman KEO, Wikstrom KF. Safranine as a probe of the mitochondrial membrane potential. FEBS Lett. 1976;68:191-7.

Alphey MS, Leonard GA, Gourley DG, Tetaud E, Fairlamb AH, Hunter WN. The high resolution crystal structure of recombinant *Crithidia fasciculata* tryparedoxin-I. J Biol Chem. 1999;274(36):25613-22.

Alphey MS, Bond CS, Tetaud E, Fairlamb AH, Hunter WN. The structure of reduced tryparedoxin peroxidase reveals a decamer and insight into reactivity of 2Cys-peroxiredoxins. J Mol Biol. 2000;300(4):903-16.

Anderson SK, Gallinger S, Roder J, Frey J, Young HA, Ortaldo JR. A cyclophilin-related protein involved in the function of natural killer cells. Proc Natl Acad Sci USA. 1993;90(2):542-6.

Andreyev A, Bondareva TO, Dedukhova VI, Mokhova EN, Skulachev VP, Tsofina LM, et al. The ATP/ADP-antiporter is involved in the uncoupling effect of fatty acids on mitochondria. Eur J Biochem. 1989;182(3):585-92.

Aragon AM, Cavalle CT, A., Frühbeck GS, A., Santidrian S. Mitogenicity of isolectins isolated from *Phaseolus vulgaris L. var. athropurpurea* in rat spleen lymphocytes. Food Research International. 1993;26(6):451-3.

Baines CP, Kaiser RA, Purcell NH, Blair NS, Osinska H, Hambleton MA, et al. Loss of cyclophilin D reveals a critical role for mitochondrial permeability transition in cell death. Nature. 2005;434(7033):658-62.

Bantel H, Engels IH, Voelter W, Schulze-Osthoff K, Wesselborg S. Mistletoe lectin activates caspase-8/FLICE independently of death receptor signaling and enhances anticancer drug-induced apoptosis. Cancer Res. 1999;59(9):2083-90.

Barret M, Burchmore R, Stich A, Lazzari J, Frasch A, Cazzulo JJ. The Trypanosomiases. Lancet. 2003;362:1469-80.

Beltrao EI, Correia MT, Figueredo-Silva J, Coelho, L C. Binding evaluation of Isoform 1 from *Cratyllia mollis* lectins to human mammary tissues. Appl Biochem Biotechnol. 1998;74(3):125-34.

Benoist H, Culerrier R, Poiroux G, Segui B, Jauneau A, Van Damme EJ, et al. Two structurally identical mannose-specific jacalin-related lectins display different effects on human T lymphocyte activation and cell death. J Leukoc Biol. 2009;86(1):103-14.

Bergsma DJ, Eder C, Gross M, Kersten H, Sylvester D, Appelbaum E, et al. The cyclophilin multigene family of peptidyl-prolyl isomerases. Characterization of three separate human isoforms. J Biol Chem. 1991;266(34):23204-14.

Berlett BS, Stadtman ER. Protein oxidation in aging, disease, and oxidative stress. J Biol Chem. 1997;272(33):20313-6.

Bernardes CF, Meyer-Fernandes JR, Basseres DS, Castilho RF, Vercesi AE. Ca^{2+}-dependent permeabilization of the inner mitochondrial membrane by 4,4'-diisothiocyanatostilbene-2,2'-disulfonic acid (DIDS). Biochim Biophys Acta. 1994;1188:93-100.

Bernardi P. Modulation of the mitochondrial cyclosporin A-sensitive permeability transition pore by the proton electrochemical gradient. Evidence that the pore can be opened by membrane depolarization. J Biol Chem. 1992;267(13):8834-9.

Bezerra SF, Vieira VLA, Carvalho Jr LB. Proteases no trato digestivo de peixes. Biotecnologia Ciência e Desenvolvimento. 2001;22:26-9.

Bhowal J, Guha AK, Chatterjee BP. Purification and molecular characterization of a sialic acid specific lectin from the phytopathogenic fungus *Macrophomina phaseolina*. Carbohydr Res. 2005;340(12):1973-82.

Bourguignon SC, de Souza W, Souto-Padron T. Localization of lectin-binding sites on the surface of *Trypanosoma cruzi* grown in chemically defined conditions. Histochem Cell Biol. 1998;110(5):527-34.

Boveris A, Chance B. The mitochondrial generation of hydrogen peroxide. General properties and effect of hyperbaric oxygen. Biochem J. 1973;134(3):707-16.

Boveris A, Cadenas E, Stoppani AO. Role of ubiquinone in the mitochondrial generation of hydrogen peroxide. Biochem J. 1976;156(2):435-44.

Boyd WC, Shapleigh E. Specific Precipitating Activity of Plant Agglutinins (Lectins). Science. 1954;119(3091):419.

Branche C, Ochaya S, Aslund L, Andersson B. Comparative karyotyping as a tool for genome structure analysis of *Trypanosoma cruzi*. Mol Biochem Parasitol. 2006;147(1):30-8.

Brazil V, Entlicher G. Complexity of lectins from the hard roe of perch (*Perca fluviatilis* L.). The International Journal of Biochemistry & Cell Biology. 1999;31:431-42.

Breckenridge DG, Xue D. Regulation of mitochondrial membrane permeabilization by BCL-2 family proteins and caspases. Curr Opin Cell Biol. 2004;16(6):647-52.

Brener Z. *Trypanossoma cruzi*: taxonomy, morphology and life cicle. In: Wendel S, Brener Z, Camargo ME, Rassi A, editors. Chaga's disease (American trypanosomiasis): its impact on transfusion and clinical medicine São Paulo: ISBT; 1992. p.13-30.

Bringaud F, Riviere L, Coustou V. Energy metabolism of trypanosomatids: adaptation to available carbon sources. Mol Biochem Parasitol. 2006;149(1):1-9.

Broekemeier KM, Dempsey ME, Pfeiffer DR. Cyclosporin A is a potent inhibitor of the inner membrane permeability transition in liver mitochondria. J Biol Chem. 1989;264(14):7826-30.

Brustovetsky N, Klingenberg M. Mitochondrial ADP/ATP carrier can be reversibly converted into a large channel by Ca^{2+}. Biochemistry. 1996;35(26):8483-8.

Bua J, Aslund L, Pereyra N, Garcia GA, Bontempi EJ, Ruiz AM. Characterisation of a cyclophilin isoform in *Trypanosoma cruzi*. FEMS Microbiol Lett. 2001;200(1):43-7.

Burleigh BA, Andrews NW. Signaling and host cell invasion by *Trypanosoma cruzi*. Current Opinion in Microbiology. 1998;1:461-65.

Cadenas E, Boveris A, Ragan CI, Stoppani AO. Production of superoxide radicals and hydrogen peroxide by NADH-ubiquinone reductase and ubiquinol-cytochrome c reductase from beef-heart mitochondria. Arch Biochem Biophys. 1977;180(2):248-57.

Cadenas E, Boveris A. Enhancement of hydrogen peroxide formation by protophores and ionophores in antimycin-supplemented mitochondria. Biochem J. 1980;188(1):31-7.

Campbell AK. Intracellular calcium. Its Universal role as regulator. New York: John Wiley & Sons Limited; 1983.

Carafoli E. Intracellular calcium homeostasis. Annu Rev Biochem. 1987;56:395-433.

Carranza JC, Kowaltowski AJ, Mendonca MA, de Oliveira TC, Gadelha FR, Zingales B. Mitochondrial bioenergetics and redox state are unaltered in *Trypanosoma cruzi* isolates with compromised mitochondrial complex I subunit genes. J Bioenerg Biomembr. 2009;41(3):299-308.

Castellani O, Ribeiro LV, Fernandes JF. Differentiation of *Trypanosoma cruzi* in culture. J Protozool. 1967;14(3):447-51.

Castilho RF, Meinicke AR, Almeida AM, Hermes-Lima M, Vercesi AE. Oxidative damage of mitochondria induced by Fe(II)citrate is potentiated by Ca^{2+} and includes lipid peroxidation and alterations in membrane proteins. Arch Biochem Biophys. 1994;308(1):158-63.

Castilho RF, Kowaltowski AJ, Meinicke AR, Vercesi AE. Oxidative damage of mitochondria induced by Fe(II)citrate or t-butyl hydroperoxide in the presence of Ca^{2+}: effect of coenzyme Q redox state. Free Radic Biol Med. 1995;18(1):55-9.

Castilho RF, Kowaltowski AJ, Vercesi AE. The irreversibility of inner mitochondrial membrane permeabilization by Ca^{2+} plus prooxidants is determined by the extent of membrane protein thiol cross-linking. J Bioenerg Biomembr. 1996;28(6):523-9.

Cavada BS, Santos CF, Grangeiro TB, Nunes EP, Sales PV, Ramos RL, et al. Purification and characterization of a lectin from seeds of *Vatairea macrocarpa* Duke. Phytochemistry. 1998;49(3):675-80.

Cazzulo JJ. Intermediate metabolism in *Trypanosoma cruzi*. J Bioenerg Biomembr. 1994;26(2):157-65.

Chagas C. Nouvelle espèce de trypanosomiase humaine. Bulletin de la Société de Pathologie Exotique. 1909;2:304-7.

Chance B, Sies H, Boveris A. Hydroperoxide metabolism in mammalian organs. Physiol Rev. 1979;59(3):527-605.

Cheung AH, Wong JH, Ng TB. *Musa acuminata* (Del Monte banana) lectin is a fructose-binding lectin with cytokine-inducing activity. Phytomedicine. 2009;16(6-7):594-600.

Chung JJ, Ratnapala LA, Cooke IM, Yanagihara AA. Partial purification and characterization of a hemolysin (CAH1) from *Hawaiian box* jellyfish (*Carybdea alata*) venom. Toxicon. 2001;39(7):981-90.

Cinerman B, Cinerman S. Parasitologia humana e seus fundamentos gerais. São Paulo: Atheneu; 1999. p.85-7.

Coelho JLC, Vercesi AE. Retention of Ca^{2+} by rat liver and heart mitochondria: Effect of phosphate, Mg^{2+}, and NAD(P) redox state. Archives of Biochemistry and Biophysics. 1980;204(1):141-7.

Coelho LCBB, Silva MBR. Simple method to purify milligram quantities of the galactose-specific lectin from the leaves of *Bauhinia monandra*. Phytochemical Analysis. 2000;11:295-300.

Coelho MB, Marangoni S, Macedo ML. Insecticidal action of *Annona coriacea* lectin against the flour moth *Anagasta kuehniella* and the rice moth *Corcyra cephalonica*

(Lepidoptera: Pyralidae). Comp Biochem Physiol C Toxicol Pharmacol. 2007;146(3):406-14.

Correia MT, Coelho LC. Purification of a glucose/mannose specific lectin, isoform 1, from seeds of *Cratylia mollis* Mart. (Camaratu bean). Appl Biochem Biotechnol. 1995;55(3):261-73.

Coura JR, de Castro SL. A critical review on Chagas disease chemotherapy. Memórias do Instituto Oswaldo Cruz. 2002;97:3-24.

Crompton M, Ellinger H, Costi A. Inhibition by cyclosporin A of a Ca^{2+}-dependent pore in heart mitochondria activated by inorganic phosphate and oxidative stress. Biochem J. 1988;255(1):357-60.

Crompton M, Virji S, Ward JM. Cyclophilin-D binding proteins. Biochem Soc Trans. 1998 Nov;26(4):S330.

Crompton M. The mitochondrial permeability transition pore and its role in cell death. Biochem J. 1999;341(Pt 2):233-49.

Crompton M. Mitochondrial intermembrane junctional complexes and their role in cell death. J Physiol. 2000;529 (Pt 1):11-21.

Datta K, Usha R, Dutta SK, Singh M. A comparative study of the winged bean protease inhibitors and their interaction with proteases. Plant Physiology and Biochemistry. 2001;39:949-59.

De Souza GA, Oliveira PS, Trapani S, Santos AC, Rosa JC, Laure HJ, et al. Amino acid sequence and tertiary structure of *Cratylia mollis* seed lectin. Glycobiology. 2003;13(12):961-72.

DePierre JW, Ernster L. Enzyme topology of intracellular membranes. Annu Rev Biochem. 1977;46:201-62.

Dias JCP, Prata A, Schofield CJ. Chaga's disease in the Amazon: an overview of the current situation and perspectives for prevention. Revista da Sociedade Brasileira de Medicina Tropical 2002;35(6):669-78.

Docampo R, de Boiso JF, Stoppani AO. Tricarboxylic acid cycle operation at the kinetoplast-mitochondrion complex of *Trypanosoma cruzi*. Biochim Biophys Acta. 1978;502(3):466-76.

Docampo R, Vercesi AE. Ca^{2+} transport by coupled *Trypanosoma cruzi* mitochondria in situ. J Biol Chem. 1989;264(1):108-11.

Du C, Fang M, Li Y, Li L, Wang X. Smac, a mitochondrial protein that promotes cytochrome c-dependent caspase activation by eliminating IAP inhibition. Cell. 2000;102(1):33-42.

Duffieux F, Van Roy J, Michels PA, Opperdoes FR. Molecular characterization of the first two enzymes of the pentose-phosphate pathway of Trypanosoma brucei. Glucose-6-phosphate dehydrogenase and 6-phosphogluconolactonase. J Biol Chem. 2000;275(36):27559-65.

Elgavish S, Shaanan B. Lectin-carbohydrate interactions: different folds, common recognition principles. Trends Biochem Sci. 1997;22(12):462-7.

Fagian MM, Pereira-da-Silva L, Martins IS, Vercesi AE. Membrane protein thiol cross-linking associated with the permeabilization of the inner mitochondrial membrane by Ca^{2+} plus prooxidants. J Biol Chem. 1990;265(32):19955-60.

Fairlamb AH, Cerami A. Metabolism and functions of trypanothione in the Kinetoplastida. Annu Rev Microbiol. 1992;46:695-729.

Ferranti R, da Silva MM, Kowaltowski AJ. Mitochondrial ATP-sensitive K^+ channel opening decreases reactive oxygen species generation. FEBS Lett. 2003;536(1-3):51-5.

Festjens N, Vanden Berghe T, Vandenabeele P. Necrosis, a well-orchestrated form of cell demise: signalling cascades, important mediators and concomitant immune response. Biochim Biophys Acta. 2006;1757(9-10):1371-87.

Finzi JK, Chiavegatto CW, Corat KF, Lopez JA, Cabrera OG, Mielniczki-Pereira AA, et al. *Trypanosoma cruzi* response to the oxidative stress generated by hydrogen peroxide. Mol Biochem Parasitol. 2004;133(1):37-43.

Fournier N, Ducet G, Crevat A. Action of cyclosporine on mitochondrial calcium fluxes. J Bioenerg Biomembr. 1987;19(3):297-303.

Galluzzi L, Kroemer G. Necroptosis: a specialized pathway of programmed necrosis. Cell. 2008;135(7):1161-3.

Garlid KD, Orosz DE, Modriansky M, Vassanelli S, Jezek P. On the mechanism of fatty acid-induced proton transport by mitochondrial uncoupling protein. J Biol Chem. 1996;271(5):2615-20.

Gastman B, Wang K, Han J, Zhu ZY, Huang X, Wang GQ, et al. A novel apoptotic pathway as defined by lectin cellular initiation. Biochem Biophys Res Commun. 2004;316(1):263-71.

Ghosh S, Majumder M, Majumder S, Ganguly NK, Chatterjee BP. Saracin: A lectin from *Saraca indica* seed integument induces apoptosis in human T-lymphocytes. Arch Biochem Biophys. 1999;371(2):163-8.

Giacomello M, Drago I, Pizzo P, Pozzan T. Mitochondrial Ca^{2+} as a key regulator of cell life and death. Cell Death Differ. 2007;14(7):1267-74.

Goldstein IJ, Hughes RC, Monsigny M, Osawa T, Sharon N. What should be called a lectin? Nature. 1980;255:66.

Gornall AG, Bardawill CJ, David MM. Determination of serum proteins by means of the biuret reaction. J Biol Chem. 1949;177(2):751-66.

Green DR, Reed JC. Mitochondria and apoptosis. Science. 1998;281(5381):1309-12.

Green DR. Apoptotic pathways: paper wraps stone blunts scissors. Cell. 2000;102(1):1-4.

Green DR, Kroemer G. Pharmacological manipulation of cell death: clinical applications in sight? J Clin Invest. 2005;115(10):2610-7.

Grijalba MT, Vercesi AE, Schreier S. Ca^{2+}-induced increased lipid packing and domain formation in submitochondrial particles. A possible early step in the mechanism of Ca^{2+}-stimulated generation of reactive oxygen species by the respiratory chain. Biochemistry. 1999;38(40):13279-87.

Guida MC, Esteva MI, Camino A, Flawia MM, Torres HN, Paveto C. *Trypanosoma cruzi*: *in vitro* and *in vivo* antiproliferative effects of epigallocatechin gallate (EGCg). Exp Parasitol. 2007;117(2):188-94.

Gunter TE, Pfeiffer DR. Mechanisms by which mitochondria transport calcium. Am J Physiol. 1990;258(5 Pt 1):C755-86.

Gurtler RE, Segura EL, Cohen JE. Congenital transmission of *Trypanosoma cruzi* infection in Argentina. Emerg Infect Dis. 2003;9(1):29-32.

Guzman-Partida AM, Robles-Burgueno MR, Ortega-Nieblas M, Vazquez-Moreno I. Purification and characterization of complex carbohydrate specific isolectins from wild legume seeds: *Acacia constricta* is (vinorama) highly homologous to *Phaseolus vulgaris* lectins. Biochimie. 2004;86(4-5):335-42.

Halestrap AP, Kerr PM, Javadov S, Woodfield KY. Elucidating the molecular mechanism of the permeability transition pore and its role in reperfusion injury of the heart. Biochim Biophys Acta. 1998;1366(1-2):79-94.

Handschumacher RE, Harding MW, Rice J, Drugge RJ, Speicher DW. Cyclophilin: a specific cytosolic binding protein for cyclosporin A. Science. 1984;226(4674):544-7.

Hansson MJ, Mansson R, Morota S, Uchino H, Kallur T, Sumi T, et al. Calcium-induced generation of reactive oxygen species in brain mitochondria is mediated by permeability transition. Free Radic Biol Med. 2008;45(3):284-94.

Haworth RA, Hunter DR. The Ca^{2+}-induced membrane transition in mitochondria. II. Nature of the Ca^{2+} trigger site. Arch Biochem Biophys. 1979;195(2):460-7.

Heise N, Opperdoes FR. Purification, localisation and characterisation of glucose-6-phosphate dehydrogenase of *Trypanosoma brucei*. Mol Biochem Parasitol. 1999;99(1):21-32.

Hermes-Lima M. How do Ca^{2+} and 5-aminolevulinic acid-derived oxyradicals promote injury to isolated mitochondria? Free Radic Biol Med. 1995;19(3):381-90.

Hochleitner EO, Bakry R, Huck CW, Flores F, Stöggl WM, Stecher G, et al. Analysis of isolectins on non-porous particles and monolithic polystyrene-divinylbenzene based stationary phases and electrospray ionization mass spectrometry. International Journal of Mass Spectrometry. 2003;223-224:519-26.

Inada NM, Zecchin KG, Alberici LC, Degasperi GR, Oliveira HCF. Mitochondrial oxidative stress and permeability transition: Tumor cell death, immune response and dyslipidemias. Free Radical Pahtophysiology. 2008:207-22.

Irigoin F, Inada NM, Fernandes MP, Piacenza L, Gadelha FR, Vercesi AE, et al. Mitochondrial calcium overload triggers complement-dependent superoxide-mediated programmed cell death in *Trypanosoma cruzi*. Biochem J. 2009;418(3):595-604.

Ito Y. Occurrence of lectins in leaves and flowers of *Sophora japonica*. Plant Science. 1986;47:77-82.

Juhaszova M, Wang S, Zorov DB, Nuss HB, Gleichmann M, Mattson MP, et al. The identity and regulation of the mitochondrial permeability transition pore: where the known meets the unknown. Ann N Y Acad Sci. 2008;1123:197-212.

Kabir S. Jacalin: a jackfruit (*Artocarpus heterophyllus*) seed-derived lectin of versatile applications in immunobiological research. J Immunol Methods. 1998;212(2):193-211.

Kaku H, Peumans WJ, Goldstein IJ. Isolation and characterization of a second lectin (SNA-II) present in elderberry (*Sambucus nigra* L.) bark. Arch Biochem Biophys. 1990;277(2):255-62.

Kaplan RR, Pedersen PL. Characterization of phosphate efflux pathways in rat liver mitochondria. J Biochem. 1983;212:279-88.

Kaur M, Singh K, Rup PJ, Saxena AK, Khan RH, Ashraf MT, et al. A tuber lectin from *Arisaema helleborifolium* Schott with anti-insect activity against melon fruit fly, *Bactrocera cucurbitae* (Coquillett) and anti-cancer effect on human cancer cell lines. Arch Biochem Biophys. 2006;445(1):156-65.

Kawagishi H, Mitsunaga S, Yamawaki M, Ido M, Shimada A, Kinoshita T, et al. A lectin from mycelia of the fungus Ganoderma lucidum. Phytochemistry. 1997;44(1):7-10.

Kawagishi H, Takagi J, Taira T, Murata T, Usui T. Purification and characterization of a lectin from the mushroom *Mycoleptodonoides aitchisonii*. Phytochemistry. 2001;56(1):53-8.

Kennedy JF, Paiva PMG, Correia MTS, Cavalcanti MSM, Coelho LCBB. Lectins, versatile proteins of recognition: a review. Carbohydrate Polymers. 1995;26:219-30.

Klingenberg M. Uncoupling proteins--how do they work and how are they regulated. IUBMB Life. 2001;52(3-5):175-9.

Kokoszka JE, Waymire KG, Levy SE, Sligh JE, Cai J, Jones DP, et al. The ADP/ATP translocator is not essential for the mitochondrial permeability transition pore. Nature. 2004;427(6973):461-5.

Konozy EH, Mulay R, Faca V, Ward RJ, Greene LJ, Roque-Barriera MC, et al. Purification, some properties of a D-galactose-binding leaf lectin from *Erythrina indica* and further characterization of seed lectin. Biochimie. 2002;84(10):1035-43.

Konozy EH, Bernardes ES, Rosa C, Faca V, Greene LJ, Ward RJ. Isolation, purification, and physicochemical characterization of a D-galactose-binding lectin from seeds of *Erythrina speciosa*. Arch Biochem Biophys. 2003;410(2):222-9.

Kowaltowski AJ, Castilho RF, Grijalba MT, Bechara EJ, Vercesi AE. Effect of inorganic phosphate concentration on the nature of inner mitochondrial membrane alterations mediated by Ca^{2+} ions. A proposed model for phosphate-stimulated lipid peroxidation. J Biol Chem. 1996A;271(6):2929-34.

Kowaltowski AJ, Castilho RF, Vercesi AE. Opening of the mitochondrial permeability transition pore by uncoupling or inorganic phosphate in the presence of Ca^{2+} is dependent on mitochondrial-generated reactive oxygen species. FEBS Lett. 1996B;378(2):150-2.

Kowaltowski AJ, Netto LE, Vercesi AE. The thiol-specific antioxidant enzyme prevents mitochondrial permeability transition. Evidence for the participation of reactive oxygen species in this mechanism. J Biol Chem. 1998;273(21):12766-9.

Kowaltowski AJ, Vercesi AE. Mitochondrial damage induced by conditions of oxidative stress. Free Radic Biol Med. 1999;26(3-4):463-71.

Kowaltowski AJ. Alternative mitochondrial functions in cell physiopathology: beyond ATP production. Braz J Med Biol Res. 2000;33(2):241-50.

Kowaltowski AJ, Castilho RF, Vercesi AE. Mitochondrial permeability transition and oxidative stress. FEBS Lett. 2001;495(1-2):12-5.

Kowaltowski AJ, Vercesi AE. Reactive oxygen generation by mitochondria. In: Lemasters JJ, L. NA, editors. Mitochondria in Pathogenesis. New York: Kluwer Academic / Penum Publishers; 2001. p.281-94.

Kowaltowski AJ, de Souza-Pinto NC, Castilho RF, Vercesi AE. Mitochondria and reactive oxygen species. Free Radic Biol Med. 2009;47(4):333-43.

Krauskopf A, Eriksson O, Craigen WJ, Forte MA, Bernardi P. Properties of the permeability transition in VDAC1(-/-) mitochondria. Biochim Biophys Acta. 2006;1757(5-6):590-5.

Krauss S, Zhang CY, Lowell BB. The mitochondrial uncoupling-protein homologues. Nat Rev Mol Cell Biol. 2005;6(3):248-61.

Kroemer G, Galluzzi L, Vandenabeele P, Abrams J, Alnemri ES, Baehrecke EH, et al. Classification of cell death: recommendations of the Nomenclature Committee on Cell Death 2009. Cell Death Differ. 2009;16(1):3-11.

Lazarou M, McKenzie M, Ohtake A, Thorburn DR, Ryan MT. Analysis of the assembly profiles for mitochondrial- and nuclear-DNA-encoded subunits into complex I. Mol Cell Biol. 2007;27(12):4228-37.

Lehninger AL, Vercesi A, Bababunmi EA. Regulation of Ca^{2+} release from mitochondria by the oxidation-reduction state of pyridine nucleotides. Proc Natl Acad Sci U S A. 1978;75(4):1690-4.

Lehninger AL. The mitochondrion: molecular basis of structure and function. New York: W. A. Benjamin, Inc.;1964.

Lei HY, Chang CP. Induction of autophagy by concanavalin A and its application in anti-tumor therapy. Autophagy. 2007;3(4):402-4.

Leite AC, de Lima RS, Moreira DR, Cardoso MV, Gouveia de Brito AC, Farias Dos Santos LM, et al. Synthesis, docking, and in vitro activity of thiosemicarbazones, aminoacyl-thiosemicarbazides and acyl-thiazolidones against *Trypanosoma cruzi*. Bioorg Med Chem. 2006;14(11):3749-57.

Lemasters JJ, Theruvath TP, Zhong Z, Nieminen AL. Mitochondrial calcium and the permeability transition in cell death. Biochim Biophys Acta. 2009;1787(11):1395-401.

Lenartowicz E, Bernardi P, Azzone GF. Phenylarsine oxide induces the cyclosporin A-sensitive membrane permeability transition in rat liver mitochondria. J Bioenerg Biomembr. 1991;23(4):679-88.

Lima VLM, Correia MTS, Cechinel YMN, Sampaio CAM, Owen JS, Coelho LCBB. Immobilized *Cratylia mollis* lectin as a potential matrix to isolate plasma glycoproteins, including lecithin-cholesterol acyltransferase. Carbohydrate Polymers. 1997;33:27-32.

Lis H, Sharon N. Lectins in higher plants. In: Marcus A, editor. The Biochemistry of Plants, a Comprehensive Treatise. 6 ed; 1981. p.371-447.

Liu B, Li CY, Bian HJ, Min MW, Chen LF, Bao JK. Antiproliferative activity and apoptosis-inducing mechanism of Concanavalin A on human melanoma A375 cells. Arch Biochem Biophys. 2009;482(1-2):1-6.

Lorenzo HK, Susin SA, Penninger J, Kroemer G. Apoptosis inducing factor (AIF): a phylogenetically old, caspase-independent effector of cell death. Cell Death Differ. 1999;6(6):516-24.

Lu HG, Zhong L, Chang KP, Docampo R. Intracellular Ca^{2+} pool content and signaling and expression of a calcium pump are linked to virulence in *Leishmania mexicana amazonesis* amastigotes. J Biol Chem. 1997;272(14):9464-73.

Lyu SY, Park WB, Choi KH, Kim WH. Involvement of caspase-3 in apoptosis induced by Viscum album var. coloratum agglutinin in HL-60 cells. Biosci Biotechnol Biochem. 2001;65(3):534-41.

Macedo DV, Ferraz VL, Pereira-da-Silva L, Vercesi AE. Ca^{2+}-dependent NAD(P^{+})-induced alterations in membrane permeability of rat liver mitochondria. New York: Ed. J. Lemasters, Plenum; 1988;535-42.

Macedo ML, das Gracas Machado Freire M, da Silva MB, Coelho LC. Insecticidal action of *Bauhinia monandra* leaf lectin (BmoLL) against *Anagasta kuehniella* (Lepidoptera: Pyralidae), *Zabrotes subfasciatus* and *Callosobruchus maculatus* (Coleoptera: Bruchidae). Comp Biochem Physiol A Mol Integr Physiol. 2007;146(4):486-98.

Machuka JS, Okeola OG, Van Damme Els JM, Chrispeels MJ, Van Leuven F, Peumans WJ. Isolation and partial characterisation of galactose-specific lectins from *African yam* beans, Sphenostyles stenocarpa Harms. Phytochemistry. 1999;51(6):721-8.

Maciel EV, Araujo-Filho VS, Nakazawa M, Gomes YM, Coelho LC, Correia MT. Mitogenic activity of *Cratylia mollis* lectin on human lymphocytes. Biologicals. 2004;32(1):57-60.

Mandal DK, Nieves E, Bhattacharyya L, Orr GA, Roboz J, Yu QT, et al. Purification and characterization of three isolectins of soybean agglutinin. Evidence for C-terminal truncation by electrospray ionization mass spectrometry. Eur J Biochem. 1994;221(1):547-53.

Mateo H, Marín C, Pérez-Cordón G, Sánchez-Moreno M. Purification and biochemical characterization of four iron superoxide dismutases in *Trypanosoma cruzi*. Memórias do Instituto Oswaldo Cruz. 2008;103(3):271-6.

Maugeri DA, Cazzulo JJ. The pentose phosphate pathway in *Trypanosoma cruzi*. FEMS Microbiol Lett. 2004;234(1):117-23.

Mehrotra S, Kakkar P, Viswanathan PN. Mitochondrial damage by active oxygen species in vitro. Free Radic Biol Med. 1991;10(5):277-85.

Meister A, Anderson ME. Glutathione. Annu Rev Biochem. 1983;52:711-60.

Merryfield ML, Lardy HA. Ca^{2+}-mediated activation of phosphoenolpyruvate carboxykinase occurs via release of Fe^{2+} from rat liver mitochondria. J Biol Chem. 1982;257(7):3628-35.

Mertens JJ, Gibson NW, Lau SS, Monks TJ. Reactive oxygen species and DNA damage in 2-bromo-(glutathion-S-yl) hydroquinone-mediated cytotoxicity. Arch Biochem Biophys. 1995;320(1):51-8.

Miletti LC, Koerich LB, Pacheco LK, Steindel M, Stambuk BU. Characterization of D-glucose transport in *Trypanosoma rangeli*. Parasitology. 2006;133(Pt 6):721-7.

Mitchell P. Coupling of phosphorylation to electron and hydrogen transfer by a chemi-osmotic type of mechanism. Nature. 1961;191:144-8.

Mo H, Van Damme EJ, Peumans WJ, Goldstein IJ. Isolation and characterization of an N-acetyl-D-galactosamine-binding lectin from *Dutch iris* bulbs which recognizes the blood group A disaccharide (GalNAc alpha 1-3Gal). J Biol Chem. 1994;269(10):7666-73.

Moreno SN, Silva J, Vercesi AE, Docampo R. Cytosolic-free calcium elevation in Trypanosoma cruzi is required for cell invasion. J Exp Med. 1994;180(4):1535-40.

Moreno SN, Docampo R. Calcium regulation in protozoan parasites. Curr Opin Microbiol. 2003;6(4):359-64.

Moure A, Sineiro J, Domínguez H. Extraction and functionality of membrane-concentrated protein from defatted *Rosa rubiginosa* seeds. Food Chemistry. 2001;74:327-39.

Murta SM, Gazzinelli RT, Brener Z, Romanha AJ. Molecular characterization of susceptible and naturally resistant strains of *Trypanosoma cruzi* to benznidazole and nifurtimox. Mol Biochem Parasitol. 1998;93(2):203-14.

Nakagawa T, Shimizu S, Watanabe T, Yamaguchi O, Otsu K, Yamagata H, et al. Cyclophilin D-dependent mitochondrial permeability transition regulates some necrotic but not apoptotic cell death. Nature. 2005;434(7033):652-8.

Nelson DL, Cox MM. Lehninger Principles of Biochemistry. 3. ed. Worth Publishers; New York, USA, 2000.

Netto LE, Kowaltowski AJ, Castilho RF, Vercesi AE. Thiol enzymes protecting mitochondria against oxidative damage. Methods Enzymol. 2002;348:260-70.

Newman DJ, Cragg GM, Snader KM. The influence of natural products upon drug discovery. Nat Prod Rep. 2000;17(3):215-34.

Ng TB, Yu YL. Isolation of a novel heterodimeric agglutinin from rhizomes of *Smilax glabra*, the Chinese medicinal material tufuling. Int J Biochem Cell Biol. 2001;33(3):269-77.

Nicholls DG. The bioenergetics of brown adipose tissue mitochondria. FEBS Lett. 1976;61(2):103-10.

Nicholls DG, Brand MD. The nature of the calcium ion efflux induced in rat liver mitochondria by the oxidation of endogenous nicotinamide nucleotides. Biochem J. 1980;188(1):113-8.

Nicholls DG, Åkerman KEO. Mitochondrial calcium transport. Biochim Biophys Acta. 1982;683:57-88.

Nicholls DG, Ferguson SV. Proton Current and Respiratory Control. Bioenergetics 3. 3 ed. London: Academic Press Inc.; 2002. p.69-75.

Nicotera P, Bellomo G, Orrenius S. Calcium-mediated mechanisms in chemically induced cell death. Annu Rev Pharmacol Toxicol. 1992;32:449-70.

Nomura K, Ashida H, Uemura N, Kushibe S, Ozaki T, Yoshida M. Purification and characterization of a mannose/glucose-specific lectin from *Castanea crenata*. Phytochemistry. 1998;49(3):667-73.

Ohba H, Bakalova R, Muraki M. Cytoagglutination and cytotoxicity of Wheat Germ Agglutinin isolectins against normal lymphocytes and cultured leukemic cell lines--relationship between structure and biological activity. Biochim Biophys Acta. 2003;1619(2):144-50.

Oliveira MD, Andrade CA, Santos-Magalhaes NS, Coelho LC, Teixeira JA, Carneiro-da-Cunha MG, et al. Purification of a lectin from *Eugenia uniflora* L. seeds and its potential antibacterial activity. Lett Appl Microbiol. 2008;46(3):371-6.

O.P.S. Estimacción cuantitativa de la erfermedad de Chagas en las Américas. Montevideo, Uruguay: Organização Pan Americana da Saúde; 2006.

Oshikawa K, Aoki K, Yoshino Y, Terada S. Purification and characterization of a basic amino acid-specific peptidase from seeds of jack bean (*Canavalia ensiformis*). Biosci Biotechnol Biochem. 2000;64(10):2186-92.

Osuna A, Castanys S, Rodriguez-Cabezas MN, Gamarro F. *Trypanosoma cruzi*: calcium ion movement during internalization in host HeLa cells. Int J Parasitol. 1990;20(5):673-6.

Oudrhiri N, Farcet JP, Gourdin MF, Divine M, Bouguet J, Fradelizi D, et al. Mechanism of accessory cell requirement in inducing IL 2 responsiveness by human T4 lymphocytes that generate colonies under PHA stimulation. J Immunol. 1985;135(3):1813-8.

Paiva PMG, Coelho LCBB. Purification and Partial Characterization of two lectins isoforms from *Cratylia mollis* Mart. (Camaratu Bean). Applied Biochemistry and Biotecnology. 1992;36:113-8.

Paulin JJ. The chondriome of selected trypanosomatids. A three-dimensional study based on serial thick sections and high voltage electron microscopy. J Cell Biol. 1975;66(2):404-13.

Peumans WJ, Van Damme EJ. Lectins as plant defense proteins. Plant Physiol. 1995;109(2):347-52.

Peumans WJ, Van Damme EJ. Plant lectins: specific tools for the identification, isolation, and characterization of O-linked glycans. Crit Rev Biochem Mol Biol. 1998A;33(3):209-58.

Peumans WJ, Van Damme EJM. Plant lectins: Proteins with important perspectives in biotechnology. Biotechnology and Genetic Engineering Reviews. 1998B;15:199-228.

Peumans WJ, Van Damme EJ, Barre A, Rouge P. Classification of plant lectins in families of structurally and evolutionary related proteins. Adv Exp Med Biol. 2001;491:27-54.

Piacenza L, Alvarez MN, Peluffo G, Radi R. Fighting the oxidative assault: the *Trypanosoma cruzi* journey to infection. Current Opinion in Microbiology. 2009;12:415–21.

Pitella J. Central nervous system involvmentin Chaga's disease. An updating. Rev Inst Med Trop. 1993;35:111-6.

Podolsky MJ, Lasker A, Flaminio MJ, Gowda LD, Ezekowitz RA, Takahashi K. Characterization of an equine mannose-binding lectin and its roles in disease. Biochem Biophys Res Commun. 2006;343(3):928-36.

Potenza M, Galat A, Minning TA, Ruiz AM, Duran R, Tarleton RL, et al. Analysis of the Trypanosoma cruzi cyclophilin gene family and identification of Cyclosporin A binding proteins. Parasitology. 2006;132(Pt 6):867-82.

Putney JW, Jr., Bird GS. The signal for capacitative calcium entry. Cell. 1993;75(2):199-201.

Ratanapo S, Ngamjunyaporn W, Chulavatnatol M. Interaction of a leaf lectin with a phytopathogenic bacterium, *P. syringae pv mori*. . Plant Science. 1998;139:141-8.

Ratanapo S, Ngamjunyaporn W, Chulavatnatol M. Interaction of a mulberry leaf lectin with a phytopathogenic bacterium, *P. syringae* pv mori. Plant Sci. 2001;160(4):739-44.

Ravagnan L, Roumier T, Kroemer G. Mitochondria, the killer organelles and their weapons. J Cell Physiol. 2002;192(2):131-7.

Reed DJ. Review of the current status of calcium and thiols in cellular injury. Chem Res Toxicol. 1990;3(6):495-502.

Rego EJ, de Carvalho DD, Marangoni S, de Oliveira B, Novello JC. Lectins from seeds of *Crotalaria pallida* (smooth rattlebox). Phytochemistry. 2002;60(5):441-6.

Reina-San-Martin B, Cosson A, Minoprio P. Lymphocyte polyclonal activation: a pitfall for vaccine design against infectious agents. Parasitol Today. 2000;16(2):62-7.

Rossi CS, Lehninger AL. Stoichiometry of Respiratory Stimulation, Accumulation of Ca^{++} and Phosphate, and Oxidative Phosphorylation in Rat Liver Mitochondria. J Biol Chem. 1964;239:3971-80.

Sá RA, Santos ND, da Silva CS, Napoleao TH, Gomes FS, Cavada BS, et al. Larvicidal activity of lectins from *Myracrodruon urundeuva* on *Aedes aegypti*. Comp Biochem Physiol C Toxicol Pharmacol. 2009;149(3):300-6.

Samartsev VN, Mokhova EN, Skulachev VP. The pH-dependent reciprocal changes in contributions of ADP/ATP antiporter and aspartate/glutamate antiporter to the fatty acid-induced uncoupling. FEBS Lett. 1997;412(1):179-82.

Santos ACO, Peixoto CA, Coelhoo LCBB. Ultrastructural analysis and immunocytochemical localization of isolectins in Cratylia mollis seeds. Micron. 2004;35(7):613-18.

Scheffler IE. Mitochondria make a come back. Adv Drug Deliv Rev. 2001;49(1-2):3-26.
Schmunis GA. A tripanossomíase americana e seu impacto na saúde pública das Américas. In: Brener Z, Andrade Z, editors. *Trypanosoma cruzi* e a doença de Chagas. Rio de Janeiro: Guanabara Koogan; 2000. p.1-3.

Schmunis GA. Epidemiology of Chagas disease in non-endemic countries: the role of international migration. Mem Inst Oswaldo Cruz. 2007;102 Suppl 1:75-85.

Schmunis GA. The globalization of Chagas disease. Ser. IS, editor.; 2007.

Schneider H, Charara N, Schmitz R, Wehrli S, Mikol V, Zurini MG, et al. Human cyclophilin C: primary structure, tissue distribution, and determination of binding specificity for cyclosporins. Biochemistry. 1994;33(27):8218-24.

Schneider WC, Hogeboom GH. Cytochemical studies of mammalian tissues; the isolation of cell components by differential centrifugation: a review. Cancer Res. 1951;11:1-22.

Sengupta S, Singh S, Sengupta LK, Bisen PS. Phytolectins: natural molecules with immense biotechnological potential. Indian J Exp Biol. 1997;35(2):103-10.

Sharon N, Lis H. Legume lectins--a large family of homologous proteins. FASEB J. 1990;4(14):3198-208.

Sharon N, Lis H. The structural basis for carbohydrate recognition by lectins. Adv Exp Med Biol. 2001;491:1-16.

Skulachev VP. Fatty acid circuit as a physiological mechanism of uncoupling of oxidative phosphorylation. FEBS Lett. 1991;294(3):158-62.

Spierings D, McStay G, Saleh M, Bender C, Chipuk J, Maurer U, et al. Connected to death: the (unexpurgated) mitochondrial pathway of apoptosis. Science. 2005;310(5745):66-7.

Sprong T, Mollness TE, Neeleman C, Swinkels D, Netea MG, Van Der Meer JW, et al. Mannose-binding lectin is a critical factor in systemic complement activation during meningococcal septic shock. Clin Infect Dis. 2009;49(9):1380-6.

Strasser A, O'Connor L, Dixit VM. Apoptosis signaling. Annu Rev Biochem. 2000;69:217-45.

Stryer L. Bioquímica. 5 ed. Rio de Janeiro: Guanabara Koogan; 2004.

Surolia A, Sharon N, Schwarz FP. Thermodynamics of monosaccharide and disaccharide binding to Erythrina corallodendron lectin. J Biol Chem. 1996;271(30):17697-703.

Sutton HC, Winterbourn CC. On the participation of higher oxidation states of iron and copper in Fenton reactions. Free Radic Biol Med. 1989;6(1):53-60.

Tarleton RL, Reithinger R, Urbina JA, Kitron U, Gurtler RE. The challenges of Chagas Disease-- grim outlook or glimmer of hope. PLoS Med. 2007;4(12):e332.

Teigelkamp S, Aschel T, Mundt C, Gothel SF, Cronshagen U, Lane WS, et al. The 20kD protein of human [U4/U6.U5] tri-snRNPs is a novelcyclophilin that forms a complex with the U4/U6-specific 60 kD and 90 kD proteins. RNA. 1998;4:127-41.

Thornberry NA, Lazebnik Y. Caspases: enemies within. Science. 1998;281(5381):1312-6.

Tsivileva OM, Nikitina VE, Loshchinina EA. Isolation and characterization of *Lentinus edodes* (Berk.) singer extracellular lectins. Biochemistry (Mosc). 2008;73(10):1154-61.

Turrens JF, Boveris A. Generation of superoxide anion by the NADH dehydrogenase of bovine heart mitochondria. Biochem J. 1980;191(2):421-7.

Turrens JF, Alexandre A, Lehninger AL. Ubisemiquinone is the electron donor for superoxide formation by complex III of heart mitochondria. Arch Biochem Biophys. 1985;237(2):408-14.

Turrens JF. The role of succinate in the respiratory chain of *Trypanosoma brucei* procyclic trypomastigotes. Biochem J. 1989;259(2):363-8.

Turrens JF. Superoxide production by the mitochondrial respiratory chain. Biosci Rep. 1997;17(1):3-8.

Turrens JF. Oxidative stress and antioxidant defenses: a target for the treatment of diseases caused by parasitic protozoa. Mol Aspects Med. 2004;25(1-2):211-20.

Valente SAS, Valente VDC, Pinto AYN, César MJB, dos Santos MP, Miranda COS, et al. Analysis of an acute Chagas disease outbreak in the Brazilian Amazon: human cases, triatomines, reservoir mammals parasites. Transactions of the Royal Society of Tropical Medicine and Hygiene. 2009;103:6.

Valle VG, Fagian MM, Parentoni LS, Meinicke AR, Vercesi AE. The participation of reactive oxygen species and protein thiols in the mechanism of mitochondrial inner membrane permeabilization by calcium plus prooxidants. Arch Biochem Biophys. 1993;307(1):1-7.

van Loo G, Schotte P, van Gurp M, Demol H, Hoorelbeke B, Gevaert K, et al. Endonuclease G: a mitochondrial protein released in apoptosis and involved in caspase-independent DNA degradation. Cell Death Differ. 2001;8(12):1136-42.

Vega N, Perez G. Isolation and characterisation of a *Salvia bogotensis* seed lectin specific for the Tn antigen. Phytochemistry. 2006;67(4):347-55.

Vercesi AE. Dissociation of $NAD(P)^+$-stimulated mitochondrial Ca^{2+} efflux from swelling and membrane damage. Arch Biochem Biophys. 1984A;232(1):86-91.

Vercesi AE. Possible participation of membrane thiol groups on the mechanism of $NAD(P)^+$-stimulated Ca^{2+} efflux from mitochondria. Biochem Biophys Res Commun. 1984B;119(1):305-10.

Vercesi AE, Pereira-da-Silva L. NADP redox state and mitochondrial Ca^{2+} efflux: a controversial issue. Braz J Med Biol Res. 1984;17(3-4):353-6.

Vercesi AE. The participation of NADP, the transmembrane potential and the energy-linked NAD(P) transhydrogenase in the process of Ca^{2+} efflux from rat liver mitochondria. Archives of Biochemistry and Biophysics. 1987;252(1):171-8.

Vercesi AE, Hermes-Lima M, Meyer-Fernandes JR, Vieyra A. Calcium inhibition of the ATP in equilibrium with [32P]Pi exchange and of net ATP synthesis catalyzed by bovine submitochondrial particles. Biochim Biophys Acta. 1990;1020(1):101-6.

Vercesi AE, Hoffmann ME, Bernardes CF, Docampo R. Regulation of intracellular calcium homeostasis in *Trypanosoma cruzi*. Effects of calmidazolium and trifluoperazine. Cell Calcium. 1991;12(5):361-9.

Vercesi AE, Bernardes CF, Hoffmann ME, Gadelha FR, Docampo R. Digitonin permeabilization does not affect mitochondrial function and allows the determination of the mitochondrial membrane potential of Trypanosoma cruzi in situ. J Biol Chem. 1991;266(22):14431-4.

Vercesi AE, Hoffmann ME. Generation of reactive oxygen metabolites and oxidative damage in mitochondria: the role of calcium. Methods in Toxicology "Mitochondrial Dysfunction". In: Jones DP, Lash LH, editors. New York: Academic Press; 1993, 2, chapter 21.

Vercesi AE. Ca^{2+} transport and oxidative damage of mitochondria. Braz J Med Biol Res. 1993A;26(5):441-57.

Vercesi AE, Moreno SN, Docampo R. Ca^{2+}/H^{+} exchange in acidic vacuoles of *Trypanosoma brucei*. Biochem J. 1994;304 (Pt 1):227-33.

Vercesi AE, Martins IS, Silva MAP, Leite HMF, Cuccovia IM, Chaimovich H. Pumping plants. Nature. 1995;375:24.

Vercesi AE, Kowaltowski AJ, Grijalba MT, Meinicke AR, Castilho RF. The role of reactive oxygen species in mitochondrial permeability transition. Biosci Rep. 1997;17(1):43-52.

Verhagen AM, Ekert PG, Pakusch M, Silke J, Connolly LM, Reid GE, et al. Identification of DIABLO, a mammalian protein that promotes apoptosis by binding to and antagonizing IAP proteins. Cell. 2000;102(1):43-53.

W.H.O. Technical Report Series, Control of Chagas disease. Geneva: World Health Organization; 2002. Available from: http:\\www.who.int.

Walter A, Gutknecht J. Monocarboxylic acid permeation through lipid bilayer membranes. J Membr Biol. 1984;77(3):255-64.

Watabe S, Hiroi T, Yamamoto Y, Fujioka Y, Hasegawa H, Yago N, et al. SP-22 is a thioredoxin-dependent peroxide reductase in mitochondria. Eur J Biochem. 1997;249(1):52-60.

Wilkinson SR, Meyer DJ, Taylor MC, Bromley EV, Miles MA, Kelly JM. The *Trypanosoma cruzi* enzyme TcGPXI is a glycosomal peroxidase and can be linked to trypanothione reduction by glutathione or tryparedoxin. J Biol Chem. 2002;277(19):17062-71.

Wongkham S, Wongkham C, Boonsiri P, Simasathiansophon S, Trisonthi C, Atisook K. Isolectins from seeds of *Artocarpus lakoocha*. Phytochemistry. 1995;40(5):1331-4.

Woodfield K, Ruck A, Brdiczka D, Halestrap AP. Direct demonstration of a specific interaction between cyclophilin-D and the adenine nucleotide translocase confirms their role in the mitochondrial permeability transition. Biochem J. 1998;336 (Pt 2):287-90.

Wu AM, Wu JH, Tsai MS, Herp A. Carbohydrate specificity of an agglutinin isolated from the root of *Trichosanthes kirilowii*. Life Sci. 2000;66(26):2571-81.

Yakubu MA, Majumder S, Kierszenbaum F. Changes in *Trypanosoma cruzi* infectivity by treatments that affect calcium ion levels. Mol Biochem Parasitol. 1994;66(1):119-25.

Yokoyama N, Hayashi N, Seki T, Pante N, Ohba T, Nishii K, et al. A giant nucleopore protein that binds Ran/TC4. Nature. 1995;376(6536):184-8.

Zamzami N, Hirsch T, Dallaporta B, Petit PX, Kroemer G. Mitochondrial implication in accidental and programmed cell death: apoptosis and necrosis. J Bioenerg Biomembr. 1997;29(2):185-93.

Zecchin KG, Seidinger AL, Chiaratti MR, Degasperi GR, Meirelles FV, Castilho RF, et al. High Bcl-2/Bax ratio in Walker tumor cells protects mitochondria but does not prevent H_2O_2-induced apoptosis via calcineurin pathways. J Bioenerg Biomembr. 2007;39(2):186-94.

Zhang P, Liu B, Kang SW, Seo MS, Rhee SG, Obeid LM. Thioredoxin peroxidase is a novel inhibitor of apoptosis with a mechanism distinct from that of Bcl-2. J Biol Chem. 1997;272(49):30615-8.

Zheng S, Li C, Ng TB, Wang HX. A lectin with mitogenic activity from the edible wild mushroom Boletus edulis Process Biochemistry. 2007;42(12):1620-24.

Zhou M, Diwu, Z, Panchuk-Voloshina N, Haugland R P. A stable nonfluorescent derivative of resofurin for the fluorometric determination of trace hydrogen peroxide: applications in detecting the activity of phagocyte NADPH oxidase and other oxidases. Anal Biochem. 1997;253(2):162-68.

Zimmermann KC, Bonzon C, Green DR. The machinery of programmed cell death. Pharmacol Ther. 2001;92(1):57-70.

Zoratti M, Szabo I. The mitochondrial permeability transition. Biochim Biophys Acta. 1995;1241(2):139-76.

7 – APÊNDICES

APÊNDICE I

---------- Mensagem Original ----------
Assunto: Re: Manuscript submission for JBB - Fernandes et al
De: "Pete Pedersen" <ppederse@jhmi.edu>
Data: Qua, Dezembro 23, 2009 8:10 pm
Para: "Anibal Vercesi" <anibal@unicamp.br>

Dear Anibal:
I apologize for the delay in the review of your manuscript entitled
"Mechanism of Trypanosoma cruzi Death Induced by Craylia mollis Seed Lectin" Nevertheless, I am happy to say that it was found to be novel, potentially very important, and clearly written. Could you please send me a Word copy with the figures in jpeg or some other suitable format? You may wish to connect the points in Figures 2A and 2B. I will then submit it to the publishers.
All the best,
Pete
Peter L. Pedersen
Editor, J. Bioenergetics and Biomembranes

APÊNDICE II

BJ www.biochemj.org

Biochem. J. (2009) **418**, 595–604 (Printed in Great Britain) doi:10.1042/BJ20081981

Mitochondrial calcium overload triggers complement-dependent superoxide-mediated programmed cell death in *Trypanosoma cruzi*

Florencia IRIGOÍN*†, Natalia M. INADA‡[1], Mariana P. FERNANDES‡, Lucía PIACENZA†§, Fernanda R. GADELHA‖, Anibal E. VERCESI‡ and Rafael RADI†§[2]

*Departamento de Histología y Embriología, Facultad de Medicina, Universidad de la República, Montevideo, Uruguay, †Center for Free Radical and Biomedical Research, Facultad de Medicina, Universidad de la República, Avda. Gral. Flores 2125, 11800 Montevideo, Uruguay, ‡Labóratorio de Bioenergética, Departamento de Patologia Clínica, Faculdade de Ciências Médicas, Unicamp, Campinas, Brazil, §Departamento de Bioquímica, Facultad de Medicina, Universidad de la República, Montevideo, Uruguay, and ‖Instituto de Biologia, Unicamp, Campinas, Brazil

The epimastigote stage of *Trypanosoma cruzi* undergoes PCD (programmed cell death) when exposed to FHS (fresh human serum). Although it has been known for over 30 years that complement is responsible for FHS-induced death, the link between complement activation and triggering of PCD has not been established. We have previously shown that the mitochondrion participates in the orchestration of PCD in this model. Several changes in mitochondrial function were described, and in particular it was shown that mitochondrion-derived $O_2^{\bullet-}$ (superoxide radical) is necessary for PCD. In the present study, we establish mitochondrial Ca^{2+} overload as the link between complement deposition and the observed changes in mitochondrial physiology and the triggering of PCD. We show that complement activation ends with the assembly of the MAC (membrane attack complex), which allows influx of Ca^{2+} and release of respiratory substrates to the medium. Direct consequences of these events are accumulation of Ca^{2+} in the mitochondrion and decrease in cell respiration. Mitochondrial Ca^{2+} causes partial dissipation of the inner membrane potential and consequent mitochondrial uncoupling. Moreover, we provide evidence that mitochondrial Ca^{2+} overload is responsible for the increased $O_2^{\bullet-}$ production, and that if cytosolic Ca^{2+} rise is not accompanied by the accumulation of the cation in the mitochondrion and consequent production of $O_2^{\bullet-}$, epimastigotes die by necrosis instead of PCD. Thus our results suggest a model in which MAC assembly on the parasite surface allows Ca^{2+} entry and its accumulation in the mitochondrion, leading to $O_2^{\bullet-}$ production, which in turn constitutes a PCD signal.

Key words: apoptosis, membrane attack complex (MAC), oxidative phosphorylation, reactive oxygen species (ROS), *Trypanosoma cruzi*, trypanosomatid.

INTRODUCTION

Trypanosoma cruzi is a protozoan parasite of the order Kinetoplastida that causes Chagas' disease, an infection that affects several million people in rural regions of Latin America (http://www.who.int/tdr/diseases/chagas/swg_chagas.pdf; [1]). The lifecycle of *T. cruzi* involves an insect vector and a mammalian host, as well as different forms of the parasite adapted to extremely different environments. In the insect vector, the epimastigotes replicate and transform into the non-proliferative, mammalian-infective stage, namely the metacyclic trypomastigotes. In the mammalian host, the parasite again alternates between a replicative, intracellular stage, namely the amastigote, and a non-replicative, extracellular form, namely the bloodstream trypomastigote. With no immediate prospect of a vaccine and problems associated with current chemotherapies, the development of new treatments is an urgent priority. In this respect, basic research in mechanisms that control parasite life and death may contribute to the discovery of new potential targets for drug development.

For a long time it was assumed that PCD (programmed cell death) arose along with multicellular organisms [2]. However, features similar to those described in metazoan cell apoptosis have also been reported in a variety of unicellular eukaryotes, including several members of Kinetoplastida (reviewed in [3–8]). These features include condensation of nuclear chromatin and DNA fragmentation, loss of $\Delta\psi_m$ (mitochondrial inner membrane potential), release of cytochrome *c* to the cytosol and PS (phosphatidylserine) exposure on the cell surface. In several cases, it was observed that PCD occurred along with the activation of proteases able to cleave typical substrates of caspases, central players in the orchestration of metazoan cell apoptosis, and the use of caspase inhibitors blocked some of the features associated with trypanosomatid PCD. However, there is still little information about the pathways and actors involved in triggering, regulating and executing PCD in trypanosomatids.

T. cruzi was the first unicellular organism in which PCD was described. In 1995, Ameisen et al. [9] showed that epimastigotes maintained in culture for 1–2 weeks without medium renewal transformed into metacyclic trypomastigotes or died showing morphological features of apoptosis. Those features were also observed in epimastigotes killed by the complement system when exposed to FHS (fresh human serum) [9,10]. In this case, epimastigote PCD involved activation of caspase-like activities, DNA fragmentation and maintenance of plasma membrane integrity assessed by [^{3}H]uridine release [10]. Parasite death was completely prevented by a caspase-3 inhibitor and partially

Abbreviations used: AA, antimycin A; $[Ca^{2+}]_i$, intracellular Ca^{2+} concentration; FCCP, carbonyl cyanide *p*-trifluoromethoxyphenylhydrazone; FHS, fresh human serum; fura 2/AM, fura 2 acetoxymethyl ester; IHS, heat-inactivated human serum; MAC, membrane attack complex; MitoSOX, 3,8-phenanthridinediamine, 5-(6′-triphenylphosphoniumhexyl)-5,6-dihydro-6-phenyl; MPT, mitochondrial permeability transition; SOD, superoxide dismutase; PCD, programmed cell death; PI, propidium iodide; PS, phosphatidylserine; RCR, respiratory control ratio; ROS, reactive oxygen species; TUNEL, terminal deoxynucleotidyl transferase-mediated dUTP nick-end labelling; $\Delta\psi_m$, mitochondrial inner membrane potential.

[1] Present address: Laboratorio de Biofotonica, Instituto de Física, Universidade de São Paulo, São Carlos, Brazil.

[2] To whom correspondence should be addressed (email rradi@fmed.edu.uy).

inhibited by L-arginine through nitric oxide-dependent pathways [10]. Recently, our group has established that, similar to what happens in metazoans, the mitochondrion was involved in orchestrating PCD in this model. Shortly after the exposure of epimastigotes to FHS, a decrease in cell respiration was observed, together with loss of $\Delta\psi_m$, increased production of $O_2^{\bullet-}$ (superoxide radical) and release of cytochrome *c* to the cytosol [11]. Overexpression of mitochondrial SOD (superoxide dismutase) partially inhibited epimastigote death, suggesting a central role of $O_2^{\bullet-}$ in signalling/executing PCD in this model [11]. However, no information was obtained about the link between complement activation on the parasite surface and the observed changes in mitochondrial physiology and the triggering of PCD.

Activation of the complement system on cell surfaces can end with the assembly of the MAC (membrane attack complex) that forms a pore in the plasma membrane. The consequences of MAC assembly were thoroughly studied in red blood cells, in which it leads to osmotic lysis [12]. However, on nucleated cells, such consequences are more complex, ranging from necrosis to apoptosis, cell proliferation and differentiation, depending on the cell type and the amount of MAC deposited (reviewed in [13–15]). Complement-dependent PCD, observed in several mammalian models [16–18], has been proposed to involve either signalling through cytosolic domains of the MAC or Ca^{2+}-dependent mechanisms. In other models of PCD, increases in mitochondrial Ca^{2+} and concomitant production of ROS (reactive oxygen species) by this organelle have been associated with apoptotic death (reviewed in [19–21]). However, mitochondrial Ca^{2+} overload has not been established as a link between complement deposition and PCD in mammalian cells.

In the present study, we have deepened the understanding of the mechanisms that govern PCD in *T. cruzi*. Using the model of epimastigotes exposed to FHS, in which there is the most information, we have identified mitochondrial Ca^{2+} overload as the link between complement activation, changes in mitochondrial function and $O_2^{\bullet-}$-dependent PCD.

MATERIALS AND METHODS

Parasites

T. cruzi epimastigotes (Tulahuen-2) were cultured at 28 °C in 33 g/l brain heart infusion medium, 3 g/l tryptose, 0.02 g/l haemin, 0.4 g/l KCl and 4 g/l Na_2HPO_4, supplemented with decomplemented 10 % (v/v) fetal bovine serum, glucose (0.3 g/l), streptomycin sulfate (0.2 g/l) and penicillin (200 000 units/l). Mid-exponential-phase parasites (5 days) were collected by centrifugation at 800 ***g*** for 10 min and washed twice with the corresponding buffer before the experiments. Cell density was determined by counting in a Neubauer chamber.

Induction and evaluation of *T. cruzi* PCD

Parasite PCD was induced by incubating, at 28 °C, 3×10^8 epimastigotes/ml in PBS-Glc [PBS (1.5 mM KH_2PO_4, 8.0 mM Na_2HPO_4, 2.7 mM KCl and 137 mM NaCl) containing 5 mM glucose] with 20 % (v/v) FHS. FHS was obtained from healthy volunteers, snap-frozen in liquid nitrogen and stored at −80 °C until used. Serum in which the complement system was inactivated by heating at 56 °C for 30 min [IHS (heat-inactivated human serum)] was used as a control in all the experiments. In some experiments, cells were challenged with FHS in the presence of 0.8 mM EGTA and 0.2 mM $MgCl_2$ in order to chelate extracellular Ca^{2+}. Cell death was assessed by measuring cell proliferation by using [^{3}H]thymidine (American Radiolabeled Chemicals) incorporation [10]. The induction of apoptosis was evaluated by: (i) assessing the exposure of PS together with the maintenance of plasma membrane integrity, and (ii) analysing DNA fragmentation. PS exposure was evaluated after 2 h of challenge by staining 1×10^6 cells with Annexin V conjugated with Alexa Fluor® 488 (Invitrogen) according to the manufacturer's protocol. Before analysing the samples, 1 μg/ml PI (propidium iodide) was added so as to evaluate plasma membrane integrity. Cells were then analysed by flow cytometry, in a FACSCalibur™ apparatus (Becton Dickinson). DNA fragmentation was evaluated (i) after 6 h of exposure to the stimuli using the TUNEL (terminal deoxynucleotidyl transferase-mediated dUTP nick-end labelling) kit (Invitrogen) according to the manufacturer's instructions and analysing the samples by flow cytometry, and (ii) after 24 h of exposure to the stimuli by analysing DNA fragments by agarose-gel electrophoresis as previously described [10].

Evaluation of complement activation on epimastigote surface

Complement activation was evaluated by determining the amount of C3d (the fragment of C3 that remains covalently attached to cell surfaces after complement activation) deposited on epimastigotes after 2 h of incubation with serum. After washing the cells thoroughly with PBS-Glc in order to remove all the C3 that was not covalently attached to the cell surface, cells were stained with a rabbit anti-human C3d antibody (Dako, Denmark), followed by an anti-rabbit IgG conjugated with Alexa Fluor® 488 (Invitrogen), and analysed by flow cytometry. In addition, MAC assembly on the parasite surface was evaluated on equivalent samples by staining cells with an anti-human MAC monoclonal antibody (Dako), which recognizes a neo-epitope of C9 that is exposed when the protein is part of the MAC. Cells were then incubated with an anti-mouse IgG conjugated with FITC (Sigma) and analysed by flow cytometry.

Exposure of epimastigotes to digitonin or ionomycin

In order to evaluate the participation of Ca^{2+} in the changes observed in mitochondrial physiology, epimastigotes were permeabilized with 1 fmol of digitonin per cell, an amount of digitonin that does not disturb the mitochondrial inner membrane [22], in the presence of 0.4 mM $CaCl_2$ or 0.1 mM EGTA as a control. The concentration of Ca^{2+} was chosen so as to mimic the amount of Ca^{2+} present during the exposure of epimastigotes to 20 % FHS. Cells were resuspended at 2×10^7 cells/ml in 20 mM Hepes (pH 7.4), 10 mM KH_2PO_4, 2 mM $MgCl_2$ and 200 mM sucrose, incubated at 28 °C with digitonin plus Ca^{2+} or EGTA, and then several parameters were evaluated: (i) the amount of Ca^{2+} accumulated in the mitochondrion after 10 min of permeabilization, (ii) cell respiration and (iii) mitochondrial $O_2^{\bullet-}$ production at different times after permeabilization. In other experiments, epimastigotes were exposed to the Ca^{2+} ionophore ionomycin (Alexis Biochemicals). Cells at 2.5×10^7 cells/ml in 50 mM Hepes (pH 7.4), 116 mM NaCl, 5.4 mM KCl, 0.8 mM $MgSO_4$ and 5.5 mM glucose (Hepes-Glc) were incubated at 28 °C with different concentrations of ionomycin (1, 5, 10 and 20 μM) in the presence of 0.4 mM $CaCl_2$ or 0.1 mM EGTA as a control. The following parameters were evaluated at the indicated times after incubation with ionomycin: (i) cytosolic Ca^{2+} levels, (ii) cell proliferation after 1 h, (iii) mitochondrial Ca^{2+} after 10 min, (iv) mitochondrial $O_2^{\bullet-}$ production, (v) PS exposure and plasma membrane integrity after 2 h and (vi) DNA fragmentation after 6 and 24 h.

Spectrofluorimetric determination of cytosolic Ca^{2+} levels

Cells (1×10^9 cells/ml) in Hepes-Glc buffer were loaded with 6 μM fura 2/AM (fura 2 acetoxymethyl ester) (Invitrogen) for 45 min at 28 °C. Cells were then washed twice so as to

eliminate excess of probe. Loaded cells were challenged with the stimulus, and at different times 2.5×10^7 cells were collected by centrifugation at 800 *g* for 5 min and resuspended in 1 ml of buffer, and the excitation spectrum (300–400 nm) of fura 2 was recorded at $\lambda_{em} = 510$ nm in an Aminco Bowman Series 2 fluorimeter (Thermo). $[Ca^{2+}]_i$ (intracellular Ca^{2+} concentration) was calculated by using the following formula [23]:

$$[Ca^{2+}]_i = K_d[(R_x - R_{min})/(R_{max} - R_x)] \times S$$

where K_d is the dissociation constant of the fura 2–Ca^{2+} complex (224 nM), and R_x, R_{max} and R_{min} are the ratio of fluorescence at 340 nm (maximum λ_{ex} for Ca^{2+}-bound fura 2) and fluorescence at 380 nm (maximum λ_{ex} for free fura 2) for the sample, saturating Ca^{2+} and Ca^{2+}-free conditions respectively. R_{max} and R_{min} were obtained by recording spectra of loaded control cells first permeabilized with 200 μM digitonin in the presence of 1 mM $CaCl_2$ (R_{max}) and then after the addition of 8 mM EGTA (pH 8) (R_{min}).

Spectrophotometric determination of mitochondrial Ca^{2+}

Mitochondrial Ca^{2+} was quantified as previously described [24] by releasing it through dissipation of $\Delta\psi_m$ in cells permeabilized with digitonin. Ca^{2+} in the medium was then estimated measuring the changes in the absorbance spectrum of Arsenazo III [25], using the SLM Aminco DW2000 spectrophotometer at the wavelength pair 675–685 nm. Briefly, after challenge with different stimuli, cells were collected by centrifugation at 800 *g* for 5 min, rinsed in 20 mM Hepes (pH 7.2), 1 mM $MgCl_2$, 2.5 mM Na_2HPO_4 and 200 mM sucrose, and resuspended in 2 ml of the same buffer at 2.5×10^7 cells/ml in the presence of 5 mM succinate, 40 μM Arsenazo III, 40 μM digitonin (1.6 fmol of digitonin per cell) and 5 μM AA (antimycin A) or 1 μM CCCP (carbonyl cyanide *m*-chlorophenylhydrazone). When indicated, Ca^{2+} stored in other compartments was released by the addition of 10 μM A23187. Calibration was performed by recording changes in absorbance after the addition of known amounts of $CaCl_2$.

High-resolution respirometry

Epimastigote respiration was evaluated using Oxygraph 2K (Oroboros Instruments). Cells were washed with respiration buffer (20 mM Hepes, pH 7.4, 10 mM KH_2PO_4, 2 mM $MgCl_2$ and 200 mM sucrose) and resuspended at 2×10^7 cells/ml, and O_2 consumption was recorded at 28 °C. The rate of O_2 consumption was calculated by means of the equipment software (DataLab) and was expressed as pmol of $O_2 \cdot s^{-1} \cdot ml^{-1}$. Cell respiration was evaluated after a 30 min exposure to FHS or IHS as a control. In some cases, serum-treated cells were permeabilized with 1 fmol of digitonin per cell while respiration was being measured. In other experiments, cells without previous treatment were permeabilized with 1 fmol of digitonin per cell in the presence of 0.4 mM $CaCl_2$ or 0.1 mM EGTA. The following compounds were added when indicated: 5 mM succinate, 2 mM ADP, 2 μg/ml oligomycin, 1 μM FCCP (carbonyl cyanide *p*-trifluoromethoxyphenylhydrazone) and 5 μM AA.

Fluorimetric detection of mitochondrial-derived $O_2^{\bullet-}$

Mitochondrial $O_2^{\bullet-}$ production was evaluated during the exposure of epimastigotes to ionomycin or digitonin in the presence or absence of Ca^{2+} using the fluorescent, $O_2^{\bullet-}$-sensitive, mitochondrial-targeted probe MitoSOX [3,8-phenanthridinediamine, 5-(6′-triphenylphosphoniumhexyl)-5,6-dihydro-6-phenyl; Invitrogen] [11]. Cells (3×10^8 cells/ml) were loaded with 5 μM MitoSOX for 10 min at room temperature (22 °C) and then washed with the corresponding buffer before the assays. Loaded cells were exposed to the stimuli, and after different times the fluorescence of 2×10^7 cells/200 μl, for the experiments involving ionomycin, and 5×10^6 cells/250 μl, for the experiments involving digitonin, was measured in a fluorescence microplate reader (FLUOStar Galaxy; BMG Labtechnologies) at $\lambda_{ex} = 510$ nm and $\lambda_{em} = 580$ nm. In some of the experiments, cells were exposed to 10 μM AA, a stimulus known to induce $O_2^{\bullet-}$ production by mitochondria.

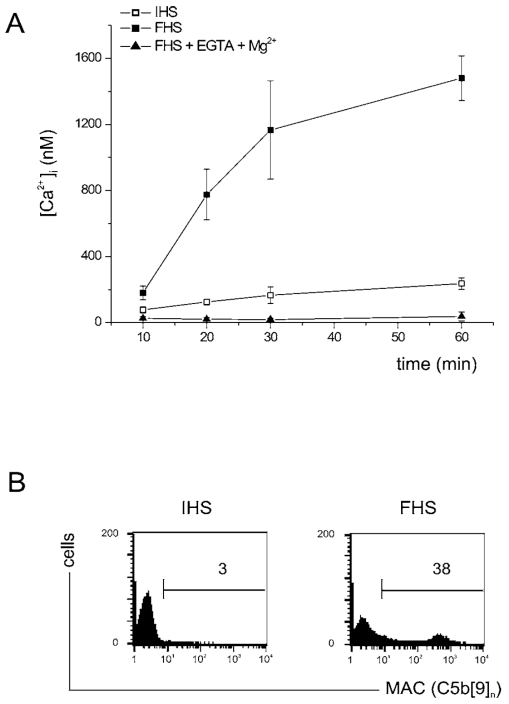

Figure 1 Cytosolic Ca^{2+} levels and MAC deposition on epimastigote surface after exposure to FHS

(**A**) Epimastigote were loaded with fura 2/AM, incubated at 28 °C with 20 % FHS, IHS or FHS in the presence of 8 mM EGTA and 2 mM $MgCl_2$, and their $[Ca^{2+}]_i$ was determined as explained in the Materials and methods section. Results are expressed as means ± S.D. for four independent experiments. (**B**) The assembly of the MAC on epimastigotes incubated for 2 h with FHS was studied by flow cytometry after staining cells with a monoclonal antibody that recognize a neo-epitope of C9 exposed when the protein is part of the complex. The percentage of MAC-positive cells is expressed in each plot. Histograms are representative of two independent experiments.

RESULTS

Exposure of epimastigotes to FHS induces a rapid accumulation of Ca^{2+} in the mitochondrion

In order to assess the participation of Ca^{2+} in the triggering of PCD, changes in the intracellular levels of the cation were evaluated in epimastigotes exposed to FHS. Cytosolic Ca^{2+} levels were estimated at different times after exposure

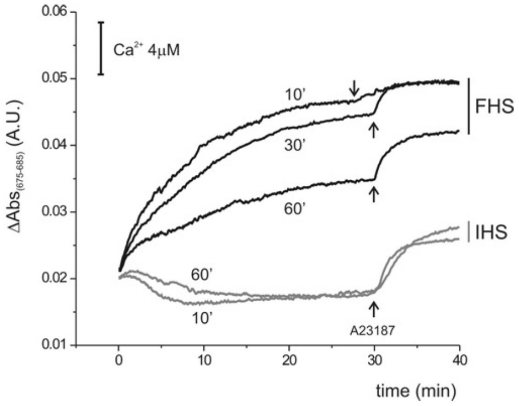

Figure 2 Mitochondrial Ca^{2+} accumulation induced by exposure to FHS

The amount of Ca^{2+} stored in the mitochondria was quantified by releasing it to the medium after dissipation of $\Delta\psi_m$ with AA in cells permeabilized with digitonin, and measuring changes in the absorbance spectrum of Arsenazo III as described in the Materials and methods section. Cells were incubated with 20% IHS or FHS for the indicated times. After washing, cells were resuspended in a buffer containing 40 μM digitonin, 5 μM AA, 5 mM succinate and 40 μM Arsenazo III, and the difference in absorbance at 675 and 685 nm was recorded over time. Arrows indicate the addition of 10 μM A23187, a Ca^{2+} ionophore. Traces are representative of at least six independent experiments. A.U., arbitrary units.

of parasites to FHS, IHS or FHS in the presence of 8 mM EGTA and 2 mM Mg^{2+}. The last condition was used to chelate extracellular Ca^{2+}, allowing complement activation to occur through the Ca^{2+}-independent, Mg^{2+}-dependent, alternative pathway. Exposure of cells to FHS produced a rapid increase in cytosolic Ca^{2+}, which rose from approx. 70 nM to 800 nM after 20 min (Figure 1A). Depletion of extracellular Ca^{2+} completely abrogated this increase, suggesting that FHS induced an influx of extracellular Ca^{2+} rather than a mobilization of the cation from intracellular stores. Ca^{2+} influx takes place through the assembly of the MAC on the epimastigote surface (Figure 1B), a pore that is freely permeable to ions.

In all eukaryotic cells, cytosolic Ca^{2+} is kept at very low concentrations (10–100 nM) by pumping out across the plasma membrane and by sequestration in intracellular compartments, such as the endoplasmic reticulum and mitochondria. Whereas the former has high affinity and low capacity, mitochondria have lower affinity for Ca^{2+} transport but enormous capacity for Ca^{2+} storage [24,26]. The driving force for Ca^{2+} movement into the mitochondria is the electrical component of $\Delta\psi_m$, which determines a net negative charge in the mitochondrial matrix. Obviously then, Ca^{2+} influx transiently dissipates $\Delta\psi_m$. Taking into account that mitochondria were quickly compromised in epimastigotes exposed to FHS [11], the accumulation of Ca^{2+} in this organelle was explored. Thus mitochondrial Ca^{2+} levels were estimated by releasing the cation into the medium through the dissipation of $\Delta\psi_m$ in permeabilized cells [24]. Mitochondria from epimastigotes exposed to FHS for 10 min released approx. 0.5 fmol of Ca^{2+} per cell, whereas Ca^{2+} released from mitochondria of control cells was almost undetectable (Figure 2). Cells exposed to FHS for longer times also released Ca^{2+} from their mitochondria, although in smaller amounts. Taking into account the number of cells and the volume occupied by the mitochondrion in each cell (approx. 12%; [27]), the total Ca^{2+} concentration in the mitochondrion of cells exposed to FHS for 10 min was estimated at 80–140 mM (depending on the experiment). Thus the influx of extracellular Ca^{2+} induced by FHS was paralleled by mitochondrial Ca^{2+} overload.

FHS-induced changes in mitochondrial respiration were explained by substrate loss and Ca^{2+} overload

Exposure of epimastigotes to FHS induced a rapid decrease in cell respiration and $\Delta\psi_m$, impairment of ATP synthesis and ADP transport into the mitochondria, as well as increased production of $O_2^{\bullet-}$ [11]. In order to explain these observations and their relationship with the accumulation of Ca^{2+} in the mitochondria, O_2 consumption on intact and digitonin-permeabilized cells was assessed by high-resolution respirometry.

Epimastigotes incubated with FHS for 30 min showed a 54% reduction in O_2 consumption with respect to control cells, i.e. the cells treated with IHS (Table 1A). Interestingly, the addition of succinate increased the respiration rates of FHS-treated cells

Table 1 Rates of O_2 consumption of epimastigotes exposed to different stimuli

Cell respiration was evaluated by high-resolution respirometry at 28°C. Rates of O_2 consumption were calculated by the instrument software and expressed as pmol of $O_2 \cdot s^{-1} \cdot ml^{-1}$. (A) O_2 consumption by cells pre-incubated for 30 min at 28°C with 20% FHS or IHS as a control. (B) The same experiment as in (A) but cells were permeabilized with 1 fmol of digitonin per cell after challenge with FHS or IHS. In (A) and (B), 'basal' corresponds to respiration of cells after 30 min of incubation with FHS or IHS. (C) O_2 consumption of cells permeabilized with digitonin in the presence of 0.1 mM EGTA or 0.4 mM $CaCl_2$. In this case, 'basal' corresponds to rates of respiration of cells before any treatment. When indicated, the following compounds were added: 5 mM succinate, 2 mM ADP, 2 μg/ml oligomycin, 1 μM FCCP, 5 μM AA, 0.4 mM $CaCl_2$, 0.1 mM EGTA and 1 fmol of digitonin per cell. Results shown are the means ± S.D. for three (A, B) and two (C) independent experiments. n.a., not applicable, n.d., not determined.

	Rates of O_2 consumption ($pmol \cdot s^{-1} \cdot ml^{-1}$)						
	Basal	+Digitonin	+Succinate	+ADP	+Oligomycin	+FCCP	+AA
(A) Epimastigotes+IHS/FHS							
IHS	49.9 ± 0.6	n.a.	49 ± 1	47 ± 2	16 ± 2*[2]	49.5 ± 0.9	4 ± 2
FHS	23 ± 6	n.a.	52 ± 2*[1]	54 ± 2	32 ± 2*[2]	44 ± 6	3 ± 2
(B) Epimastigotes+IHS/FHS, then permeabilized with digitonin							
IHS	54.6 ± 0.2	22 ± 2	30.9 ± 0.4	47 ± 4*[3]	n.d.	65 ± 5*[2]	1.1 ± 0.1
FHS	29.5 ± 0.7	16 ± 2	46 ± 3	49 ± 2	n.d.	60 ± 1*[2]	1.7 ± 0.4
(C) Epimastigotes permeabilized with digitonin+EGTA/Ca^{2+}							
EGTA	60 ± 7	15 ± 1	23 ± 2	53 ± 3*[3]	n.d.	65 ± 5	0.4 ± 0.4
Ca^{2+}	61 ± 7	7 ± 2	52 ± 3	55 ± 8	n.d.	58 ± 10	0.5 ± 0.4

*Significant difference ($P < 0.05$ by Student's t test) from [1]basal respiration, [2]respiration in the presence of ADP and [3]respiration in the presence of succinate.

to the level of control ones, whereas it had no effect on the latter (Table 1A), suggesting loss of respiratory substrates due to the partial permeabilization of the plasma membrane by the MAC. The subsequent addition of ADP did not enhance further the respiration of FHS-treated cells (Table 1A). The addition of oligomycin, an inhibitor of ATP synthase, decreased O_2 consumption, the effect being more pronounced in control cells (decrease of 68 % with respect to basal respiration) than in FHS-treated cells (decrease of 42 % with respect to respiration in the presence of succinate). However, in these experiments it was difficult to compare the two groups of cells, as in the ones exposed to IHS, respiration was based on endogenous substrates, whereas FHS-treated cells were using non-limiting amounts of exogenously added succinate. Thus, in order to compare both groups under the same conditions, the plasma membrane was permeabilized and respiration on exogenous substrates was measured. It is important to take into account that trypanosomatids possess a single, very large, mitochondrion that is almost impossible to isolate in an intact form. In order to bypass this difficulty, the strategy normally used is the permeabilization of the plasma membrane with a concentration of digitonin that does not affect the mitochondrial inner membrane [22]. Table 1(B) shows respiration of digitonin-permeabilized cells that were previously treated for 30 min with FHS or IHS. Cells exposed to IHS showed a decrease in respiration after permeabilization of the plasma membrane due to the loss of endogenous substrates, a moderate increase (1.4-fold) in respiration after addition of succinate, and a significant rise in O_2 consumption after addition of ADP (Table 1B). Mitochondrial coupling is usually evaluated by the RCR [respiratory control ratio; respiration in the presence of succinate+ADP (state 4)/respiration in the presence of succinate (state 3)], which equalled 1.50 in control cells. Contrarily, cells exposed to FHS showed a 2.8-fold increase in respiration after addition of succinate, they did not display further increase after ADP addition (RCR was 1.07), and only a moderate one was observed with FCCP (Table 1B). Thus it seemed that exposure of epimastigotes to the death stimulus led to a loss of respiratory substrates as well as a partial uncoupling of the mitochondrion.

Coupling between electron transport and ATP synthesis depends on $\Delta\psi_m$. It was shown that Ca^{2+} accumulated in the mitochondria of FHS-treated cells, a process expected to decrease $\Delta\psi_m$. This could explain the apparent uncoupling observed in mitochondria of cells exposed to FHS. In order to assess this hypothesis directly, cells were permeabilized with digitonin in the presence or absence of Ca^{2+}, and then mitochondrial Ca^{2+} accumulation and cell respiration were evaluated. It was observed that cells permeabilized in the presence of Ca^{2+} for 10 min accumulated in the mitochondria approx. 0.8 fmol of Ca^{2+} per cell (Figure 3A), an amount similar to that estimated in cells exposed to FHS. Moreover, cells permeabilized in the presence of Ca^{2+} showed a pattern of O_2 consumption very similar to the one observed with epimastigotes exposed to FHS (Table 1C): decrease in respiration after plasma membrane permeabilization, 7.3-fold increase in respiration after addition of succinate, and no significant further increase after ADP (RCR = 1.04) or FCCP addition. Contrarily, mitochondria of cells permeabilized in the absence of Ca^{2+} were coupled, showing an RCR of 2.29 (Table 1C). Also, it was determined that mitochondria of cells permeabilized in the presence of Ca^{2+} produced measurable amounts of $O_2^{\bullet-}$, a fact that was not observed in the absence of the cation (Figure 3B). Thus accumulation of Ca^{2+} in the mitochondrion explains the apparent uncoupling of mitochondria as well as the increase in $O_2^{\bullet-}$ production observed in cells exposed to FHS [11].

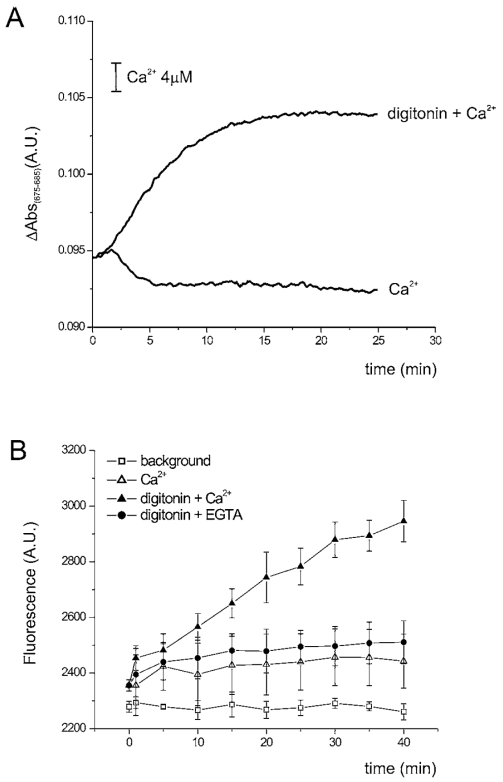

Figure 3 Mitochondrial Ca^{2+} and $O_2^{\bullet-}$ production in cells permeabilized in the presence of Ca^{2+}

Epimastigotes were permeabilized by incubation with 1 fmol of digitonin per cell at 28 °C in the presence of 0.4 mM $CaCl_2$ or 0.1 mM EGTA as a control. (**A**) Ca^{2+} stored in the mitochondria after a 10 min exposure to digitonin plus Ca^{2+} or Ca^{2+} alone was estimated as described in Figure 2. The plot is representative of two independent experiments. (**B**) Mitochondrial $O_2^{\bullet-}$ production was evaluated using the fluorescent probe MitoSOX. Results are expressed as mean fluorescence (in arbitrary units) ± S.D. for three independent experiments. 'Background' indicates cells not loaded with the probe; 'Ca^{2+}' indicates cells exposed to 0.4 mM Ca^{2+} in the absence of digitonin; 'digitonin + Ca^{2+}' indicates cells permeabilized with digitonin in the presence of 0.4 mM Ca^{2+}; 'digitonin + EGTA' indicates cells permeabilized with digitonin in the presence of 0.1 mM EGTA.

Mitochondrial Ca^{2+} overload is needed for triggering PCD in *T. cruzi* epimastigotes

A link between mitochondrial Ca^{2+} overload and the triggering of PCD was explored. First, parasites were exposed to FHS in the presence of EGTA and Mg^{2+}, a condition that was previously shown to inhibit Ca^{2+} influx into the cell (Figure 1A). Under this condition, cell death was not observed after 1 h of challenge (Figure 4A), it was significantly reduced after longer incubations (results not shown) and DNA fragmentation was not detected (Figure 4B). However, restricting complement activation to the alternative pathway through chelation of Ca^{2+} resulted in an important reduction in complement activation on the parasite surface, as indicated by 80 % less C3d deposited on cells incubated with FHS+EGTA+Mg^{2+} with respect to

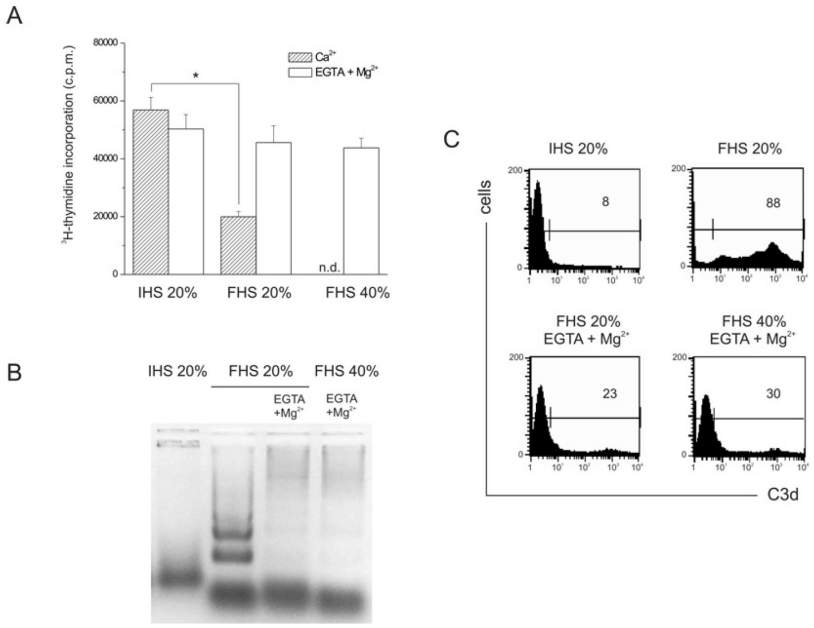

Figure 4 Effects of extracellular Ca^{2+} chelation on FHS-dependent parasite death and complement activation

Epimastigotes were incubated with 20 % IHS or FHS in the presence or absence of 8 mM EGTA+2 mM $MgCl_2$ and 40 % FHS with 8 mM EGTA+2 mM $MgCl_2$. (**A**) Cell death was evaluated after 1 h of incubation by assessing cell proliferation by measuring [^{3}H]thymidine incorporation. Results are expressed as means ± S.D. for the radioactivity measured for triplicates. Results are representative of two independent experiments. The asterisk indicates significant difference ($P < 0.05$ by the Student's t test) between the indicated conditions; n.d., not determined. (**B**) DNA fragmentation was evaluated 24 h after exposure to the stimuli by agarose-gel electrophoresis. (**C**) Complement activation was assessed by analysing C3d deposition on parasite surface by flow cytometry. The percentage of C3d-positive cells, indicative of the extent of complement activation under each condition, is expressed in each plot. Histograms are representative of two independent experiments.

FHS-treated cells (Figure 4C). This implied that epimastigotes activated the complement system by the Ca^{2+}-dependent pathways, a fact that was underestimated in previous studies [28]. In addition, the observation did not make it possible to establish a direct link between complement-mediated Ca^{2+} influx and triggering of PCD, as the eventual involvement of other complement-dependent events could not be ruled out. As an alternative approach, the use of an intracellular chelating agent {BAPTA/AM [bis-(*o*-aminophenoxy)ethane-*N*,*N*,*N*′,*N*′-tetra-acetic acid tetrakis(acatoxymethyl ester)]} was attempted, but it was revealed to be not fully effective in attenuating the increase in intracellular Ca^{2+} (results not shown).

Then, an indirect approach to associate mitochondrial Ca^{2+} with PCD was used. It consisted in evaluating cellular status after ionomycin-mediated Ca^{2+} influx. First, different concentrations of ionomycin were tested, so as to choose one that produced a Ca^{2+} influx similar to the one observed with FHS. This was achieved only with high concentrations of ionomycin (10–20 μM) (Figure 5), which were then used for evaluating mitochondrial Ca^{2+} overload, mitochondrial $O_2^{\bullet-}$ production and cell death. First, it was observed that the ionophore, although increasing the cytosolic Ca^{2+} levels, did not allow the accumulation of the cation in the mitochondrion (Figure 6A). This was due to the ionophore itself, which also mediates the mobilization of Ca^{2+} out of the mitochondrion. Secondly, under these conditions, formation of $O_2^{\bullet-}$ in the mitochondrion was not detected (Figure 6B), reinforcing the idea that mitochondrial Ca^{2+} overload is the cause of the increased $O_2^{\bullet-}$ generation observed in cells exposed to FHS or permeabilized with digitonin in the presence of Ca^{2+}. Cells exposed to ionomycin and Ca^{2+} died after 1–2 h of challenge (Figure 7A). Interestingly, the analysis of different parameters so as to discriminate necrotic from apoptotic-like death showed that ionomycin induced necrosis rather than apoptosis: plasma membrane integrity was not maintained after 2 h of challenge (Figure 7B) and DNA fragmentation was not detected either by TUNEL and flow cytometry (Figure 7C) or by resolving DNA fragments by using agarose-gel electrophoresis (Figure 7D). In summary, the results obtained with ionomycin showed that a rise in cytosolic Ca^{2+}, if not paralleled by its accumulation in the mitochondrion and the concomitant production of $O_2^{\bullet-}$, led to necrotic rather than to apoptotic death.

DISCUSSION

It has been known since 1975 that *T. cruzi* epimastigotes, contrarily to the mammalian infective forms, are killed by complement [28]. Epimastigote death was described in the cited work and subsequent ones from the 1980s in terms of necrosis [28–30]. This idea was reasonable at that time, when the concept of PCD was only arising and there was no evidence that complement could induce another type of cell death apart from necrosis. However, it has now been established that complement kills epimastigotes through a process with morphological characteristics of apoptosis

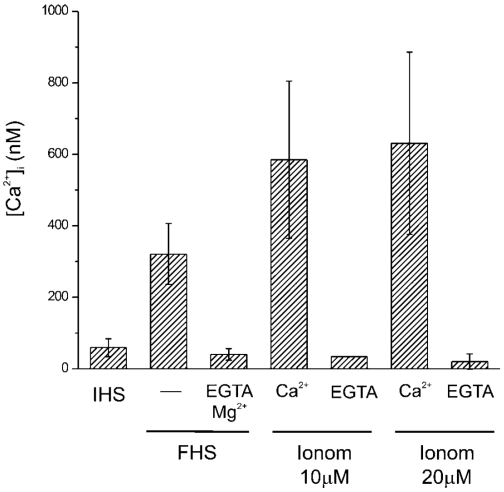

Figure 5 Comparison of cytosolic Ca^{2+} levels after challenge of epimastigotes with FHS or ionomycin

Cytosolic Ca^{2+} levels were estimated as in Figure 1. Cells preloaded with fura 2 were exposed to 20% IHS, FHS and FHS in the presence of 8 mM EGTA+2 mM Mg^{2+}, or 10 or 20 μM ionomycin (Ionom) in the presence of 0.4 mM $CaCl_2$ or 0.1 mM EGTA. After a 30 min incubation at 28 °C, the $[Ca^{2+}]_i$ was determined. Results are expressed as means ± S.D. for at least four independent experiments.

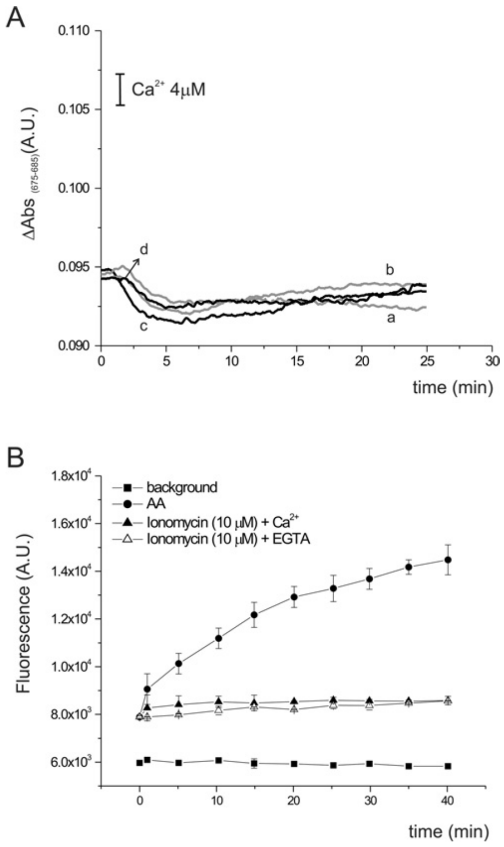

Figure 6 Mitochondrial Ca^{2+} and $O_2^{\bullet-}$ production in cells challenged with ionomycin

Epimastigotes were exposed to ionomycin in the presence of 0.4 mM Ca^{2+} or 0.1 mM EGTA. (**A**) Mitochondrial Ca^{2+} levels were estimated as described in Figure 2 after a 10 min exposure to Ca^{2+} alone (line a), ionomycin 20 μM+EGTA (line b), ionomycin 20 μM+Ca^{2+} (line c) or ionomycin 5 μM+Ca^{2+} (line d). (**B**) Mitochondrial $O_2^{\bullet-}$ production was evaluated as described in Figure 3(B). Results are expressed as mean fluorescence (in arbitrary units) ± S.D. for three independent experiments. 'Background' indicates cells not loaded with the probe; 'AA' indicates cells exposed to 10 μM AA, an inhibitor of complex III of the respiratory chain, known to stimulate $O_2^{\bullet-}$ production.

[9,10]. We have used this model to learn about the molecular mechanisms that govern PCD in this parasite. We showed that, as it happens in metazoans, the mitochondrion is a central organelle in the orchestration of PCD [11]. Changes in mitochondrial function, and, in particular, the production of $O_2^{\bullet-}$, were identified as key events in the signalling/execution of the process [11]. In the present study, we establish mitochondrial Ca^{2+} overload as the link between the observed mitochondrial changes and the activation of the complement system on the parasite surface.

The complex changes in mitochondrial function observed previously in epimastigotes exposed to FHS [11] can be reinterpreted in the light of the results presented in the current study. In addition to allowing the influx of Ca^{2+}, MAC deposition led to a partial loss of respiratory substrates and was thus responsible for the decrease in cell respiration observed (Table 1A and [11]). However, it is important to note that this loss was not total, as it was possible to decrease O_2 consumption further by additional permeabilization of the plasma membrane with digitonin (Table 1B). Thus, after treatment with FHS, electrons are still being delivered to the respiratory chain, albeit at lower rates. The study of cell respiration also showed that after challenge with FHS, the mitochondrion became partially uncoupled (Table 1B). This phenomenon is in line with the observed massive accumulation of Ca^{2+} by this organelle (Figure 2), a process expected to reduce $\Delta\psi_m$ and thus inhibit ATP synthesis [31], two events known to occur soon after exposure to FHS [11]. In agreement with this scenario, it was possible to mimic the changes in respiration observed in epimastigotes exposed to FHS by permeabilizing the plasma membrane with digitonin in the presence of Ca^{2+} (Table 1C).

Calcium overload was also responsible for the increased production of $O_2^{\bullet-}$ observed in epimastigotes exposed to FHS. A connection between these two phenomena has been reported in several other eukaryotic, and especially mammalian, systems (reviewed in [19–21]); however, the mechanisms underlying such a link have not been clearly unravelled. In fact, the connection is certainly counterintuitive, as an influx of Ca^{2+} into mitochondria is expected to dissipate $\Delta\psi_m$, an event normally associated with decreased ROS production. Moreover, Ca^{2+} overload and ROS have been implicated in the induction of the MPT (mitochondrial permeability transition), a non-selective increase in inner membrane permeability. Although the mitochondria of epimastigotes accumulated high amounts of Ca^{2+} during exposure to FHS (Figure 2), MPT did not occur, coincident with a previous work that showed that the *T. cruzi* mitochondrion is extremely resistant to MPT [24]. In agreement, it was observed that even after 1 h of exposure to FHS, the mitochondrion was able to take up Ca^{2+} from the medium (see Supplementary Figure S1 at

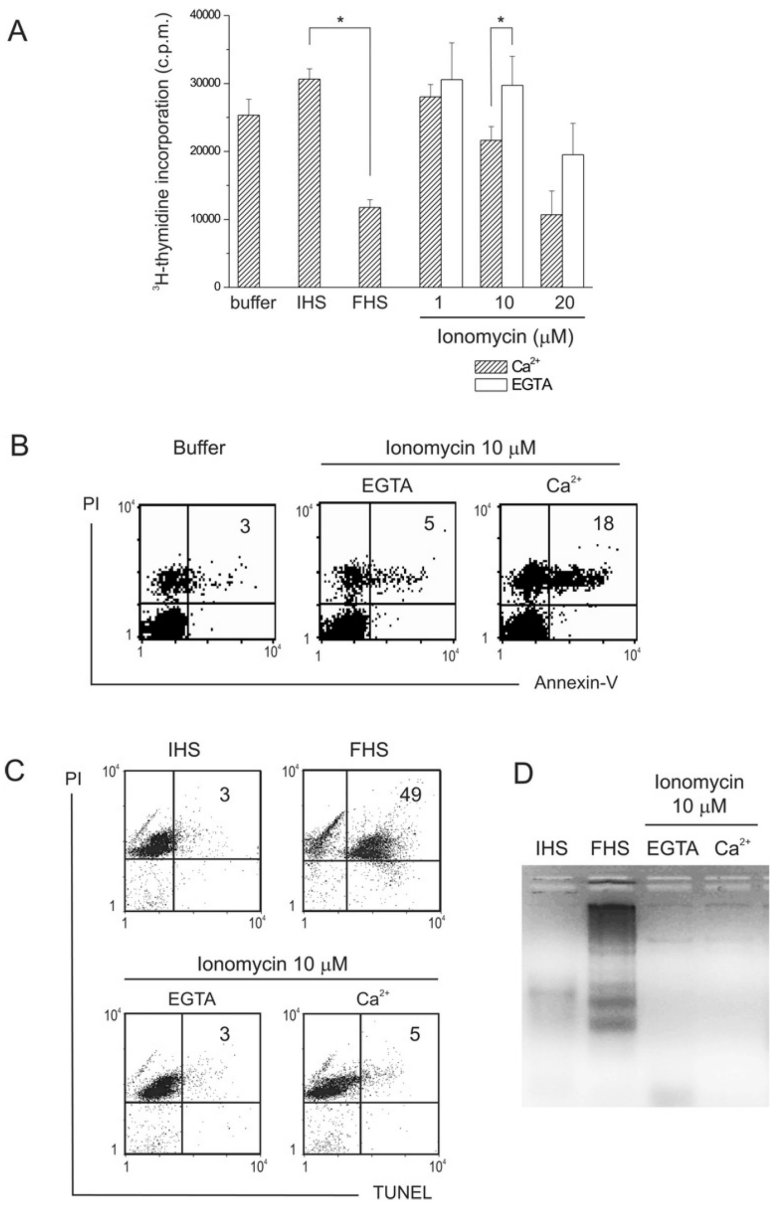

Figure 7 Calcium-dependent, ionomycin-induced cell death

Cells were exposed to ionomycin (1, 10 and 20 μM) in the presence of 0.4 mM Ca^{2+} or 0.1 mM EGTA. For comparison, cells were incubated in parallel with 20 % IHS, FHS or buffer. (**A**) Cell death was evaluated after 1 h of challenge by assessing cell proliferation by measuring [^{3}H]thymidine incorporation. Results are expressed as means $\pm$ S.D. for quadruplicates. Results are representative of two independent experiments. The asterisk indicates significant difference ($P < 0.05$ by the Student's t test) between the indicated conditions. (**B**) PS exposure and plasma membrane integrity were evaluated after 2 h of incubation with the stimuli, by staining cells with Annexin V–Alexa Fluor® 488 and PI and analysing the fluorescence by using flow cytometry. Numbers shown in the quadrants corresponding to double-positive cells indicate the percentage of cells undergoing necrotic death. Results are representative of two independent experiments. (**C**) DNA fragmentation was analysed after 6 h of incubation with the stimuli using the TUNEL assay and flow cytometry. Numbers shown in the quadrants corresponding to double-positive cells indicate the percentage of cells undergoing apoptosis. Note that in the TUNEL assay, PI is used as a counterstain rather than to indicate membrane integrity, as cells are permeabilized during the technique. Results are representative of two independent experiments. (**D**) DNA fragmentation was evaluated 24 h post-stimuli by resolving cytosolic DNA fragments on agarose-gel electrophoresis.

http://www.BiochemJ.org/bj/418/bj4180595add.htm), something that would not be possible after MPT.

We have obtained evidence that mitochondrial Ca^{2+} overload was directly associated with the triggering of PCD through the production of $O_2^{\bullet-}$. When the cytosolic Ca^{2+} rise was not paralleled by mitochondrial overload and $O_2^{\bullet-}$ production, as happened in cells exposed to ionomycin (Figures 6A and 6B), PCD was not activated (Figures 7B–7D). Thus signalling and/or execution of PCD in *T. cruzi* may involve molecules that can be modified by $O_2^{\bullet-}$-dependent oxidation/reduction. These targets probably do not react readily with H_2O_2, the product of $O_2^{\bullet-}$ dismutation, as overexpression of mitochondrial SOD, which is expected to increase the steady-state levels of H_2O_2, protected parasites from FHS-induced death [11]. It is interesting to note that ROS appear as central players in several models of trypanosomatid PCD, either acting as inductors [32,33] or participating in the signalling/execution of the process [11,34–36]. Indeed, early reports on *T. cruzi* cell death induced by β-lapachone, a redox cycling agent, showed morphological features that could be compatible with PCD [37].

In mammalian cells exposed to complement, mitochondrial Ca^{2+} overload frequently leads to necrosis, due to a complete loss of mitochondrial function and an associated energetic crisis [38]. Why does *T. cruzi* respond to complement-dependent Ca^{2+} rise by triggering PCD instead of necrosis? Some clues may be found in peculiar characteristics of the *T. cruzi* metabolism. One is the high capacity of the *T. cruzi* mitochondrion for Ca^{2+} storage, and its resistance to MPT [24]. This allows the organelle to act as an efficient buffer for high rises in cytosolic Ca^{2+} without collapsing completely, and to serve as a source of redox signals. In addition, *T. cruzi* has special organelles for Ca^{2+} storage, the acidocalcisomes (reviewed in [39]), whose participation in Ca^{2+} homoeostasis in this model was not explored. Lastly, *T. cruzi*, as well as the other trypanosomatids, have an extraordinary capacity for obtaining ATP from glycolysis [40], and this is probably the main source of energy for completion of the apoptotic programme once the mitochondrion becomes unable to perform oxidative phosphorylation.

FUNDING

This work was funded by the Howard Hughes Medical Institute [grant number 55005527] and the ICGEB (International Centre of Genetic Engineering and Biotechnology; Italy) [grant number CGEB CRP/URU 06-03] (to R. R.); the Fondo Clemente Estable (Uruguay) [grant number FCE 2004/10027] and Amsud Pasteur through a travel award (to F. I.); and the FAPESP (Fundação de Amparo à Pesquisa do Estado de São Paulo; Sao Paulo, Brazil) [grant number 2006/59786-0] (to A. E. V.). M. P. F. is a graduate student supported by a fellowship from the CAPES (Coordenação de Aperfeiçoamento de Pessoal de Nível Superior). R. R. is an International Research Scholar of the HHMI (Howard Hughes Medical Institute).

REFERENCES

1 Barrett, M. P., Burchmore, R. J., Stich, A., Lazzari, J. O., Frasch, A. C., Cazzulo, J. J. and Krishna, S. (2003) The trypanosomiases. Lancet **362**, 1469–1480
2 Vaux, D. L., Haecker, G. and Strasser, A. (1994) An evolutionary perspective on apoptosis. Cell **76**, 777–779
3 Ameisen, J. C. (2002) On the origin, evolution, and nature of programmed cell death: a timeline of four billion years. Cell Death Differ. **9**, 367–393
4 Bruchhaus, I., Roeder, T., Rennenberg, A. and Heussler, V. T. (2007) Protozoan parasites: programmed cell death as a mechanism of parasitism. Trends Parasitol. **23**, 376–383
5 Debrabant, A., Lee, N., Bertholet, S., Duncan, R. and Nakhasi, H. L. (2003) Programmed cell death in trypanosomatids and other unicellular organisms. Int. J. Parasitol. **33**, 257–267
6 Deponte, M. (2008) Programmed cell death in protists. Biochim. Biophys. Acta **1783**, 1396–1405
7 Duszenko, M., Figarella, K., Macleod, E. T. and Welburn, S. C. (2006) Death of a trypanosome: a selfish altruism. Trends Parasitol. **22**, 536–542
8 Nguewa, P. A., Fuertes, M. A., Valladares, B., Alonso, C. and Perez, J. M. (2004) Programmed cell death in trypanosomatids: a way to maximize their biological fitness? Trends Parasitol. **20**, 375–380
9 Ameisen, J. C., Idziorek, T., Billaut-Mulot, O., Tissier, J. P., Potentier, A. and Ouaissi, A. (1995) Apoptosis in a unicellular eukaryote (*Trypanosoma cruzi*): implications for the evolutionary origin and role of programmed cell death in the control of cell proliferation, differentiation and survival. Cell Death Differ. **2**, 285–300
10 Piacenza, L., Peluffo, G. and Radi, R. (2001) L-Arginine-dependent suppression of apoptosis in *Trypanosoma cruzi*: contribution of the nitric oxide and polyamine pathways. Proc. Natl. Acad. Sci. U.S.A. **98**, 7301–7306
11 Piacenza, L., Irigoín, F., Alvarez, M. N., Peluffo, G., Taylor, M. C., Kelly, J. M., Wilkinson, S. R. and Radi, R. (2007) Mitochondrial superoxide radicals mediate programmed cell death in *Trypanosoma cruzi*: cytoprotective action of mitochondrial iron superoxide dismutase overexpression. Biochem. J. **403**, 323–334
12 Mayer, M. M. (1972) Mechanism of cytolysis by complement. Proc. Natl. Acad. Sci. U.S.A. **69**, 2954–2958
13 Cole, D. S. and Morgan, B. P. (2003) Beyond lysis: how complement influences cell fate. Clin. Sci. (London) **104**, 455–466
14 Fishelson, Z., Attali, G. and Mevorach, D. (2001) Complement and apoptosis. Mol. Immunol. **38**, 207–219
15 Rus, H. G., Niculescu, F. I. and Shin, M. L. (2001) Role of the C5b-9 complement complex in cell cycle and apoptosis. Immunol. Rev. **180**, 49–55
16 Hughes, J., Nangaku, M., Alpers, C. E., Shankland, S. J., Couser, W. G. and Johnson, R. J. (2000) C5b-9 membrane attack complex mediates endothelial cell apoptosis in experimental glomerulonephritis. Am. J. Physiol. Renal Physiol. **278**, F747–F757
17 Nauta, A. J., Daha, M. R., Tijsma, O., van de Water, B., Tedesco, F. and Roos, A. (2002) The membrane attack complex of complement induces caspase activation and apoptosis. Eur. J. Immunol. **32**, 783–792
18 Shimizu, A., Masuda, Y., Kitamura, H., Ishizaki, M., Ohashi, R., Sugisaki, Y. and Yamanaka, N. (2000) Complement-mediated killing of mesangial cells in experimental glomerulonephritis: cell death by a combination of apoptosis and necrosis. Nephron **86**, 152–160
19 Brookes, P. S., Yoon, Y., Robotham, J. L., Anders, M. W. and Sheu, S. S. (2004) Calcium, ATP, and ROS: a mitochondrial love-hate triangle. Am. J. Physiol. Cell Physiol. **287**, C817–C833
20 Camello-Almaraz, C., Gomez-Pinilla, P. J., Pozo, M. J. and Camello, P. J. (2006) Mitochondrial reactive oxygen species and Ca^{2+} signaling. Am. J. Physiol. Cell Physiol. **291**, C1082–C1088
21 Vercesi, A. E., Kowaltowski, A. J., Oliveira, H. C. and Castilho, R. F. (2006) Mitochondrial Ca^{2+} transport, permeability transition and oxidative stress in cell death: implications in cardiotoxicity, neurodegeneration and dyslipidemias. Front. Biosci. **11**, 2554–2564
22 Vercesi, A. E., Bernardes, C. F., Hoffmann, M. E., Gadelha, F. R. and Docampo, R. (1991) Digitonin permeabilization does not affect mitochondrial function and allows the determination of the mitochondrial membrane potential of *Trypanosoma cruzi in situ*. J. Biol. Chem. **266**, 14431–14434
23 Thomas, A. P. and Delaville, F. (1991) The use of fluorescent indicators for measurements of cytosolic-free calcium concentration in cell populations and single cells. Cellular Calcium. A Practical Approach (McCormack, J. G. and Cobbold, P. H., eds), pp. 1–54, IRL Press, Oxford, U.K.
24 Docampo, R. and Vercesi, A. E. (1989) Ca^{2+} transport by coupled *Trypanosoma cruzi* mitochondria *in situ*. J. Biol. Chem. **264**, 108–111
25 Scarpa, A. (1979) Measurements of cation transport with metallochromic indicators. Methods Enzymol. **56**, 301–338
26 Nicholls, D. G. (2005) Mitochondria and calcium signaling. Cell Calcium **38**, 311–317
27 Lazardi, K., Urbina, J. A. and de Souza, W. (1990) Ultrastructural alterations induced by two ergosterol biosynthesis inhibitors, ketoconazole and terbinafine, on epimastigotes and amastigotes of *Trypanosoma* (*Schizotrypanum*) *cruzi*. Antimicrob. Agents Chemother. **34**, 2097–2105
28 Nogueira, N., Bianco, C. and Cohn, Z. (1975) Studies on the selective lysis and purification of *Trypanosoma cruzi*. J. Exp. Med. **142**, 224–229.
29 Joiner, K., Sher, A., Gaither, T. and Hammer, C. (1986) Evasion of alternative complement pathway by *Trypanosoma cruzi* results from inefficient binding of factor B. Proc. Natl. Acad. Sci. U.S.A. **83**, 6593–6597
30 Schenkman, S., Guther, M. L. and Yoshida, N. (1986) Mechanism of resistance to lysis by the alternative complement pathway in *Trypanosoma cruzi* trypomastigotes: effect of specific monoclonal antibody. J. Immunol. **137**, 1623–1628

31 Moreno-Sanchez, R. (1985) Regulation of oxidative phosphorylation in mitochondria by external free Ca^{2+} concentrations. J. Biol. Chem. **260**, 4028–4034
32 Das, M., Mukherjee, S. B. and Shaha, C. (2001) Hydrogen peroxide induces apoptosis-like death in *Leishmania donovani* promastigotes. J. Cell Sci. **114**, 2461–2469
33 Ridgley, E. L., Xiong, Z. H. and Ruben, L. (1999) Reactive oxygen species activate a Ca^{2+}-dependent cell death pathway in the unicellular organism *Trypanosoma brucei brucei*. Biochem. J. **340**, 33–40
34 Figarella, K., Uzcategui, N. L., Beck, A., Schoenfeld, C., Kubata, B. K., Lang, F. and Duszenko, M. (2006) Prostaglandin-induced programmed cell death in *Trypanosoma brucei* involves oxidative stress. Cell Death Differ. **13**, 1802–1814
35 Sen, N., Das, B. B., Ganguly, A., Mukherjee, T., Bandyopadhyay, S. and Majumder, H. K. (2004) Camptothecin-induced imbalance in intracellular cation homeostasis regulates programmed cell death in unicellular hemoflagellate *Leishmania donovani*. J. Biol. Chem. **279**, 52366–52375
36 Sudhandiran, G. and Shaha, C. (2003) Antimonial-induced increase in intracellular Ca^{2+} through non-selective cation channels in the host and the parasite is responsible for apoptosis of intracellular *Leishmania donovani* amastigotes. J. Biol. Chem. **278**, 25120–25132
37 Docampo, R., Lopes, J. N., Cruz, F. S. and Souza, W. (1977) *Trypanosoma cruzi*: ultrastructural and metabolic alterations of epimastigotes by beta-lapachone. Exp. Parasitol. **42**, 142–149
38 Papadimitriou, J. C., Phelps, P. C., Shin, M. L., Smith, M. W. and Trump, B. F. (1994) Effects of Ca^{2+} deregulation on mitochondrial membrane potential and cell viability in nucleated cells following lytic complement attack. Cell Calcium **15**, 217–227
39 Docampo, R., de Souza, W., Miranda, K., Rohloff, P. and Moreno, S. N. (2005) Acidocalcisomes: conserved from bacteria to man. Nat. Rev. Microbiol. **3**, 251–261
40 Bringaud, F., Riviere, L. and Coustou, V. (2006) Energy metabolism of trypanosomatids: adaptation to available carbon sources. Mol. Biochem. Parasitol. **149**, 1–9

Received 30 September 2008/2 December 2008; accepted 3 December 2008
Published as BJ Immediate Publication 3 December 2008, doi:10.1042/BJ20081981

Biochem. J. (2009) **418**, 595–604 (Printed in Great Britain) doi:10.1042/BJ20081981

SUPPLEMENTARY ONLINE DATA

Mitochondrial calcium overload triggers complement-dependent superoxide-mediated programmed cell death in *Trypanosoma cruzi*

Florencia IRIGOÍN*†, Natalia M. INADA‡[1], Mariana P. FERNANDES‡, Lucía PIACENZA†§, Fernanda R. GADELHA‖, Anibal E. VERCESI‡ and Rafael RADI†§[2]

*Departamento de Histología y Embriología, Facultad de Medicina, Universidad de la República, Montevideo, Uruguay, †Center for Free Radical and Biomedical Research, Facultad de Medicina, Universidad de la República, Avda. Gral. Flores 2125, 11800 Montevideo, Uruguay, ‡Labóratorio de Bioenergética, Departamento de Patologia Clínica, Faculdade de Ciências Médicas, Unicamp, Campinas, Brazil, §Departamento de Bioquímica, Facultad de Medicina, Universidad de la República, Montevideo, Uruguay, and ‖Instituto de Biologia, Unicamp, Campinas, Brazil

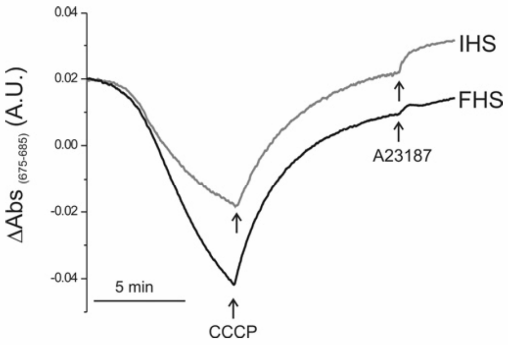

Figure S1 Mitochondrial Ca^{2+} uptake after treatment of epimastigotes with FHS

Epimastigotes were incubated with IHS or FHS for 1 h and then permeabilized with digitonin in the presence of succinate. Under this condition, mitochondria were allowed to take up Ca^{2+} from the medium, which was shown by a decrease in the absorbance changes of Arsenazo III. Arrows indicate the addition of 3 μM CCCP, so as to inhibit mitochondrial Ca^{2+} uptake through dissipation of $\Delta\psi_m$, and 10 μM A23187, so as to release Ca^{2+} from other compartments. Traces are representative of at least three independent experiments.

Received 30 September 2008/2 December 2008; accepted 3 December 2008
Published as BJ Immediate Publication 3 December 2008, doi:10.1042/BJ20081981

[1] Present address: Laboratorio de Biofotonica, Instituto de Física, Universidade de São Paulo, São Carlos, Brazil.
[2] To whom correspondence should be addressed (email rradi@fmed.edu.uy).

APÊNDICE III

EUKARYOTIC CELL, Nov. 2009, p. 1706–1720 Vol. 8, No. 11
1535-9778/09/$12.00 doi:10.1128/EC.00066-09

Goa1p of *Candida albicans* Localizes to the Mitochondria during Stress and Is Required for Mitochondrial Function and Virulence▽†

Adrienne Bambach,[1] Mariana P. Fernandes,[2] Anup Ghosh,[3] Michael Kruppa,[1] Deepu Alex,[1] Dongmei Li,[1] William A. Fonzi,[1] Neeraj Chauhan,[1] Nuo Sun,[1] Orlando A. Agrellos,[1,4] Anibal E. Vercesi,[2] Ronda J. Rolfes,[3] and Richard Calderone[1]*

Department of Microbiology and Immunology, Georgetown University Medical Center, Washington, DC[1]; Departamento de Patologia Clínica, Universidade Estadual de Campinas, Campinas, Brazil[2]; Department of Biology, Georgetown University, Washington, DC[3]; and Universidade Federal do Rio de Janeiro, Rio de Janeiro, Brazil[4]

Received 27 February 2009/Accepted 18 August 2009

Using a Tn*7* transposon library of *Candida albicans*, we have identified a mutant that exhibited sensitivity in drop plate assays to oxidants such as menadione and hydrogen peroxide. To verify the role of the mutated gene in stress adaptation, null mutants were constructed and phenotypically characterized. Because of its apparent functions in growth and oxidant adaptation, we have named the gene *GOA1*. Goa1p appears to be unique to the CTG subclade of the *Saccharomycotina*, including *C. albicans*. Mutants of *C. albicans* lacking *goa1* (strain GOA31) were more sensitive to 6 mM H_2O_2 and 0.125 mM menadione than the wild type (wt) or a gene-reconstituted (GOA32) strain. The sensitivity to oxidants correlated with reduced survival of the GOA31 mutant in human neutrophils and avirulence compared to control strains. Other phenotypes of GOA31 include reduced growth and filamentation in 10% serum, Spider, and SLAD agar media and an inability to form chlamydospores. Since Goa1p has an N-terminal mitochondrion localization site, we also show that green fluorescent protein-tagged Goa1p shows a mitochondrionlike distribution during oxidant or osmotic stress. Further, the inability of GOA31 to grow in medium containing lactate, ethanol, or glycerol as the sole carbon source indicates that the mitochondria are defective in the mutant. To determine how Goa1p contributes to mitochondrial function, we compared the wt, GOA32, and GOA31 strains for mitochondrial electrical membrane potential, respiration, and oxidative phosphorylation. We now show that GOA31, but not the wt or GOA32, had decreased respiration and mitochondrial membrane potential such that mutant cells are unable to drive oxidative phosphorylation. This is the first report in *C. albicans* of a respiratory defect caused by a loss of mitochondrial membrane potential.

Antioxidant proteins are part of the fungal cellular response to reactive oxidant species (ROS) in *Candida albicans*, both in vivo when the organism encounters phagocytic cells or competitors on the mucosal surfaces of humans or in vitro when confronted with external or internal metabolically generated ROS. Interestingly, increased ROS production in *C. albicans*, and probably fungi in general, occurs following treatment with antifungal compounds, such as diallyl disulfide (the active ingredient in garlic) and with miconazole, observations that may explain in part the activity of these compounds (35, 39).

To counter the stress induced by ROS, a number of antioxidant proteins are induced in *C. albicans*, including catalases (43, 58), superoxide dismutases (30, 40), and enzymes that require the cofactor glutathione (13). Biosynthesis of trehalose also provides protection against oxidant stress (4, 27, 41). Of the mitogen-activated protein kinase (MAPK) signal pathways that regulate new gene transcription during stress, the MKC1 MAPK and HOG1 MAPK (for hyperosmotic glycerol) pathways are prominent in a number of yeasts and filamentous fungi in regard to adaptation to hyperosmotic and/or oxidant stress (2, 3, 5, 6, 11, 12, 18–21, 29, 44, 50, 52, 55). Transcription factors such as Cap1p are also critical to oxidant resistance (7, 20, 21, 60). The Cek2 MAPK is not apparently required for stress adaptation (14).

Resistance to stress in *C. albicans* is complex but, in general, genes can be assigned to two categories based upon transcriptional profiling: (i) genes that make up a general response (or core) profile to common stress conditions such as osmotic, oxidative, and heavy metal and (ii) genes that are specific for each stress condition (20, 21, 52). In *C. albicans* a core transcriptional response to all stress conditions included genes that encode redox regulation, mitochondrial activity, carbohydrate metabolism, and cell wall biogenesis, among others (20). Interestingly, the core stress response set of genes in *C. albicans* is much smaller than that of *Saccharomyces cerevisiae* or *Schizosaccharomyces pombe*, suggesting that *C. albicans* relies more upon diversity in gene transcription to counter stress conditions (20, 52). A common theme is that most stress conditions result in an increase in ROS during cellular respiration. Thus, resistance to osmostress, for example, requires restoration of redox potential, reduction of ROS, and increased mitochondrial function.

Adaptation to stress in *C. albicans* is also most likely critical

* Corresponding author. Mailing address: Department of Microbiology and Immunology, Georgetown University Medical Center, Medical/Dental Bldg., 312SE, Washington, DC 20007. Phone: (202) 687-1137. Fax: (202) 687-1800. E-mail: calderor@georgetown.edu.

† Supplemental material for this article may be found at http://ec.asm.org/.

▽ Published ahead of print on 28 August 2009.

TABLE 1. Strains of *C. albicans* used in this study

Strain	Genotype	Source or reference
DAY286	*ura3*::*imm434*/*ura3*::*imm434 his1*::*hisG*/*his1*::*hisG arg4*::*hisG*/*arg4*::*hisG*,*ARG4*,*URA3*	56
SC5314	Clinical isolate; Ura^+ parent of CAI4	23
CAI4	*ura3*::*imm434*/*ura3*::*imm434*	23
DAY185	*ura3*Δ::λ*imm434*/*ura3*Δ::λ*imm434 his1*::*hisG*/*HIS1*::*his1*::*hisG arg4*::*hisG*/*URA3*::*ARG4*::*arg4*::*hisG*	16
BWP17	*ura3*::*imm434*/*ura3*::*imm434 his1*::*hisG*/*his1*::*hisG arg4*::*hisG*/*arg4*::*hisG*	56
SN148	*arg4*Δ/*arg4*Δ *leu2*Δ/*leu2*Δ *his1*Δ/*his1*Δ*ura3*Δ::*imm434*/*ura3*::*imm434 iro1*Δ::*imm434*/*iro1*Δ::*imm434*	46
GOA21	*goa1*::*UAU1*/*goa1*::*URA3 ura3*::*imm434*/*ura3*::*imm434 his1*::*hisG*/*his1*::*hisG arg4*::*hisG*/*arg4*::*hisG*	This study
GOA31	*goa1*::*URA3*/*goa1*::*ARG4 arg4*/*arg4leu2*/*leu2 his1*/*his1ura3*Δ::*imm434*/*ura3*::*imm434 iro1*::*imm434*	This study
GOA41	*goa1*::*URA3*/*goa1*::*ARG4 ura3*::*imm434*/*ura3*::*imm434 his1*::*hisG*/*his1*::*hisG arg4*::*hisG*/*arg4*::*hisG*	This study
GOA22	*goa1*::*UAU1*/*goa1*::*URA3*::*GOA1-HIS1*	This study
GOA32	*goa1*::*URA3*/*goa1*::*ARG4*::*GOA1-HIS1*	This study
GOA42	*goa1*::*URA3*/*goa1*::*ARG4*::*GOA1-HIS1*	This study
GOA-GFP	*GOA1*/*GOA1-GFP-URA3 ura3*::*imm434*/*ura3*::*imm434*	This study

to interactions of the organism during encounters with host defenses. For example, innate immunity including phagocytic killing by human polymorphonuclear cells (PMNs) and activated macrophages is critical to protection against blood-borne *Candida* species. Unactivated macrophages provide some protection although less so than neutrophils. This important observation has been demonstrated both clinically (neutropenic patients are susceptible to blood-borne candidiasis) and experimentally (25, 26, 47). In the latter instance, a sevenfold-greater killing of *C. albicans* by PMNs was reported compared to blood monocytes; additionally, germination of the organism occurred in monocytes. Similar data have been previously reported by another group (38). After phagocytosis, in both PMNs and monocytes, the expression of many fungal genes associated with oxidative stress responses was especially prominent (25). However, it would appear that resistance to oxidant stress, and probably other anti-*Candida* factors, was achieved only in infected monocytes. Thus, in neutropenic patients, the paradigm is that mononuclear phagocytes are less able to kill the organism that, in turn, favors spread of the organism in tissues.

We have identified a gene (*GOA1*) from *C. albicans* whose deletion results in oxidative sensitivity. One of the features of this protein is that it becomes localized to the mitochondria during oxidant stress. In the absence of *GOA1*, we show that mitochondrial functions are compromised as revealed by a decrease in respiration and membrane potential. We hypothesize that Goa1p provides functions that relate to its role in mitochondria energetics especially during stress.

MATERIALS AND METHODS

Strains, strain maintenance, and plasmids. All strains used in the present study are listed in Table 1 and were maintained as frozen stocks and propagated on yeast extract-peptone-dextrose (YPD) agar when needed (1% yeast extract, 2% peptone, 2% glucose, 2% agar). Plasmids pGEM-URA3, pRS-ARG4, and pGEM-HIS1 were provided by Aaron Mitchell (56, 57). To create pGEM-HIS1-GOA1, *GOA1* was amplified by using primers listed in Table 2, which contained flanking BamHI restriction sequences. The PCR product was purified and di-

TABLE 2. Primer sets used in this study

Primer	Sequence	Application
AnuKOF	CAGCCATTAAGAGATTGCCAATAAAATAACTAAGAATCACAAACC CTGGTGCTAAATTGCGTTTTCCCAGTCACGACGTT	URA3/ARG4 disruption cassette: 5′ region of *GOA1*
AnuKOR	CCAAGTAAAACACCCCTTGAATTATCAGTATGCCAACATGTTTCAT TGTTTGTGTTAGTAATTGTGGAATTGTGAGCGGATA	URA3/ARG4 disruption cassette: 3′ region of *GOA1*
ABA-REV-BamHIF	GGATCCGGCATTCAATGTCTGCGTGC	Upstream region of *GOA1* with BamHI restriction sequence to create GOA32 and GOA42
ABA-REV-BamHIR	GGATCCCTCCCATGACGAAATGACG	Downstream region of *GOA1* with BamHI restriction sequence to create GOA32 and GOA42
19.3818F	ACGTGCACCCACGGTATTACATCA	*GOA1* specific
19.3818R	ACTTCTGATCTCCAATTCGGGCAA	*GOA1* specific
AnuDIAGF	GGGTCAGGCAGGGGTTACCTA	Confirm intergration at the *GOA1* locus
AnuDIAGR	CACGGTGTTTTGGGTACCTCTC	Confirm intergration at the *GOA1* locus
SouthernF	ACTTCTGAATTTGATGGATCTCGGA	Generate probe for Southern blot
SouthernR	AGCAATCCAACAGGTGGACCTAGA	Generate probe for Southern blot
GOA-GFPF	CACAAAGCTTGAAAGTAAAGCATTAATGCAAAGTGACATATACA AATCTCTCAACAAAGAAAATCAGAATGGTGGTGGTTCTAAAGG TGAAGAATTATT	GFP cassette, 3′ region of *GOA1* excluding stop codon
GOA-GFPR	TATCAGTATGCCAACATGTTTCATTGTTTGTGTTAGTAATTTTTGA GCTTGCATTCCTAGTCGGAATACGTCTAGAAGGACCACCTTTG ATTG	GFP cassette, downstream of *GOA1*

gested with BamHI restriction enzymes and ligated into pGEM-HIS1, which had been digested using BamHI.

Construction of *GOA1* deletion mutants. GOA21 was obtained from a transposon mutagenized library (16). In addition to GOA21, we constructed two other *GOA1* deletion mutants, GOA31 and GOA41. To do this, cassettes for transformation were designed by amplifying *ARG4* and *URA3* from plasmids pRS-ARG4 and pGEM1-URA3 using the primers described in Table 2. Primers containing the *GOA1* flanking sequences were also used for PCR amplification, and *URA3* or *ARG4* was inserted within the *GOA1* flanking sequences (46). Cassettes were then transformed into SN148 to generate GOA31 or into BWP17 to generate GOA41 (see Fig. 1A [only GOA31 is shown]).

Construction of the gene reconstituted strains GOA22, GOA32, and GOA42. GOA22 was constructed as follows. *GOA1* was amplified by using primers listed in Table 2. The PCR product was purified and digested with NdeI and ligated into pGEM-HIS1, which had been digested by using NdeI. The pGEM-HIS1-GOA1 plasmid was linearized by using SalI and subsequently transformed into GOA21 (Fig. 1B). The integration and orientation of *GOA1* were confirmed by PCR using primers listed in Table 2. GOA32 and GOA42 were constructed as follows. *GOA1* was amplified using primers listed in Table 2, which contained flanking BamHI restriction sequences. The PCR product was purified, digested with BamHI, and ligated into pGEM-HIS1, which had been digested by using BamHI. The pGEM-HIS1-GOA1 plasmid was linearized using EcoRI and subsequently transformed to yield strains GOA32 and GOA42.

Southern hybridization. We utilized standard methods for doing Southern blot hybridization (8, 23). Purified *C. albicans* genomic DNA was isolated and digested with NdeI and separated by gel electrophoresis and transferred to a nylon membrane. The reaction proceeded overnight in a solution containing 0.4 M NaOH and 1 M NaCl. The membrane was then placed in a neutralization buffer (0.5 M Tris, 1 M NaCl [pH 7.2]), UV cross-linked and placed in a 2× SSC (1× SSC is 0.15 M NaCl plus 0.015 M sodium citrate) solution for hybridization. A 600-bp probe was generated by PCR with primers (Table 2) containing sequences upstream of and within *GOA1*. The probe (Fig. 1C) was purified and labeled with [^{32}P]dCTP. All blots were hybridized at 68°C in a solution containing 0.5 M NaH_2PO_4 (pH 7.2), 7% sodium dodecyl sulfate, and 1 mM EDTA. After hybridization, the membranes were washed with decreasing concentrations of SSC and sodium dodecyl sulfate. All membranes were imaged by using a Storm phosphorimager (Amersham Biosciences) (Fig. 1D).

Screening of the transposon mutant library for oxidant sensitivity. Approximately 400 transposon insertion mutants were evaluated for oxidant sensitivity by plating each strain on YPD agar medium containing 0, 4, 6, or 8 mM H_2O_2 using a pin replicator. Plates were incubated at 30°C for 48 h and growth was evaluated. Strains that failed to grow or exhibited reduced growth from at least three experiments were screened further by plating known numbers of cells onto YPD medium containing either hydrogen peroxide or menadione as described below.

Determination of generation time and growth measurements. To determine generation times of all strains, yeast cells from overnight cultures grown at 30°C were diluted to a starting optical density at 600 nm (OD_{600}) of 0.10 in 50 ml of YPD broth containing leucine, histidine, arginine, and uridine. Cultures were incubated at 30°C, the OD_{600} was recorded hourly for 12 h or 20 h (see Results for details), and the generation times were calculated by using the method of Walia and Calderone (55).

Drop plate sensitivity assays. According to the method of Chauhan et al. (11), the sensitivity of all strains to oxidant and osmotic stress was tested by plating serial dilutions of 5×10^1 to 5×10^5 cells (each in a total of 5 μl) onto YPD agar plates containing 6 mM H_2O_2 or 0.125 mM menadione. Yeast cells were obtained from overnight cultures grown in YPD broth at 30°C, washed with saline, and standardized by hemacytometer counts. The growth of each strain was evaluated for sensitivities after 48 h of incubation at 30°C.

Strains were also evaluated for their growth on YNB (yeast nitrogen base) agar supplemented with histidine (20 mg/ml) and leucine (30 mg/ml) containing 2% glucose, 4% glycerol, 4% lactate, or 6% ethanol. Drop plates were incubated at 30°C for 5 days and then photographed.

PMN killing and phagocytosis assays. Neutrophil killing assays were performed as previously described (18, 49). Briefly, PMNs were isolated from the peripheral blood of healthy human volunteers by dextran sedimentation and centrifuged through the lymphocyte separation medium Polymorphprep (Axis-Shield). PMNs were enriched in number by a brief hypotonic lysis of erythrocytes and then suspended in RPMI 1640 medium containing 10% fetal bovine serum (FBS). Cells were judged as >99% viable by trypan blue dye exclusion. Strains were grown in YPD broth overnight as described above, washed with phosphate-buffered saline (PBS; pH 7.4), and then opsonized with 50% human serum for 30 min at 37°C. PMNs and opsonized yeasts (collected by centrifugation) were suspended in RPMI medium containing 10% FBS at a ratio of 10:1 (10^7 PMNs to 10^6 yeasts). Cultures were incubated at 37°C for 3 h, centrifuged, and suspended in water to lyse the neutrophils. Serial dilutions were performed of the yeast cells, and 100 μl was plated onto YPD agar. Plates were incubated for 48 h at 30°C, at which time CFU were counted. The percent killing was calculated by using the following formula for each strain: [(CFU without PMNs) − (CFU with PMNs/CFU without PMNs)] × 100.

To determine the percent phagocytosis of all strains, we used the method of Klippel and Bilitewski (34). Human neutrophils were prepared as described above. For fluorescence labeling, 10^7 yeasts were harvested by centrifugation (13,000 rpm, 5 min, 4°C), washed twice with PBS, and stained with 1 ml of carboxyfluorescein diacetate succinimidyl ester (CFSE; Molecular Probes, Leiden, The Netherlands; 500 μM in PBS–0.1% dimethyl sulfoxide) for 1.5 h at 37°C. Stained cells are green in color. Yeasts were washed three times in PBS to remove the residual dye. For phagocytosis assays, in brief, 6×10^5 PMNs/ml/well were incubated with CFSE-labeled *Candida* (1:2) for 30 min at 30°C in a final volume of 400 μl. Samples were kept on ice until immediately before analysis. To quench the fluorescence of yeasts that were not internalized, trypan blue (0.2%, final concentration) was added. The images were analyzed and captured with a Zeiss Axiovert 200M microscope, coupled with a digital camera (magnification, ×400). Thus, intracellular (phagocytized) cells appear green, whereas nonphagocytized yeasts are red. We determined the percentage of PMN that contained phagocytized yeasts of each strain, as well as the number of yeast cells per PMN per strain, from 20 fields of mixed suspensions.

Morphogenesis assays. For these experiments, cells from an overnight culture grown in YPD were washed, and 250 cells of each strain were plated on YPD, 10% serum, Spider, and SLAD agar media and incubated at 37°C for 5 days according to standard procedures (8, 15). Representative colonies were then photographed.

Chlamydospore formation was evaluated by spotting 10 μl of an overnight yeast culture (10^5 cells) of each strain onto cornmeal agar, placing a coverslip over the cells, and incubating the cultures for 5 days in the dark at room temperature. Subsequently, chlamydospore formation was evaluated for each strain by light microscopy. Cultures were photographed by using an Olympus DP12 microscope equipped with a digital camera.

Murine model of hematogenously disseminated candidiasis. We followed the method of Calera et al. (8) to evaluate the virulence of a set of wild-type (wt), null, and gene-reconstituted strains. All strains were grown overnight in YPD at 30°C. Cells were washed in PBS (pH 7.2), counted by using a hemacytometer, and suspended in PBS. Three groups of 13 female BALB/c mice (Harlan) were injected intravenously via the lateral tail vein with 10^6 yeast cells in 50 μl of SC5314, GOA31, and GOA32 samples. At 24, 48, and 72 h postinfection, one mouse per group was euthanized. One kidney from each animal was removed, fixed in 10% formalin, and prepared for histological examination using the periodic acid-Schiff stain. The other kidney was removed, weighed, and homogenized in PBS. The homogenates were diluted and plated on YPD agar containing 50 μg per ml of streptomycin to inhibit bacterial growth. The plates were incubated at 30°C and, after 48 h, the number of colonies was counted to determine fungal load per gram of kidney. All remaining mice were observed for signs of morbidity twice per day. If moribund, animals were euthanized by cervical dislocation.

Construction of GOA1-GFP. Using primers (Table 2) containing sequences from the 3′ end of *GOA1* (excluding the stop codon) and downstream of *GOA1*, as well as containing sequences of the green fluorescent protein (GFP)-URA3 cassette from plasmid pGFP-URA3, a GOA-GFP cassette was amplified by PCR. This cassette was transformed into CAI4. The resultant strain was verified by PCR (data not shown).

Mitochondrial colocalization. Strain GOA-GFP was grown at 30°C overnight and then diluted to a starting OD_{600} of 0.10 in 50 ml of YPD broth. Cells were incubated at 30°C and upon reaching log-phase were stained with 250 nM MitoTracker Red (Molecular Probes) for 45 min. Cells were washed and stressed with 1 M NaCl or 5 mM H_2O_2 for 15 min, or grown in glycerol-YP for 15 min, and then imaged by using an Olympus Fluoview-FV300 laser scanning confocal system.

Spheroplast formation. Cultured GOA31, GOA32, or SC5314 cells in exponential phase were harvested by centrifugation from 350-ml of cultures from YPD medium, and the cells were washed with cold water, followed by a wash using buffer A (1 M sorbitol, 10 mM $MgCl_2$, 50 mM Tris-HCl [pH 7.5]). Cells were suspended in buffer A (3 ml/g of cells) containing 30 mM dithiothreitol. After 15 min of incubation at 30°C with shaking, the cells were harvested by centrifugation, suspended in buffer A containing lyticase (1 mg/g of cells) and 1 mM dithiothreitol, and incubated at 30°C until ca. 90% of the cells converted to spheroplasts (60 to 80 min). The digestion was stopped by the addition of an equal volume of ice-cold buffer A, and spheroplasts were washed twice with the

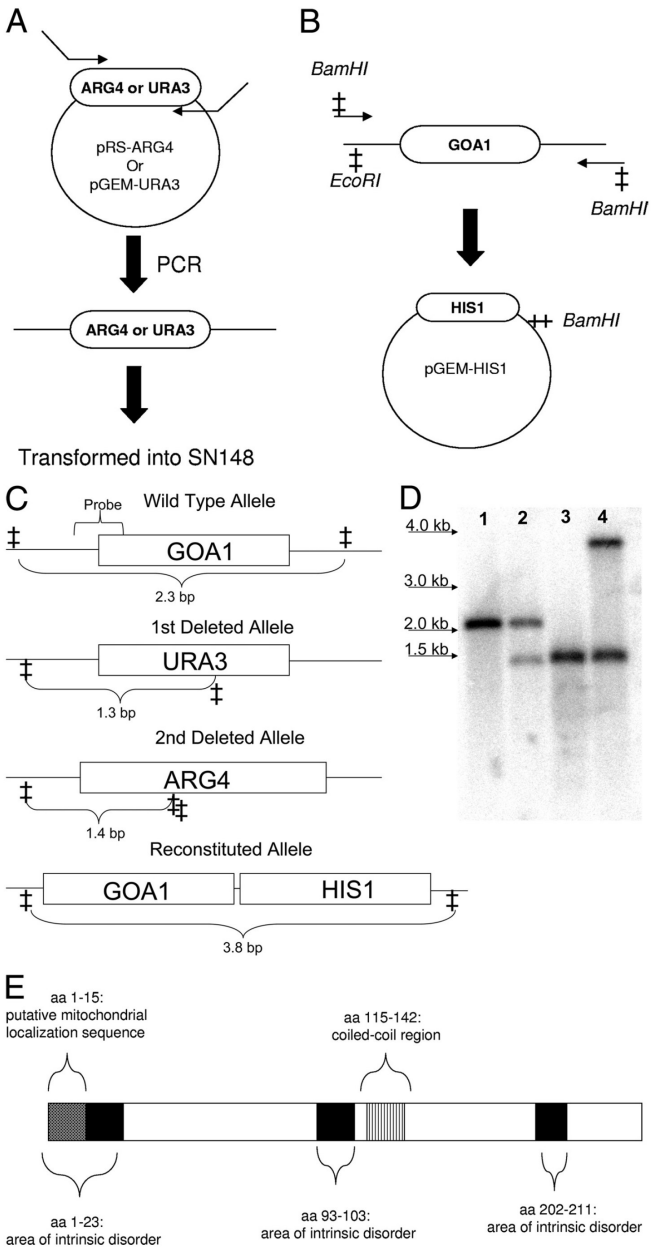

FIG. 1. Construction of the *goa1*Δ deletion mutant (GOA31) and its gene-reconstituted derivative GOA32. (A) Cassettes for transformation were constructed by amplifying *ARG4* and *URA3* from plasmids pRS-ARG4 and pGEM-URA3 using primers homologous to sequences upstream and downstream of *GOA1* (Table 2). These cassettes were then transformed into SN148 to create GOA31 and into BWP17 to generate GOA41 (data not shown). (B) *GOA1* was amplified using primers containing BamHI restriction sites. pGEM-HIS1 and the amplified *GOA1* fragment were digested with BamHI and the *GOA1* fragment inserted into pGEM-HIS1. The plasmid was digested with EcoRI and transformed into GOA31 to

same buffer. Protein concentration of the final suspension was determined using the biuret assay (28) in the presence of 0.2% deoxycholate.

Mitochondrial membrane potential. The mitochondrial membrane potential ($\Delta\Psi_m$) of permeabilized cells (spheroplasts) was monitored by measuring the fluorescence spectrum of Safranine O on a RF5301PC Shimadzu spectrofluorophotometer (Kyoto, Tokyo, Japan) operating at excitation and emission wavelengths of 495 and 586 nm, respectively, and with slit widths of 5 nm (24). All experiments were performed at 28°C with 1 mg of spheroplasts in 2 ml containing 5 μM Safranine O, 5 mM succinate, and 0.05% bovine serum albumin. Relative changes in membrane potential were expressed as arbitrary fluorescence units.

Oxygen uptake. Oxygen uptake was measured polarographically at 28°C using a Clark-type electrode (Hansatech Instruments, Ltd., England) with 1 mg of spheroplasts in 1 ml of standard incubation medium containing 125 mM sucrose, 65 mM KCl, 10 mM HEPES (pH 7.2), 2.5 mM KH_2PO_4, and 1 mM $MgCl_2$ with 1 mg of spheroplasts.

Statistical analysis. The Student *t* test was used for all analyses. Differences were considered significant when P was <0.05.

RESULTS

Isolation of GOA21 from a UAU insertion mutant library. A library of ~400 transposon insertion mutants was used to screen for oxidant-sensitive strains on YPD agar plates containing 0, 4, 6, and 8 mM H_2O_2. From this primary screen, 34 strains exhibited a peroxide sensitive phenotype and were further evaluated for sensitivity to both peroxide and menadione in drop-plate assays. Of these strains, a single mutant designated strain GOA21, named for growth and oxidant adaptation, was chosen for further study based upon its sensitivity to both peroxide and menadione and its slower growth rate (see below). The DNA sequence corresponding to the transposon insertion site was provided by Aaron Mitchell. The open reading frame (19.3818) encodes a protein of 279 amino acids (aa) in length. SMART (Simple Modular Architecture Research Tool) analysis indicated protein domains that include a putative mitochondrial localization signal (aa 1 to 15), areas of intrinsic disorder (aa 1 to 23, 93 to 103, and 202 to 211), and a coiled-coil domain (aa 115 to 142) (Fig. 1E).

Orthologs of Goa1p were identified by BLAST comparison with fungal, plant, and animal genomes in the NCBI database and genomics provided by the Fungal Genome Initiative at the Broad Institute. The presence of orthologs was confined to species within the CTG subclade of the *Saccharomycotina*, so named because the CTG codon of most of the species within this subclade has been reassigned from leucine to serine (17, 22). An apparent ortholog was present in each of the available genome sequences of species within this subclade, even those that have lost the codon reassignment. There are no known homologues in *Saccharomyces cerevisiae* or other human pathogens except the *Candida* species in this subclade.

Construction of null strains GOA31 and GOA41. To address the concern of secondary mutations due to the use of the TN7 transposon insertion cassette in the original library, we constructed new deletion mutants in the SN148 and BWP17 backgrounds (Fig. 1A). Cassettes for transformation were constructed by amplifying *ARG4* and *URA3* from plasmids pRS-ARG4 and pGEM-URA3 using primers containing sequences homologous to regions upstream and downstream of *GOA1*. The null mutant GOA31 was constructed by using these cassettes in the transformation of strain SN148 (46). The same cassettes were used to construct a second null mutant (GOA41) using BWP17 as the parental strain (not shown). Here, we describe only data from GOA31, although GOA41 exhibited similar phenotypes in assays described below.

To reconstitute *GOA1* into its native locus, the gene was amplified using primers containing BamHI restriction sites and subcloned into the BamHI site of pGEM-HIS1 (Fig. 1B). pGEM-HIS1 and amplified *GOA1* were digested with BamHI, ligated to create pGEM-HIS-GOA1, and evaluated by PCR to ensure that *GOA1* was inserted. After digestion with EcoRI, the cassette was transformed into GOA31 to generate strains GOA32 and GOA42 from GOA41 (only GOA31 and 32 are shown). All strains were confirmed by Southern Blot (Fig. 1C and D). Subsequent results in the present study will focus on strains GOA31 and GOA32.

A strain lacking *GOA1* has a longer generation time. To determine the generation time for each strain, overnight grown cells in YPD (30°C) were diluted to a starting OD_{600} of 0.10, and growth was monitored hourly spectrophotometrically (OD_{600}) for 12 h at 30°C (Fig. 2). The data represent averages from three independent experiments for the strains indicated and three replicates per time point. The wt strains SN148 and SC5314 doubled at 2.09 and 1.88 h, respectively ($P = 0.009$). In contrast, GOA31 (*goa1*/*goa1*) doubled significantly more slowly at 2.9 h ($P = 0.0005$ versus SN148). The *GOA1* reconstituted strain (GOA32) had a doubling time equal to SC5134 of 1.86 h (P = not significant versus SC5314; $P = 0.003$ versus SN148; and $P = 0.0002$ versus GOA31). We also found that GOA31 had a longer lag phase than the parental or gene-reconstituted strains and did not reach the same density at stationary phase (Fig. 2), even if incubation was carried out for 20 h (not shown). Therefore, *GOA1* is required for optimum growth and did not reach the same stationary phase by 12 h as wt cells, or even at 20 h (data not shown).

Goa1p protects cells against some oxidants. We tested the sensitivity of the strains to H_2O_2, *tert*-butyl hydrogen peroxide, menadione, and potassium superoxide. Cells were grown overnight, dilutions were plated on YPD agar containing each oxidant mentioned above, and the plates were incubated at 30°C for 48 h. Compared to the wt, GOA31 showed increased sensitivity to 6 mM H_2O_2 and to 0.125 mM menadione (Fig. 3A). Resistance to these oxidants was partially or completely restored in GOA32. There was no difference in growth among strains on YPD agar containing *tert*-butyl hydrogen peroxide and potassium superoxide (data not shown). Thus, *GOA1* is required for protection to some but not all types of oxidants, a result we have observed with the *C. albicans ssk2*Δ null mutant (54). We also evaluated the killing of each strain (10^7 cells/

create GOA32. (C) Restriction maps of *GOA1* and derived constructs. (D) Southern hybridization. Strains were digested with NdeI (sites are indicated with a cross). Lanes 1 to 4: 1, SC5314; 2, heterozygote; 3, GOA31; 4, GOA32. The probe for the blot is shown in Fig. 1C. (E) The Goa1p of *C. albicans*. Goa1p is 279 aa in length. The cross-hatched box (aa 1 to 15) indicates a putative mitochondrial localization signal. The black boxes (aa 1 to 23, 93 to 103, and 202 to 211) indicate areas of intrinsic disorder. The vertical-lined box (aa 115 to 142) indicates a coiled-coil region.

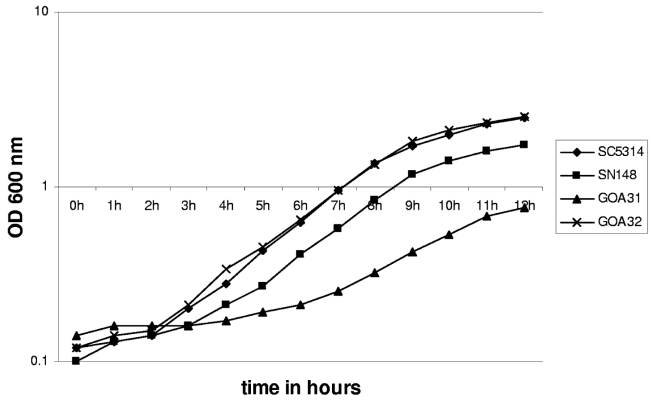

FIG. 2. Deletion of *GOA1* results in a longer generation time. The growth curves of strains SC5314, SN148, GOA31, and GOA32 are shown. Strains were grown overnight in YPD, transferred to fresh YPD at an OD_{600} of 0.1, and incubated at 30°C. The absorbance was measured every 1 h for 12 h, and the generation times were calculated. The growth curves represent the averages of three experiments and three replicates per time point per strain. Generation times: GOA31, 2.9 h; GOA32, 1.8 h; SC5314, 1.8 h; SN148, 2.09 h.

strain) in the presence of 10 mM H_2O_2 by incubating strains with H_2O_2 for 6 h (Fig. 3B). The concentration chosen for this assay was greater than the drop plate assays since we also used a greater number of yeast cells (10^7 per strain). We found that

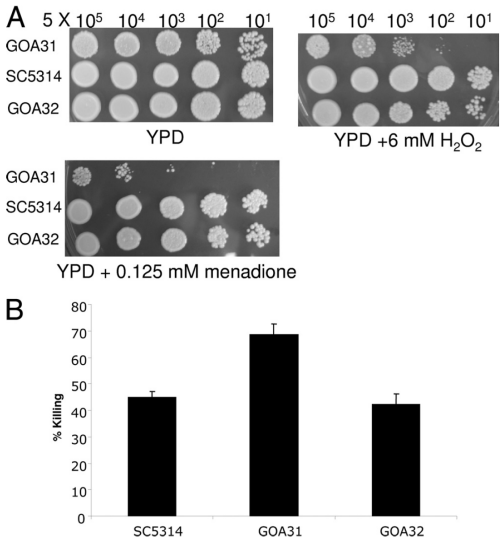

FIG. 3. The GOA31 strain is sensitive to H_2O_2 and menadione and is killed significantly more by H_2O_2. (A) Drop plate assays of strains GOA31, GOA32, and wt (SC5314) cells in the presence of H_2O_2 or menadione. Strains were grown overnight and standardized as described in Materials and Methods. Pictured is the growth of strains on YPD or YPD containing H_2O_2 (6 mM) or menadione (0.125 mM) at yeast cell concentrations of 5×10^5, 10^4, 10^3, 10^2, and 50 cells. Plates were incubated at 30°C for 48 h. (B) Killing of strains was determined in vitro by incubating 10^7 yeasts with 10 mM H_2O_2. Samples were removed after 6 h of incubation at 30°C, and dilutions were plated on YPD agar.

GOA31 was killed to a significantly greater extent than wt or GOA32 by H_2O_2 ($P = 0.03$, GOA31 versus GOA32).

The *GOA*-null strains are more sensitive to killing by neutrophils. Since GOA31 is sensitive to oxidant stress imposed by incubating cells in medium containing menadione or H_2O_2, we hypothesized that this strain would be more sensitive to killing by PMNs. To measure killing of all strains, PMNs were isolated and mixed with yeasts previously opsonized with 50% human serum at a 10:1 (PMN-to-yeast) ratio in RPMI medium containing 10% FBS for 2 h at 37°C. PMNs were then lysed with water, the yeast cells were plated on YPD agar, and cultures were incubated for 48 h at 30°C. Colonies were counted from three independent experiments, and the averages are shown in Fig. 4A. The survival of GOA31 cells was significantly less than that of wt cells ($P = 0.018$) and lower for GOA32 than GOA31 ($P = 0.04$), while there was a significant difference observed between wt and GOA32 strains ($P = 0.05$). Killing of the original transposon mutant GOA21 versus its parental strain (DAY286) by PMNs was significantly greater also, similar to the results with GOA31 (data not shown). Thus, these experiments indicate a correlation between the sensitivity of the *goa1*Δ null mutant to hydrogen peroxide and menadione and survival in human PMNs.

Reduced survival of the GOA31 null mutant than the wt or the reconstituted strains might be associated with a higher amount of phagocytosis by neutrophils. To address this issue, we determined the percentage of neutrophils that phagocytized each strain by observing 20 microscope fields of PMN-yeast mixtures. We found that the percentage of phagocytosis was unexpectedly lower for GOA31 than the wt or reconstituted strains (ca. 67% for SC5314, 26% for GOA31, and 63% GOA32 ($P = 0.0001$, wt versus GOA31; $P = 0.01$, GOA31 versus GOA32, and wt = GOA32) (Fig. 4B). We also determined the number of yeast cells of each strain per PMN, which was, on average, wt = 3.4, GOA31 = 1.1, and GOA32 = 1.8 (data not shown). The differences between GOA31 and both the wt and GOA32 strains were significant ($P = 0.0001$, wt versus GOA31; $P = 0.005$, GOA31 versus GOA32; wt versus

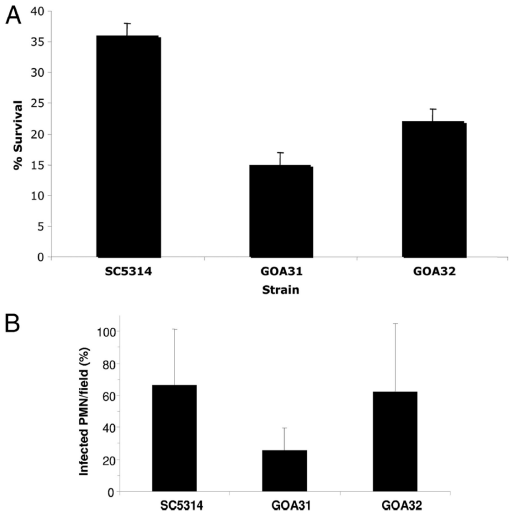

FIG. 4. GOA31 is killed more by human PMNs than wt or GOA32 but is phagocytized less. (A) GOA31 is more susceptible to killing by PMNs. Strains were grown overnight at 30°C, standardized, opsonized with human serum, mixed with human PMNs at a ratio of 10:1 (PMNs to yeast), and incubated at 37°C for 3 h, after which PMNs were lysed, and the yeast cell suspensions were plated on YPD plates (30°C for 48 h). The colonies were counted, and the percent survival was calculated. GOA31 versus SC5314, $P = 0.018$. (B) Percent phagocytosis by human PMNs of wt, GOA31, and GOA32 strains. Phagocytosis was determined by mixing CFSE-treated, green fluorescing yeast cells of each strain with PMNs. Subsequently, after phagocytosis for 30 min, extracellular, green fluorescent yeasts were quenched with trypan blue, whereas internalized yeasts remained green. The percentage of PMN cells containing green fluorescing yeasts was greater with wt and GOA32 cells than with GOA31 cells.

GOA32, P = not significant). Thus, these data indicate that the increased killing (reduced survival) of GOA31 is not associated with greater phagocytosis or a greater number of GOA31 cells per PMN. In fact, we found less phagocytosis of GOA31, suggesting that killing occurs by a different mechanism.

***GOA1* is required for morphogenesis and chlamydospore formation.** The role of *C. albicans* genes in nutrient stress can be evaluated in medium lacking specific carbon sources or low nitrogen (15). Most often, wt cells under these conditions convert from yeast to hyphal growth. To determine whether *GOA1* is required for the yeast-to-hyphal transition, we evaluated the morphogenesis and growth of all strains on YPD (nutrient rich), 10% serum, spider, and SLAD agar at 37°C for a minimum of 5 days (Fig. 5A). In a comparison of the strains, there were 3- to 10-fold differences in the colony diameters. On YPD agar, GOA31 colonies were smaller than those of wt and GOA32 strains, a finding consistent with the slower growth rate and longer lag phase (Fig. 2). On 10% serum agar, GOA31 colonies were smaller that those of the wt and GOA32, and all strains formed filaments, although GOA31 hyphae were considerably shorter in length than those of the wt but the same as GOA32 (Fig. 5A). On Spider and especially SLAD agar media, GOA31 colonies appeared minute and lacked filamentation. Each of these phenotypes was partially restored in GOA32, indicating a gene dosage-related phenotype. Thus, *GOA1* is required for morphogenesis under the conditions tested.

Chlamydospore formation by all strains was also evaluated. To do this, 10-μl portions of overnight grown YPD cultures were standardized to cell number, spotted onto cornmeal Tween agar plates, and then covered with a glass coverslip. The plates were then allowed to incubate at room temperature for up to 5 days in the dark. GOA31 was unable to form chlamydospores compared to wt cells, while chlamydospore production in GOA32 was intermediate to that of wt and GOA31, indicating that *GOA1* is required for chlamydospore formation (Fig. 5B).

***GOA1* is required for virulence in a hematogenously disseminated murine model of candidiasis.** To investigate the role of Goa1p in virulence, wt, GOA31 and GOA32 strains were inoculated intravenously into immunocompetent mice. The survival of mice over a 21-day period of time was determined for each strain, as shown in Fig. 6, and the colonization of their kidneys determined from mice infected for 24 to 72 h. We found that mice infected with wt cells rapidly succumbed to the infection during 4 days, whereas mice infected with the null strain GOA31 survived for at least 3 weeks. Mice infected with the gene-reconstituted strain (GOA32) showed attenuation of virulence, such that 40% survived for 21 days. Tissue loads of the organism, expressed as CFU/g of kidney, were relatively constant for all strains over the course of 72 h but much lower in strain GOA31 (Table 3). Hyphae were visible in kidneys of infected animals, although much more difficult to find in mice infected with GOA31 (data not shown). These data clearly demonstrate that Goa1p is required for virulence in this murine model.

Goa1p is translocated from the cytoplasm to mitochondria during oxidant and osmotic stress. Since Goa1p has a putative mitochondrial localization signal, we tagged Goa1p with GFP and performed fluorescence microscopy. Cells were grown to early log phase in YPD and then stained with MitoTracker (Molecular Probes) in order to visualize mitochondria. Cells were either treated or not with 5 mM H_2O_2 or 1.0 M NaCl or had glycerol substituted for glucose. We observed that, in unstressed cells, Goa1p was located in a punctuate pattern in the cytoplasm; the fluorescent signal was not uniformly coincident with the MitoTracker signal, indicating that Goa1p is not generally found in the mitochondria (Fig. 7A). However, upon either peroxide or osmotic stress, Goa1p partially relocalizes to the mitochondria as evidenced by merged photographs that indicate superimposition of GFP and MitoTracker (Fig. 7B, peroxide, and Fig. 7C, osmotic; see also Fig. S1 in the supplemental material). Goa1p also shows a mitochondrionlike distribution when cells were incubated in glycerol as a carbon source (data not shown). These data indicate that during peroxide or osmotic stress, the function of Goa1p is probably related to its ability to translocate to mitochondria.

To determine whether Goa1p is critical for mitochondria function, we evaluated growth of all strains on YNB medium supplemented with 2% glucose or nonfermentable carbon sources such as glycerol, lactate, and ethanol. We observed that while wt and GOA32 grew on all carbon sources, GOA31 was unable to utilize glycerol, lactate, or ethanol (Fig. 8). We

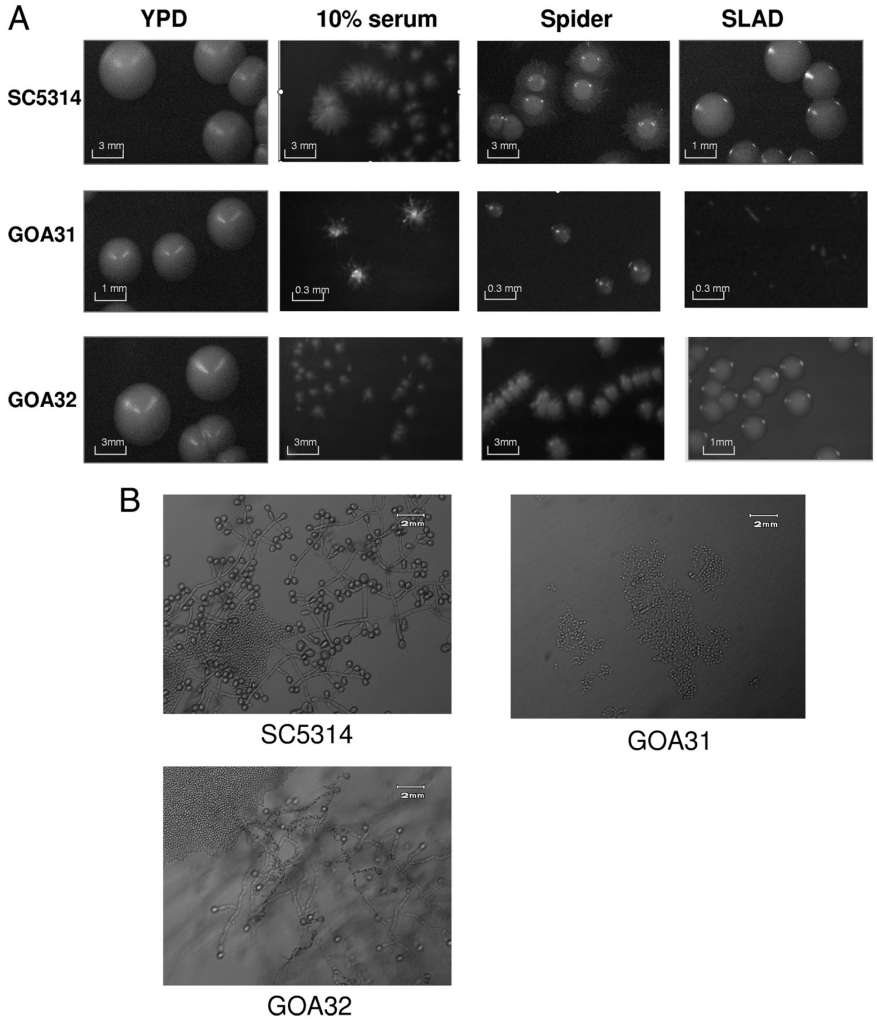

FIG. 5. GOA31 is compromised in growth on hypha-inducing media and lacks chlamydospore formation compared to other strains. (A) GOA31 colonies are smaller than those of wt and GOA32 and fail to filament or filament less extensively on 10% serum, Spider, or SLAD medium than other strains. Strains SC5314, GOA31, and GOA32 (indicated to the left of the figure) were grown overnight in YPD at 30°C and counted, and an equal number were incubated at 37°C on YPD, 10% serum, Spider, and SLAD agars for 48 h. Representative colonies are indicated. Note that the differences in the colony sizes of the strains on filamentation or YPD medium. A bar in each photograph indicates 0.3, 1, or 3 mm. (B) GOA31 fails to form chlamydospores compared to wt and GOA32 strains, which is intermediate in spore formation compared to wt and GOA31 strains. Cells of all strains were plated on cornmeal-Tween agar and incubated in the dark at room temperature for 5 days. After 5 days, chlamydospore formation was viewed by using light microscopy.

surmise that mitochondria function in the mutant was compromised as the nonfermentable carbon sources were not utilized via mitochondrial oxidation.

Mitochondria of GOA31 have defective membrane potential and reduced respiration. Safranine O is a dye whose fluorescence spectrum shifts as it binds to and stacks upon increasingly polarized inner mitochondrial membranes (1). The spectral shift is related to a developed mitochondrial membrane potential ($\Delta\Psi_m$) up to at least 170 mV (1) and can be monitored by using a spectrofluorophotometer operating at excitation and emission wavelengths of 495 and 586 nm, respectively (9). Figure 9A shows that spheroplasts suspended in the stan-

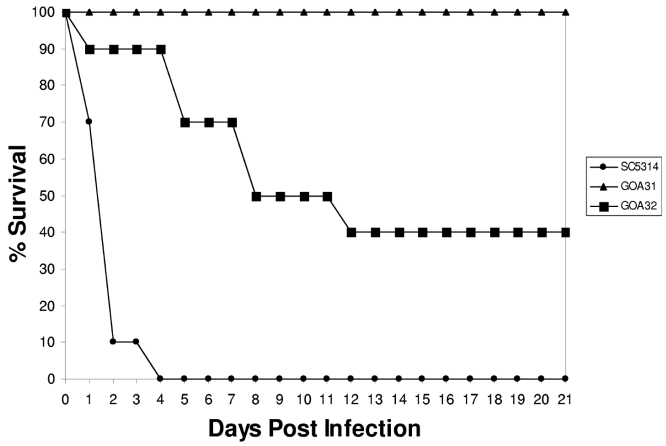

FIG. 6. GOA31 is avirulent in a murine model of hematogenously disseminated candidiasis. Mice were infected with 10^6 cells of each strain (wt, GOA31, and GOA32) in a murine model of hematogenously disseminated candidiasis. The survival of mice at 0 to 21 days postinfection is shown for each strain.

dard buffer containing 5 mM succinate as a substrate and 5 μM safranine was followed by a large decrease in fluorescence, which reached a steady state after a period of about 2 min. The blue line (Fig. 9A) shows that the addition of ADP to the experiment with the SC5314 spheroplasts, after the fluorescence had stabilized, was followed by an increase in fluorescence compatible with the utilization of the electrochemical proton potential to drive ADP phosphorylation by the F_oF_1-ATP synthase, as previously observed with *Candida parapsilosis* (9) and *C. albicans* (32). As expected, this fluorescence increase was reversed by carboxyatractyloside (CAT), an inhibitor of the adenine nucleotide translocase (Fig. 9A, black line). After CAT addition, the $\Delta\Psi_m$ returned to values slightly higher than the initial value, suggesting that, even in the absence of exogenous ADP, the mitochondria were using the membrane potential to phosphorylate endogenous ADP. The addition of FCCP, a protonophore, promoted a fast downward deflection of the trace compatible with depolarization of the inner mitochondrial membrane and return of safranine to the water phase. In contrast to the SC5314 spheroplasts, the GOA31 spheroplasts developed a very small $\Delta\Psi_m$ that was not modified by the addition of ADP, strongly indicating that this strain is not able to oxidatively phosphorylate ADP (Fig. 9A, green line). Figure 9B shows that GOA32 spheroplasts develop a $\Delta\Psi_m$ similar to SC5314 spheroplasts, allowing ADP phosphorylation consistent with the development of a membrane potential. Compatible with the $\Delta\Psi_m$ experiments of both SC5314 and GOA32 strains, respiration supported by endogenous substrates was similar and much faster than the GOA31 respiration (Fig. 10). The respiratory rates for strains SC5314, GOA32, and GOA31 were 13.62, 15.06, and 5.56 nM O_2/min/mg of protein, respectively.

TABLE 3. CFU counts in mice infected with strains of *C. albicans*[a]

C. albicans strain	Log_{10} CFU/g of tissue (mean ± SD) in kidneys at:		
	24 h	48 h	72 h
SC5314	6.0 ± 0.3	6.6 ± 0.2	6.6 ± 0.2
GOA31	3.7 ± 0.3	3.2 ± 0.1	3.0 ± 0.2
GOA32	5.8 ± 0.4	5.5 ± 0.3	5.2 ± 0.2

[a] At 24, 48, and 72 h postinfection, mice were sacrificed, and the CFU of each strain were determined by plating homogenates of kidneys on YPD agar. Cultures were incubated at 30°C, and colonies were counted after a 48-h incubation.

DISCUSSION

From a transposon mutant library of *C. albicans*, a gene was identified that provided adaptation to 6 mM H_2O_2 (16). Subsequently, null mutants were constructed in two strain backgrounds, and both exhibited sensitivity to peroxide and menadione. Since mutants lacking this gene also had growth defects, the gene was named *GOA1* to indicate its functions in both growth and oxidant adaptation. A thorough search of the literature and genome databases indicated its absence in *S. cerevisiae* as well as non-*Candida* human pathogenic fungi but a similarity to proteins only from the CTG subclade of the *Saccharomycotina* that includes, in addition to *C. albicans*, five other human pathogenic *Candida* species (17, 22). SMART analysis of the protein revealed an N-terminal mitochondrial localization domain as well as a coiled-coil and intrinsic disorder domains, the latter two of which indicate that it may functionally be important in its interactions with other proteins. Interestingly, Goa1p is required for optimal growth in the presence of H_2O_2 and menadione in vitro as well as optimum survival in human PMNs. Presumably, the latter function is associated with the ability to partially withstand the ROS of these phagocytes. Our data on killing of strains by PMNs was not related to a difference in the percent phagocytosis since wt cells were phagocytized more than GOA31. Our interpretation of this observation is that GOA31 is more susceptible to extracellular killing by PMN, which has been shown to be part of

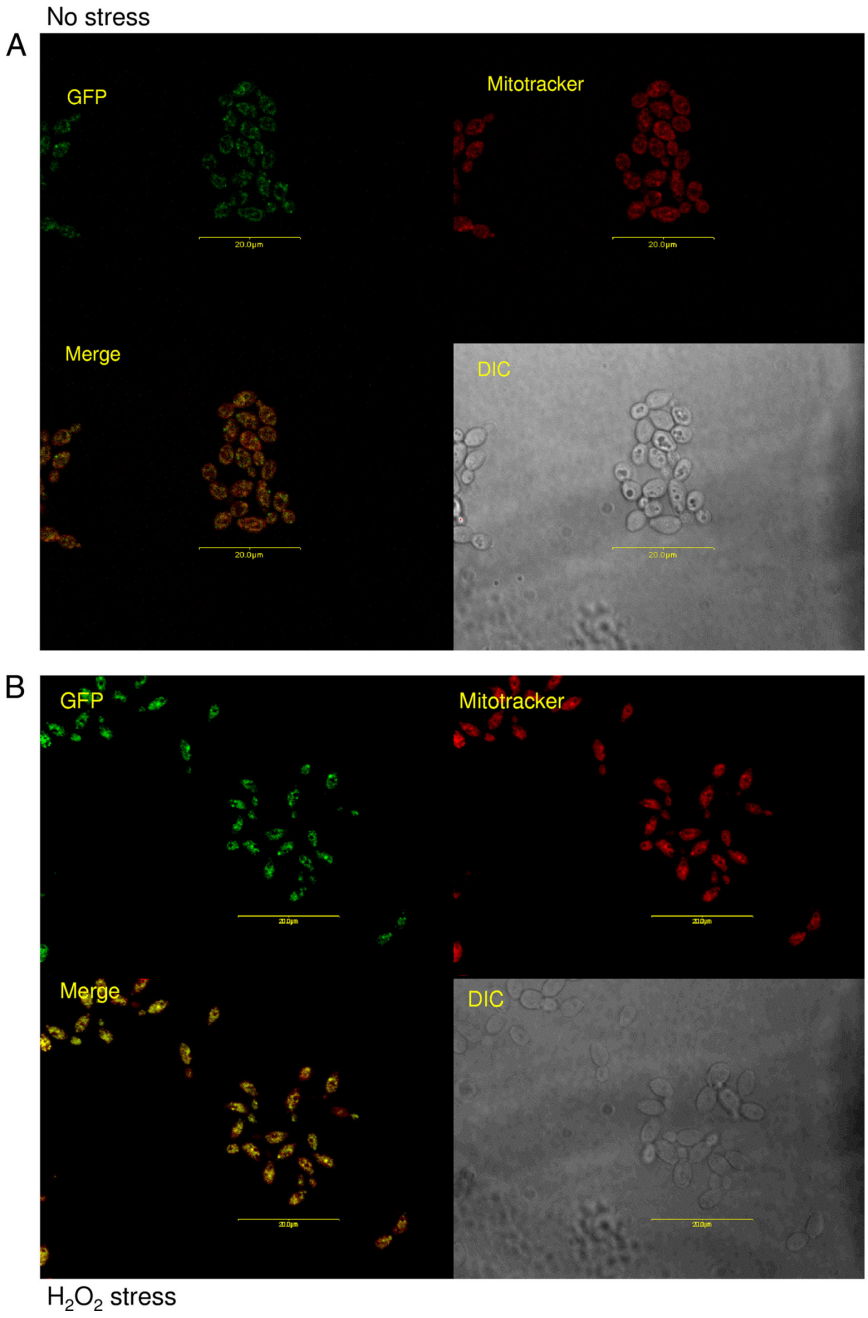

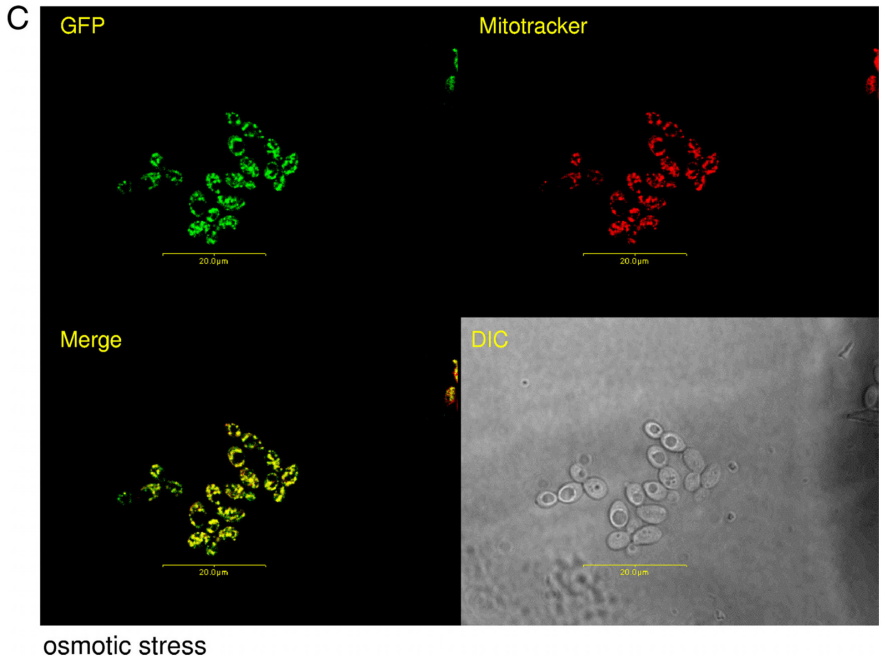

FIG. 7. Translocation of Goa1p to mitochondria is dependent upon peroxide or osmotic stress and a nonfermentative (glycerol) carbon source. A Goa1p-GFP fusion was incubated at 30°C, grown to early log phase, stained with MitoTracker Red (Molecular Probes/Invitrogen) for 45 min, washed, and subjected to treatment regimes for 20 min in YPD. Cells were immediately viewed by using fluorescence confocal microscopy. (A) Unstressed; (B) 5 mM hydrogen peroxide; (C) 1.0 M NaCl.

the PMN killing repertoire of *C. albicans* (25). Alternatively, while the percent PMN phagocytosis is lower in GOA31, the intracellular killing is still greater. Of importance, Goa1p is also required for virulence in a hematogenously disseminated murine model of candidiasis. The null strain GOA31 was totally avirulent in this model and, based upon tissue counts, the organism colonized (or persisted) in kidney tissue to a much lower extent than wt and GOA32.

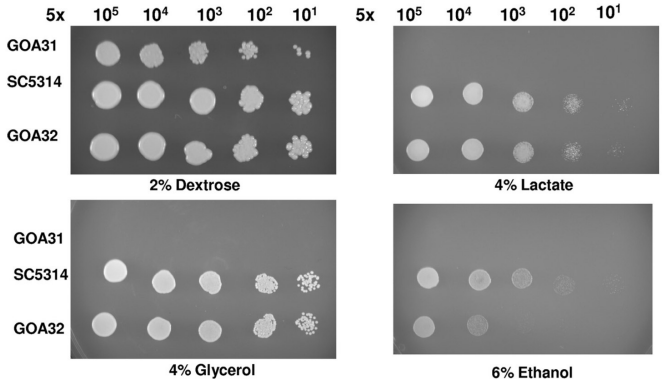

FIG. 8. The GOA31 mutant is unable to utilize nonfermentable carbon sources. Drop plate assays of wt, GOA32, and GOA31 strains on YNB agar medium supplemented with histidine, leucine, and either 2% glucose, 4% glycerol, 4% lactate, or 6% ethanol. GOA31 is able to grow only on YNB plus 2% glucose.

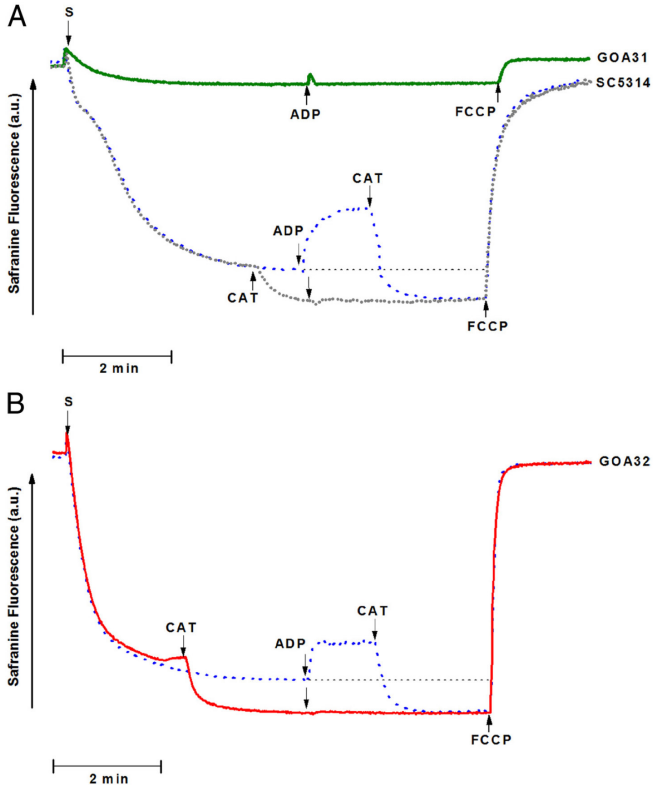

FIG. 9. Electrical membrane potential ($\Delta\Psi_m$) in different strains of *C. albicans*. GOA31 is unable to drive the phosphorylation of ADP. Spheroplasts (S, 1 mg/ml) were added to a reaction medium containing 125 mM sucrose, 65 mM KCl, 10 mM HEPES (pH 7.2), 2.5 mM KH_2PO_4,1 mM $MgCl_2$, 5 μM Safranine O, and 5 mM succinate in a total volume of 2 ml. Additions—200 μM ADP, 0.5 μM CAT, and 1 μM FCCP—are indicated by the arrows. (A) The dark green line represents GOA31 spheroplasts; the blue and black lines represent experiments performed with SC5314 spheroplasts in the absence (blue) or presence (black) of CAT (dashed line), respectively. (B) Experiments performed with GOA32 spheroplasts. The results shown are representative of four independent experiments performed in duplicate. a.u., arbitrary units.

One of the more striking phenotypes of strain GOA31 was its minimal growth on media that induce filamentation such as 10% serum, SLAD, and Spider agar media. This observation demonstrates the importance of respiratory metabolism in filamentation of *C. albicans*. Interestingly, there remains a controversy over the role of metabolic status associated with morphogenesis since both a need for and a lack of an intact respiratory pathway have been both suggested as important (10, 36, 37, 42, 54). Our data support the former conclusion.

Because of its mitochondrial localization signal, we integrated a *GOA1-GFP* cassette in wt cells and monitored translocation of the protein with or without stress to determine whether in fact the protein shuttled to the mitochondria during stress. In stressed cells or those grown in glycerol, the protein did partially relocalize to the mitochondria from the cytoplasm, whereas in unstressed cells, Goa1p was not associated with mitochondria. It is clear that adaptation to these stress conditions requires extensive energy production and mitochondria activity (see below). Cellular ROS accumulation is an outcome of increased cell metabolism and in addition, as cells sense increased external ROS, a stress response is induced to adapt cells. The relationship between stress adaptation and energy metabolism has been shown by others. During treatment with peroxide or high salinity, genes associated with energy production and mitochondrial functions are upregulated in *S. cerevisiae* (48, 59) and the halotolerant black yeast, *Hortaea werneckii* (53). In *S. cerevisiae*, respiration-associated transcripts (metabolism and energy functions) were especially strongly induced within 30 min of osmotic stress and persisted throughout exposure (59). The authors of that study showed that after treatment with high salinity, ca. 10% of the open reading frames were changed transcriptionally, and ca. 9% of the altered transcripts included open reading frames functionally important in providing energy via mitochondrial activities. In addition, a number of genes referred to as "cell

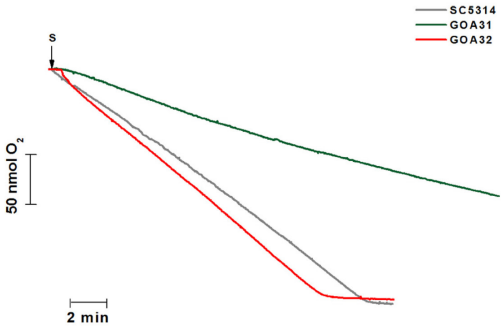

FIG. 10. The GOA31 strain shows a significantly reduced rate of respiration compared to wt and GOA32 strains, as measured by oxygen consumption. The test system (final volume, 1 ml, 28°C) contained 125 mM sucrose, 65 mM KCl, 10 mM HEPES (pH 7.2), 2.5 mM KH_2PO_4, and 1 mM $MgCl_2$. The addition of *C. albicans* spheroplasts (1 mg/ml) is indicated by an arrow. The results shown are a representative trace from four independent experiments performed in duplicate. Respiratory rates for each strain are listed in the text.

defense" transcripts, including those for glycerol and trehalose production and cell detoxification (glutaredoxin and metallothionein) also increased significantly. Posas et al. (48) showed that a number of functional gene families are induced early during saline stress, including carbohydrate metabolism (as represented by increased glycerol, glycogen, and trehalose content), sugar transporters, protein biosynthesis, ion homeostasis, and signal transduction. Clearly, osmotic stress can cause the loss of mitochondrial functions and apoptotic programmed cell death, as evidenced by mitochondrial swelling, reduction of mitochondrial inner membranes, and increased production of ROS (51). Growth of *H. werneckii* in a hypersaline medium resulted in increased ATP synthesis and oxidative damage protection (53). In the same study, the authors identified the 14-3-3 protein-encoding gene *HwBMH1* that localized to the mitochondria during hypersaline stress but not during growth of cells in physiological saline. In *S. cerevisiae*, the Bmh1/2 proteins are thought to be involved in the regulation of the mitochondrial proteome, especially in regard to carbohydrate metabolism (31). Transcriptional studies of stress responses have been carried out in *C. albicans*, although there were differences reported in regard to whether or not this organism has a core stress response (20, 21, 52). If a core stress response to adapt cells to oxidative, osmotic, or heavy metal (Cd^{2+}) stress does exist in *C. albicans*, it apparently upregulates a smaller set of genes compared to *S. cerevisiae* or *S. pombe*. The core stress response includes genes involved in redox regulation, cell wall biogenesis, protein folding and degradation, and carbohydrate metabolism, as well as genes encoding mitochondrial activities. In summary, it appears that an increase in energy metabolism is part of a stress response in a variety of yeasts and that adaptation to most stress conditions includes regulation of redox conditions and ROS detoxification.

Little is known about the coordination of events that shuttle cytoplasmic proteins to the mitochondria during stress in *C. albicans* although the literature is abundant with studies in other eukaryotes (reviewed in reference 45). About 10 to 15% of nuclear genes encode mitochondrial proteins, and they are recognized by translocase receptors that are of two general groups of proteins: transmembrane outer proteins and transmembrane inner proteins. Goa1p, by nature of its intrinsic and coiled-coil domains, may have functions related to protein escorting that are critical to translocation.

There are no other reports of proteins in *C. albicans* that are translocated to the mitochondria that play a role in membrane potential and ATP synthesis. *C. albicans* Hmi1p, like that of *S. cerevisiae*, has a C-terminal mitochondria targeting signal. Deletion of *HMI1* causes fragmentation of mtDNA, reduction of mtDNA mass, and loss of nucleoid distribution, but the deletion is not lethal, and the deleted strain is able to grow on nonfermentable carbon sources, unlike the *goa1*Δ null mutant (33). Recently, a *hog1*Δ null mutant was shown to be sensitive to inhibitors of the respiratory chain, with an enhanced respiratory basal rate and increased ROS production, although oxidant-detoxifying enzymes were elevated (2). However, mutant cells were able to still undergo oxidative phosphorylation even though the mitochondrial membrane potential was lower (2). In our studies, the functional activity of Goa1p is clearly related to its ability to mediate membrane integrity and, in the presence of peroxide, this event is lethal in the GOA31 strain. The studies described here focused upon the suggested protein escort function in which Goa1p may participate, as well as the identity of mitochondrial proteins lacking in GOA31.

ACKNOWLEDGMENTS

We thank Aaron Mitchell for providing the transposon mutant library and Alexander Johnson for *C. albicans* SN148. The fluorescence microscopy was done in the Lombardi Core microscopy facility. We thank Guillermo Palchik of the Lombardi Comprehensive Cancer Center Microscopy (LCCC) for his technical assistance and Luzia Lyra for help with the *C. albicans* cultures in the Laboratory of Clinical Pathology at the State University of Campinas. We also thank Cheryl Gale (The University of Minnesota) for providing the *GFP-URA3* plasmid.

Our study was supported by a National Institutes of Health grant (NIH-NIAID-43465) to R.C. This study was supported in part by the LCCC, Imaging Shared Resource, and U.S. Public Health Service grants 2P30-CA-51008 and 1S10 RR15768-01. O.A.A. was supported by the National Counsel of Technological and Scientific Development (CNPq/Brazil). N.C. is the recipient of an NIH-NIAID grant (AI076084) and an American Heart Association National Scientist Development Grant (0635108N).

REFERENCES

1. **Åkerman, K. E. O., and K. Wikstrom.** 1976. Safranine as a probe of the mitochondrial membrane potential. FEBS Lett. **68:**191–197.
2. **Alonso-Monge, R., S. Cavalheiro, C. Nombela, E. Rial, and J. Pla.** 2009. The Hog1 MAP kinase controls respiratory metabolism in the fungal pathogen *Candida albicans*. Microbiology **155:**413–423.
3. **Alonso-Monge, R., E. Navarro-Garcia, A. Romain, B. Negredo, C. Eisman, C. Nombela, and J. Pla.** 2003. The HOG1 MAP Kinase is essential in the oxidative stress response and chlamydospore formation in *Candida albicans*. Eukaryot. Cell **2:**351–361.
4. **Alvarez-Peral, F., O. Zaragoza, Y. Pedreno, and J. Arguelles.** 2002. Protective role of trehalose during severe oxidative stress caused by hydrogen peroxide and the adaptive oxidative stress response in *Candida albicans*. Microbiology **148:**2599–2606.
5. **Arana, D., R. Alonso-Monge, C. Du, R. Calderone, and J. Pla.** 2007. Differential susceptibility of mitogen-activated protein kinase pathways to oxida-

tive-mediated killing by phagocytes in the fungal pathogen *Candida albicans*. Cell. Microbiol. **9:**1647–1659.
6. **Arana, D., C. Nombela, R. Alonso, and J. Pla.** 2005. The Pbs2 MAP kinase kinase is essential for the oxidative stress response in the fungal pathogen *Candida albicans*. Microbiology **151:**1033–1049.
7. **Bahn, V. S., and P. Sundstrom.** 2001. *CAP1*, an adenylate cyclase-associated protein gene, regulates bud-hypha transition, filamentous growth, and cyclic AMP levels and is required for virulence of *Candida albicans*. J. Bacteriol. **183:**3211–3223.
8. **Calera, J. A., X.-J. Zhao, and R. Calderone.** 2000. Defective hyphal formation and avirulence caused by a deletion of the *CSSK1* response regulator gene in *Candida albicans*. Infect. Immun. **68:**518–525.
9. **Cavalheiro, R. A., F. Fortes, J. Borecky, V. C. Faustinoni, A. Z. Schreiber, and A. E. Vercesi.** 2004. Respiration, oxidative phosphorylation, and uncoupling protein in *Candida albicans*. Braz. J. Med. Biol. Res. **37:**1455–1461.
10. **Chattaway, F., R. Bishop, R. Holmes, F. Odds, and A. Barlow.** 1973. Enzyme activities associated with carbohydrate synthesis and breakdown in yeast and mycelial forms of *Candida albicans*. Microbiology **75:**97–109.
11. **Chauhan, N., D. Inglis, J. Pla, D. Li, J. A. Calera, and R. Calderone.** 2003. The *SSK1* of *Candida albicans* is associated with oxidative stress adaptation and cell wall biosynthesis. Eukaryot. Cell **2:**1018–1024.
12. **Chauhan, N., J.-P. Latge, and R. Calderone.** 2006. Signaling and oxidant adaptation in *Candida albicans* and *Aspergillus fumigatus*. Nat. Microbiol. Rev. **4:**435–444.
13. **Chaves, G. M., S. Bates, D. MacCallum, and F. Odds.** 2007. *Candida albicans GRX2*, encoding a putative glutaredoxin, is required for virulence in a murine model. Genet. Mol. Res. **6:**1051–1063.
14. **Chen, J., J. Chen, S. Lan, and H. Liu.** 2002. A conserved mitogen-activated protein kinase pathway is required for mating in *Candida albicans*. Mol. Microbiol. **46:**1335–1344.
15. **Csank, C., K. Schroppel, E. Lebrerer, D. Harcus, O. Mohamed, S. Melocha, D. Thomas, and M. Whiteway.** 1998. Roles of the *Candida albicans* mitogen-activated protein kinase homologue Cek1 in hyphal development and systemic candidiasis. Infect. Immun. **66:**2713–2721.
16. **Davis, D. A., V. M. Bruno, L. Loza, S. G. Filler, and A. P. Mitchell.** 2002. *Candida albicans* Mds3p, a conserved regulator of pH responses and virulence identified through insertional mutagenesis. Genetics **162:**1573–1581.
17. **Diezmann, S., C. Cox, G. Schonian, R. Vilgalys, and T. G. Mitchell.** 2004. Phylogeny and evolution of medical species of *Candida* and related taxa: a multigenic analysis. J. Clin. Microbiol. **42:**5624–5635.
18. **Du, C., R. Calderone, J. Richert, and D. Li.** 2005. Deletion of the *SSK1* response regulator gene of *Candida albicans* contributes to enhanced killing by human polymorphonuclear neutrophils. Infect. Immun. **73:**865–871.
19. **Eisman, B., R. Alonso Monge, D. Arana, E. Roman, C. Nombela, and J. Pla.** 2006. The Cek1 and Hog1 mitogen-activated protein kinases play complementary roles in cell wall biogenesis and chlamydospore formation in the fungal pathogen *Candida albicans*. Eukaryot. Cell **5:**347–358.
20. **Enjalbert, B., D. Smith, M. Cornell, I. Alam, S. Nicholls, A. J. P. Brown, and J. Quinn.** 2006. Role of the Hog1 stress activated protein kinase in the global transcriptional response to stress in the fungal pathogen. *Candida albicans.* Mol. Biol. Cell **17:**1018–1032.
21. **Enjalbert, B., A. Nantel, and M. Whiteway.** 2003. Stress-induced gene expression in *Candida albicans*: absence of a general stress response. Mol. Biol. Cell **14:**1460–1467.
22. **Fitzpatrick, D. A., M. E. Logue, J. Stajich, and G. Butler.** 2006. A fungal phylogeny based on 42 complete genomes derived from supertree and combined gene analysis. BMC Evol. Biol. **6:**99–114.
23. **Fonzi, W., and M. Y. Irwin.** 1993. Isogenic strain construction and gene mapping in *Candida albicans*. Genetics **134:**3648–3655.
24. **Fortes, F., R. Castilho, R. Catisti, R. E. Carnieri, and A. E. Vercesi.** 2001. Ca^{2+} induces a cyclosporin A-insensitive permeability transition pore in isolated potato tuber mitochondria mediated by reactive oxygen species. J. Bioenerg. Biomembr. **33:**43–51.
25. **Fradin, C., P. de Groot, D. MacCallum, M. Schaller, F. Klis, F. Odds, and B. Hube.** 2005. Granulocytes govern the transcriptional response, morphology and proliferation of *Candida albicans* in human blood. Mol. Microbiol. **56:**397–415.
26. **Fradin, C., M. Kretschmar, T. Nichterlein, C. Gaillarding, C. d'Enfert, and B. Hube.** 2003. Stage-specific gene expression of *Candida albicans* in blood. Mol. Microbiol. **47:**1523–1543.
27. **Gonzales-Parraga, J. Hernandez, and J. C. Arguelles.** 2003. Role of antioxidant enzymatic defenses against oxidative stress H_2O_2 and the acquisition of oxidative tolerance in *Candida albicans*. Yeast **20:**161–169.
28. **Gornall, A., C. Bardawill, and M. Davis.** 1949. Determinations of serum proteins by means of the biuret reaction. J. Biol. Chem. **177:**751–766.
29. **Hohmann, S.** 2002. Osmotic stress signaling and osmoadaptation in yeasts. Microbiol. Mol. Biol. Rev. **66:**300–372.
30. **Hwang, C., Y. Baek, H. Yim, and S. Kang.** 2003. Protective roles of mitochondrial manganese-containing superoxide dismutase against various stresses in *Candida albicans*. Yeast **29:**929–941.
31. **Ichimura, T., H. Kubota, T. Goma, N. Mizushima, Y. Ohsumi, M. Iwago, K. Kakiuchi, H. Shekhar, T. Shinkawa, M. Taoka, T. Ito, and T. Isobe.** 2004. Transcriptomic and proteomic analysis of a 14-3-3 gene-deficient yeast. Biochemistry **43:**6149–6158.
32. **Jarmuszkiewicz, W., G. Milani, F. Fortes, A. Z. Schreiber, F. E. Sluse, and A. E. Vercesi.** 2000. First evidence and characterization of an uncoupling protein in fungi kingdom: CpUCP of *Candida parapsilosis*. FEBS Lett. **467:**145–149.
33. **Joers, P., J. Gerhold, T. Sedman, S. Kuusk, and J. Sedman.** 2007. The helicase CaHmi1p is required for wild-type mitochondrial DNA organization in *Candida albicans*. FEMS Yeast Res. **7:**118–130.
34. **Klippel, N., and U. Bilitewski.** 2007. Phagocytosis assay based on living *Candida albicans* for the detection of effects on macrophage function. Anal. Lett. **40:**1400–1411.
35. **Kobayashi, D., K. Kondo, N. Uehara, S. Otokozawa, N. Tsuji, A. Yagihashi, and N. Watanabe.** 2002. Endogenous reactive oxygen species is an important mediator of the miconazole effect. Antimicrob. Agents Chemother. **46:**3113–3117.
36. **Land, G., W. McDonald, R. Stjernholm, and L. Friedman.** 1975. Factors affecting filamentation in *Candida albicans*: changes in respiratory activity of *Candida albicans* during filamentation. Infect. Immun. **12:**119–127.
37. **Land, G., W. McDonald, R. Stjernholm, and L. Friedman.** 1975. Factors affecting filamentation in *Candida albicans*: relationship of the uptake and distribution of proline to morphogenesis. Infect. Immun. **11:**1014–1023.
38. **Lehrer, R. I., and M. J. Cline.** 1969. Interaction of *Candida albicans* with human leukocytes and serum. J. Bacteriol. **98:**996–1004.
39. **Lemar, K., M. Aon, S. Cortassa, B. O'Rouke, C. Muller, and D. Lloyd.** 2007. Diallyl disulphide depletes glutathione in *Candida albicans*. Yeast **24:**695–706.
40. **Martchenko, M., A.-M. Alarco, D. Harcus, and M. Whiteway.** 2004. Superoxide dismutases in *Candida albicans*: transcriptional regulation and functional characterization of the hyphal-induced *SOD5* gene. Mol. Biol. Cell **15:**456–467.
41. **Martinez-Esparza, M., A. Aguniaga, P. Gonzalez-Parraga, P. Garcia-Penarrubia, T. Jouault, and J. C. Arguelles.** 2007. Role of trehalose in resistance to macrophages killing: study with a *tps/tps* trehalose-deficient mutant of *Candida albicans*. Clin. Microbiol. Infect. **13:**384–394.
42. **McDonough, J., V. Bhattacherjee, T. Sadlon, and M. Hostetter.** 2002. Involvement of *Candida albicans* NADH dehydrogenase complex I in filamentation. Fungal Genet. Biol. **36:**117–127.
43. **Nakagawa, Y., T. Kanbe, and I. Mizugchi.** 2003. Disruption of the human pathogenic yeast *Candida albicans* catalase gene decreases survival in mouse-model infection and elevates susceptibility to higher temperature and to detergents. Microbiol. Immunol. **47:**395–403.
44. **Navarro-Garcia, F., R. Alonso-Monge, H. Rico, J. Pla, R. Sentandreu, and C. Nombela.** 1998. A role for the MAP kinase gene *MKC1* in cell wall construction and morphological transitions in *Candida albicans*. Microbiology **144:**411–421.
45. **Neupert, W., and J. M. Hermann.** 2007. Translocation of proteins into mitochondria. Annu. Rev. Biochem. **76:**723–749.
46. **Noble, S., and A. D. Johnson.** 2005. Strains and strategies for large-scale gene deletion studies of the diploid human fungal pathogen *Candida albicans*. Eukaryot. Cell **4:**298–309.
47. **Pfaller, M. A., and D. J. Diekema.** 2007. Epidemiology of invasive candidiasis: a persistent public health problem. Clin. Microbiol. Rev. **20:**133–163.
48. **Posas, F., J. Chambers, J. Heyman, J. Hoeffler, E. de Nadal, and J. Arino.** 2000. The transcriptional response of yeast to saline stress. J. Biol. Chem. **275:**17249–17255.
49. **Roilides, E., K. Uhlig, D. Venzon, P. Pizzo, and T. Walsh.** 1992. Neutrophil oxidative burst in response to blastoconidia and pseudohyphae of *Candida albicans*: augmentation by granulocyte colony-stimulating factor and interferon-gamma. J. Infect. Dis. **166:**668–673.
50. **San Jose, C., R. Alonso-Monge, R. Perez-Diaz, J. Pla, and C. Nombela.** 1996. The mitogen-activated protein kinase *HOG1* gene controls glycerol accumulation in the pathogenic fungus *Candida albicans*. J. Bacteriol. **178:**5850–5852.
51. **Silva, R., R. Sotoca, B. Johansson, P. Ludovico, F. Sansonetty, M. Silva, J. Peinado, and M. Corte-Real.** 2005. Hyperosmotic stress induces metacaspase-and mitochondria-dependent apoptosis in *Saccharomyces cerevisiae*. Mol. Microbiol. **58:**824–834.
52. **Smith, D. A., S. Nicholls, B. Morgan, A. J. P. Brown, and J. Quinn.** 2004. A conserved stress-activated protein kinase regulates a core stress response in the human pathogen *Candida albicans*. Mol. Biol. Cell **15:**4179–4190.
53. **Vaupotic, T., P. Veranic, P. Jenoe, and A. Plemenitas.** 2008. Mitochondrial mediation of environmental osmolytes discrimination during osmoadaptation in the extremely halotolerant black yeast *Hortaea werneckii*. Fungal Genet. Biol. **45:**994–1007.
54. **Vellucci, V., S. Gygax, and M. Hostetter.** 2007. Involvement of *Candida albicans* pyruvate dehydrogenase complex protein X (Pdx1) in filamentation. Fungal Genet. Biol. **44:**979–990.
55. **Walia, A., and R. Calderone.** 2007. The *SSK2* MAPKKK of *Candida*

albicans is required for oxidant adaptation in vitro. FEMS Yeast Res. **8:**287–299.
56. **Wilson, R., D. Davis, B. Enloe, and A. Mitchell.** 2000. A recyclable *Candida albicans URA3* cassette for PCR through gene disruption with short homology. J. Bacteriol. **181:**1868–1874.
57. **Wilson, R., D. Davis, B. Enloe, and A. Mitchell.** 2000. A recyclable *Candida albicans URA3* cassette for PCR-product-directed gene disruption. Yeast **16:**65–70.
58. **Wysong, D. R., L. Christin, A. Sugar, P. W. Robbins, and R. D. Diamond.** 1998. Cloning and sequencing of a *Candida albicans* catalase gene and effects of disruption of this gene. Infect. Immun. **66:**1953–1961.
59. **Yale, J., and H. J. Bohnert.** 2001. Transcript expression in *Saccharomyces cerevisiae* at high salinity. J. Biol. Chem. **276:**15996–16007.
60. **Zhang, X., M. De Micheli, S. Coleman, D. Sanglard, and W. S. Moye-Rowley.** 2000. Analysis of the oxidative stress regulation of the *Candida albicans* transcription factor, Cap1p. Mol. Microbiol. **36:**618–629.